UNIVERSITÉ DE STRASBOURG

Thèse présentée pour obtenir le grade de Docteur de l'Université de Strasbourg

Discipline : Sciences Pharmaceutiques
Spécialité : Pharmacie galénique et délivrance de médicaments
Ecole doctorale : Ecole Doctorale Des Sciences Chimiques

Présentée par :
Ikram Ullah KHAN

Microfluidic-assisted synthesis and release properties of multi-domain polymer microparticles drug carriers

Soutenue le 24 octobre 2014

Directeur de Thèse :	Thierry VANDAMME	Professeur, Université de Strasbourg
Co-Directeur de Thèse :	Christophe SERRA	Professeur, Université de Strasbourg
Rapporteur Externe :	Lorenz MEINEL	Professeur, Université de Würzburg
Rapporteur Externe :	Cécile NOUVEL	Maître de conférences, Université de Lorraine
Examinateur Externe :	Michael KÖHLER	Professeur, Université Technique d'Ilmenau
Examinateur Interne :	Youri ARNTZ	Maître de conférences, Université de Strasbourg

Laboratoire de Pharmacie Biogalénique, Faculté de Pharmacie, Université de Strasbourg, 74 Route du Rhin BP 60024 67401 ILLKIRCH Cedex

I would like to dedicate my thesis to beloved parents,
especially my deceased mother (may Alllah keep her soul in eternal peace), family members & teachers for their love, guidance and prayers

Preface

This PhD dissertation started almost three year back with search to find a new, reliable and efficient technique to develop microparticles. Microcarriers are considered as a suitable alternative for macrocarriers because in comparison microparticles cause less toxicity, dose dumping, intra subject variability and local irritation. Conventional encapsulation methods can cause wastage of polymer, polydisperse particles and variation of drug release from batch to batch. So there is a need to establish new techniques that can fabricate different types of microparticles with high encapsulation efficiency, batch to batch uniformity and potential new characteristic features.

My search ended when I came through a project offered by Prof. Thierry F. Vandamme in collaboration with Prof. Christophe A. Serra on the use of "microfluidic techniques" to develop different drug loaded microcarriers. These techniques allow a better control over material composition, droplet size and thus particle size. Thus I used several capillary-based microfluidic devices to develop microbeads, Janus, core-shell and Trojan particles. All these particles were obtained by starting with monomers in solution and later polymerized by UV initiated polymerization. Particles were monodispersed in size and had high encapsulation efficiency. They can be used for different oral drug release strategies like controlled release (Microbeads), co-delivery (Janus), targeted dual delivery (Core-shell) and delivery of drug-loaded nanoparticles (Trojan).

Ikram Ullah Khan
University of Strasbourg, Strasbourg
France

Contents

Acknowledgment

All praise is to Allah, the lord of the entire universe, the gracious and the merciful. Countless thanks to Allah, who gave me opportunity, capability and courage to accept microfluidic project as a challenge and proceeded successfully to defend PhD. I pray, the results I obtained during my PhD research will benefit all the mankind. This thesis in its current form is due to the assistance and support of several people. It's a good opportunity to express my sincere thanks to all of them.

My parent university, Government College University Faisalabad, Pakistan for providing funding support for doctoral studies.

Prof. Thierry F Vandamme and Prof. C.A Serra for accepting me as PhD student and providing guidance and facilities for research project. During research they provided opportunity to communicate research results at several international conferences. I would like to express my special appreciation and thanks to efforts of Prof. C.A Serra for providing all necessary knowledge and guidance for proper understanding and handling of microfluidic technique. Wish to be kind hearted, lively, enthusiastic and energetic like him. Nicolas Anton for his help in experimental design and figures in research articles.

Words are inadequate to express my thanks to colleagues at Government College University Faisalabad especially Asif Massud and Mohsin Ali and my friends in Strasbourg Muhammad Rafiq, Zahid Rasul, Waseem, Azhar Ayaz, Madha, Khalid, Kareem and so on for their moral support, encouragement, love and care which help me withstand all the frustration encountered during my research work and also for their company which cheered me day and night.

Word of thanks to colleague at ICPEES (Alice Arbenz, Marie Reulier, Stéphanie Laurichesse, Dambarudhar, Camille Carré, Yu wei, F.-X. Pierrot, A. Rothan, S. Ding, R. Nasreddine, Salima Nedjari, Murielle Oster, Ibrahim Bulut, Patricia, A. Allouch, L. Stolch) and CAMB. I am especially thankful to officemates (Alice Arbenz, Marie Reulier, Stéphanie Laurichesse) for advice and friendly assistance whenever in trouble, especially for their help with the French administrative paperwork and translation of many French letters. Also to technical staff at ICPEES, ICS, CAMB and IGBMC for different techniques like SEM, TEM, MTT assay, DSC, FTIR, DLS etc.

I cannot finish without thanking my family members. I pay sincere and heartfelt admiration to my loving father, mother (May Allah keep her soul in eternal peace), brothers, sister's aunts and uncles for their prayers and well wishes. Although, I was far away from them but conversation with them was a source of mental satisfaction for me. Finally I would like to thank my better half, who joined me in Strasbourg during the last few months of PhD thesis. Her presence during this period was a source of mental satisfaction. Thanks for making my life easy and comfortable.

Ikram Ullah Khan

University of Strasbourg, Strasbourg

France

Abbreviations and notations

Abbreviations

µRMX	Elongational-flow micro reactor mixer
5-FU	5-Fluorouracil
A	Alginate
AAc	Acrylic acid
Ac	Acrylamide
API	Active pharmaceutical ingredient
ASHF	Hydroxypropylmethylcellulose acetate succinate based polymer
ATRP	Atom transfer radical polymerization
BCS	Biopharmaceutical classification systems
BSA	Bovine serum albumin
BzMA	Benzyl methacrylate
CdTe	Cadmium telluride
CEA	2 carboxyethyl acrylate
CEL	Celecoxib
CMC	Carboxymethylcellulose
CMC	Critical micellar concentration
CV	Coefficient of variation
DCM	Dichloromethane
dex-HEMA	Dextran-hydroxyethyl methacrylate
DMEM	Dulbecco's Modified Eagle's Medium
DSC	Differential scanning calorimetry
EA	Ethyl acrylate
EC	Ethyl cellulose
F-FITC	Bi-perfluoro-tagged fluorescein isothiocyanate
FITC	Fluorescein isothiocyanate
FTIR	Fourier transform infrared spectroscopy
GIT	Gastrointestinal tract
GPC	Gel permeation chromatography
HCPK	1-hydroxycyclohexyl phenyl ketone

HRP	Horse radish peroxidase
ID	Internal diameter
LD50	Median lethal dose
LTCC	Low temperature co-fired ceramics
MA	Methyl acrylate
MBA	N,N-methylene bis acrylamide
MMA	Methyl methacrylate
MTT	Tetrazolium dye
NIPAM	N-isopropylacrylamide
NIST	National Institute of Standards and Technology
NSAIDs	Nonsteroidal anti-inflammatory drugs
P	Pectin
PBS	Phosphate buffer solution
PCL	Polycaprolactone
PDI	Polydispersity index
PDMS	Polydimethylsiloxane
PEEK	Polyether ether ketone
PEI	Polyethyleneimine
PGDMA	Poly(1,3-glyceroldimethacrylate)
PLA	Poly(DL-lactic acid)
PLGA	Poly(lactic-co-glycolic acid)
PLLA	Poly(L-Lactic Acid)
PMMA	Poly(methyl methacrylate)
PMVEMA	Poly(methyl vinyl ether-co-maleic acid)
PNIPAM	Poly(N-isopropylacrylamide)
poly(AA-co-CEA)	Poly(acrylamide-co-carboxy ethyl acrylate)
PSi NPs	Porous silicon nanoparticles
PTFE	Polytetrafluoroethylene
PVP	Polyvinylpyrrolidone
QDs	Quantum dots
SDS	Sodium dodecyl sulphate
SQUID	Super conducting quantum interference device

TEM	Transmission electron microscopy
TMEDA	Tetramethylethylenediamine
TPGDA	Tripropylene glycol diacrylate
Vn	Vitronectin
VPTT	Volume phase transition temperature
XRD	X-ray Diffraction

Notations

Mw	Molecular weight (g/mole)
Q_c	Continuous phase flow rate (µL/min)
Q_d	Dispersed phase flow rate (µL/min)
Q_i	Inner phase flow rate (µL/min)
Q_m	Middle phase flow rate (µL/min)
Tg	Glass transition temperature (^oC)
η	Polymer solution viscosity (mPa.s)

Résumé de thèse

Microfluidic-assisted synthesis and release properties of multi-domain polymer microparticles drug carriers

1 Introduction

La libération de principes actifs dépend des caractéristiques inhérentes aux différentes voies d'administration. La voie orale est la voie d'administration la plus commode pour administrer un médicament et pour laquelle il existe encore actuellement différents obstacles et défis. Des systèmes de libération de principes actifs contrôlés à partir de systèmes unitaires sont actuellement en émergence pour résoudre des problèmes d'administration mais posent encore des problèmes comme la libération complète et ciblée. Afin de surmonter ces problèmes, une solution consiste à utiliser des formes microparticulaires contenant des principes actifs. Ces microparticules sont préparées par une technique dite de microencapsulation dans laquelle des principes actifs, solides, liquides ou gaz sont enfermé dans une microparticule grâce à la formation d'une couche périphérique d'un tiers matériel. Cette technique est largement utilisée dans plusieurs systèmes de délivrance de médicaments depuis sa première application en 1930. L'administration de médicaments sous forme de microparticules offre plusieurs avantages : la protection du principe actif, une libération contrôlée, une réduction de la fréquence d'administration, un meilleur confort pour le patient. Les méthodes de routine pour fabriquer ces microparticules souffrent cependant de coefficients de variation élevés (10 à 50%), de variabilités entre lots, d'une faible efficacité d'encapsulation et requièrent une grande quantité d'ingrédients. Par conséquent, il est souhaitable d'utiliser des méthodes qui permettent de surmonter ces problèmes. J'ai donc utilisé des systèmes microfluidiques pour résoudre ces problèmes. J'ai ainsi pu générer plusieurs morphologies de microparticules non conventionnelles qui ont servi de support pour le développement de nouvelles stratégies visant la co-délivrance de deux molécules actives et la réduction de la fréquence des prises tout en résolvant les problèmes inhérents liés à leur incompatibilité et différence de solubilité. Au cours de mon doctorat j'ai ainsi étudié quatre types différents de morphologies de microparticules à savoir: des microbilles, des particules Janus, des particules troyennes ainsi que différents types de particules coeur-écorce (Fig. 1).

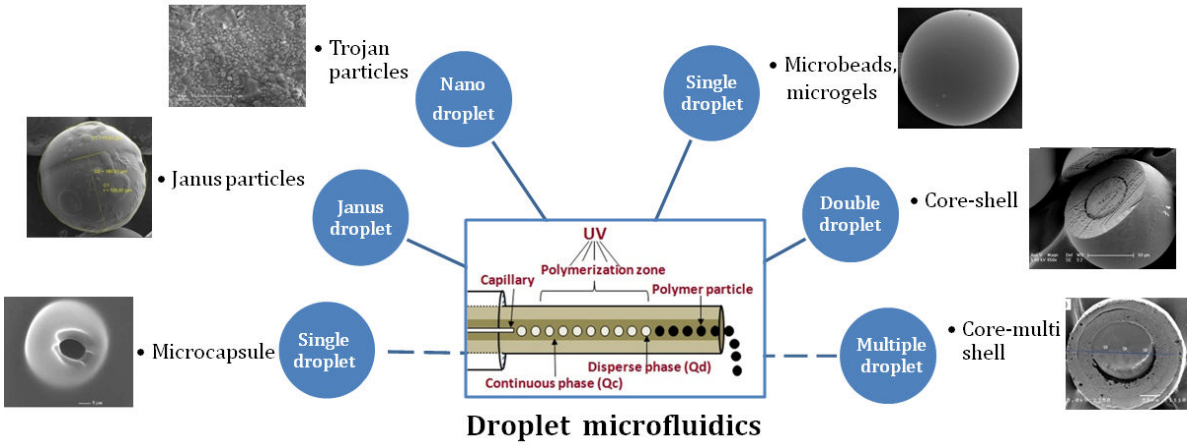

Fig. 1. Développements potentiels de différentes morphologies de particules par des modifications mineures d'un dispostif microfluidique constitué de capillaires. Les traits pleins concernent les particules développées dans le cadre de cette thèse de doctorat. Les traits pointillés concernent des morphologies de particules actuellement en prospection.

2. Microbilles

Des microbilles monodisperses de poly (tripropylène glycol diacrylate-co-acrylate d'éthyle) et chargées en kétoprofène ont été préparées en utilisant un dispositif microfluidique capillaire à co-écoulement et une irradiation UV pour déclencher une polymérisation radicalaire. Ces microbilles avaient un diamètre compris entre 200 et 380 µm et un coefficient de variation (rapport entre l'écart type de la distribution des diamètres et le diamètre moyen) inférieur à 5%. Les conditions d'obtention ont été optimisées afin d'éviter la dégradation des molécules actives dans les conditions expérimentales. Ainsi l'intensité de l'irradiation UV fut maintenue à un niveau minimum et la polymérisation fut conduite loin de la longueur d'onde d'absorption des principes actifs. Cela fut confirmé par des analyses FTIR dans lesquelles fut observé le pic caractéristique du kétoprofène et par des études XRD qui révélèrent son caractère amorphe une fois encapsulé. Les courbes de DSC ont permis d'obtenir des informations sur la température de transition vitreuse (Tg) et indiquèrent que cette dernière croissait lorsque la proportion massique de tripropylène glycol diacrylate augmentait dans les formulations testées. Des clichés de microscopie SEM montrèrent des tailles uniformes de microbilles avec une surface lisse pour toutes les formulations. L'efficacité d'encapsulation fut significativement élevée avec des valeurs comprises entre 80% to 100%. Les rapports des débits des phases continue et dispersée (Qc/Qd) ont été modifiés de manière à obtenir différentes dimensions de particules. Lorsque le rapport

Qc/Qd augmentait, la taille des gouttelettes était plus petite et leur interdistance plus grande. Dans toutes les conditions étudiées, le régime hydrodynamique était le goutte-à-goutte (Fig. 2a). De plus il a été montré que la taille des gouttelettes et des particules filles était influencée par la concentration d'acrylate d'éthyle: plus la concentration était élevée, plus les gouttelettes et particules étaient petites (Fig. 2b,d).

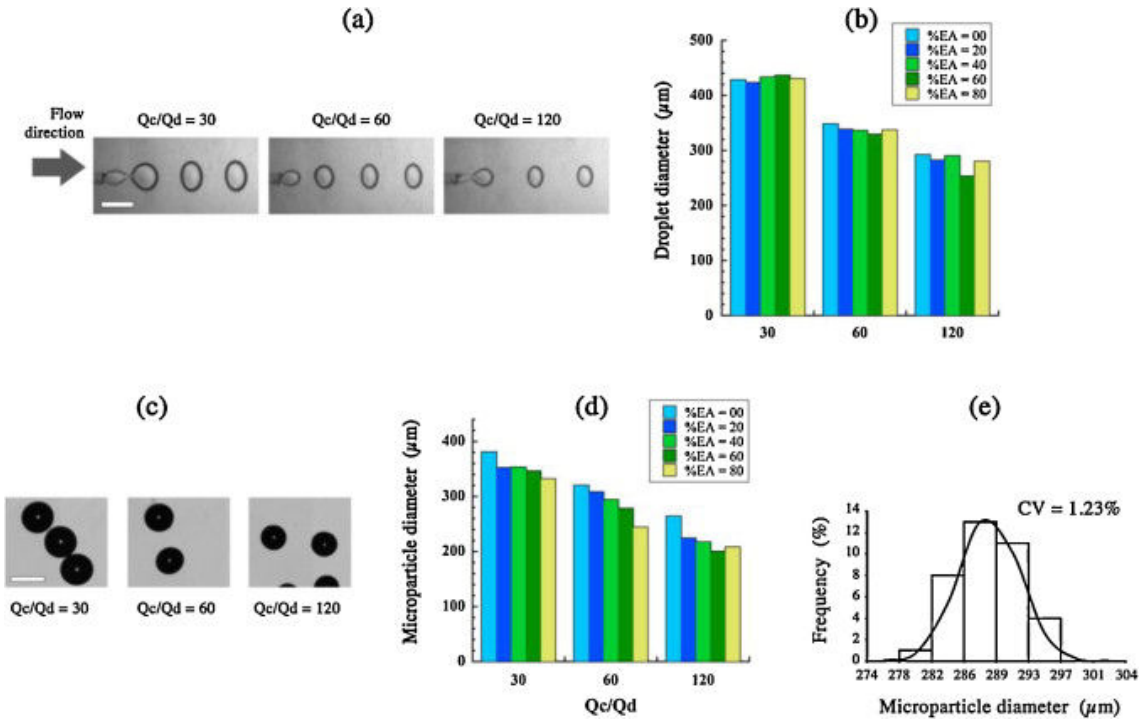

Fig. 2. Images optiques de la formation des gouttelettes (a) et des microbilles (c), l'échelle équivaut à 500 µm. Influence du rapport des débits des phases continue et dispersée ainsi que de la fraction massique d'acrylate d'éthyle sur le diamètre des gouttelettes (b) et des microbilles (d). Histogramme de tailles des microparticules pour une formulation ne contenant pas d'acrylate d'éthyle et obtenue avec Qc/Qd=120 (e).

La libération de kétoprofène a été étudiée à pH 1,2 et dans un tampon phosphate USP de pH 6,8. Toutes les formulations montraient une libération négligeable à faible pH alors que la libération variait à des pH plus élevés et dépendait du pourcentage en poids d'acrylate d'éthyle. Lorsque la concentration en acrylate d'éthyle augmentait, la libération de principe actif augmentait également et atteignait 100% en 24 heures pour des formulations contenant 80% d'acrylate d'éthyle (Fig. 3). Toutes les formulations montrèrent une bonne corrélation ($R^2 \geq 0.98$) avec le modèle de Korsmeyers Peppas et les valeurs de l'exposant (n) furent comprises entre 0.5 et 1 suggérant ainsi que la libération du

kétoprofène suit un mécanisme de diffusion non Fickien (résultats publiés dans International Journal of Pharmaceutics).

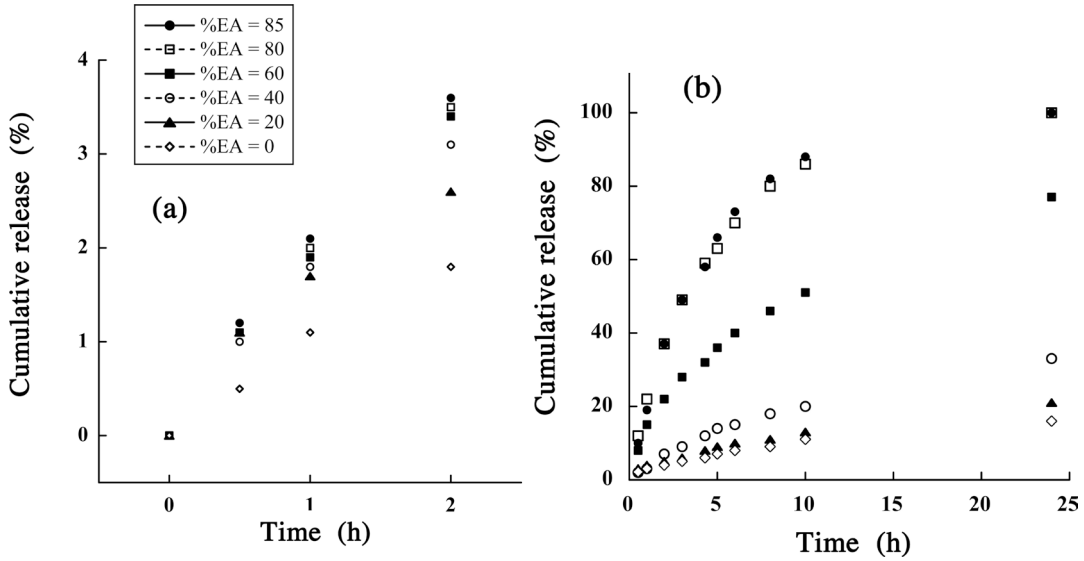

Fig. 3. Profils cumulés de libération du kétoprofène encapsulé dans des microbilles pour différentes fractions d'acrylate d'éthyle à pH 1,2 (a) et pH 6,8 (b).

3. Particules de type Janus

Une particule qui possède deux ou plusieurs compartiments séparés dont les compositions ou la nature chimique sont différentes est appelée particule "Janus". Ces particules peuvent être utilisées pour encapsuler deux molécules différentes, chacune d'elles dans un compartiment. La libération des molécules dépend de la nature des matrices polymères et de leurs densités de réticulation. Pour développer des particules Janus de poly(acrylamide)/poly(acrylate de méthyle) chargées en principes actifs, le dispositif de microfluidique décrit ci-dessus a été modifié de sorte à ajouter un second capillaire disposé juste à côté du premier de façon à ce que les deux phases dispersées puissent être libérées au même moment. Les dimensions des particules Janus sont comprises entre 59 et 240 µm et sont produites par polymérisation radicalaire en utilisant l'amorcée par irradiation UV. Ce système a été caractérisé en termes de débit des phases continue et dispersée, de composition en monomère des deux compartiments, de la nature et de la concentration en agent tensio-actif, du diamètre du tube collecteur de sortie et de l'intensité UV. Il a été observé que tous ces facteurs peuvent être contrôlés de manière adéquate de sorte à obtenir des particules de différentes formes allant de particules de types cœur-écorce à des particules bi-compartimentées. Pour obtenir ces dernières, une faible concentration en

agent tensio-actif (0,75% en poids) était nécessaire lorsque les deux phases dispersées étaient délivrées au même débit alors qu'à concentration élevée en agent tensio-actif, les débits des phases dispersées doivent être différentiés. Des particules de petite taille ont été obtenues en diminuant le diamètre interne du tube collecteur, en augmentant les débits de la phase continue par rapport à ceux de la phase dispersée (Qc/Qd) et en utilisant une section promouvant une focalisation hydrodynamique. L'analyse infra-rouge par transformée de Fourrier a mis en évidence que la polymérisation des monomères était complète et l'essai de cytotoxicité a montré que les particules étaient biocompatibles en ayant une DL 50 de 9 mg/ml. Les résultats des tests MTT furent confirmés par le marquage à l'iodure de propidium et à la calcéine AM qui ont respectivement la particularité de colorer les cellules mortes et vivantes (Fig. 4).

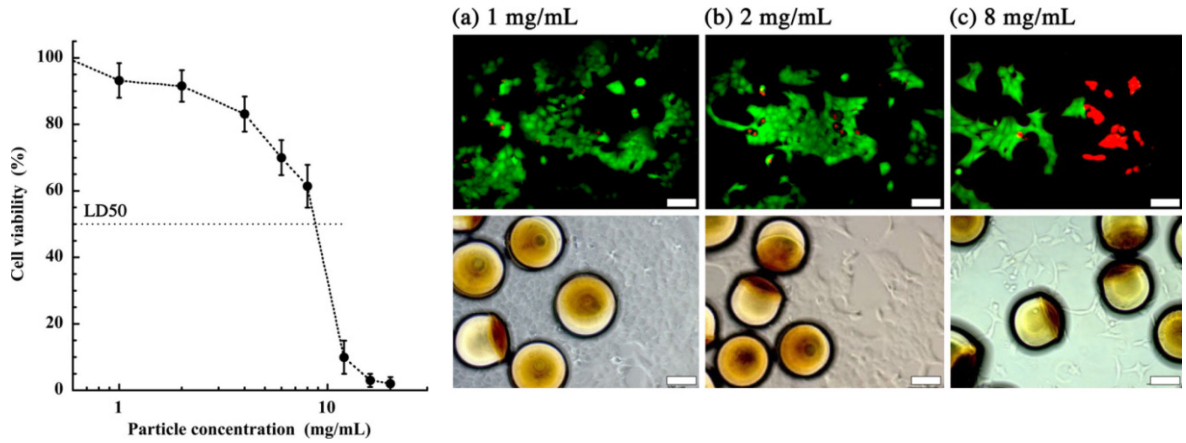

Fig. 4. Graphique présentant la viabilité des cellules après une exposition d'une lignée cellulaire hépatique BNL-CL2 à différentes concentrations massiques de particules Janus. Les images a, b et c (bas) montrent les cellules hépatiques après 24h d'incubation au contact des particules Janus. Les images du haut sont une visualisation fluorescente de ces cellules après marquage à l'iodure de propidium et à la calcéine AM. La barre d'échelle représente 100 µm.

Le kétoprofène et la fluorescéine de sodium ont tous deux été libérés de façon soutenue à pH 6,8 et limitée à pH 1,2. La libération des principes actifs était plus rapide à partir des grandes particules et résultait de la distribution irrégulière des deux phases et du renfoncement des plus grandes particules comme cela a été observé par microscopie électronique à balayage (Fig. 5). Par rapport au principe actif hydrophobe, la libération de la fluorescéine sodique de caractère hydrophile était beaucoup plus lente et pourrait être

attribuée à une faible charge et taux d'encapsulation initial ; de plus la libération de la fluorescéine de sodium peut être modulée en changeant la concentration en agent de réticulation. En diminuant la concentration de ce dernier, la densité de réticulation s'en trouve réduite augmentant de fait les mailles du réseau. Cela a pour conséquence de donner plus de liberté de mouvement au solvant et au principe actif. Ainsi peut-on contrôler la vitesse de libération individuelle des deux principes actifs par ajustement de la densité de réticulation des deux compartiments. Le mécanisme de libération des deux principes actifs modèles s'effectue dans ce cas par diffusion Fickienne (résultats publiés dans International Journal of Pharmaceutics).

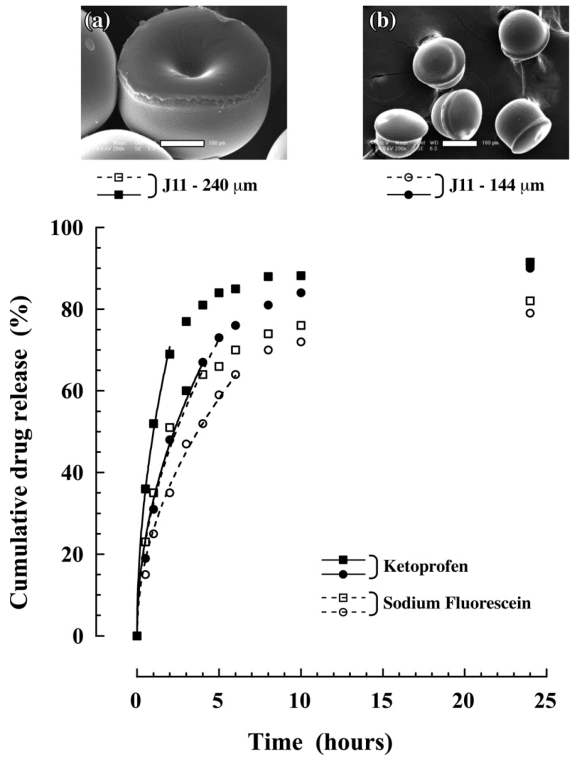

Fig. 5. Effet de la morphologie et de la taille des particules vecteurs sur la libération des principes actifs modèles. Les particules Janus de 240 µm ont été obtenues dans un tube de 1.6 mm de diamètre interne et leur cliché SEM montre des indentations (a) alors que celui des particules de 144 µm obtenues dans un tube de 1.6 mm présente une structure uniforme sans défaut (b). Les courbes de libération démontrent que 60% du principe actif a diffusé suivant la seconde loi de Fick modifiée. Les débits des phases hydrophobe et hydrophile étaient tous deux égales à 2 µL/min alors que la phase continue (huile de silicone) fut pompée au débit de 240 µL/min. L'intensité de la source UV était de 40%. La barre d'échelle des clichés SEM représente 100 µm.

4 Cœur-écorce

Une modification supplémentaire fut apportée au dispositif microfluidique de base décrit précédemment de manière à ce que les deux capillaires fussent arrangés de façon coaxiale. Ce faisant, il a été possible de produire des “gouttelettes doubles” (une gouttelette dans une autre gouttelette) qui furent ensuite polymérisées de sorte à donner une morphologie de type cœur-écorce. Le cœur de ces particules est constitué de poly (acrylate de méthyle) avec du kétoprofène tandis que leur écorce ou coquille était composée de poly (acrylamide) contenant du chlorhydrate de ranitidine. La taille de ces particules variait entre 100 et 151 µm en changeant le rapport des débits (Qc/Qm) de la phase continue (Qc) et de la phase écorce (Qm). Le diamètre du cœur variait de 58 à 115 µm en augmentant le rapport des débits (Qm/Qi) de la phase écorce et du cœur (Qi) (Fig. 6).

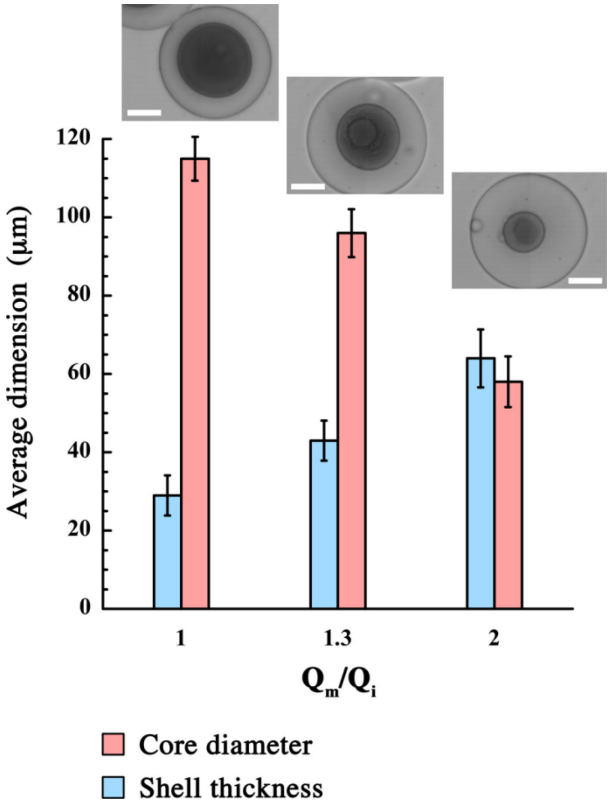

Fig. 6. Effet de Q_m/Q_i sur le diamètre du cœur et sur l’épaisseur de l’écorce. Les photos ci-dessous montrent les images optiques des particules coeur-écorce prises immédiatement après la polymérisation. Les barres d'erreur indiquent l'écart type (n=3) et les barres d'échelle représentent toutes 55 µm.

L’analyse infra-rouge par transformée de fourrier a confirmé la polymérisation complète des phases du cœur et de l’écorce. L'analyse MTT montre la variation dans la

viabilité des cellules dans des conditions de non contact et de contact avec moins de cytotoxicité pour le premier. Pour développer des particules sensibles au pH pour le ciblage du colon, quelques pourcents en poids d'un monomère sensible au pH (acrylate de beta-carboxyethyle) ont été ajoutés à la phase écorce. Le cœur et l'écorce contenaient les mêmes principes actifs respectivement hydrophobe et hydrophile comme dans le cas précédent. L'écorce sensible au pH prévient la libération des deux molécules encapsulées à faible pH mais progressivement accroît leur taux de libération avec un maximum de libération au pH du côlon, à 7,4 (Fig. 7). (résultats publiés dans International Journal of Pharmaceutics)

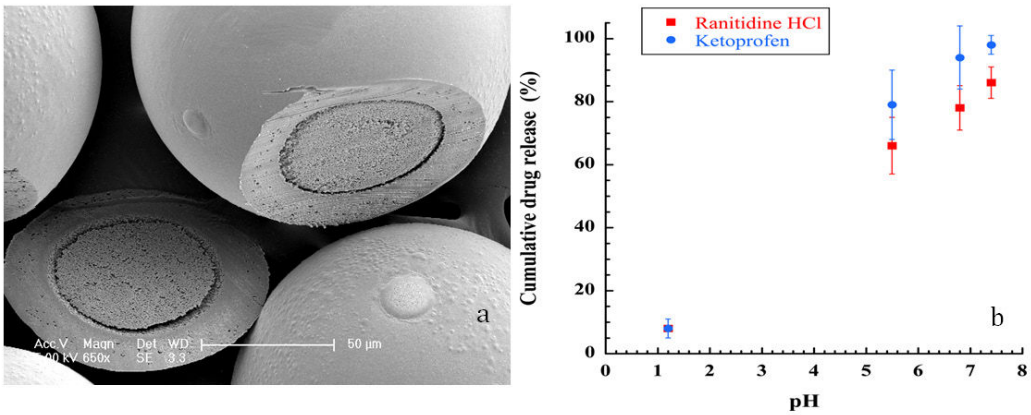

Fig. 7. Photographie SEM d'une particule cœur-écorce dont les sections révèlent clairement les deux compartiments. Le cœur est chargé avec 10% en poids de kétoprofène alors que l'écorce contient 1% en poids de chlorhydrate de ranitidine (a). Profils de libération des deux principes actifs (b).

5 Particules troyennes

Les nanoparticules encapsulées dans des microparticules sont appelées particules troyennes. Ces constructions sont utiles car elles permettent la libération de nanoparticles par voie orale et pulmonaire quand les méthodes conventionnelles ne peuvent les apporter directement sur le site d'absorption. Les méthodes courantes de fabrication des particules troyennes sont chronophages et impliquent de multiples étapes. Au cours de ce travail doctoral, j'ai développé un procédé microfluidique semi-continu en deux étapes pour produire facilement des microparticules troyennes à partir de nanoemulsions. Un micromélangeur à flux élongationnel (µRMX) a été employé d'abord pour produire des nanoémulsions pour lesquelles la taille des gouttelettes était comprise entre 98 to 132 nm (PDI = 0,162) en ajustant simplement les paramètres opératoires tels que la concentration

en surfactant et le temps de mélange. Par la suite, la nanoémulsion a été émulsifiée dans le système microfluidique capillaire à co-écoulement mentionné ci-dessus (Fig. 8). Les microgouttelettes ainsi obtenues furent ensuite polymérisées en ligne pour donner lieu aux microparticules troyennes. La section transversale de ces particules a révélé par analyse microscopique à balayage que le kétoprofène était encapsulé dans des nanoparticules d'acrylate d'éthyle et elles-mêmes incluses dans une matrice de poly(acrylamide) (Fig. 9). La libération des nanoparticules et du kétoprofène a été réalisée dans une solution tampon phosphate USP de pH 6,8. Les particules troyennes libèrent 35% du principe actif encapsulé en 24 heures tandis que la libération des nanoparticules était confirmée en observant le milieu de libération par microscopie à transmission (Fig. 8). (résultats soumis à International Journal of Pharmaceutics)

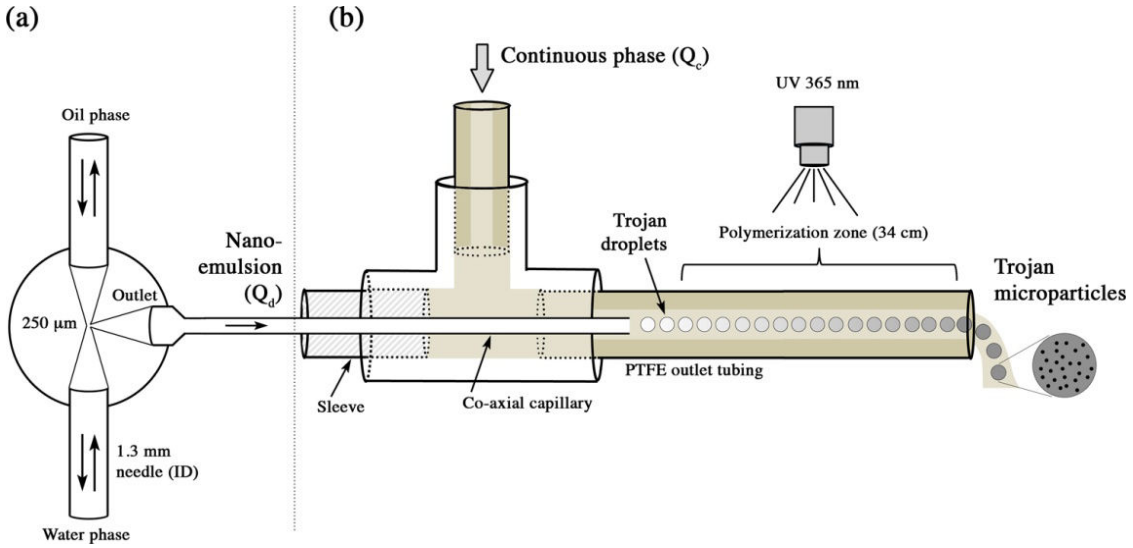

Fig. 8. Sytème microfluidique pour la production de microparticules: a) micromélangeur à flux élongationnel pour la production de nanoémulsion; b) générateur de goutte à un capillaire pour la production des microparticules troyenne.

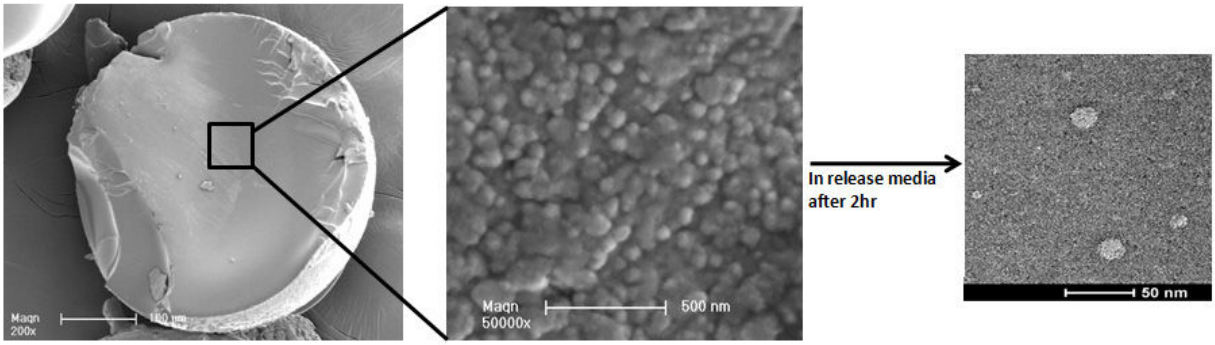

Fig. 9. Photographie SEM de la section transversale d'une microparticule troyenne chargée de nanoparticules d'acrylate d'éthyle chargées de kétoprofène; cliché TEM du milieu de dissolution après libération des nanoparticules.

6 Conclusion

Des dispositifs microfluidiques à capillaires ont été conçus, assemblés et utilisés avec succès afin de produire des vecteurs microparticulaires polymères multi-domaine monodisperses en taille. Les particules monocompartimentales ont libéré le principe actif encapsulé en fonction du rapport massique entre les monomères bifonctionnel et monofonctionnel. Dans des particules de type Janus, deux molécules sont libérées de manière contrôlée en 24 heures et leurs libérations furent modulées en fonction de la fraction massique d'agent réticulant. Des particules cœur-écorce pH-sensibles ont été développées pour un ciblage double de principes actifs. Des particules troyennes ont été développées avec succès par une nouvelle méthode semi-continue qui pourrait être employée à l'avenir pour assurer la libération de nanoparticles dans le tractus gastro-intestinal. De manière générale, il fut montré qu'un contrôle efficace des propriétés de libération des microparticules élaborées avait été obtenu. Il fut également démontré que ces propriétés pouvaient être facilement modulées simplement en ajustant les paramètres opératoires (débit des phases en présence, conception du dispositif microfluidique, etc…) ainsi que les paramètres de composition (densité de réticulation, nature et concentration des (co)monomères, etc.).

Introduction to thesis

This thesis aims at investigating the role and applications of microfluidic techniques in the area of drug delivery. Microfluidics is the science of manipulation and flow of small amounts of fluid in devices having at least one extremely small characteristic dimension (typically few hundreds of microns). This technique took birth in 1990s due to combine efforts of different scientific groups across the globe. In a short period of time, microfluidics has found many applications in a lot of scientific fields such as chemistry, chemical engineering, materials science, pharmaceutical and biology.

First chapter of this thesis will give a brief description of drug delivery and more specifically the role and technological issues related to microparticulate forms of delivery. Then scientific evidences will be provided to demonstrate that these issues can be solved using microfluidic techniques with examples in the production of size-tunable microspheres, microcapsules, microgels, core-shell particles etc. It turned out that most of the efforts were directed to the use of microchannel-based techniques for simple morphologies with little focus on capillary-based microfluidic devices and complex morphologies.

Second chapter appears in thesis under heading of "materials and methods". It will provide details of all the microfluidic devices used, chemicals, characterization techniques and procedures. While discussing the latter; great care will be taken to describe the minute details of the different steps which are necessary to obtain reproducible results.

Third chapter will be dedicated to the presentation, discussion and comment of the first set of experimental results obtained for plain and Janus particles. The first section deals with ketoprofen loaded microbeads of poly(ethyl acrylate-co-tripropyleneglycol diacrylate) prepared using a single capillary-based microfluidic device. Prepared microbeads will be characterized by FTIR, XRD and DSC for detection of possible interactions and state of ketoprofen. Effect of continuous to disperse phase flow rate ratio on droplet and particle size, encapsulation efficiency and drug release will be investigated. Later these microbeads will be prepared using different combination of mono- and bi-functional monomers to vary the matrix density and thus the release of ketoprofen. Second section deals with bi-compartmental morphology which will be prepared in a side-by-side capillary-based microfluidic device, a modified version of the previous single capillary-based microfluidic device. Poly(acrylamide)/poly(methyl acrylate) Janus particles will be developed with aim to

incorporate two different molecules (namely sodium fluorescein and ketoprofen) in a single microparticle which otherwise is a difficult task. This system will be characterized in terms of continuous to disperse phase flow rate ratio, monomer composition of the two compartments, crosslinker, surfactant nature and concentration, outlet tube diameter and UV intensity on particle size and morphology. *In vitro* studies on cell lines will be performed to ensure the cytocompatibility of Janus particles. Finally release studies will be carried out as a function of particle size, UV intensity and crosslinker concentration.

Fourth chapter is titled "Core-shell and Trojan particles". Core-shell particles are routinely prepared in non-microfluidic methods but are time consuming and involve multiple steps procedures. It has already been demonstrated by different groups that core-shell particles can be prepared in a single step with appropriate microfluidic devices. All the attempts focused on protection of core encapsulated active pharmaceutical agent. Here I will try to incorporate two different APIs in core and shell respectively for targeted dual delivery. A two co-axial capillaries-based microfluidic setup will be used to prepare pH sensitive poly(methyl acrylate) core - poly(acrylamide-co-carboxyethyl acrylate) shell particles. First this system will be characterized in terms of outer, middle and inner phases flow rate ratios and their effect on overall particle size, core diameter and shell thickness. Cytocompatibility of core-shell particles will be assessed on cell lines. Finally release studies will be carried out as a function of shell thickness and pH of release media. Second part of this chapter deals with the development of a continuous process to synthesize Trojan particles for oral delivery of nanoparticles. These nano-in-micro systems are routinely prepared in multiple steps. My microfluidic setup is based on nanoemulsion templating. First nanoemulsions of ethyl acrylate and methyl acrylate are produced in a continuous phase containing acrylamide, cross linker and photoinitiator using an elongational-flow micromixer. Then this micromixer is linked to a single capillary-based microfluidic device to generate polymerizable droplets and later fixed to get poly(acrylamide) Trojan particles embedded with ketoprofen loaded poly(ethyl acrylate) and poly(methyl acrylate) nanoparticles. Effect of operating parameters and surfactant concentration on size of nanodroplets will be investigated. Later on release of nanoparticles and ketoprofen in buffer solution will be demonstrated. Presence and release of nanoparticles will be confirmed by SEM and TEM.

Finally chapter 5 will highlight the most prominent results and establish a link between the experimental chapters. It will also present my vision of the overall outcome of microfluidics in drug delivery.

Chapter 6 will summarize the content of this PhD thesis and will also present the perspectives that can be foreseen in light of the work accomplished.

Chapter 1
Drug delivery and microfluidics

This chapter gives a brief overview of drug delivery, microencapsulation and role of microparticulate carrier system in drug delivery. Furthermore this chapter will explore current up to date literature to shed light on different microfluidic techniques and their role and importance in developing different drug loaded carriers.

This chapter is mainly composed of the following accepted review articles and book chapters.

- ✓ **Review articles**

  *1: Serra C.A., B. Cortese, **I.U. Khan**, N. Anton, M.H.J.M. de Croon, V. Hessel, T. Ono and T. Vandamme, Coupling microreaction technologies, polymer chemistry and processing to produce polymeric micro and nanoparticles with controlled size, morphology and composition, Macromol. React. Eng. (2013), 7 (9) 414-439 (Invited article)*

  *2: **I.U Khan**, C.A. Serra, N. Anton and T. Vandamme. Microfluidics: a focus on improved cancer targeted drug delivery systems: Journal of controlled release (2013), 172(3):1065-74*

  *3: **I.U Khan**, C.A. Serra, N. Anton and T. Vandamme.* Production of nanoparticle drug delivery systems with microfluidic tools*. Expert Opinion on Drug Delivery.* doi:10.1517/17425247.2015.974547

- ✓ **Book Chapters**

  *1: Serra, C. A., **Khan, I.U**., Cortese, B., de Croon, M. H. J. M., Hessel, V., Ono, T., Anton, N. and Vandamme, T. (2013). Microfluidic Production of Micro- and Nanoparticles. Encyclopedia of Polymer Science and Technologys*

  *2: **Khan, I.U**, Serra, C. A, Masood M.I, Shahzad Y, Vandamme T.F. Microfluidic-Conceived Drug-Loaded Micro-Carriers" (2014) Encyclopedia of Biomedical Polymers and Polymeric Biomaterials (Accepted)*

Contents

1.1 Drug delivery

Drug delivery is a general term that refers to the process or methods of administering active pharmaceutical ingredients (APIs) for mitigation or cure of a diseases condition. Mostly drugs are delivered with help of vehicle which influences the pharmacological activity of drugs, thus insuring safe, reliable and effective use of API. Drug delivery systems improves efficacy and safety by taking control of rate, time and place of release of drugs in the body (Perrie Y and Rades T, 2009) (Swarbrick J and JC, 2002). Drugs are delivered by different route of administration and their selection depends on the localization of disease in particular organ, desired effect, product availability and physical, biological and chemical barriers that a drug has to cross before reaching site of action (Swarbrick J and JC, 2002). Drugs may be administered directly to the disease organ or given systemically to target a diseased organ. They can be classified according to their physical state (Liquid, semisolid and solid dosage forms) or mechanism of release of drug (Immediate, modified release dosage forms) or route of administration (Perrie Y and Rades T, 2009). A classification of drug delivery systems based on anatomical routes is shown in Table 1.1.

Table 1.1: Classification of drug delivery systems based on route of administration

	Drug delivery Systems	**Route**
1	Gastrointestinal	Oral
		Rectal
2	Parenteral	Subcutaneous injection
		Intramuscular injection
		Intravenous injection
		Intra arterial injection
3	Transnasal	Nasal
4	Pulmonary	Administered via respiratory tract
5	Transdermal	Skin

Oral route of drug administration is one of most widely used route of administration for both conventional as well as for novel drug delivery systems. This route is preferred due ease of administration, safety and general acceptance by patients (Ranade, 1991; Thanki et al., 2013). While administering drug through oral route, several factors have to be kept in

mind like transit time in gastrointestinal tract (GIT) which varies in individuals depending on fed state and type of dosage form. pH of GIT varies in different parts that affects ionization of drug thus affecting their solubility and absorption (Perrie Y and Rades T, 2009). Oral route of administration also offers certain challenges like poor uptake of APIs, local irritation with nonsteroidal anti-inflammatory drugs (NSAIDs) (del Favero, 1986), certain APIs are rapidly metabolized in liver by first pass effect, some are chemically unstable at low pH of stomach and others are degraded by enzymes, low aqueous solubility and bioavailability for certain APIs, delivery of drug to target site and release of drug at therapeutically effective rate (Agrawal et al.; Mrsny, 2012; Perrie Y and Rades T, 2009). These factors had lead to development of sustained and controlled drug delivery system.

Different unit dosage forms like modified release tablets, osmotic pumps, gastro retentive drug delivery systems etc. are developed to meet above mentioned challenges. In comparison to single unit dosage form microparticulate form of drug delivery system are more advantages due to their small size and have tendency to accumulate in inflamed areas of the body (Mathew et al., 2007; Singh MN, 2010). These advantages can be summarized as follows:

- Less dependent on gastric emptying time
- Less inter and intra-subject variability
- Better distribution and less likely to cause local irritation
- Reduced risk of systemic toxicity
- Less chance of dose dumping
- Ease of administration
- Enhanced bioavailability
- Provides protection and stability to encapsulated materials, thus overall improving therapeutic effect of pharmaceuticals (Eiamtrakarn et al., 2002; Nokhodchi A, 2002; Singh MN, 2010).

1.2 Microparticles

Barrett K. Green (September 11, 1906 – August 29, 1997) was an American scientist and known as the inventor of microencapsulation. This technique is used to fabricate microparticles that involves modification of API properties by applying a thin coating of polymer to individual core materials in the range of 5 to 5000 µm (Bakan, 1986; Ranjha et al., 2009) while others say 1 to 1000 µm (Park and Yeo, 2006). This technique was first introduced in 1930 and since then is widely used in several drug delivery applications (Park and Yeo, 2006; Tran et al., 2011) for encapsulation of small drug molecules as well as macromolecules like nucleic acid, proteins and hormones (Hung et al., 2010), taste and odor masking, protection of drug, enhance solubility of poorly soluble drugs and cell encapsulation (Park and Yeo, 2006). Encapsulation provides several advantages like protection of drug from light, heat, surrounding media etc., improve absorption of drug, reduced side effects, sustained release, reduced administration frequency, patient compliance and comfort (Nokhodchi A, 2002; Tran et al., 2011). Therefore, microencapsulation is a promising alternative to address the current challenges of drug delivery.

1.2.1 Prerequisites for ideal microparticle carriers

All the materials used for the preparation of microparticles should ideally fulfill the following prerequisites:

- Duration of action should be longer
- Control release of contents
- Increase of therapeutic efficiency
- Protection of drug
- Reduction of toxicity
- Biocompatibility
- Sterilizability
- Drug stability
- Water solubility or dispersability

1.2.2 General methods to synthesize microparticles

Over the years numbers of microencapsulation techniques have been developed. These techniques are selected depending on the nature of the polymer, the drug, the intended use and duration of therapy. During preparation of microparticles, the choice of the optimal method has an uttermost importance for the efficient entrapment of the active substance (Hincal AA and S., 2005). Moreover, the method of preparation and its choice is also determined by some formulation and technology related factors as mentioned below:

- A single method never serves to incorporate all the drugs. It's important to understand the physicochemical properties of drug and find suitable polymer and encapsulation method (Park and Yeo, 2006).
- The particle size requirements for specific application may be different from others. In fact, volume of a sphere is proportional to the third power of the radius ($V=4/3\ \pi\ r^3$), while the surface area is proportional to the second power ($SA=4\ \pi\ r^2$). Hence, the surface area to volume ratio (SA/V) is inversely proportional to the radius. This has numerous effects on the nature and functioning of particles (Kohane, 2007). Increase in SA/V ratio increases surface exposed to media, diffusion of media and finally drug release. Size of microparticles determine the route administration for e.g. there is no upper limit for administration via oral route but reducing size from 7.2 µm to 2.1 µm doubles the gastrointestinal tract adsorption. For pulmonary route the particle size should be 3 µm whereas for subcutaneous, intramuscular, intravitreal administration route it should be between 10 to 250 µm. Size also influences distribution of drug thus influencing drug release properties. For instance in the microspheres with size of 10-20 µm drug distributes uniformly while if size is larger than 40 µm, hydrophilic drugs tends to distribute near the surface whereas hydrophobic one are shifted towards core. So, the size of microparticle should be such that it contains reasonable amount of active ingredient and comfortable for administration (Tran et al., 2011).
- Precise role of particle shape in drug delivery is not yet clear but degradation of microparticles to release drug, transport of particles in body regardless of mode of administration and their targeting ability is affected by their shape (Xu et al., 2009b). For e.g. disc shape red blood cells (10 µm) can easily pass through liver but for nanoparticles size should be at least 200 nm.

- The API should not be adversely affected by the encapsulation process. This stability issue is most common with protein or nucleic acid encapsulation, which are sensitive to various chemical and physical stresses (Park and Yeo, 2006). The instability issue brings about two major problems: a) incomplete and little release of the API 2) immunogenicity or toxicity by degraded drugs (van de Weert et al., 2000).
- Reproducibility of the release profile.
- There should be no toxic products associated with the final product.

Microencapsulation is used in pharmaceutical industry since 1960s for a) bad taste and odor masking, b) conversion of liquids to solids for ease of handling, c) protection of APIs from harsh surrounding environment, d) safe handling of toxic substances, e) preventing volatilization, f) separation of incompatible materials, g) help in dispersion of water insoluble substances, h) for sustained, controlled and targeted release and i) reduction of dose dumping (Burgess DJ and AJ, 2002).

Synthetic polymers are now materials of choice for the controlled release as well as targeted microparticulate carriers. The initial work was carried out on non-biodegradable polymers but later on the interest has shifted to the biodegradable polymers. Encapsulation methods can be broadly divided into three categories namely a) Chemical methods, b) Physico-chemical methods and c) Physico-mechanical methods (Table 1.2) (Jyothi et al., 2010; Tomaro-Duchesneau et al., 2013).

Table 1.2: Classification of microencapsulation techniques

Chemical	**Physico-chemical**	**Physico-mechanical**
Interfacial polymerization	Coacervation and phase separation	Spray drying and congealing
In situ polymerization	Sol-gel encapsulation	Fluid bed coating
Poly condensation	Supercritical fluid technology	Pan coating
Interfacial crosslinking	Ionotropic gelation	Vibrating nozzle/vibrating jet
		Solvent evaporation
		Solvent extraction

a) Chemical methods

Chemical methods are based on polymerization or polycondensation mechanisms that may be implemented in a variety of different ways to produce nanoparticles, composite membranes, microparticles and microcapsules. For instance, in case of

microcapsule with a liquid core, wall is formed in situ by polymerization between monomers present in the core and material's surface (e.g. interfacial polymerisation, in situ polymerization etc) (Abderrahmen et al., 2011).

b) Physico-chemical methods

Here formation of particles depends on phase separation in colloidal system. Usually a soluble shell material aggregates around the core material to form a solid wall (Abderrahmen et al., 2011).

c) Physico-mechanical methods

In these methods wall material is mechanically applied or condensed around the core material (Abderrahmen et al., 2011).

1.2.3 Limitations of traditional microencapsulation methods

In order to be an effective drug delivery system, microparticles should have high encapsulation efficiency, uniform size distribution, provide protection to drug during encapsulation and storage, ease of administration and controlled release (Tran et al., 2011). However, most of the microencapsulation methods developed to date failed to achieve aforementioned goals because of i) high particle size distribution with coefficient of distribution (CV) in the range of 10 to 50%, ii) batch to batch variation, iii) poor encapsulation efficiency (Xu et al., 2009b) and vi) initial burst release. Apart from these factors, there may be waste of materials and in general large amount of ingredients are used. Particle size distribution and batch to batch variation resulting from traditional methods can affect rate of microparticle degradation, stability of drug, drug loading and it's release rate (Sansdrap and Moës, 1993; Su et al., 2009). Furthermore, uneven particle size can promote aggregation and can cause clogging of needles during parenteral administration (Xu et al., 2009b). Poor encapsulation could be due to slow removal of solvent and slow solidification of particles (Yeo and Park, 2004) which allows the drug to escape in surrounding medium. Furthermore, small size particles also exhibit low encapsulation efficiency due to higher surface area/volume ratio, thus increasing chances for the drug to dissolve in continuous phase during solidification of droplet (Su et al., 2009). High initial burst release is attributed to un equal distribution of drug in particles (Fu et al., 2005). Thus it's obvious that particle size and distribution play an important role in controlling different

important aspects of drug loaded particles. So far, different methods like acoustic excitation, spinning oil film, replica molding etc are developed to control the droplet size and hence the size of microparticles. However, these techniques did not catch much attention due to their complexity and cost.

1.3 Microfluidics

Microfluidics is the discipline of science that deals with flow and manipulation of small amount of fluid retained in confined space either natural or synthetic with at least one dimension less than 1000 µm (Khan et al., 2013b; Whitesides, 2006) and on the other hand if one dimension is in nano range it is called nanofluidics (Eijkel and Berg, 2005) as elaborated in figure 1.1.

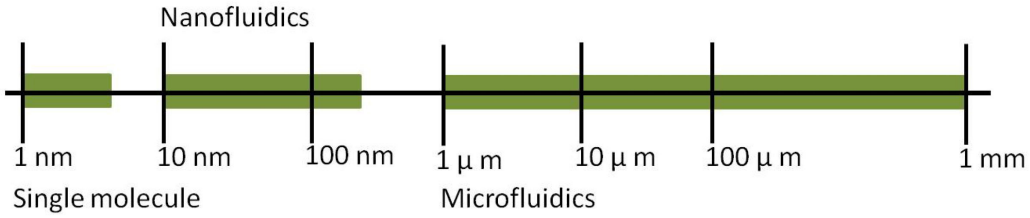

Figure 1.1: Typical dimensions of micro- and nanofluidics

Microfluidics is a newly developing branch of science and has ability to address different areas of research like analysis, electronics, physics, biomedicine, pharmaceutical sciences etc. This field of research is still at its infancy and there is strong urge to understand basic principles before applying it in any area of research. It's attraction in multiple areas of research lies in microdimension where fluid behavior differs from macroscale i.e. laminar in microfluidics and turbulent at macroscale due to low and high Reynolds numbers respectively.

Birth of microfluidics can be traced way back to 1950 where it appeared for the first time in different chromatographic systems. During that period different scientist like Golay's (Golay, 1957) theoretical work on gas chromatography and Van Deemter (van Deemter et al., 1956) on liquid chromatography showed that by reducing the diameter of open column and packed column particle size could result in improve performance. After that people started fabricating column in micrometer range. At the same time capillary electrophoresis

was under development for separation of biomolecules, here too small size capillaries were found to improve separation process (Tian and Finehout, 2009).

First microfluidic system appeared in 1979, where Terry *et al.* from Stanford University fabricated a miniature gas chromatograph air analyzer on a silicon wafer (Terry et al., 1979) as shown in figure 1.2. Afterwards scientist continued to develop miniaturized system with improved performance. But real boost to microfluidic field occurs in 1990s due to combined effort of several researchers. They focused on capillary electrophoresis which is a powerful technique for DNA sequencing, forensic analysis, *polymerase chain reaction* etc. and is faster than gel electrophoresis. However, this technique is also limited by single sample analysis at time (Woolley and Mathies, 1994). Although this problem could be resolved by miniaturized systems where several samples are analyzed rapidly in parallel.

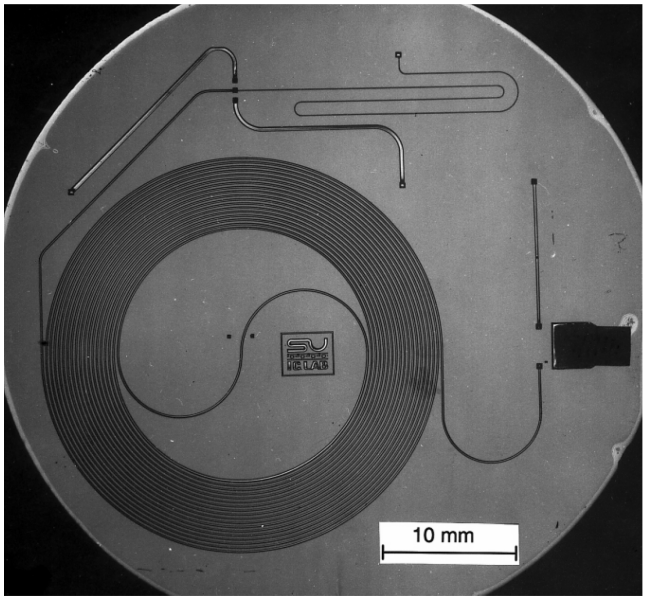

Figure 1.2: Gas chromatograph air analyzer developed by Terry et al.(Terry et al., 1979).

Manz *et al.* in 1992 showed for first time on chip capillary electrophoresis system (Manz et al., 1992) and in the same year Mathies *et al.* designed a array of capillaries for DNA electrophoresis that provided a new method for high-throuput sequencing of DNA (Mathies and Huang, 1992). Then in 1993 Harrison *et al.* fabricated a micro- capillary electrophoresis system on glass for separation of amino acid (Harrison DJ et al., 1993) and in 1994 Woolley and Mathies miniaturized a microfluidic capillary gel electrophoresis system for DNA analysis (Woolley and Mathies, 1994). This boom was further confirmed when we

look at Scopus data. In between 1991 and 2014 one can find 29,959 and 26,447 documents by searching word “microfluidic” and “microfluidics” respectively. One further analysis, only 508 documents are found in the area of “pharmacolgy, toxicology and pharmaceutics” (Figure 1.3 and 1.4). It’s necessary to understand why from just 2 documents in 1991, the number raised to 29,959 in 2014. In following section I will briefly outline advantages offered by miniaturization over macroscale devices that drive researchers to use microfluidics.

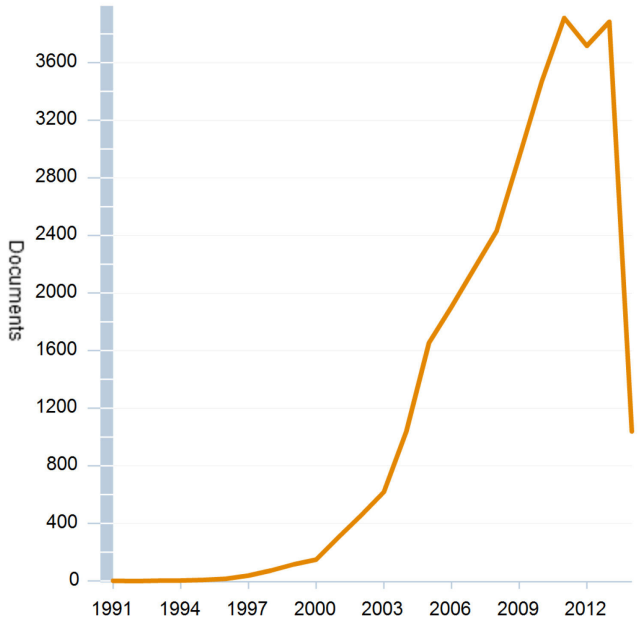

Figure 1.3: Scopus analysis of word “microfluidic” shows real boom in this area.

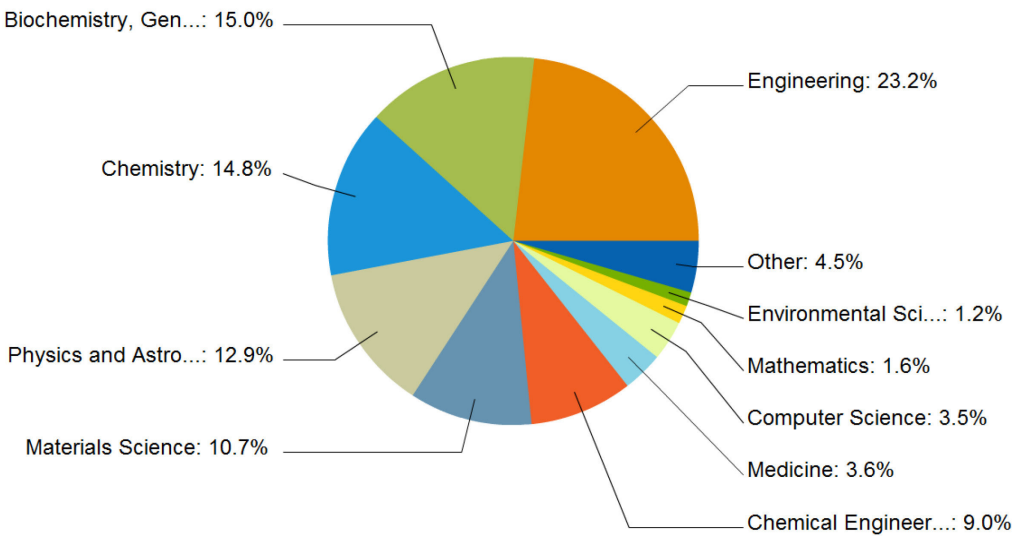

Figure 1.4: Subject wise analysis of data shows biggest chunk of documents comes from engineering flowed by biochemistry and physics respectively.

1.3.1 Advantages and disadvantages of microfluidic tools

Microdimension of microfluidic tools provides different advantages that could be summarized as follows 1) consumption of small quantity of reagents normally 10^2 to 10^3 times less than conventional methods thus addressing safety (anticancer drugs, biological and radioactive) and economic issues; 2) improved mass and heat transfer due large surface; 3) provides precise control over flow, i.e. laminar flow due to small Reynolds number where viscous forces are dominant; 4) continuous flow operations; 5) reduces mixing time; 6) low power consumption; 7) rapidly produces libraries of different materials by changing composition and fluid phase flow rate; 8) production of particles where coefficient of variation is less than 5% and high encapsulation efficiency; 9) miniaturization allows portability and on spot analysis due integration and low power consumption; 10) parallelization on microfluidic chips allows high throughput and multiple analysis at a time; 11) faster analysis and quick response due to shorter diffusion distances and 12) allows rapid screening of nanoparticles during different phases of clinical development (Khan et al., 2013b; Serra et al., 2013; Tian and Finehout, 2009; Valencia et al., 2012). Apart from advantages it has certain disadvantages for e.g. it's a new technology and not fully understood yet. Dominance of surface forces (surface tension, electrical, van der Waals, and surface roughness) at micro scale makes certain reactions more complex than macroscale. In microfluidics as signal drop is generated at time, so emulsification is time taking process and per hour production is low. Although several attempts are made by different group to overcome this problem by parallelization of channels on same chip (Serra et al., 2013).

1.3.2 Microfluidic devices

There are two most commonly used devices for production of particles namely microchannels or microcapillaries as shown in figure 1.5.

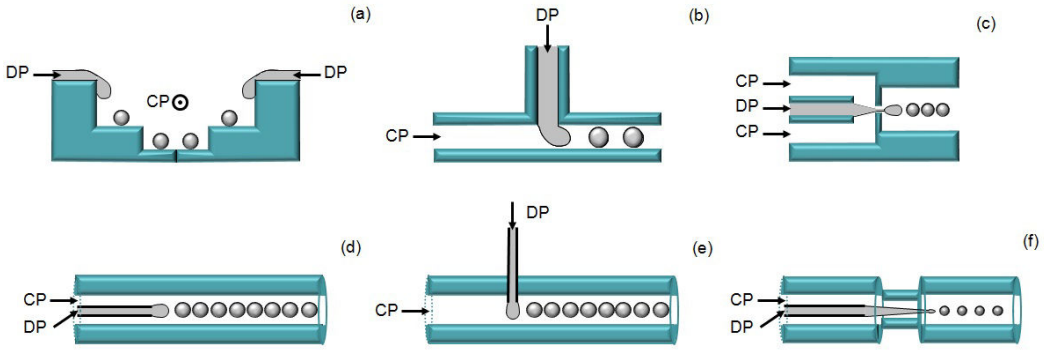

Figure 1.5: Graphic presentation of most commonly used microfluidic devices. Microchannel-based devices: a) terrace-like device, b) T-junction device, c) flow-focusing device. Capillary-based devices: d) co-flow device, e) cross-flow device, f) flow focusing device. CP and DP represent continuous and dispersed phase respectively.

Microchannel-based devices are fabricated by different microfabrication processes like micromilling, micromachining, lithography and mold replication using range of materials such as metal, glass, silicon or polymer. In comparison capillary based systems are developed from cheap commercially available parts but are as much efficient as microchannel-based devices (Khan et al., 2013a). Fabrication of microchannel based systems is costly and time taking but are easier to manipulate and can be paralleled to achieve large yields. Capillary based system can be fabricated in less time and can be operated in aggressive chemical conditions, but some time it is difficult to align the capillaries and place them in parallel (Wang et al., 2011). Further details about these systems can be read from review articles published by Serra *et al*. (Serra and Chang, 2008), Wang *et al*. (Wang et al., 2011), Zhao *et al*. (Zhao and Middelberg, 2011) and Zhao *et al*. (Zhao, 2013).

In microfluidic one can generate multiple or single emulsions. For single emulsions, dispersed phase is injected into another immiscible or partially immiscible liquid phase. Droplets are sheared off at the junction where the two phases meet by competition between the shear stress imposed by the flow of the continuous phase and the interfacial force. Bigger droplets are formed if large interfacial tension exists between continuous and dispersed phase and vice versa. On other hand smaller droplets are formed with higher shear stress and vice versa. Same principle is involved in generation of multiple emulsions except that device is different from one used for single emulsion and are broadly categorized as two-step and one-step methods (Zhao, 2013).

1.3.3 Microfluidic conceived drug loaded microcarriers

Microfluidic production of microparticles can be listed under three categories: Droplet- and multiphase-based methods, Photolithography based methods and Supra-particle synthesis by assembly of colloids (Dendukuri and Doyel, 2009). In first category droplets are solidified downstream by chemical or physical means like polycondensation, ionic crosslinking, radical polymerization, thermosetting, solvent evaporation or extraction

(Khan et al., 2013a) as demonstrated in figure 1.6. In photolithographic technique photo-polymerizable solution flowing within a microchannel is irradiated with UV light through a patterned mask of desirable shape, placed in the objective of a microscope (Dendukuri and Doyel, 2009; Serra and Chang, 2008). The last category involves manipulation or alteration of preexisting microparticles into more complex structures or ''supraparticles'' with possibility to introduce 3D properties but is not commonly used (Dendukuri and Doyel, 2009). Microparticles of different morphologies are developed to use them as drug carriers. Each one has their own pros and cons. In following section I will briefly discuss synthesis, characterization and application of drug loaded morphologies ranging from simple to complex one.

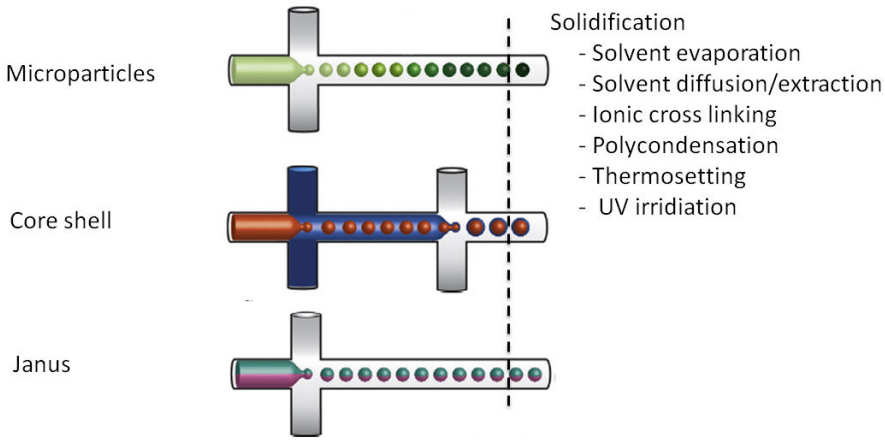

Figure 1.6: Figure represents the formation of different morphologies and subsequent solidification step by different approaches.

1.3.3.1 Microgels

Hydrogels are water swollen crosslinked polymeric structures. Depending upon the network composition they can undergo abrupt volume changes in response to variations in surroundings such as pH, temperature, ionic strength, presence of specific compounds (Hussain A, 2011) or electric field; and release the entrapped ingredients in their matrix like drugs, proteins, cells and functional nanoparticles (Wang et al., 2011). Hydrogels are classified by size as macrogels and microgels. Macrogels are bulk gels ranging anywhere from a millimeter to a few centimeter while colloidally stable hydrogel particles that ranges from 100 nm to several hundred microns in size are called microgels (Das M, 2008). In microfluidic device synthesis of hydrogels requires two steps, i.e. generation of precursor droplets and solidification. Solidification is carried out either by photopolymerization, heat

driven polymerization and physical methods like evaporation (Wang et al., 2011). In recent years microgels are finding reasonable interest in drug delivery due to their biocompatibility and drug entrapment in polymeric network (De Geest et al., 2005). Activity of sensitive compounds with low or high molecular weights can be significantly prolonged in biological environment by encapsulating them in microgels. Secondly their performance and application usually depend upon their size and shape, just like many living micro-systems such as red blood cells that holds a particular shape for a specific application (Hu Y, 2012). In following section we will highlight how easily particle size, shape, composition, targeting and release behavior is tuned by changing microfluidic process parameters.

1.3.3.1.1 Non targeted Microgels

To get biodegradable carriers for protein drugs, De Geest and coworkers synthesized dextran-hydroxyethyl methacrylate (dex-HEMA) microgels in polydimethylsiloxane (PDMS) microchannels. Aqueous phase containing 30% w/w dex-HEMA and photoinitiator are emulsified by a mineral oil and cured downstream by UV irradiation. It was found that mineral oil alone was not able to prevent the coalescence of droplets so they added 4% v/v of nonionic surfactant (ABIL EM-90). They obtained 10 µm sized microgels at low Reynolds number while at higher rates coalescence occurred.

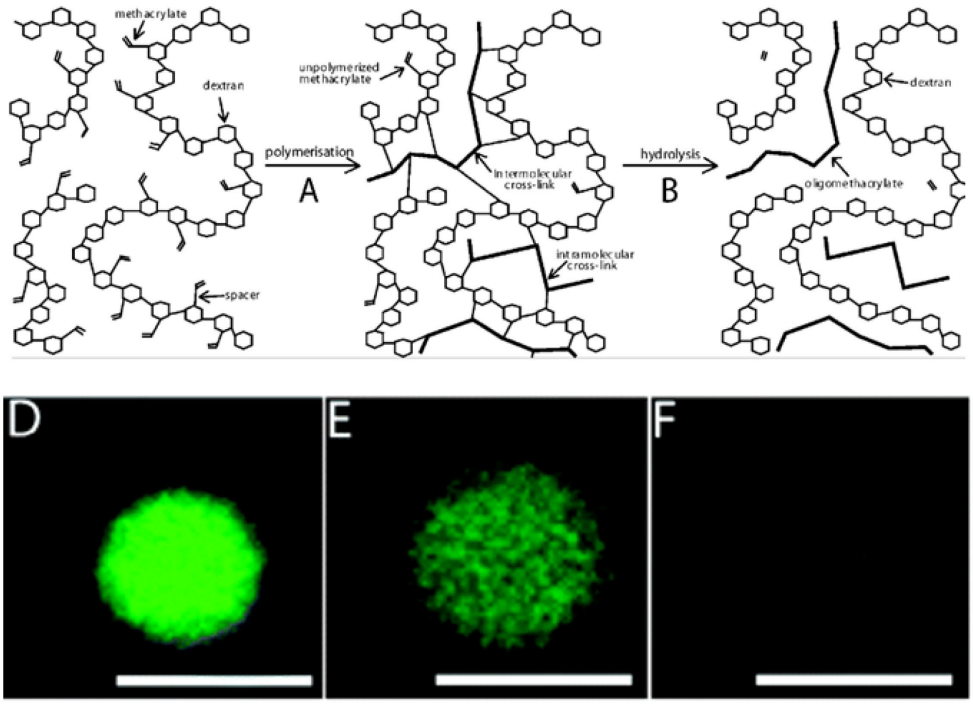

Figure 1.7: Schematic and confocal microscopic images showing degradation of carbonate ester group by hydrolysis which connect polymerized methacrylate and dextran chain and subsequent release of fluorescein isothiocyanate (FITC) labeled BSA. Scale bars represent 10µm (De Geest et al., 2005).

Fluorescein labeled bovine serum albumin (BSA) was encapsulated with one 100% efficiency. Confocal microscopic images of dex-HEMA microgels shows entrapment and release of fluorescein labeled BSA. These microgels sterically entrap BSA and when they are degrade by hydrolysis of carbonate ester group which connects dextran and methacrylate chain , pore size increases thus facilitating the release of BSA (Figure 1.7) (De Geest et al., 2005).

In another study Hu *et al*. fabricated alginate microgels with varied shapes, such as spherical, mushroom or pear like, by combining microfluidics and external ionic crosslinking. They obtained this by simply changing viscosity of the gelation bath, collecting height and interfacial tension. Spherical particles were obtained with low viscosity of gelation bath and combination of cross linkers (Ba^{+2} & $Ca^{+}2$). They demonstrated release behavior of iopamidol varied significantly with differences in morphologies (Figure 1.8) (Hu Y, 2012).

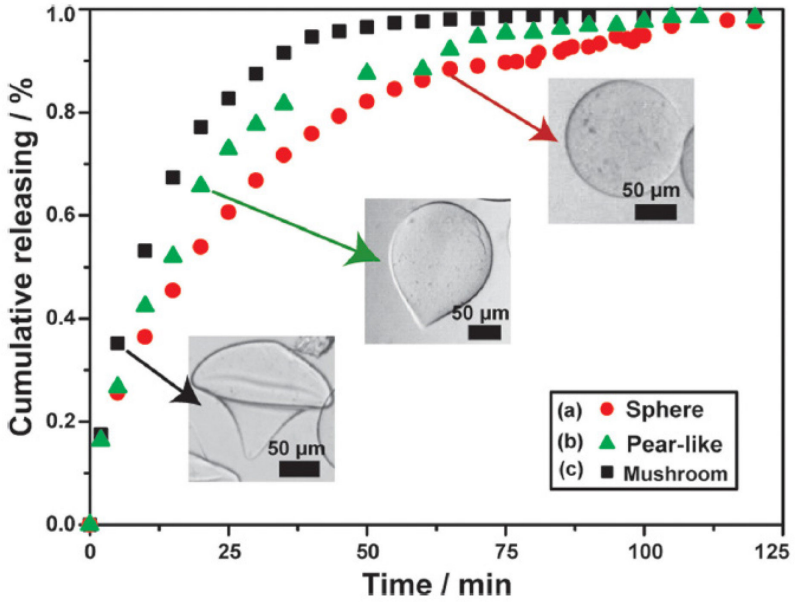

Figure 1.8: Iopamidol release behavior from spherical, pear and mushroom like alginate microgels. This variation was attributed to difference of surface area, crosslinking degree and uniformity of particles (Hu Y, 2012).

1.3.3.1.2 Targeted Microgels

Design of controlled release and site-specific drug delivery has attracted great interest of scientific community from the chemical, materials, and especially in pharmaceutical sciences. Incorporation of these features dramatically improves drug efficacy and reduce the side effects (Zhang et al., 2006).

In traditional microencapsulation methods number of successful attempts are made to develop targeted microspheres, microcapsules, microgels and other carriers but only limited attempts are made to develop targeted systems. Same was case in microfluidic technique as well. In order to get targeted microgels for protein delivery in microfluidics, Fang *et al*. used pectin (P) or alginate (A) or mixture of alginate and carboxymethylcellulose (CMC). Pectin and alginate contain carboxylic group in their structure thus making them pH sensitive. The rapid chaotic mixing of polymers and their ionotropic gelation with crosslinking agent was achieved in winding flow-focusing channel type device, using mineral oil as continuous phase. Particles are collected in buffer solution with different concentration of $CaCl_2$ and $FeCl_3$ for completion of gelation. Microparticles obtained lies in the range of 40-100 µm with CV less than 5%.

Pectin and alginate microgels do not show appreciable swelling at pH 1.2 and 5 but swelling rate was improved with addition of CMC. In bi-polymer particles, alginate crosslinked by calcium ion act as the backbone and CMC contributes to pore formation by electrostatic repulsion from the highly hydrophilic carboxyl groups in their structure. It was further observed that ferric ion as an additional crosslinking agent considerably increased the swelling and stability which are attributed to stable electrostatic interaction between ferric ion and hydrophilic OH and COOH in bi-polymer particles of CMC and alginate. Stability was also affected by mixing method of bi-polymers.

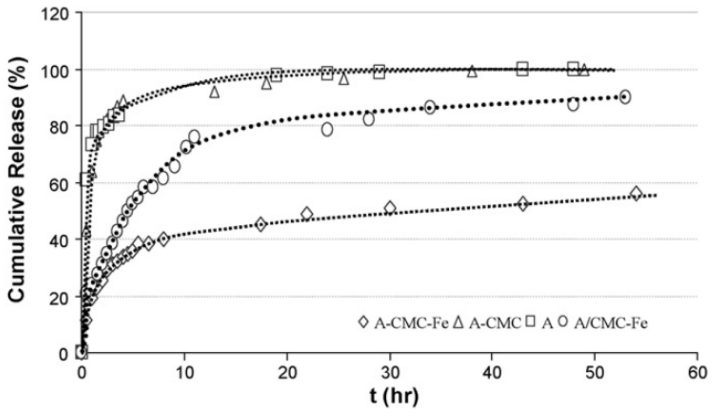

Figure 1.9: *In vitro* release studies showing rapid and sustained release properties at pH 7.4 whereas temperature was maintained at 37°C (Fang and Cathala, 2011).

In vitro BSA release profile demonstrated that microparticles crosslinked with both calcium and ferric ions induced a significant delayed release properties as compared to the ones crosslinked solely with calcium ion which was attributed to slow degradation (Fang and Cathala, 2011). Hydrogel particles are proving to be important drug delivery system for range of drugs and can be used for immediate, controlled and targeted release and their fabrication by microfluidic methods could achieve better control over their size, shape, targeting and release properties.

1.3.3.2 Microcapsules

Microcapsules are reservoir type systems with regular or irregular shapes that contain a well defined core and envelope. The core consists either in a hollow cavity filled with solid particles or liquid or gas phases surrounded by a polymeric envelope (Obeidat, 2009). Recently a considerable interest has been directed towards the development of polymeric microcapsules which have potentials in drug and enzyme delivery (Abraham et al., 2006). Microcapsules are manufactured by different techniques that are broadly categorized as physical and chemical routes. These traditional methods have limitations like a poor control of the particle size, encapsulation efficiency, waste of material, huge consumption of energy etc. which can be overcome by microfluidic methods. In microfluidics, microcapsules are fabricated by droplet or double emulsion templates which are solidified by solvent evaporation, solvent extraction, layer by layer deposition and supramolecular host guest chemistry (Zhao et al., 2006).

1.3.3.2.1 Non Targeted microcapsules

Huang *et al.* fabricated monodispersed genipin-gelatin microcapsules in a poly(methyl methacrylate) (PMMA) based cross-junction microchannel-based setup (Figure 1.10). The pregel solution of gelatin (1% w/v), genipin (2% w/v) and *5-Fluorouracil* (1 mg/mL) was initially compressed to arrow shape and then to droplets by sunflower seed oil in cross-flow channels. The final product was obtained by collecting emulsion of pregel solution in 10% w/v genipin aqueous solution that acted as crosslinker to form water insoluble genipin-

gelatin microcapsules (Figure 1.10). They were able to increase the droplet size by keeping oil phase flow rate constant and increasing the flow rate of aqueous phase. All the formulations showed similar degree of crosslinking and swelling behavior.

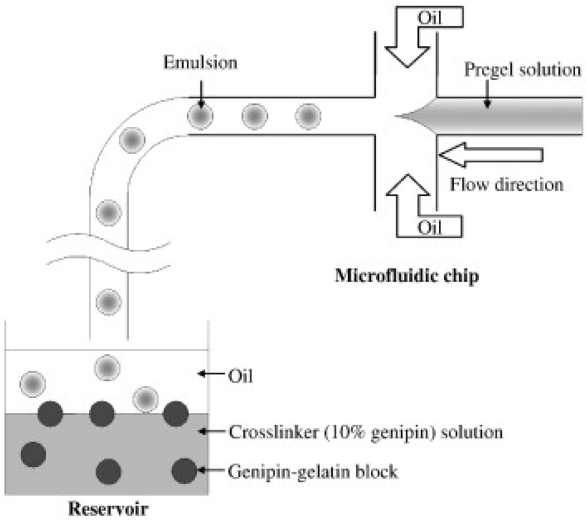

Figure 1.10: Emulsification of pregel solution and crosslinking of genipin-gelatin in reservoir container (Huang et al., 2009).

Release rate of encapsulated 5-FU become faster with a decrease in microcapsule size due to a reduction in the diffusion path and an increased surface area per volume unit. So, particles with diameter of 124 µm showed sustained release behavior for three hours and those above 280 µm sustained release behavior for 12h. Higuchi kinetics reveals that all formulations release the drug by diffusion (Huang et al., 2009).

Abraham *et al.* developed spherical polymeric microcapsules encapsulating congo red dye in crossed network microchannels of silicon with glass pyrex window for visualization. They synthesized poly(styrene-b-methylmethacrylate) by atom transfer radical polymerization (ATRP) polymerization and estimated their molecular weight and polydispersity index (PDI) by gel permeation chromatography (GPC). Then prepolymer in dichloromethane (DCM) was emulsified by continuous phase containing 3% PVA where supramolecular self assembly of block copolymer leads to formation of microcapsules (Figure 1.11). Obtained droplets were collected on hydrophilic silicon wafers and dried slowly to evaporate the solvent during which their size reduced from 80 to 40 µm. Microcapsules have hollow cavities with porous surface as confirmed by SEM after removing a part of the membrane by plasma ashing (Figure 1.12)

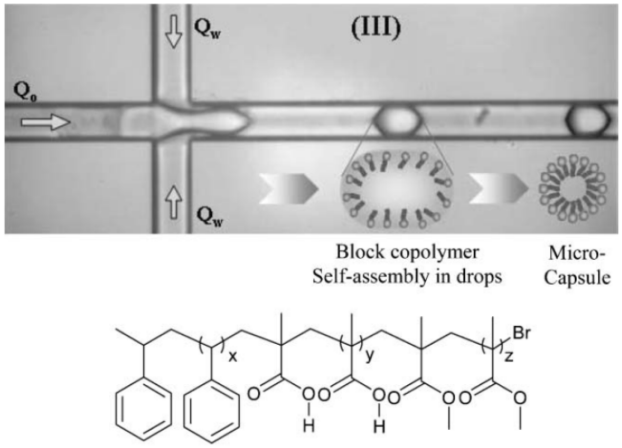

Figure 1.11: Self assembly of block copolymer in microchannels which leads to formation of microcapsules. Amphiphilic poly(styrene-b-methylmethacrylate) block copolymer is also shown (Abraham et al., 2006) which do not ionizes thus does not swells.

Congo red dye was loaded by immersing microcapsules in 30 ml of distilled water containing 6.5 $*10^{-6}$ g/cc congo red dye. Release studies were carried out at pH 7 or 7.8 and different temperatures. Release was faster in first few hours and cumulative drug release increases with increase of pH and temperature (Figure 1.12).

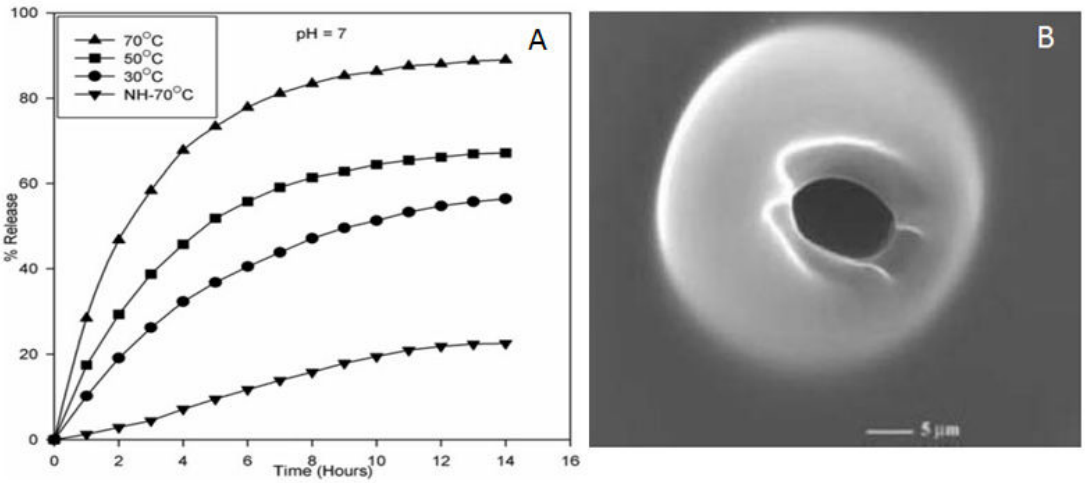

Figure 1.12: A) In vitro studies showing variation in release as function of temperature at pH 7 from hydrolyzed microcapsules. The hydrolysis of PMMA block was carried out using 20% diluted sulfuric acid solution to get hydrophilic methacrylic acid groups. For comparison purpose, the release of dye from non hydrolyzed polymer microcapsule is also shown (▼) at 70 °C. B) hollow cavity of microcapsule can be seen after removing a part of the membrane by plasma ashing (Abraham et al., 2006).

This release behavior was due to combine effect of presence of ionizable groups in block copolymer which ionizes to higher extent at higher pH and leads to higher swelling and higher drug release. Secondly, stability of dye enhanced at higher pH due to its ionization which results in increased diffusion. Furthermore, higher temperature also enhances ionization and helps in faster release (Abraham et al., 2006).

Liquid core poly(L-Lactic Acid) (PLLA) microcapsules were developed by Lensen and coworkers by utilizing flow focusing microchannels. Discontinuous phase (polymer solution in DCM with dodecane 3% by volume, dye, oil-red-O as model drug) was broken into droplets by 1% by weight of PVA aqueous solution. Droplets were collected in double distilled water and left until DCM evaporated completely. As the DCM evaporates floating dodecane filled capsules were obtained. This was because dodecane is a non solvent of PLLA which results in separation between polymer and dodecane. Dodecane was subsequently removed by lyophlization and DSC results confirmed absence of dodecane. They observed a broad size distribution at low flow rates of the continuous phase (dispersed phase constant) due to satellite formation. At optimal flow rate of continuous phase (35 ml/hr) capsules with average diameter of 50 µm were obtained.

At higher speed, capsules with hole on one side were observed which was due to partial engulfment of liquid core by polymer rich droplets. These droplets were formed by phase separation within emulsion droplet when good solvent evaporates (DCM). These polymer rich droplets then move to interface and engulf original droplets. Moreover, it was only possible to make core-shell microcapsules with high molecular weight PLLA. SEM of crushed lyophilized microcapsules revealed a wall thickness of 3 µm. Release studies showed a large release in first hour due to combination of release of drug from shell (entrapped during encapsulation) and core (pore formation in shell due to hydrolysis) (Lensen et al., 2010).

1.3.3.2.2 Targeted microcapsules

Microcapsules response to surrounding environmental stimuli like pH, temperature, glucose, magnetic field are used in therapeutics, biotechnology, drug delivery, biosensors etc. where they change their physical, chemical or colloidal properties to trigger the release of encapsulated material. Cancer cells utilizes more sugar than normal cell to meet the

nutritional requirements for fast growth (Khan et al., 2013b). So, glucose responsive microcapsule could be used for treatment of diabetes and cancer. Zhang *et al.* used double emulsification in microfluidic device to get glucose responsive hydrogel microcapsules of poly(N-isopropylacrylamide-co-3-aminophenylboronic acid-co-acrylic acid) (p(NIPAM-co-AAPBA-co-AAc)). In shell the PNIPAM segment was thermo-responsive, AAPBA moiety act as glucose-responsive component and hydrophilic AAc serves to adjust the volume phase transition temperature of the shell (Zhang et al., 2013) which was lowered by hydrophobic AAPBA. Yet in some other studies microcapsules responsive to magnetic field was fabricated by Liao *et al.* and Yang *et al*. Liao *et al.* fabricated microcapsules in 3D PDMS double emulsification devices. Walls of microcapsules are composed of either poly(L-lactic acid) or trilaurin or phosphocholine. Incorporation of γ-Fe_2O_3 nanoparticles in microcapsules make them responsive to electromagnetic waves (Liao and Su, 2010). Yang *et al.* fabricated smart microcapsules of polycaprolactone (PCL) by incorporating tamoxifen, Cadmium telluride (CdTe) quantum dots (QDs) and Fe_3O_4 nanoparticles in cross junction microchannels. They generated droplets having relative standard deviation less than 4% but showed a mean 16% reduction in the size after removal of chloroform. Fluorescent microscopic studies confirms the incorporation of CdTe quantum dots while hysteresis loop obtained by super conducting quantum interference device (SQUID) magnetometer and separation of these microcapsules in ethanol under the influence of magnetic force demonstrates magnetic properties (Figure 1.13).

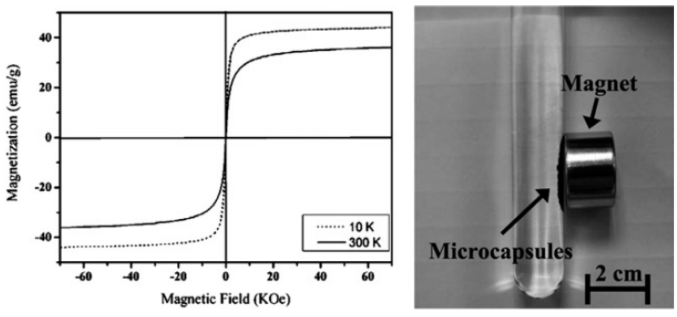

Figure 1.13: Response of microcapsules to magnetic field (Yang et al., 2009).

These microcapsules show biphasic release providing loading and maintenance dose over two days (10% burst release, 78% in 24h and 100% in two days). There size lies in the range of 50 to 200 µm and could be used for combined magnetic targeting, fluorescent imaging and drug release (Yang et al., 2009). To conclude this part, microcapsules for drug release

properties were fabricated in microchannel based microfluidic systems using different approaches like solvent evaporation, ATRP polymerization and crosslinking methods. These microcapsules were monodispersed and showed sustained or targeted release of active ingredients while in some cases was used for imaging purpose.

1.3.3.3 Microparticles

Rapid development of new and potent molecules necessitates the development of more effective and safer drug delivery systems. Controlled release systems are developed to address different problems raised with traditional systems. Microspheres or microparticles are one of the controlled release system and defined as solid, approximately spherical particles ranging from 1 to 1000 µm (Burgess DJ and AJ, 2002). They are homogeneous structures made up of one or more miscible polymers in which API is dispersed throughout the matrix. They are widely used as drug carriers for controlled and targeted drug release. Administration of drugs in the form of microspheres usually improves the treatment by providing the localization of the active substance at the site of action and by prolonging release of drugs. Furthermore, entrapped sensitive drugs such as peptides and proteins may be protected against chemical and enzymatic degradation. Finally, these particles insure patient comfort and compliance by reducing dosing frequency. So far, in microfluidics mostly poly(lactic-co-glycolic acid) (PLGA) and chitosan are frequently used to fabricate drug loaded microparticles and will be discussed in different sections.

1.3.3.3 1 PLGA microparticles

PLGA is widely used as drug delivery carrier and as scaffolds for tissue engineering. It is a Food and drug administration approved biodegradable, biocompatible polymer having long clinical experience, favorable degradation characteristics and has been extensively used to deliver drugs, proteins and macromolecules such as DNA, RNA and peptides (Makadia HK and SJ., 2011). So PLGA microspheres are being considered as the pharmaceutical products of the future (Hincal AA and S., 2005). In microfluidics also, researchers focused on development of PLGA particles for different applications. For instance Xu *et al*. compared the PLGA microparticles obtained by conventional emulsification process and microfluidic flow-focusing technique. In the later, bupivacaine and PLGA in dichloromethane were broken into droplets by 1% aqueous solution of PVA and finally DCM was removed by rotary evaporator.

The obtained particles showed a polydispersity index of 3.9%. Authors varied the size of particles by changing the flow rates of the continuous phase and found a threshold value at which system forms co laminar flow and no droplets. Flow focused based particles showed more controlled release and small burst release than the particles formed with conventional single emulsion technique. It is due to monodispersity and uniform distribution of drug within the particles, while in conventional method more drug is accumulated on surface. This is confirmed by treating microparticles with 1M aqueous HCl solution. No prominent surface changes were observed in microparticles with flow-focusing method while several pores could be seen on the surface of particles formed with emulsification method due to rich drug domains at or near the surface of particles (Figure 1.14) (Xu et al., 2009b).

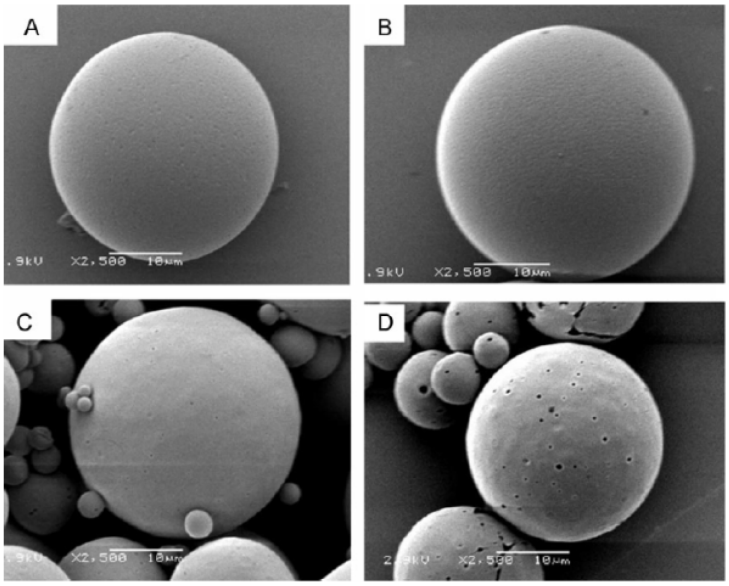

Figure 1.14: Microparticles before (A, C) and after (B, D) treatment with 1 M HCl for 1h. Particles fabricated using microfluidic device are (A, B) and particles prepared from conventional single emulsion method are (C, D) (Xu et al., 2009b).

Hung and coworkers were able to encapsulate fluorescein in PLGA microparticles and nanoparticles by microfluidics for its potential use as ocular drug delivery system. For microparticles they used flow focusing microchannels with solvent evaporation (Figure 1.15). They obtained particles ranging from 3 to 30 µm with a narrow size distribution (CV<3%) and showed an increase in the size of microparticles with increasing concentration of polymer in solvent (Hung et al., 2010).

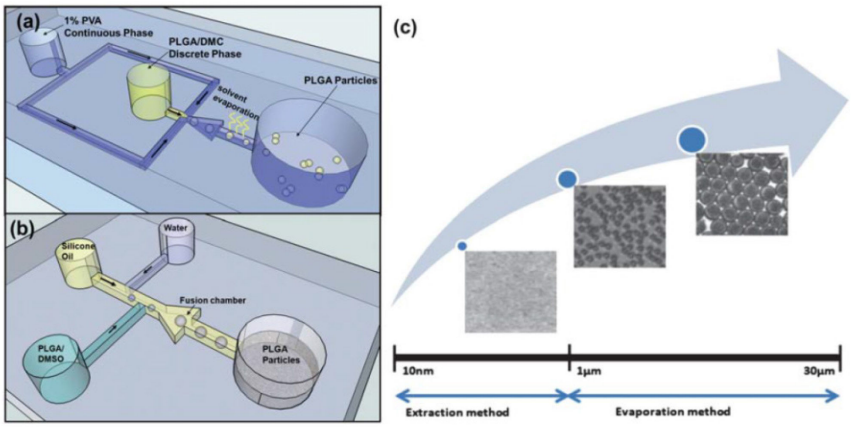

Figure 1.15: Schematic drawing for solvent evaporation for microparticles (a) and solvent extraction technique for PLGA nanoparticles (b). Particles with different sizes can be obtained with both methods (c) (Hung et al., 2010).

Holgado and coworkers compared lidocaine loaded PLGA microparticles by solvent evaporation and flow focusing device as shown in figure 1.16.

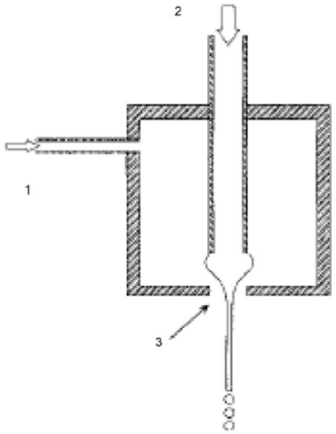

Figure 1.16: Flow-focusing setup for the synthesis of lidocaine loaded PLGA microparticles: continuous (1) dispersed phase (2) and flow focused area (3) (Holgado et al., 2008).

Microparticles obtained by solvent evaporation method were spherical with broad size distribution while with flow-focusing they were spherical with narrow size distribution. Furthermore, no effect of drug concentration and polymer type on morphology was observed. DSC studies showed absence of drug polymer interaction and distribution of drug at molecular level. Drug loading in microparticles increased with increased concentration of drug in solvent. It was further observed that microparticles formed with PLGA carrying free carboxylic end groups have higher drug loading due to hydrogen bonding between drug and

this free end group. Finally, it was observed that flow-focusing method yielded microparticles with higher drug loading than solvent evaporation method. This was because particles formed by flow-focusing were more hydrophobic as observed by surface thermodynamic studies and secondly loss of drug during flow focusing was negligible. Lidocaine release from microparticles was biphasic due to combination of diffusion and degradation process. In all the cases higher drug release was observed from microparticles formed with solvent evaporation process. This was due to formation of more hydrophobic microparticles by flow-focusing method which ultimately decreases degradation rate and therefore drug release (Holgado et al., 2008).

Low temperature co-fired ceramics (LTCC) technique can be a good option for fabrication of microfluidic devices and offers several advantages over other microfabrication technologies. Ribeiro-Costa and co workers utilized LTCC passive micromixers for protein loaded PLGA microsphere. They constructed eight different kinds of micromixers (Figure 1.17).

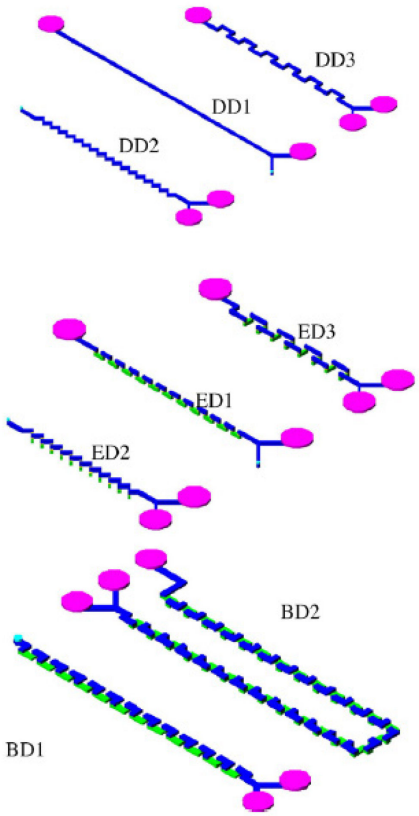

Figure 1.17: LTCC micromixers for synthesis of protein loaded PLGA microspheres. Different 2D and 3D geometries namely DD1 (straight channel micromixer), DD2 (Zig-zag 2D

micromixer), DD3 (Square-wave 2D-XY micromixer), ED2 (Zig-zag 3D micromixer), ED1 (Square-wave 3D-XZ micromixer) with similar dimensions. Two 3D mixers includes BD1 and BD2 (Serpentine 3D micromixer) with channel of 77 and 172 mm respectively (Ribeiro-Costa et al., 2009).

They prepared microspheres by conventional w/o/w solvent evaporation method and then by using micromixers. In the latter case, organic phase consisted of w/o emulsion of aqueous solution of BSA in PLGA dissolved in DCM. 3% PVA solution was injected through one of inlet of mixer and organic phase through the second inlet. Obtained droplets were stirred at 500 rpm for 4h to evaporate DCM. All the microspheres are spherical with narrow size distribution which was little influenced by geometry of micromixer. Encapsulation efficiency of microspheres produced by LTCC micromixer ranges from 61 to 75% suggesting these micromixers are suitable tools for the continuous production of drug loaded carriers (Ribeiro-Costa et al., 2009).

In some cases constant release of active ingredient is not required due to multiple factors like high metabolism, short half life, a limited absorption window or development of receptor tolerance. Hence, in conventional methods different strategies were used to improve the drug release from microparticles like pore forming agents, blend of hydrophilic and hydrophobic polymers etc. In microfluidics Duncanson *et al.* developed porous microspheres of poly(DL-lactic acid)(PLA) and PLGA in microfluidic glass-capillary device. Perfluorinated-dendrimer-dye was used as permanent geometric template for pores. As PLGA degrades faster than PLA so for release studies PLGA microspheres were used. So, porous PLGA microsphere helps in faster release of encapsulated nile red at 0.1M HCL as compared to the non porous particles because polymer degrades by ester hydrolysis and was more rapid in porous microspheres due to large surface area. The size of pores can be changed by increasing dendrimer generation from 1.5 to 3.5 bearing 8 and 32 perfluoro-alkyl chains at the periphery respectively. Moreover, the presence of fluorous group in dendrimer-dye helps to retain another guest molecule by fluorous-fluorous interaction. They added bi-perfluoro-tagged fluorescein isothiocyanate (F-FITC) to microspheres (G3.5). The presence of two molecules in the porous microspheres were confirmed by confocal micrographs as shown below (Figure 1.18) (Duncanson et al., 2012).

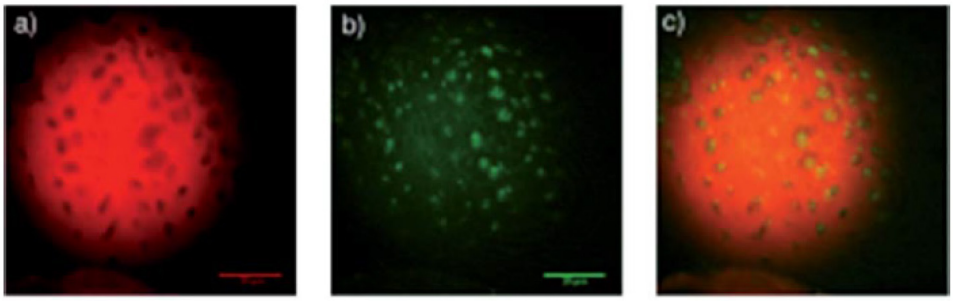

Figure 1.18: a) Confocal micrograph of the porous PLA microsphere formed with [G3.5]–dye complex and encapsulated with nile red. b) F-FITC labeled on the pores of the porous microsphere. c) Overlay of two images (Duncanson et al., 2012).

As compared to the two previous morphologies, here scientists also tried to use other types of microfluidic devices like micromixers and capillary-based devices to provide more freedom of handling while simultaneously reducing the cost of fabrication. For PLGA microparticles most of the time solvent evaporation method was used and then compared with conventional solvent evaporation technique that reveals edge of microfluidic route over counterpart techniques.

1.3.3.3.2 Chitosan microparticles

Chitosan is a versatile natural polymer and is gaining importance in biomedical and biocatalysis field. In the past few years research on chitosan-based drug delivery system have increased. Generally microparticles of chitosan are developed by emulsion crosslinking, coacervation/precipitation, spray-drying, ionic gelation and sieving method (Bansal et al., 2011). After PLGA, chitosan is being used repeatedly for development of drug loaded microparticles by microfluidic approaches using ionic gelation, solvent extraction and crosslinking method. Controlled release microspheres of ampicillin (once a day) were fabricated from chitosan utilizing cross junction (flow-focusing) microchannels. Authors claim it to be the most efficient method to produce chitosan microspheres. First w/o emulsion was generated from pregel solution of ampicillin and chitosan by sunflower seed oil. Downstream, this semi product is put in contact with 20% copper sulphate solution. Chitosan emulsion is converted to microparticles after 20 minutes of ionic gelation crosslinking in collecting reservoir (Figure 1.19). All the droplets generated have uniform

diameter and have similar inter droplet distance but as the flow rate of oil phase was increased this distance decreased along with droplet size.

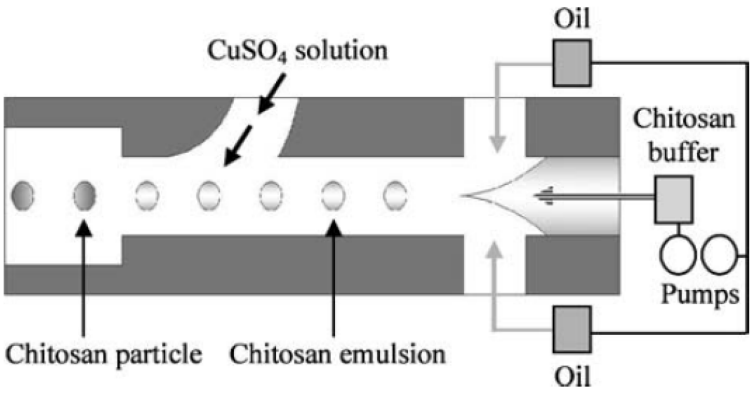

Figure 1.19: Setup used to generate chitosan microspheres by using copper sulphate solution as crosslinker (Yang et al., 2007).

Obtained particles were in the range of 100-800 µm in diameter with coefficient of variation less than 5% but after freeze drying particle size decreased with standard deviation less than 15%. Microparticles with larger diameter showed delayed release compare to microparticles with small size and hence daily dosing can be achieved by bigger particles (Figure 1.20) (Yang et al., 2007).

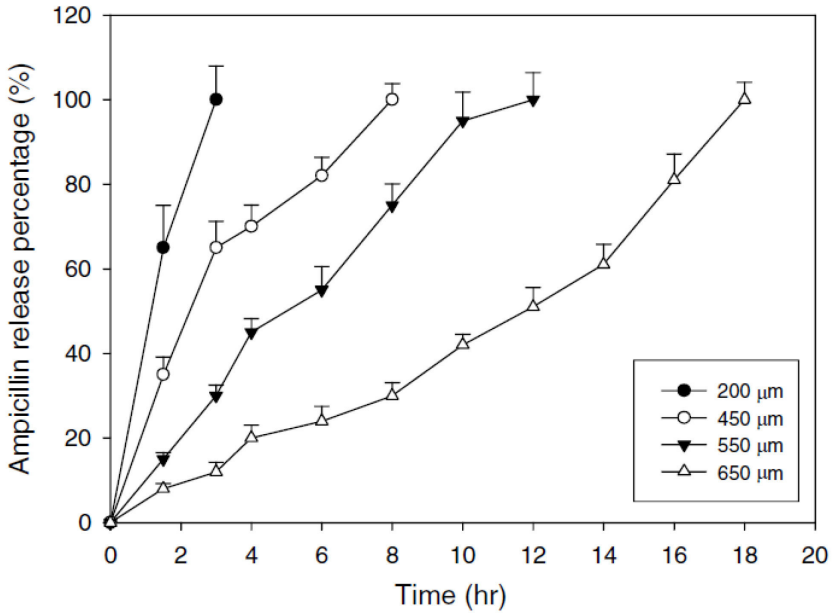

Figure 1.20: Variation in ampicillin release as function of particles diameter. Particles with small size give faster release than bigger ones (Yang et al., 2007).

Xu and coworkers reported preparation of monodispersed (CV less than 4%) BSA microspheres in the range of 100-700 µm using novel solvent extraction method in co-axial capillary microfluidic devices embedded in PMMA plate. They used 4 wt.% of chitosan in 2 wt.% acetic acid aqueous solution as dispersed phase and 2 wt.% span 80 in 30 wt.% of TOA-octyl alcohol as organic phase to generate w/o emulsion. Chitosan droplets are solidified by extracting acetic acid with tri octyl amine (TOA). All the formulations show above 95% of encapsulation efficiency. They were able to obtain different flow regimes by changing the flow rates of oil phase to water (Q_o/Q_w). When Q_o/Q_w was less than 8, plugs were observed, at ratio above 20 spherical drops were obtained. But if ratio of flow rate was greater than 8 and less than 20 then cobbles spheres were seen under microscope which was a transition region between plugs and drops (Figure 1.21).

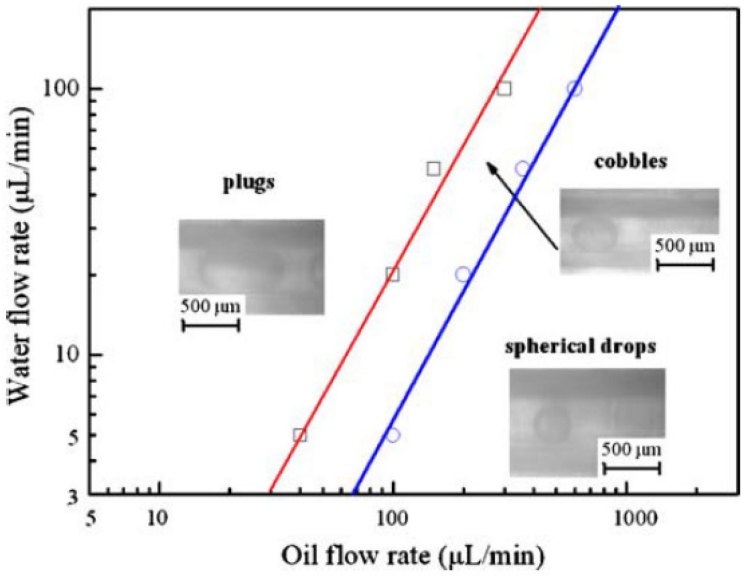

Figure 1.21: Different droplet morphologies under various flow regimes (Xu et al., 2009a).

SEM reveals spherical nature with many micro pores of various dimensions. *In vitro* release of BSA increased with decrease in size which was attributed to decrease of diffusional pathway. They concluded that BSA encapsulated microparticles with dimensions of 340 µm can be used for once daily dosing (Xu et al., 2009a).

Yet in another study Xu *et al*. developed chitosan microspheres by a novel technique combining solidification via solvent extraction and chemical crosslinking via glutraldehyde in a capillary embedded T-junction microfluidic device as described in figure 1.5b. These microspheres exhibiting potential for protein drug delivery and enzyme immobilization. By

changing the solidification time (10-35 min) and flow rates of continuous phase (400–1550 µl/min) they succeeded to obtain different structures namely porous, core-shell and solid particles. Obtained microparticles were in the range of 25 to 130 µm with coefficient of variation less than 5%. In their previous studies, it was found that microspheres formed by crosslinking with glutraldehyde have solid or core-shell structure without any pores on their surface while with solvent extraction exhibit core-shell structure with porous interior and surface. By combining both the methods better architecture was obtained as shown in the figure 1.22.

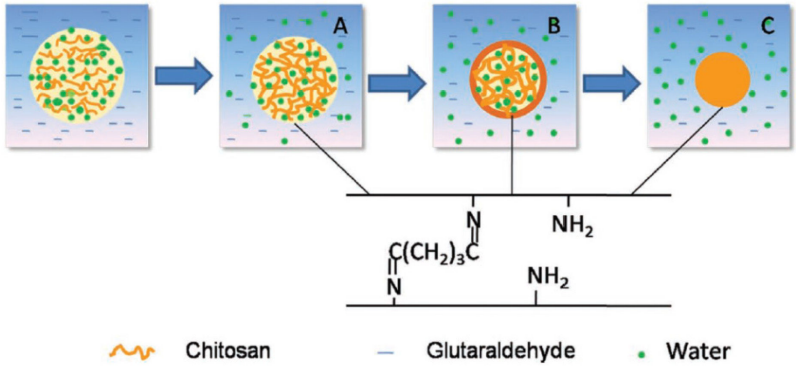

Figure 1.22: Mechanism of generation of microspheres. A) CS–G–A microspheres. B) CS–G–B microspheres. C) CS–G–C microspheres (Xu et al., 2012).

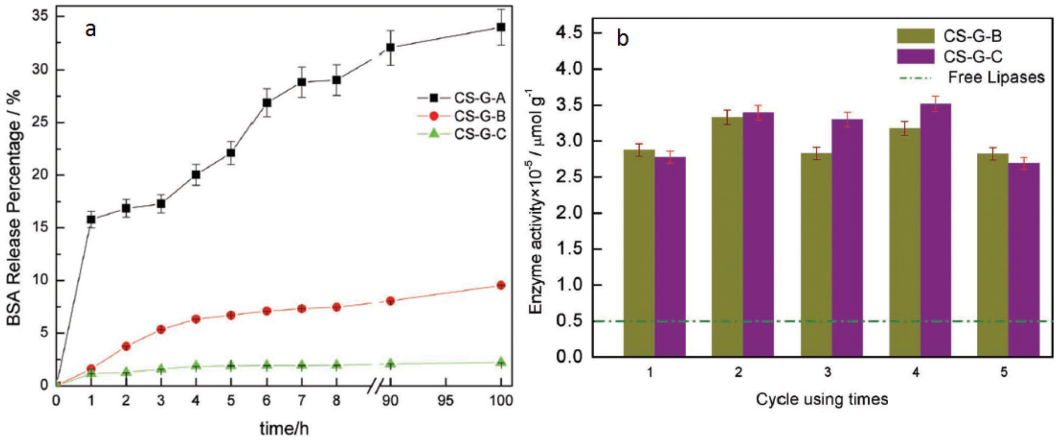

Figure 1.23: a) *In vitro* BSA release studies for the porous (■), core shell (●) and solid microspheres (▲). b) Comparison of encapsulated and free Lipases (Xu et al., 2012).

Here initially water was extracted to form pores either inside or on surface (CS-G-A (porous)) then with increasing solidification time chemical crosslinking between aldehyde and amino group on surface to form core-shell structure having solid shell and porous core

(CS-G-B (core-shell)). Afterwards as the glutraldehyde diffuses into core, shell become thicker and thicker and ultimately leads to the formation of a solid structure (CS-G-C (solid)). SEM studies confirm these transition phases. It was found that BSA release from porous formulation showed burst release and cumulative drug release up to 30%, whereas other two formulations showed release rate less than 10% (Figure 1.23). Furthermore, lipases encapsulated in core-shell and solid structures had ten times higher activity than free lipases (Fig 1.23) (Xu et al., 2012).

So far, researchers focused their attention on polymers and in limited cases on monomers for the fabrication of simple carrier morphologies (e.g. microcapsules, microgels and microspheres) for targeted or non targeted drug delivery. In following section we will address more complex morphologies.

1.3.3.3.3 Core-shell microparticles

Core-shell carriers are double-walled particles consisting of core of one polymer enclosed by a coating of the second polymer. This morphology can overcome problems encountered in single layer particles like burst effect, achieving zero-order release and incorporation and sequential release of two API (Park et al., 2010; Wang et al., 2010). Traditional methods are generally tedious and multiple steps are required. Moreover, core-shell particles produced in traditional methods show batch to batch variation and are polydisperse. Particles with such properties are not suitable for drug delivery applications especially when potent and drugs with narrow therapeutic index were used for treatment. Microfluidics gives a facile approach to develop this morphology to overcome problems of traditional methods and also develop them with different release strategies.

Yu *et al*. at Sichuan University China used coaxial capillary microfluidic device to develop thermo responsive core-shell microspheres where core was loaded with either vitamin B 12 or rhodamine B. Core of these particles were composed of poly(N-isopropylacrylamide) and shell of ethyl cellulose (EC) with PNIPAM gates for proper mechanical strength and release of entrapped material. First, EC microcapsules are fabricated via microemulsification, solvent diffusion and evaporation method and then core and pores in membrane were filled with PNIPAM by free radical polymerization (Figure 1.24).

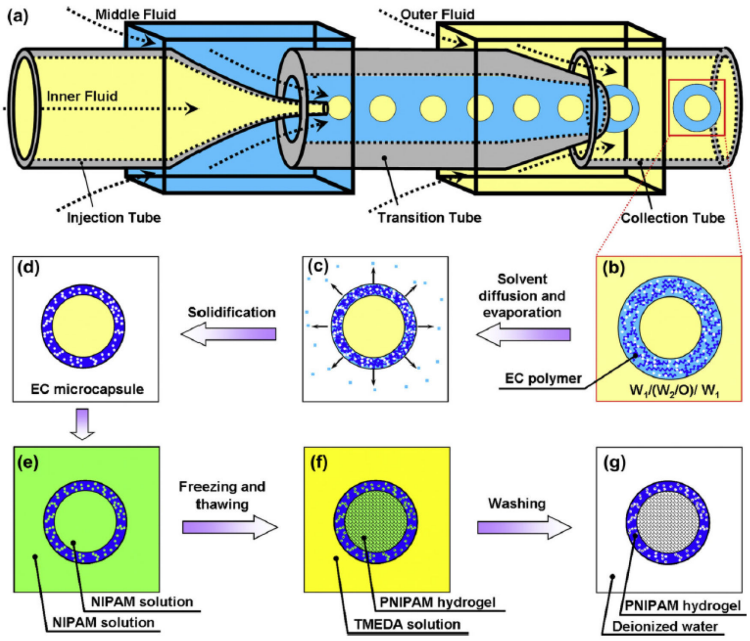

Figure 1.24: Co-axial microfluidic device and steps involved in development of core and shell structure. In first step, the hollow and porous EC shells were developed by microfluidic emulsification followed by solvent evaporation (a–d). In the second step, PNIPAM was filled in cores and porous EC shell. N-isopropylacrylamide (NIPAM) was polymerized by free radical polymerization as soon as activator tetramethylethylenediamine (TMEDA) solution diffused through shell (e–g). (Yu et al., 2012).

At temperature above the VPTT (volume phase transition temperature) of PNIPAM (33 ˚C), core and gates shrunk to release of entrapped material (Figure 1.25) (Yu et al., 2012).

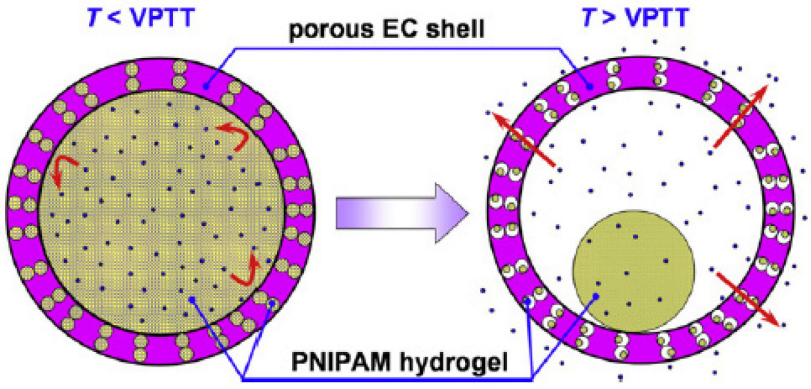

Figure 1.25: Mechanism of release of vitamin B12 and rhodamine B from core-shell particles (Yu et al., 2012).

In another study Gong *et al.* developed smart core-shell microspheres that respond to external magnetic field for smart drug delivery in channel type flow focusing PDMS chips.

1% w/v aspirin solution was encapsulated in core and magnetic nanoparticles were incorporated in shell. Afterwards shell was solidified by dewetting and crosslinking of high molecular weight chitosan by glutaraldehyde (Figure 1.26) in n-butanol injected via additional inlet in PDMS chip.

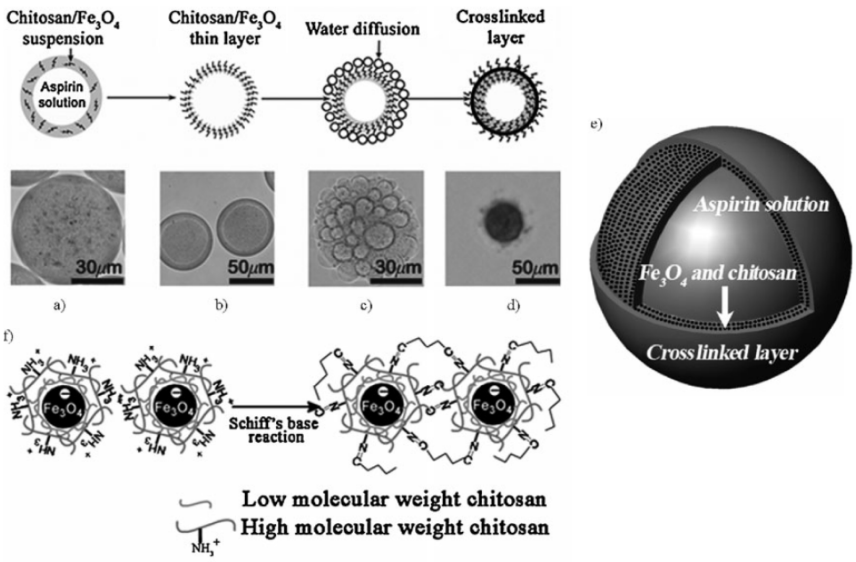

Figure 1.26: Schematic representation of various steps involved in fabrication of magnetically functionalized core-shell microspheres and e) representative structure. a) double emulsion, b) initial core/shell structure formed by the ''dewetting'' effect using n-butanol, c) dynamic permeation of water from inside the particle, d) a transparent shell layer formed through the crosslinking reaction f) After formation of particles they were further baked at 60°C for 2h to facilitate the Schiff reaction between high molecular weight chitosan molecules and glutaraldehyde (Gong et al., 2009).

Size of microsphere was in the range of 40-200 µm. FTIR confirmed the crosslinking of chitosan in shell while fluorescein labeled isothiocynate solution confirms core-shell architecture. Core-shell was also confirmed by examining cross section under SEM. These magnetic particles were observed to deform their shape under the influence of a magnetic field from spherical to spheroidal (Figure 1.27).

This deformation results in release of drug through crosslinked shell. Drug release rate was enhanced by increasing the strength of magnetic field from 0-300G and likewise by keeping magnetic strength constant at 300G and varying frequencies from 0-20 Hz (Gong et al., 2009).

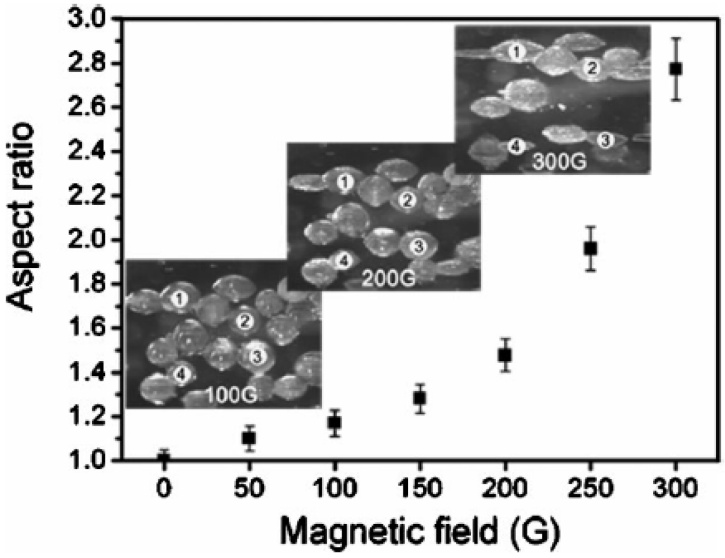

Figure 1.27: Elongation of microspheres under 100G, 200G and 300G field (Gong et al., 2009).

Multilayered microcapsules and microparticles in the range of 10 to 100µm were developed in PDMS microfluidic channel consisting of sheath flow junction (droplet generation), serpentine channel (hardening of droplet) and flow-focusing device for deposition of additional layer of polymers (Figure 1.28).

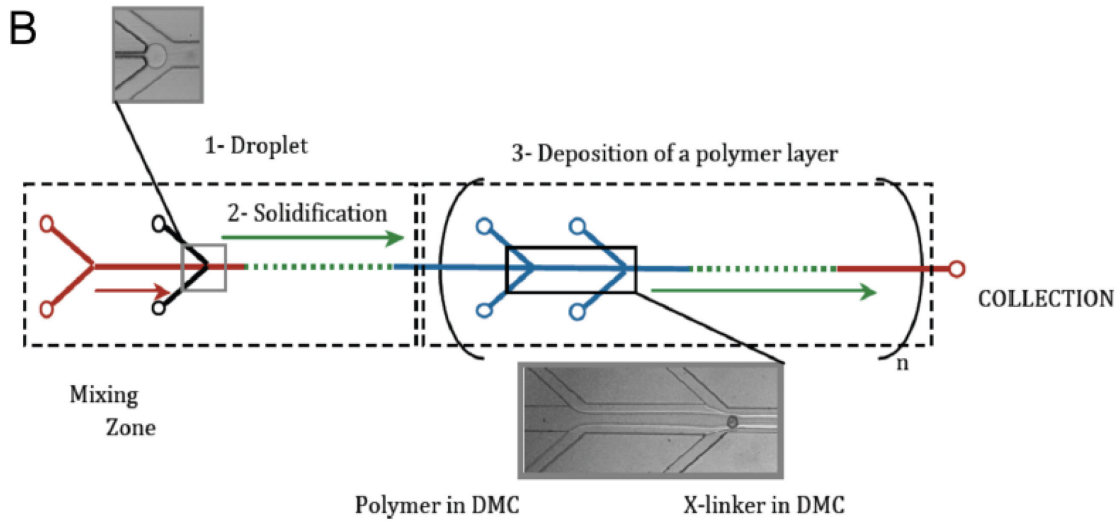

Figure 1.28: PDMS chip showing droplet generation, solidification and layering zone (Rondeau E, 2012).

Redox initiated and photo-induced reaction was used to get the diacrylated Pluronic PF-127 or PF-68 core part and then first layer of triblock PLA-PEO-PLA or

polyvinylpyrrolidone (PVP) was deposited via photo-polymerization. SEM micrographs of crosslinked pluronic microcapsules with first layer of PVP or PLA-PEO-PLA and microparticles with first layer of PVP and second layer of PLA-PEO-PLA exhibit different surface character. Deposition of PVP gives smoother surface while PLA-PEO-PLA gives rough surface. Vitamin B12 (1.35kDA), horse radish peroxidase (HRP) (44kDA) and vitronectin (Vn) (65kDA) were separately encapsulated in microparticles and release rate was compared with macrogels prepared off the chip (Figure 1.29).

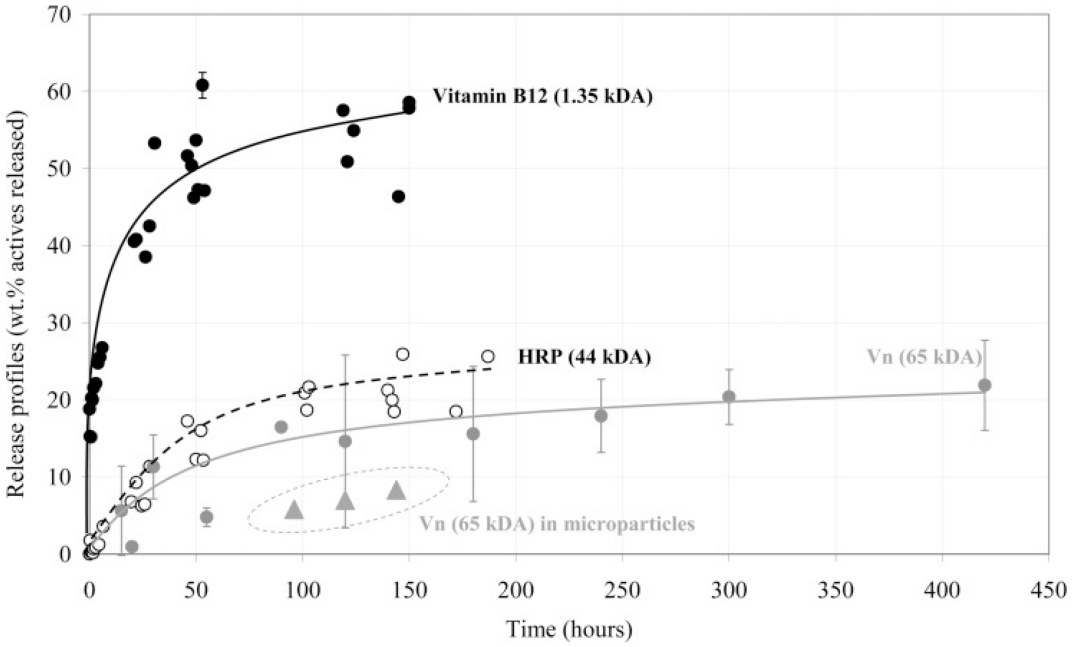

Figure 1.29: Drug release profiles for Vn (grey line), HRP (dotted line) and vitamin B12 (black line) from crosslinked diacrylated pluronic PF-127 macrogels obtained by bulk method; release profile of vitronectin (triangles) from crosslinked diacrylated pluronic PF-127 prepared in microfluidic chip (Rondeau E, 2012).

It was shown that there were differences in microstructure of bulk and microfluidic microgels which can influence the release of molecules depending on their size and structure. Microfluidic gels were denser and there was a size cut off above which release was significantly retarded which was not the case for bulk gels. Release studies indicate microparticles formed have different molecular weight cut off characteristics. Thus, by changing the local density of crosslinked microparticles and that of different layers one could use it to deliver active ingredient having different sizes (Rondeau E, 2012).

This section has showed nice attempts to make core-shell microparticles, encapsulating in their core part APIs of different characters, molecular weights or sizes. Furthermore, different approaches like magnetism, network density tuning and thermal triggering to promote the release of encapsulated material were also presented. But yet no attempt was made to encapsulate two different molecules in core and shell separately for sequential release or dual or targeted dual delivery. This kind of approach could be useful for co-delivery of two APIs at different parts of GIT.

1.3.3.3.4 Targeted microparticles

Although, extensive research is focused on producing microfluidic assisted microparticles yet little has been done for targeted carriers. Lipospheres are water-dispersible solid microparticles (0.2 to 100 µm) composed of a solid hydrophobic fat core stabilized by a monolayer of phospholipid molecules embedded on the surface. Routine methods produce gas filled liposheres with high polydispersity index (>50%) but not in the case of microfluidic methods. In routine they are used to encapsulate and deliver anti inflammatory compounds, local anesthetics, antibiotics, vaccines etc. (Khan et al., 2013b).

Hettiarachchi and coworkers prepared gas filled lipospheres, using PDMS based microfluidic chip featuring two distinct hydrodynamic flow-focusing regions. These multilayer lipospheres with oil layer of triacetin (capable of carrying bioactive molecule) sandwiched between inner gas filled core and outer lipid layer (polyethylene glycol conjugated with lipid called DSPE-PEG2000-Biotin) with avidin as targeting moieties were produced and in the range of 7.5 µm to 20 µm. They showed high encapsulation, better release profile and good acoustic activation to deliver doxorubicin locally in tumor tissues as compare to those produced by conventional agitation method (Hettiarachchi et al., 2009).

1.3.3.3.5 Composite microcarriers

Oral drug delivery is limited by poor solubility, stability and absorption which could lead to poor bioavailability in blood stream. These hurdles can be overcomed by encapsulating them in micro- or nanoparticles. It has been reported by many authors that these particles have ability to accumulate in inflamed areas and also reduce the toxic effect of irritant drugs (Ranjha et al., 2009). Nanoparticles can be beneficial for oral drug delivery

but have some inherited problems since for instance their final fate is affected by pH, ionic concentration, enzymes, mucus, motility etc. Secondly, there handling is difficult in comparison to microparticles. This situation necessitates the development of new hybrid carriers giving ability for easy handling of nanoparticles and oral delivery.

Zhang *et al.* developed multifunctional nano-in-micro hybrid carrier called PSi-PEI-PMVEMA@ASHF for colon cancer treatment. Mucoadhesive, poly(methyl vinyl ether-co-maleic acid) (PMVEMA) polymer was conjugated to porous silicon nanoparticles (PSi NPs) using polyethyleneimine (PEI) as a linker. Then targeted drug delivery system was fabricated in a microfluidic system by encapsulating PSi-PEI-PMVEMA NPs inside a pH-responsive hydroxypropylmethylcellulose acetate succinate based polymer (ASHF) (Figure 1.30 a).

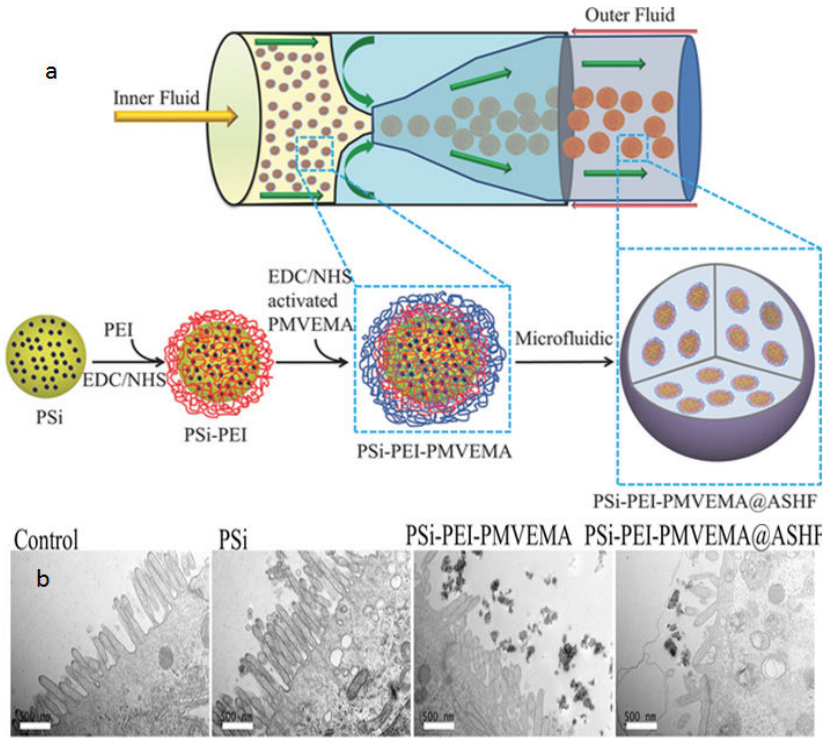

Figure 1.30: a) Microfluidic flow-focusing device for fabrication of composite particles. Enlarged images show the different steps involved in synthesis. b) TEM images of Caco-2/HT-29 cell line showed absence of PSi NPs, presence of PSi-PEI-PMVEMA NPs on microvilli and release of PSi-PEI-PMVEMA from PSi-PEI-PMVEMA@ASHF composite carrier (Zhang et al., 2014).

Size of PSi NPs was 151 nm and overall particles size was 30 µm. Here hydrophilic fluorouracil was incorporated in PSi-PEI-PMVEMA NPs and the hydrophobic celecoxib (CEL)

was dissolved in inner fluid. The composite carrier did not released CEL and 5-FU when pH was below 6.5, but at 7.4 it released both drugs within 2 hr. In Caco-2/HT-29 co-culture monolayers, PSi-PEI-PMVEMA NPs were observed and found to be attached to microvilli (Figure 1.30 b) (Zhang et al., 2014). In a similar kind of study Liu *et al.* developed pH sensitive composite particles for colon cancer treatment. They incorporated atorvastatin in porous silicon matrix and then encapsulated them in different grades of pH responsive hypromellose acetate succinate (MF or HF) microparticles containing celecoxib by microfluidic procedure. These composite carriers prevented the release of two APIs below pH 6. Above pH 6 drugs were released as function of the grade of polymer HF or MF or their combination i.e. higher the amount of HF, lower was the percentage release. But above 6.8 higher the amount of HF higher was release of APIs (Liu et al., 2014).

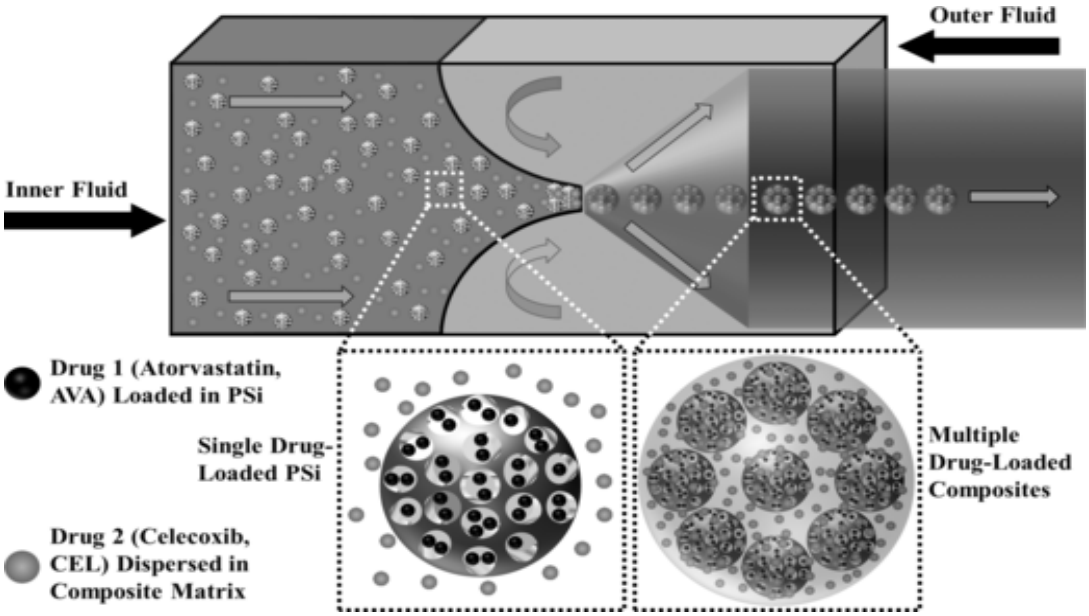

Figure 1.31: Microfluidic flow focus device to fabricate multiple drug loaded composite carrier (Liu et al., 2014).

1.3.3.3.6 Other microcarriers

When literature was further studied it was found that few groups used microfluidic derived microfibers and emulsions for encapsulation and release of various bioactive molecules. One strategy to avoid initial burst effect of microparticle was to use core-shell particles. They were obtained by adding an additional layer of polymer around the core. Microfibers also possess potential to avoid limitations of plain particles. For instance alginate

microfibers containing diclofenac was developed by Lin *et al*. using PMMA based flow-focusing chip. Alginate was crosslinked by divalent calcium ion. Diameter of these fibers could be easily varied by changing flow rate of continuous phase and are in the range of 211 to 364 µm. Under SEM, microfibers revealed uniform size cylinders arranged in a bundle-cluster morphology (Figure 32).

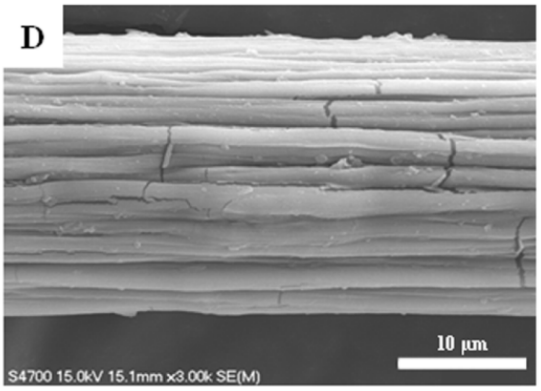

Figure 1.31: SEM image of diclofenac loaded microfibers (Lin et al., 2012).

These fibers released 91.9 ± 2.8% of diclofenac in 1.5h with zero order release. But after incorporation of magnetic iron oxide nanoparticles (5 nm in diameter), release pattern was further improved by applying external magnetic field. Thus showing release properties of fibers can be controlled externally by magnetism (Lin et al., 2012).

Neves *et al.* used terrace like microchannels (Figure 1.5a) on a silicon chip to encapsulate β-carotene or ϒ-oryzanol in O/W emulsion. Resulting emulsion have an average diameter of 27.6 µm (CV 2.3%) and 28.8 µm (CV 3.8%) respectively. β-carotene droplets remained stable and monodispersed after four month storage in darkness at 5°C. Thus this emulsification process have potential to get stable O/W emulsions with lipohilic bioactive molecules that are sensitive to oxidation and heat (Neves et al., 2008).

1.4 Conclusion

Drug delivery carriers are required for convenient and safe administration of active pharmaceutical ingredients. Microcarriers are more safe and reliable than macrocarriers. Conventional microencapsulation technique presents numerous challenges. These can be addressed by developing new methods which provide better control over droplet generation

and size. Microfluidic is newly emerging technique providing satisfactory control over size, composition and morphology with ease, safety and economy. So far in drug delivery, microfluidic techniques are not explored to full potential and are still in their infancy. Most of the times channel type microfluidic devices are used to prepare targeted and non targeted microgels, microcapsules, microparticles, core-shell particles and composite carriers.

1.5 Aims of PhD thesis

So far, capillary-based devices were not explored to their full potential; hence they were used in this work to generate different drug loaded carriers. These devices are facile to fabricate (Chapter 2) from low cost and commercially available chromatographic components. They are assembled in a short span of time in common laboratory as compared to channel-based devices which takes times and dedicated facility for fabrication. In capillary-based devices a slight modification can result in a wide range of different morphologies like microbeads, Janus (Chapter 3) Core-shell and Trojan particle (Chapter 4). The aim of this PhD work is to use such devices to develop different drug loaded morphologies for oral drug delivery. Some of these morphologies would open a new horizon for sustained, co-delivery and targeted delivery of two different molecules. Microbeads will be developed to deliver a single molecule in a sustained release manner. Janus particles will be assessed for the very first time for the co-delivery of two APIs having different solubilities. Core-shell particles will be developed to target the dual delivery of two APIs to colonic region of GIT. Trojan particles will be developed using a new semi-continuous process based on nanoemulsions as template. This will pave the way for easy and facile fabrication of composite carriers which in routine techniques require several steps. These composite carriers will be used for oral delivery of nanoparticles. All of these morphologies will start from monomers and will be polymerized using UV assisted free radical polymerization taking care of integrity of active molecules. Use of UV will avoid the utilization toxic solvents in particle manufacturing and low power consumption thus a step forward toward the concept of Green chemistry. Furthermore, many process parameters (flow rate, reagents concentration, dimension of the capillaries etc.) and material parameters (type of monomer, surfactant etc.) that could affect the formation and release properties of trapped molecules

in aforementioned particles morphologies will be studied. Finally, these morphologies will be investigated by optical microscopy, SEM, TEM, XRD, FTIR, DSC and MTT assay.

References

Abderrahmen, R., Gavory, C., Chaussy, D., Briançon, S., Fessi, H., Belgacem, M.N., 2011. Industrial pressure sensitive adhesives suitable for physicochemical microencapsulation. International Journal of Adhesion and Adhesives 31, 629-633.

Abraham, S., Jeong, E.H., Arakawa, T., Shoji, S., Kim, K.C., Kim, I., Go, J.S., 2006. Microfluidics assisted synthesis of well-defined spherical polymeric microcapsules and their utilization as potential encapsulants. Lab on a Chip 6, 752-756.

Agrawal, U., Sharma, R., Gupta, M., Vyas, S.P., Is nanotechnology a boon for oral drug delivery? Drug Discovery Today.

Bakan, J., 1986. Microencapsulation, The Theory and Practice of Industrial Pharmacy, 2 ed. Lea & Febiger, Philadelphia,.

Bansal, V., Sharma, P.K., Sharma, N., Pal, O.M., Malviya, R., 2011. Applications of Chitosan and Chitosan Derivatives in Drug Delivery. Advances in Biological Research 5, 28-37.

Burgess DJ, AJ, H., 2002. Microsphere technology and applications, in: J, S. (Ed.), Encyclopedia Of Pharmaceutical Technology. Marcel Dekker , INC New york, pp. 2328-2338.

Das M, 2008. Stimulus-Responsive Microgels: Design, Properties and Applications ,University of Toronto.

De Geest, B.G., Urbanski, J.P., Thorsen, T., Demeester, J., De Smedt, S.C., 2005. Synthesis of Monodisperse Biodegradable Microgels in Microfluidic Devices. Langmuir 21, 10275-10279.

del Favero, A., 1986. Anti-inflammatory analgesics and drugs used in rheumatoid arthritis and gout, in: Dukes, M.N.G., Beeley, L. (Eds.), Side Effects of Drugs Annual. Elsevier, pp. 76-96.

Dendukuri, D., Doyel, P.S., 2009. The Synthesis and Assembly of Polymeric Microparticles Using Microfluidics. Adv. Mater. 21, 1–16

Duncanson, W.J., Zieringer, M., Wagner, O., Wilking, J.N., Abbaspourrad, A., Haag, R., Weitz, D.A., 2012. Microfluidic synthesis of monodisperse porous microspheres with size-tunable pores. Soft Matter 8, 10636–10640.

Eiamtrakarn, S., Itoh, Y., Kishimoto, J., Yoshikawa, Y., Shibata, N., Murakami, M., Takada, K., 2002. Gastrointestinal mucoadhesive patch system (GI-MAPS) for oral administration of G-CSF, a model protein. Biomaterials 23, 145-152.

Eijkel, J.T., Berg, A., 2005. Nanofluidics: what is it and what can we expect from it? Microfluid Nanofluid 1, 249-267.

Fang, A., Cathala, B., 2011. Smart swelling biopolymer microparticles by a microfluidic approach: Synthesis, in situ encapsulation and controlled release. Colloids and Surfaces B: Biointerfaces 82, 81-86.

Fu, X., Ping, Q., Gao, Y., 2005. Effects of formulation factors on encapsulation efficiency and release behaviour in vitro of huperzine A-PLGA microspheres. Journal of Microencapsulation 22, 705-714.

Golay, M.J.E., 1957. Vapor Phase Chromatography and Telegrapher's Equation. Analytical Chemistry 29, 928-932.

Gong, X., Peng, S., Wen, W., Sheng, P., Li, W., 2009. Design and Fabrication of Magnetically Functionalized Core/Shell Microspheres for Smart Drug Delivery. Advanced Functional Materials 19, 292-297.

Harrison DJ, Fluri K, Seiler K, F.Z., Effenhauser C, A, M., 1993. Micromachining a Miniaturized Capillary Electrophoresis-Based Chemical Analysis System on a Chip. Science 261, 895-897.

Hettiarachchi, K., Zhang, S., Feingold, S., Lee, A.P., Dayton, P.A., 2009. Controllable microfluidic synthesis of multiphase drug-carrying lipospheres for site-targeted therapy. Biotechnology Progress 25, 938-945.

Hincal AA, S., C., 2005. Microsphere preparation by solvent evaporation method, in: DL, W. (Ed.), Handbook of pharmaceutical controlled release technology. Marcel Dekker, Inc. , New York, pp. 329-343.

Holgado, M.A., Arias, J.L., Cózar, M.J., Alvarez-Fuentes, J., Gañán-Calvo, A.M., Fernández-Arévalo, M., 2008. Synthesis of lidocaine-loaded PLGA microparticles by flow focusing: Effects on drug loading and release properties. International Journal of Pharmaceutics 358, 27-35.

Hu Y, W.Q., Wang J, Zhu J, Wang H, Yang Y., 2012. Shape controllable microgel particles prepared by microfluidic combining external ionic crosslinking. Biomicrofluidics 6, 26502-265029.

Huang, K.-S., Lu, K., Yeh, C.-S., Chung, S.-R., Lin, C.-H., Yang, C.-H., Dong, Y.-S., 2009. Microfluidic controlling monodisperse microdroplet for 5-fluorouracil loaded genipin-gelatin microcapsules. Journal of Controlled Release 137, 15-19.

Hung, L.-H., Teh, S.-Y., Jester, J., Lee, A.P., 2010. PLGA micro/nanosphere synthesis by droplet microfluidic solvent evaporation and extraction approaches. Lab on a Chip 10, 1820-1825.

Hussain A, K.S., Qadir MI, Massud A, Ali M, Khan IU, Saleem M, Iqbal MS, Asghar S, Gul H, 2011. Water uptake and drug release behaviour of methyl methacrylateco-itaconic acid [P(MMA/IA)] hydrogels cross-linked with methylene bis-acrylamide. J. Drug del. Sci. Tech. 21, 249-255

Jyothi, N.V.N., Prasanna, P.M., Sakarkar, S.N., Prabha, K.S., Ramaiah, P.S., Srawan, G.Y., 2010. Microencapsulation techniques, factors influencing encapsulation efficiency. Journal of Microencapsulation 27, 187-197.

Khan, I.U., Serra, C.A., Anton, N., Vandamme, T., 2013a. Continuous-flow encapsulation of ketoprofen in copolymer microbeads via co-axial microfluidic device: Influence of operating and material parameters on drug carrier properties. International Journal of Pharmaceutics 441, 809-817.

Khan, I.U., Serra, C.A., Anton, N., Vandamme, T., 2013b. Microfluidics: A focus on improved cancer targeted drug delivery systems. Journal of Controlled Release 172, 1065-1074.

Kohane, D.S., 2007. Microparticles and nanoparticles for drug delivery. Biotechnology and Bioengineering 96, 203-209.

Lensen, D., van Breukelen, K., Vriezema, D.M., van Hest, J.C.M., 2010. Preparation of Biodegradable Liquid Core PLLA Microcapsules and Hollow PLLA Microcapsules Using Microfluidics. Macromolecular Bioscience 10, 475-480.

Liao, C.-Y., Su, Y.-C., 2010. Formation of biodegradable microcapsules utilizing 3D, selectively surface-modified PDMS microfluidic devices. Biomed Microdevices 12, 125-133.

Lin, Y.-S., Huang, K.-S., Yang, C.-H., Wang, C.-Y., Yang, Y.-S., Hsu, H.-C., Liao, Y.-J., Tsai, C.-W., 2012. Microfluidic Synthesis of Microfibers for Magnetic-Responsive Controlled Drug Release and Cell Culture. PLoS ONE 7, e33184.

Liu, D., Zhang, H., Herranz-Blanco, B., Mäkilä, E., Lehto, V.-P., Salonen, J., Hirvonen, J., Santos, H.A., 2014. Microfluidic Assembly of Monodisperse Multistage pH-Responsive Polymer/Porous Silicon Composites for Precisely Controlled Multi-Drug Delivery. Small 10, 2029-2038.

Makadia HK, SJ., S., 2011. Poly Lactic-co-Glycolic Acid (PLGA) as Biodegradable Controlled Drug Delivery Carrier. Polymers (Basel) 3, 1377-1397.

Manz, A., Harrison, D.J., Verpoorte, E.M.J., Fettinger, J.C., Paulus, A., Lüdi, H., Widmer, H.M., 1992. Planar chips technology for miniaturization and integration of separation techniques into monitoring systems: Capillary electrophoresis on a chip. Journal of Chromatography A 593, 253-258.

Mathew, S., Devi, S.G., Sandhya, K.V., Sandhya, K.V., 2007. Formulation and evaluation of ketorolac tromethamine-loaded albumin microspheres for potential intramuscular administration. AAPS PharmSciTech 8, E100-E108.

Mathies, R.A., Huang, X.C., 1992. Capillary array electrophoresis: an approach to high-speed, high-throughput DNA sequencing. Nature 359, 167-169.

Mrsny, R.J., 2012. Oral drug delivery research in Europe. Journal of Controlled Release 161, 247-253.

Neves, M., Ribeiro, H., Kobayashi, I., Nakajima, M., 2008. Encapsulation of Lipophilic Bioactive Molecules by Microchannel Emulsification. Food Biophysics 3, 126-131.

Nokhodchi A, F.D., 2002. Microencapsulation of Paracetamol by Various Emulsion Techniques Using Cellulose Acetate Phthalate. Pharm Technol 26, 54–60.

Obeidat, W., M., 2009. Recent patents review in microencapsulation of pharmaceuticals using the emulsion solvent removal methods. Recent Patents on Drug Delivery & Formulation 3, 178-192.

Park, J.H., Saravanakumar, G., Kim, K., Kwon, I.C., 2010. Targeted delivery of low molecular drugs using chitosan and its derivatives. Advanced Drug Delivery Reviews 62, 28-41.

Park, K., Yeo, Y., 2006. Microencapsulation Technology, in: Swarbrick, J. (Ed.), Encyclopedia of Pharmaceutical Technology, Third Edition ed. Informa Healthcare, New York USA, pp. 2315-2327.

Perrie Y, Rades T, 2009. FASTtrack Pharmaceutics – Drug Delivery and Targeting. Pharmaceutical Press, London.

Ranade, V.V., 1991. Drug Delivery Systems 5A. Oral Drug Delivery. The Journal of Clinical Pharmacology 31, 2-16.

Ranjha, N.M., Khan, I.U., Naseem, S., 2009. Encapsulation and characterization of flurbiprofen loaded poly(ϵ-caprolactone)–poly(vinylpyrrolidone) blend microphores by solvent evaporation method. Journal of Sol-Gel Science and Technology 50, 281-289.

Ribeiro-Costa, R.M., Cunha, M.R.d., Gongora-Rubio, M.R., Michaluart-Júnior, P., Ré, M.I., 2009. Preparation of protein-loaded-PLGA microspheres by an emulsion/solvent evaporation process employing LTCC micromixers. Powder Technology 190, 107-111.

Rondeau E, C.-W.J., 2012. Formation of multilayered biopolymer microcapsules and microparticles in a multiphase microfluidic flow. Biomicrofluidics 6, 24125-2412516.

Sansdrap, P., Moës, A.J., 1993. Influence of manufacturing parameters on the size characteristics and the release profiles of nifedipine from poly(DL-lactide-co-glycolide) microspheres. International Journal of Pharmaceutics 98, 157-164.

Serra, C.A., Chang, Z., 2008. Microfluidic-Assisted Synthesis of Polymer Particles. Chemical Engineering & Technology 31, 1099-1115.

Serra, C.A., Cortese, B., Khan, I.U., Anton, N., de Croon, M.H.J.M., Hessel, V., Ono, T., Vandamme, T., 2013. Coupling Microreaction Technologies, Polymer Chemistry, and Processing to Produce Polymeric Micro and Nanoparticles with Controlled Size, Morphology, and Composition. Macromolecular Reaction Engineering 7, 414-439.

Singh MN, H.K., Ram M, Shivakumar HG., 2010. Microencapsulation: A promising technique for controlled drug delivery. Res Pharm Sci. 5, 65-77.

Su, Z., Sun, F., Shi, Y., Jiang, C., Meng, Q., Teng, L., Li, Y., 2009. Effects of Formulation Parameters on Encapsulation Efficiency and Release Behavior of Risperidone Poly(D,L-lactide-co-glycolide) Microsphere. Chemical and Pharmaceutical Bulletin 57, 1251-1256.

Swarbrick J, JC, B., 2002. Drug delivery, in: Swarbrick, J. (Ed.), Encyclopedia of Pharmaceutical Technology, Second edition ed. M. Dekker, Ed., Informa Healthcare,, New York.

Terry, S.C., Jerman, J.H., Angell, J.B., 1979. A gas chromatographic air analyzer fabricated on a silicon wafer. Electron Devices, IEEE Transactions on 26, 1880-1886.

Thanki, K., Gangwal, R.P., Sangamwar, A.T., Jain, S., 2013. Oral delivery of anticancer drugs: Challenges and opportunities. Journal of Controlled Release 170, 15-40.

Tian, W.-C., Finehout, E., 2009. Introduction to Microfluidics, Microfluidics for Biological Applications. Springer US, pp. 1-34.

Tomaro-Duchesneau, C., Saha, S., Malhotra, M., Kahouli, I., Prakash, S., 2013. Microencapsulation for the Therapeutic Delivery of Drugs, Live Mammalian and Bacterial Cells, and Other Biopharmaceutics: Current Status and Future Directions. Journal of Pharmaceutics 2013, 19.

Tran, V.-T., Benoît, J.-P., Venier-Julienne, M.-C., 2011. Why and how to prepare biodegradable, monodispersed, polymeric microparticles in the field of pharmacy? International Journal of Pharmaceutics 407, 1-11.

Valencia, P.M., Farokhzad, O.C., Karnik, R., Langer, R., 2012. Microfluidic technologies for accelerating the clinical translation of nanoparticles. Nat Nano 7, 623-629.

van de Weert, M., Hennink, W., Jiskoot, W., 2000. Protein Instability in Poly(Lactic-co-Glycolic Acid) Microparticles. Pharm Res 17, 1159-1167.

van Deemter, J.J., Zuiderweg, F.J., Klinkenberg, A., 1956. Longitudinal diffusion and resistance to mass transfer as causes of nonideality in chromatography. Chemical Engineering Science 5, 271-289.

Wang, J.-T., Wang, J., Han, J.-J., 2011. Fabrication of Advanced Particles and Particle-Based Materials Assisted by Droplet-Based Microfluidics. Small 7, 1728-1754.

Wang, W., Zhou, S., Sun, L., Huang, C., 2010. Controlled delivery of paracetamol and protein at different stages from core–shell biodegradable microspheres. Carbohydrate Polymers 79, 437-444.

Whitesides, G.M., 2006. The origins and the future of microfluidics. Nature 442, 368-373.

Woolley, A.T., Mathies, R.A., 1994. Ultra-high-speed DNA fragment separations using microfabricated capillary array electrophoresis chips. Proceedings of the National Academy of Sciences 91, 11348-11352.

Xu, J.-H., Zhao, H., Lan, W.-J., Luo, G.-S., 2012. A Novel Microfluidic Approach for Monodispersed Chitosan Microspheres with Controllable Structures. Advanced Healthcare Materials 1, 106-111.

Xu, J.H., Li, S.W., Tostado, C., Lan, W.J., Luo, G.S., 2009a. Preparation of monodispersed chitosan microspheres and in situ encapsulation of BSA in a co-axial microfluidic device. Biomed Microdevices 11, 243-249.

Xu, Q., Hashimoto, M., Dang, T.T., Hoare, T., Kohane, D.S., Whitesides, G.M., Langer, R., Anderson, D.G., 2009b. Preparation of Monodisperse Biodegradable Polymer Microparticles Using a Microfluidic Flow-Focusing Device for Controlled Drug Delivery. Small 5, 1575-1581.

Yang, C.-H., Huang, K.-S., Chang, J.-Y., 2007. Manufacturing monodisperse chitosan microparticles containing ampicillin using a microchannel chip. Biomed Microdevices 9, 253-259.

Yang, C.H., Huang, K.S., Lin, Y.S., Lu, K., Tzeng, C.C., Wang, E.C., Lin, C.H., Hsu, W.Y., Chang, J.Y., 2009. Microfluidic assisted synthesis of multi-functional polycaprolactone microcapsules: incorporation of CdTe quantum dots, Fe3O4 superparamagnetic nanoparticles and tamoxifen anticancer drugs. Lab on a Chip 9, 961-965.

Yeo, Y., Park, K., 2004. Control of encapsulation efficiency and initial burst in polymeric microparticle systems. Arch Pharm Res 27, 1-12.

Yu, Y.-L., Zhang, M.-J., Xie, R., Ju, X.-J., Wang, J.-Y., Pi, S.-W., Chu, L.-Y., 2012. Thermo-responsive monodisperse core–shell microspheres with PNIPAM core and biocompatible porous ethyl cellulose shell embedded with PNIPAM gates. Journal of Colloid and Interface Science 376, 97-106.

Zhang, H., Liu, D., Shahbazi, M.-A., Mäkilä, E., Herranz-Blanco, B., Salonen, J., Hirvonen, J., Santos, H.A., 2014. Fabrication of a Multifunctional Nano-in-micro Drug Delivery Platform by Microfluidic Templated Encapsulation of Porous Silicon in Polymer Matrix. Advanced Materials, 26, 4497-4503.

Zhang, H., Mardyani, S., Chan, W.C.W., Kumacheva, E., 2006. Design of Biocompatible Chitosan Microgels for Targeted pH-Mediated Intracellular Release of Cancer Therapeutics. Biomacromolecules 7, 1568-1572.

Zhang, M.-J., Wang, W., Xie, R., Ju, X.-J., Liu, L., Gu, Y.-Y., Chu, L.-Y., 2013. Microfluidic fabrication of monodisperse microcapsules for glucose-response at physiological temperature. Soft Matter 9, 4150-4159.

Zhao, C.-X., 2013. Multiphase flow microfluidics for the production of single or multiple emulsions for drug delivery. Advanced Drug Delivery Reviews 65, 1420-1446.

Zhao, C.-X., Middelberg, A.P.J., 2011. Two-phase microfluidic flows. Chemical Engineering Science 66, 1394-1411.

Zhao, L., Xu, L., Mitomo, H., Yoshii, F., 2006. Synthesis of pH-sensitive PVP/CM-chitosan hydrogels with improved surface property by irradiation. Carbohydrate Polymers 64, 473-480.

Chapter 2
Materials and methods

This chapter deals with all the materials, fabrication methods, procedures and techniques used to develop and characterize the four different microparticles that will be discussed in the following chapters. In order to get reproducible and reliable results, it is imperative to focus on minor details. Microfluidic devices and experimental procedure like encapsulation efficiency, drug release, drug release kinetic, MTT assay etc. are described with thorough explanations. Similarly all characterization techniques like FTIR, DSC, XRD, optical and electronic microscopy (SEM, TEM) are explained in detail. These techniques were used to characterize prepared microparticles in term of extent of polymerization, state of drug, internal and external morphology etc. In this chapter, I will first present all the microfluidic setups and then characterization and instrumental techniques procedures for each drug loaded morphology.

Contents

2.1 Materials

Methyl methacrylate (MMA), methyl acrylate (MA), benzyl methacrylate (BzMA), ethyl acrylate (EA), tripropylene glycol diacrylate (TPGDA), acrylamide (Ac), 1-hydroxycyclohexyl phenyl ketone (HCPK), potassium dihydrogen phosphate, hydrochloric acid, N,N-methylene bis acrylamide (MBA), sodium fluorescein, tween 80, silicon oil of 500 cSt, 2 carboxyethyl acrylate (CEA), ethanol, hexadecane, ethyl acetate, sodium acetate trihydrate and tetrazolium dye (MTT) were purchased from Aldrich, Germany. Sodium dodecyl sulphate (SDS), acetic acid glaciel and ranitidine HCl were purchased from Alfa Aesar, Germany. Ketoprofen was kindly gifted by Amoli Organics Ltd. India. Calcein AM and propidium iodide from eBiosience. Carob gum from Louis Francois, France. Genocure DMHA from Rahan AG Switzerland. 0.45 µm syringe filters and dialysis tubings (Spectra/Por® Dialysis membrane MWCO 3500) were purchased from Fisher, Germany and Spectrum Laboratories USA respectively. All other chemicals used were of analytical grade and used without modification.

2.2 Capillary-based microfluidic setups

2.2.1 Co-axial capillary-based microfluidic setup for microbeads

Microbeads were synthesized using modified version of the original setup developed by Serra *et al.* (Bouquey et al., 2008; Serra et al., 2007) and reported in Fig. 2.1. Briefly, the dispersed phase, comprising monomer, crosslinker, model drug and photoinitiator (Table 2.1), was injected into a continuous phase (carob solution with viscosity of 2150 cps, measured with Rheo RV 8 viscometer using spindle 6 at 50 rpm after centrifugation at 6000 G) by means of a microfluidic device comprising two syringe pumps (PHD 2000, Harvard Apparatus), a T-junction and a fused silica capillary (internal diameter 50 or 200 µm) placed in PTFE or glass outlet tubings (1.6 or 1.8 mm internal diameter, Polymicro Technologies). Once generated at the tip of the capillary, the monomer droplets were polymerized downstream by UV irradiation (Lightningcure LC8 operated at 365 nm, Hamamatsu) in a residence loop of 20 cm for typically 120 s at a suitable intensity (ca. 140 mW/cm^2 for all formulations except ke85 which requires 180 mW/cm^2; as measured by Light power meter, model C6080-13 HAMAMATSU) (Fig. 2.1). For all the formulations, obtained microbeads

were then washed with distilled water, dried at room temperature and stored in glass vials until further characterization.

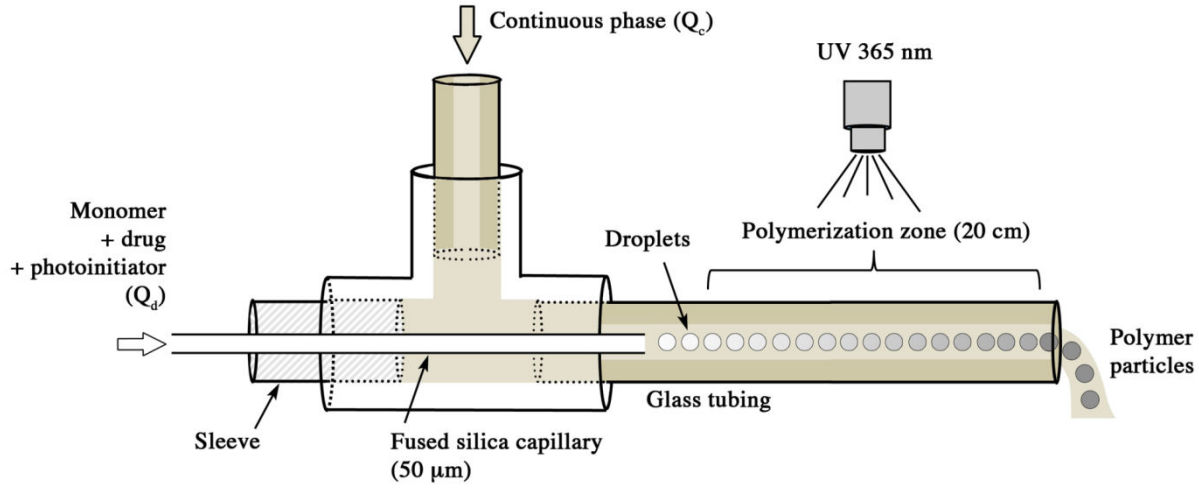

Fig. 2.1. Schematic drawing showing co-axial capillary-based microfluidic setup.

Table 2.1. Composition of formulation

	Formulation	Ketoprofen wt.%	TPGDA wt.%	MMA wt.%	BzMA wt.%	EA wt.%	HCPK wt.%	Capillary	Outlet tubing
1	K0	10	87.5	-	-	-	2.5	200 µm	1.6 mm, PTFE
2	Km0	10	67.5	20	-	-	2.5	200 µm	1.6 mm, PTFE
3	Kb0	10	67.5	-	20	-	2.5	200 µm	1.6 mm, PTFE
4	Ke0	10	87.5	-	-	-	2.5	50 µm	1.8 mm, GT
5	Ke2	10	67.5	-	-	20	2.5	50 µm	1.8 mm, GT
6	Ke4	10	47.5	-	-	40	2.5	50 µm	1.8 mm, GT
7	Ke6	10	27.5	-	-	60	2.5	50 µm	1.8 mm, GT
8	Ke8	10	7.5	-	-	80	2.5	50 µm	1.8 mm, GT
9	Ke85	10	2.5	-	-	85	2.5	50 µm	1.8 mm, GT

Tripropylene glycol diacrylate (TPGDA), 1-hydroxycyclohexyl phenyl ketone (HCPK), Methyl methacrylate (MMA), Benzyl methacrylate (BzMA), Ethyl acrylate (EA), Glass tubing (Nunthanid et al.), Polytetrafluoroethylene (PTFE)

2.2.2 Side-by-side capillaries-based microfluidic setup for Janus

Drug loaded Janus particles are fabricated by modification of the aforementioned device. Briefly this setup consist of three syringe pumps (PHD 2000, Harvard Apparatus), two T-junctions and two side-by-side capillaries (internal diameter 100 µm, Polymicro Technologies) in which flows the two different monomer dispersed phases. The capillaries are placed in the centerline of a PTFE outlet tubing (1.6, 1 or 0.5 mm internal diameter). The dispersed phases, comprising hydrophilic or hydrophobic monomer, crosslinker, model drug and photoinitiator respectively (J1 to J12, see Table 2.2) were injected into a continuous phase (silicon oil of 500 cSt) and biphasic-droplets were generated at the tip of the capillaries. Then Janus droplet morphology was fixed downstream by UV irradiation (Lightning cure LC8 operated at 365 nm, Hamamatsu) in a residence loop of 34 cm at a

suitable intensity (ca. 276 mW/cm^2 as measured by Light power meter, model C6080-13 HAMAMATSU) (Fig. 2.2). These particles were collected, washed with ethyl acetate and dried overnight at room temperature.

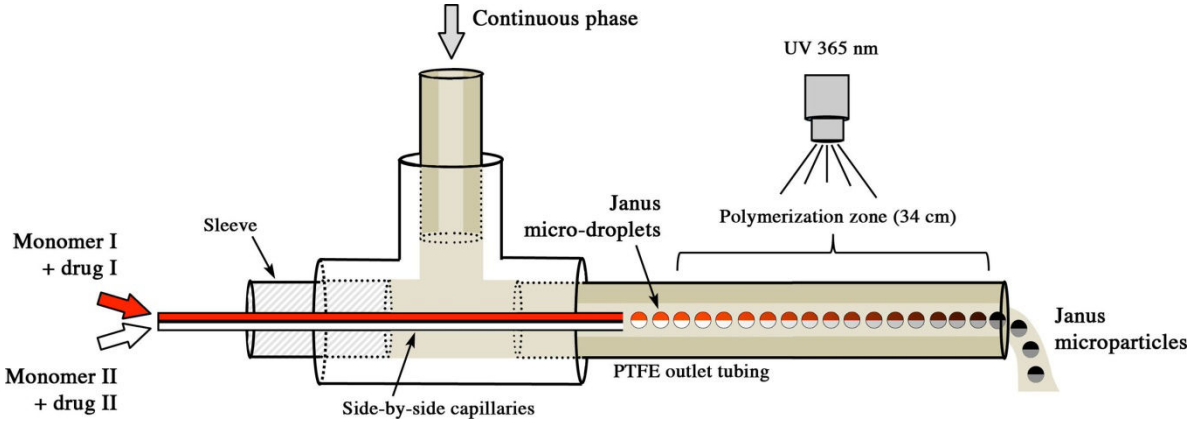

Fig. 2.2. Side-by-side capillaries-based microfluidic setup for the synthesis of drug loaded Janus particles. Each capillary had an internal diameter of 100 µm.

Table 2.2. Composition of the different formulations investigated in current study

Formulation		Ketoprofen	Methyl acrylate	TPGDA	HCPK	Sodium florescence	Acrylamide	MBA	DMHA	SDS	Tween 80	Water
J1	Km86	10	86.5	-	3.5							
	AC30%					0.05	30	6	6	1.5	1.5	54.95
J2	Km86	10	86.5	-	3.5							
	AC20%					0.05	20	4	4	1	1	69.95
J3	Km86	10	86.5	-	3.5							
	AC10%					0.05	10	2	2	0.5	0.5	84.95
J4	Km8	10	79	7.5	3.5							
	AC30%					0.05	30	6	6	1.5	1.5	54.95
J5	Km8	10	79	7.5	3.5							
	AC20%					0.05	20	4	4	1	1	69.95
J6	Km8	10	79	7.5	3.5							
	AC10%					0.05	10	2	2	0.5	0.5	84.95
J7	Km86	10	86.5	-	3.5							
	AC30% 1%Naf					1	30	6	6	1.5	1.5	54
J8	Km86	10	86.5	-	3.5							
	AC30% 1%Naf					1	30	6	6	0.75	0.75	55.5
J9	Km86	10	86.5	-	3.5							
	AC30%					1	30	6	6	0.5625	0.563	55.875
J10	Km86	10	86.5	-	3.5							
	AC30% 1%Naf					1	30	6	6	0.4688	0.4688	56.0625
J11	Km86	10	86.5	-	3.5							
	AC30%1%Naf					1	30	6	6	0.375	0.375	56.25
J12	Km86	10	86.5	-	3.5							
	AC30%1%Naf					1	30	1.5	6	0.375	0.375	60.75

Each hydrophobic phase contains 10 mg of Nigrosin black as colorant. All components are in wt.%.
MBA and DMHA are always 20 wt.% of acrylamide. In different formulations individual weight of Tween 80 and SDS was 5, 2.5, 1.875, 1.5625 and 1.25 wt.% of acrylamide.

2.2.3 Two co-axial capillaries-based microfluidic setup for Core-shell

A two co-axial capillaries-based microfluidic device was used with a slight modification as compared to the one reported earlier by Chang *et al.* (Chang et al., 2009). In brief this setup (Fig. 2.3) was composed of three syringe pumps (PHD 2000, Harvard Apparatus), two T-junctions, a hydrophilic inner capillary (fused silica tubing, internal diameter 100 µm, Polymicro Technologies) and a hydrophobic middle capillary (PEEK tubings, internal diameter 255 µm, Upchurch Scientific) co-axially arranged and placed in the centerline of a PTFE outlet tubing (1 mm internal diameter). The two dispersed phases, comprising hydrophilic or hydrophobic monomer, crosslinker, model drug and photoinitiator respectively (Table 2.3), were injected into a continuous phase (silicon oil of 500 cSt) and double droplets were generated at the tip of the capillaries. This core-shell morphology was then polymerized downstream by UV irradiation (Lightning cure LC8 operated at 365 nm, Hamamatsu) in a residence loop of 34 cm at a suitable intensity (ca. 704 mW/cm^2 as measured by a light power meter, model C6080-13, Hamamatsu). Collected particles were washed with ethyl acetate to remove silicon oil and dried overnight at room temperature.

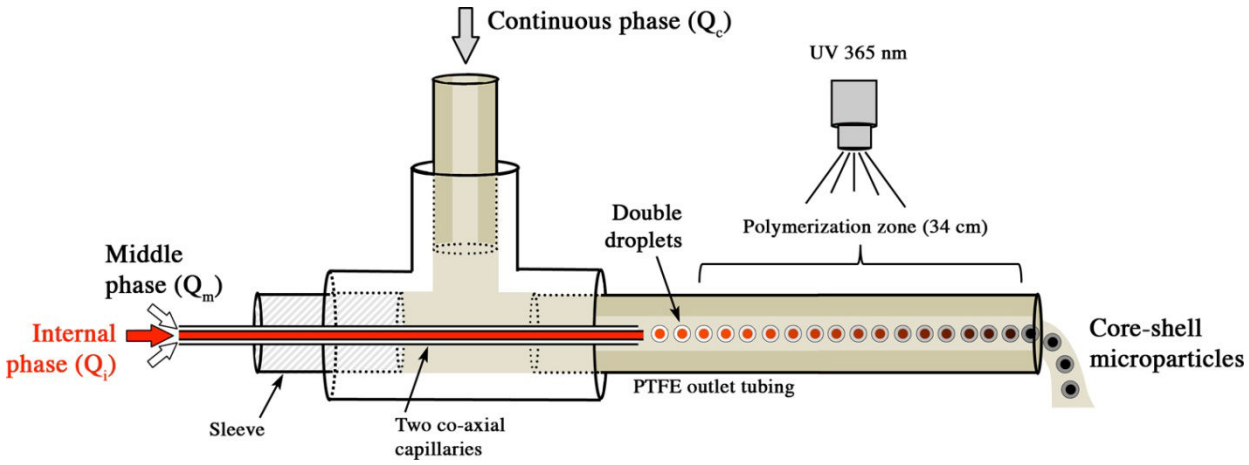

Fig. 2.3. Co-axial capillaries-based microfluidic setup for production of drug loaded core-shell particles (polytetrafluoroethylene, PTFE, polyether ether ketone, PEEK).

Table 2.3. Reference compositions of core and shell phases

S. no	Formulation	Composition						
1	C1	**Shell phase**						
		Acrylamide	MBA	DMHA	SDS	Tween 80	Ranitidine HCl	Water
		30	6	6	2	2	1	53
		Core phase						
		Ketoprofen	HCPK	Methyl acrylate				
		10	4	86				
2	C3	**Shell phase**						
		Acrylamide	CEA	MBA	DMHA	SDS	Tween 80	Ranitidine HCl	Water
		20	10	6	6	2	2	1	53
		Core phase						
		Ketoprofen	HCPK	Methyl acrylate				
		10	4	86				

All components are in wt.%. Core phase contains 10 mg of Nigrosin black as colorant.

2.2.4 µRMX-co-axial capillary-based microfluidic setup for Trojan

To synthesis Trojan particle in semi-continuous fashion, nanoemulsions were used as templates. In a first step, the nanoemulsification of an oil phase with an aqueous solution of acrylamide containing suitable quantity of photoinitiator and crosslinker (Table 2.4) was carried out with an elongation-flow micromixer (µRMX, Fig. 2.4a) having a restriction of 250 µm, a miniaturized version of a bigger RMX developed by Souilem *et al.* (Souilem et al., 2012). Authors have shown that due to its specific design, such device promotes a predominant elongational flow which is known to be more efficient than dispersive flow to break-up the to-be-dispersed phase into monodisperse nanodroplets. After a given back and forth movements through the restriction (referred as the number of cycles), this micromixer was attached to a single capillary-based microfluidic droplet generator composed of a fused silica capillary of 100 µm internal diameter (Fig. 2.4b). Resulting nanoemulsions (later on reffered as disperse phase (Q_d)) are then pumped (8 µL/min) through the co-axial capillary and droplets of nanoemulsions are obtained at the capillary tip in a stream of a continuous phase (silicon oil of 500 cSt, 240 µL/min). These droplets are finally polymerized downstream by UV irradiation (Lightningcure LC8 operated at 365 nm, Hamamatsu) in a residence loop of 34 cm at suitable intensity (ca. 536 mW/cm^2 as measured by Light power meter, model C6080-13, Hamamatsu).

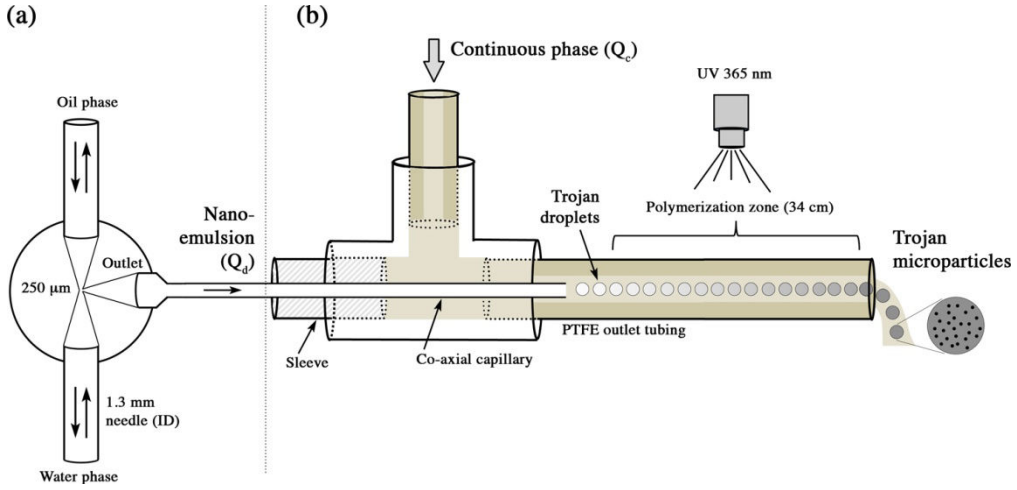

Fig 2.4. Microfluidic setup for the synthesis of Trojan microparticles. a) elongation-flow micromixer for the nanoemulsification and b) single capillary-based droplet generator and hardening of nanoemulsion droplets in a polytetrafluoroethylene (PTFE) outlet tubing to get hybrid carrier.

Table 2.4. Composition of oil and water phases for investigated nanoemulsions

Formulation	Compositions					
T0	**Oil phase (wt.%)**					
	Ketoprofen	HCPK	Ethyl acrylate	Hexadecane		
	10	2.5	87.5	3.5		
	Water phase (wt.%)					
	Acrylamide	MBA	DMHA	SDS	water	
	30	3	6	2	70	
T2	**Oil phase (wt.%)**					
	Ketoprofen	HCPK	TPGDA	Methyl acrylate	Hexadecane	
	10	3.5	7.5	79	3.16	
	Water phase (wt.%)					
	Acrylamide	MBA	DMHA	SDS	Tween 80	water
	30	3	6	3	1.5	56.5

All components are wt.%. Water phase also contains 100 µL of ethanol and in oil phase hexadecane is always 4wt.% of ethyl or methyl acrylate.

2.3. Experimental and characterization procedures

2.3.1 Microbeads

2.3.1.1 Solubility

Excess amount of ketoprofen was added to 10 mL of solutions having different pH in screw-capped glass vials. The contents were stirred magnetically at room temperature until equilibrium. The saturated solution was then filtered through 0.45 µm syringe filters. The

concentration of ketoprofen was measured after appropriate dilution by spectrophotometric (UV-2101PC Shimadzu) analysis at 260 nm (Cho and Choi, 1998).

2.3.1.2 Encapsulation efficiency

Amount of drug encapsulated in the microbeads was determined by dispersing 20 mg of drug loaded microparticles in 10 mL of ethanol and left overnight to extract all the ketoprofen from microbeads. After appropriate dilution, solution was filtered through 0.45 µm filter. Filtrate was analyzed spectrophotometrically at 260 nm (UV-2101PC Shimadzu) (Ranjha et al., 2010; Sairam et al., 2006). Encapsulation efficiency of microbeads was determined by using the following equation

$$\%\ \text{Encapsualtion efficiency} = \frac{\text{Drug encapsulated}}{\text{Drug total}} \text{X} 100 \qquad (1)$$

2.3.1.3 Droplet and particle size analysis

Optical microscope (Nikon ECLIPSE 80*i* and TS100 fitted with a camera, Pike F032B and F032C, Allied Vision Technologies) was used to monitor droplet generation and to take optical images of microbeads. About fifty polymerized microbead images were analyzed by Hiris version 3 (R & D Vision) software to determine average diameter and coefficient of variation (CV) (Bouquey et al., 2008). SEM (XL FEG/SFEG/Sirion) was used to observe the surface and morphology of the prepared microbeads.

2.3.1.4 FTIR analysis

Spectral variations are attributed to alteration in bonds that reveal characteristic vibrational frequencies, leading to frequency shifts and splitting in absorption peaks. FTIR technique was used to monitor the polymerization profiles of different functional groups and drug-polymer interactions (Nicolet 380 FT-IR Spectrometer). The spectra were recorded for pure drug, monomers and drug-loaded microbeads over a scanning range of 4000-500 cm^{-1} (Lee et al., 2003; Ranjha et al., 2009).

2.3.1.5 DSC measurements

DSC curves of pure ketoprofen and drug-loaded microbeads were recorded using TA DSC Q200 to acquire information about glass transition temperature (T_g) of copolymers and

the physical state of ketoprofen. The analysis was performed by heating the samples at the rate of 10°C/min under an inert atmosphere (Ranjha et al., 2010; Sairam et al., 2006).

2.3.1.6 XRD analysis

To investigate the physical state of drug after microencapsulation, X-ray diffraction patterns were obtained by utilizing X-ray diffractometer (**Bruker D8**). All the diffraction patterns were analyzed at scanning rate of 2° min^{-1}, over the 5-50°diffraction angle (2 θ) range.

2.3.1.7 In vitro ketoprofen release

In vitro ketoprofen release were performed by incubating 100 mg of the microbeads, in a dialysis tubing (Spectra/Por® dialysis membrane, MWCO 3500) containing 20 mL of USP phosphate buffer solution (pH =6.8). This dialysis tube was then placed in 500 mL of USP phosphate buffer solution (pH = 6.8) at 37°C and stirred magnetically at 100 rpm. At predetermined time intervals, 5 mL of dialysate was sampled and replaced by the same volume of fresh media pre-warmed at 37°C. The concentration of ketoprofen in samples was calculated by using previously constructed standard calibration curve (R^2=0.9993). In vitro release studies were performed in triplicate (n = 3) in an identical manner.

2.3.1.8 Drug release kinetics

Drug is released from microbeads matrix by different release mechanisms. Korsmeyer Peppas equation was used to model the release of ketoprofen from polymer microbeads:

$$\frac{M_t}{M_\infty} = k\, t^n \qquad (2)$$

where M_t/M_∞ is fraction of drug released at time t, k is the release rate constant incorporating structural and geometric characteristics of the studied system and n is the release exponent or diffusion exponent indicating the release mechanism. When n approximates to 0.5, a Fickian/diffusion controlled-release is implied; while 0.5 < n < 1.0 indicates a release non Fickian and 1 stands for zero order (case II transport). When n value is greater than 1.0, it indicates super case II transport. While applying this model, it was considered that no significant porosity and swelling changes in microbeads occurred during ketoprofen release (Dalmoro et al., 2012; Ranjha et al., 2009).

2.3.2 Janus

2.3.2 1 Janus structure and particle size

Different techniques were used to confirm the Janus structure that includes microscopic and spectroscopic techniques. SEM (TESCAN Vega and XL FEG/SFEG/Sirion) was used to take images of Janus particles while raman mapping was carried out to confirm different chemical nature on two sides of Janus particles. Size of Janus particles were determined by procedure described in section 2.3.1.3.

2.3.2 2 Factors affecting the shape

2.3.2.2.1 Effect of flow rate

Effect of flow rate was investigated by keeping the stream of hydrophilic phase (30 wt.% of AC) constant while changing the flow rate of hydrophobic phase (86.5 wt.% of MA).

2.3.2.2.2 Effect of surfactant

Janus particles were produced without or with surfactants. Combination of SDS and Tween 80 (3, 1.5, 1.125 and 0.75 wt.%) was added to acrylamide phase with no surfactant in hydrophobic phase.

2.3.2.2.3 Effect of monomeric composition

To investigate the influence of monomer concentration, first a solution with 30 wt.% of acrylamide was pumped side-by-side with a solution containing 86.5 wt.% of methyl acrylate. Then 7.5 wt.% of TPGDA was added to the methyl acrylate phase while keeping the same acrylamide phase content. In a new set of experiments, the composition of the hydrophilic phase was changed (30, 20, 10 wt.% of acrylamide) while keeping same hydrophobic phase content (7.5 wt.% TPGDA, 79 wt.% methyl acrylate).

2.3.2.3 Factors controlling the size of Janus particles

2.3.2.3.1 Effect of outlet diameter

In this experiment, a formulation optimized in term of different parameters like surfactant concentration (0.75 wt.% of SDS plus Tween 80), flow rate of the two dispersed

phases (2-2 µL/min) was subjected to the variation of the collecting tube internal diameter (1.6, 1 and 0.5 mm respectively) under similar conditions.

2.3.2.3.2 Effect of the flow-focusing arrangement

In order to switch from the co-flow to the flow-focusing arrangement, initial device was slightly modified to accommodate few millimeters downstream to the capillaries tips a 350 µm restriction (HPLC Liner).

2.3.2.3.3 Effect of UV intensity

Optimized formulations were polymerized under same condition except with different UV intensities i.e. 20, 40 and 80%.

2.3.2.4 Analysis of polymerization

FTIR analysis was carried out using procedure mentioned in section 2.3.1.4.

2.3.2.5 Encapsulation efficiency

Procedure described in section 2.3.1.2 was used to determine encapsulation efficiency, except 10 mL of phosphate buffer solution (PBS) of pH 6.8 was used for extraction and after 48h filtrate was analyzed at 260 and 489 nm for ketoprofen and sodium fluorescein respectively.

2.3.2.6 *In vitro* cytotoxicity testing

BNL-CL2 cells were seeded in 24-well plates at a concentration of 5×10^4 cells per well in 1 mL of medium (Dulbecco's Modified Eagle's Medium, DMEM) containing 10% fetal bovine serum, 1 wt.% glutamine, 1 wt.% of commercial solution of penicillin and streptomycin. The BNL-CL2 cells were then incubated overnight at 37 °C under a controlled atmosphere (5% CO_2 and 95 % air). Next, formulation J11 was added at different concentrations, corresponding to 0.5, 1, 2, 4, 6, 8, 12, 16 and 20 mg per well. After an incubation of 24 hr, the medium was removed and adherent cell monolayers were washed with PBS. Then, wells were filled with cell culture medium containing MTT (3-(4,5-dimethylthiazol-2-yl)-2,5-diphenyltetrazolium bromide), incubated for 2 hr at 37°C. Formazan crystals formed were dissolved in 1 mL dimethyl sulfoxide. UV absorbance was

measured at 570 nm by spectrophotometry with a microplate reader. Experiments were carried out in triplicate, and expressed as a percentage of viable cells compared to control group.

2.3.2.7 Drug release

Drug release studies were performed by using procedure described in section 2.3.1.7 except dialysis tube was placed in 250 mL of USP phosphate buffer solution and samples were analyzed at 260 and 489 nm for ketoprofen and sodium fluorescein respectively.

2.3.3 Core-shell

2.3.3.1 Particle analysis

Particle size was determined using procedure described in section 2.3.1.3.

2.3.3.2 Effect of continuous to middle phase flow rate ratio (Q_c/Q_m)

To investigate the effect of continuous to middle phase flow rate ratio (Q_c/Q_m), formulation C1 (Table 2.3) was operated under different conditions of Q_c/Q_m i.e. 240, 180 and 120, while keeping middle and inner phase flow rate constant at 2 µL/min.

2.3.3.3 Variation of core diameter

The core diameter was varied by changing the flow rate ratio of middle and internal phases (Q_m/Q_i), *i.e*. 1, 1.3 and 2 in formulation C1 (Table 2.3) at constant continuous phase flow rate of 240 µL/min.

2.3.3.4 Influence of composition on morphology

To study effect of composition on particle morphology, concentration of acrylamide in shell phase of formulation C1 was varied from the reference value of 30 wt.% down to 25 and 20 wt.% while keeping rest of composition constant. Then 40 and 20 wt.% of TPGDA were added to the core phase for the shell formulation containing 30 wt.% of acrylamide.

2.3.3.5 Monitoring of polymerization

FTIR analysis was accomplished to monitor polymerization using same procedure as mentioned in section 2.3.1.4.

2.3.3.6 Encapsulation efficiency

Refer to the section 2.3.1.2 except that particles were incubated in 20 mL of phosphate buffer solution of pH 6.8 for 72 hours and filtrate was analyzed at 260 and 315 nm for ketoprofen and ranitidine HCl respectively.

2.3.3.7 Cytotoxicity testing

2.3.3.7.1 Cell cultivation

Mouse hepatic BNL-CL2 cell line was used in this research. Cells were cultivated in Dulbecco's Modified Eagle's Medium (DMEM) supplemented with 10% fetal bovine serum and 1 wt.% of commercial Penicillin-Streptomycin (Pen Strep) solution at 37°C in a 5% CO_2 humidified atmosphere. The medium was replaced every 3-4 days after previous cell detachment using 0.02% (w/v) trypsin-EDTA solution.

2.3.3.7.2 MTT-test

MTT procedure described in section 2.3.2.6 was used for MTT assay of core-shell particles.

2.3.3.7.3 Live-dead test

BNL-CL2 cells were seeded in Millicell EZ 4 well glass slides at a density of 25000 cells per well followed by overnight incubation. Formulations were added to the cells at indicated concentrations for 24 hours of incubation at 37°C in a 5% CO_2 humidified atmosphere. Then the cells were washed 3 times with PBS and stained by additional incubation with Calcein AM which is specific for alive cells visualisation (5 µM, 20 min of incubation) and Propidium iodide for dead cells (5 µM, 10 min). Finally, the cells were washed twice with PBS, mounted in the fluorophor protector CC/Mount and observed with Zeiss Axiovert 25 fluorescent microscope equipped with Axiocam CCD camera and 40× objectives. The images were processed with Zeiss ZEN and Image J software.

2.3.3.8 Drug release studies

Refer to the section 2.3.1.7 except that dialysis tube was placed in 250 mL of USP buffer solution of pH 1.2, 5.4, 6.8 and 7.4 and samples were analyzed at 260 and 315 nm for ketoprofen and ranitidine HCl respectively.

2.3.4 Trojan

2.3.4.1 Size of Nanoemulsions

After emulsification in µRMX, the mean droplets size was determined by using dynamic light scattering (Zetasizer 3000 HS, Malvern).

2.3.4.2 Effect of cycles on nanodroplets

The oil phase and water phases were injected from both ends of the µRMX at a given volume ratio (20:80) and a constant flow rate of 5ml/min. The µRMX was operated continuously during a prescribed number of cycles 5, 15, 30, 60, 90, 120 and 150 cycles (Fig. 2.4a).

2.3.4.3 Size of Trojan particles

Size of Trojan particles was determined by using procedure described in section 2.3.1.3.

2.3.4.4 SEM of Trojan particles

SEM (XL FEG/SFEG/Sirion) was used to observe the surface, morphology and cross section of particles. The cross section was used to observe ketoprofen loaded poly(ethyl acrylate) or poly(methyl acrylate) nanoparticles embedded in the poly(acrylamide) matrix.

2.3.4.5 Release of nanoparticles

30 mg of Trojan microparticles were incubated in 20 ml of USP phosphate buffer solution at pH 6.8 at 37 $^{\circ}$C under gentle shaking at 100 rpm for two hours. Then, the solution was passed through 0.2 µm syringe filter and few drops were treated with uranyl acetate and observed under TEM (CM12 Philips and Technai G2 microscope, FEI) for detection of nanoparticles.

2.3.4.6 Encapsulation efficiency

Encapsulation efficiency was determined by method reported in section 2.3.1.2, except particles were incubated in 20 mL of phosphate buffer solution (PBS) of pH 6.8 for 48 hours and filtrate analyzed at 260 nm for ketoprofen.

2.3.4.7 Drug release of Trojan particles

Drug release studies was carried out using method described in section 2.3.1.7 except dialysis tube was placed in 250 mL of USP phosphate buffer solution of pH 6.8 and samples were analyzed at 260 nm for ketoprofen.

References

Bouquey, M., Serra, C., Berton, N., Prat, L., Hadziioannou, G., 2008. Microfluidic synthesis and assembly of reactive polymer beads to form new structured polymer materials. Chemical Engineering Journal 135, Supplement 1, S93-S98.

Chang, Z., Serra, C.A., Bouquey, M., Prat, L., Hadziioannou, G., 2009. Co-axial capillaries microfluidic device for synthesizing size- and morphology-controlled polymer core-polymer shell particles. Lab on a Chip 9, 3007-3011.

Cho, Y.J., Choi, H.K., 1998. Enhancement of percutaneous absorption of ketoprofen: effect of vehicles and adhesive matrix. International Journal of Pharmaceutics 169, 95-104.

Dalmoro, A., Barba, A.A., Lamberti, G., d'Amore, M., 2012. Intensifying the microencapsulation process: Ultrasonic atomization as an innovative approach. European Journal of Pharmaceutics and Biopharmaceutics 80, 471-477.

Lee, T.Y., Roper, T.M., Jonsson, E.S., Kudyakov, I., Viswanathan, K., Nason, C., Guymon, C.A., Hoyle, C.E., 2003. The kinetics of vinyl acrylate photopolymerization. Polymer 44, 2859-2865.

Nunthanid, J., Huanbutta, K., Luangtana-anan, M., Sriamornsak, P., Limmatvapirat, S., Puttipipatkhachorn, S., 2008. Development of time-, pH-, and enzyme-controlled colonic drug delivery using spray-dried chitosan acetate and hydroxypropyl methylcellulose. European Journal of Pharmaceutics and Biopharmaceutics 68, 253-259.

Ranjha, N., Khan, H., Naseem, S., 2010. Encapsulation and characterization of controlled release flurbiprofen loaded microspheres using beeswax as an encapsulating agent. Journal of Materials Science: Materials in Medicine 21, 1621-1630.

Ranjha, N., Khan, I., Naseem, S., 2009. Encapsulation and characterization of flurbiprofen loaded poly(ϵ-caprolactone)–poly(vinylpyrrolidone) blend micropheres by solvent evaporation method. Journal of Sol-Gel Science and Technology 50, 281-289.

Sairam, M., Babu, V.R., Naidu, B.V.K., Aminabhavi, T.M., 2006. Encapsulation efficiency and controlled release characteristics of crosslinked polyacrylamide particles. International Journal of Pharmaceutics 320, 131-136.

Serra, C., Berton, N., Bouquey, M., Prat, L., Hadziioannou, G., 2007. A Predictive Approach of the Influence of the Operating Parameters on the Size of Polymer Particles Synthesized in a Simplified Microfluidic System. Langmuir 23, 7745-7750.

Souilem, I., Muller, R., Holl, Y., Bouquey, M., Serra, C.A., Vandamme, T., Anton, N., 2012. A Novel Low-Pressure Device for Production of Nanoemulsions. Chemical Engineering & Technology 35, 1692-1698.

Chapter 3
Microbeads and Janus particles

The first section of this chapter deals with the production and characterization of plain particles, so-called microbeads. This morphology is obtained by means of a capillary-based microfluidic device and is intended for the delivery of a single active pharmaceutical agent. It will be shown that the developed device enables to get monodisperse particles with easy tuning of release profile by changing either material composition or operating parameters. The second section of this chapter deals with a side-by-side capillary-based microfluidic device developed on purpose for the production of drug loaded Janus particles. These particles have the ability to address the issue of co-delivery of two molecules having completely different physicochemical properties. Thus Janus particles allows encapsulating two active ingredients in two separate compartments while still keeping the potential to release these two APIs in a controlled manner whatever their relative solubility and compatibility which would not be the case with plain particles.

This chapter is mainly composed of the following published research articles.

1: ***Khan, I.U.**; Serra, C.A.; Anton, N.; Vandamme, T. Continuous-flow encapsulation of ketoprofen in copolymer microbeads via co-axial microfluidic device: Influence of operating and material parameters on drug carrier properties. International Journal of Pharmaceutics **2013,** 441 (1–2), 809-817.*

2: ***Khan, I. U.**; Serra, C. A.; Anton, N.; Li, X.; Akasov, R.; Messaddeq, N.; Kraus, I.; Vandamme, T. F. Microfluidic conceived drug loaded Janus particles in side-by-side capillaries device. International Journal of Pharmaceutics **2014,** 473 (1–2), 239-249.*

Contents

3.1 Continuous-flow encapsulation of ketoprofen in copolymer microbeads via co-axial microfluidic device: Influence of operating and material parameters on drug carrier properties.

Graphical Abstract

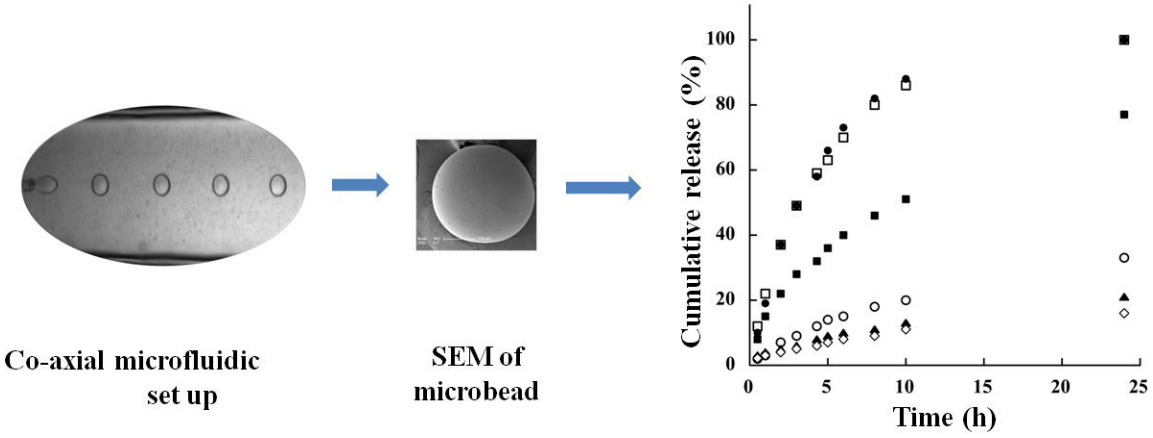

Abstract

Microchannel based microfluidic systems are able to obtain monodispersed microparticles but are limited by cost, time and channel clogging. We succeeded in on the fly encapsulation of high ketoprofen contents in acrylate-based copolymer microbeads by environment friendly UV induced free radical polymerization in off-the-shelf co-axial microfluidic device. FTIR shows complete polymerization of acrylate monomers and interaction between carboxylic group of ketoprofen and ester group of monomers. DSC and XRD confirm amorphous nature of drug in microbeads. Different comonomer content formulations show limited drug release at low pH, a helpful properties to avoid gastric irritating effect of ketoprofen associated with conventional dosage forms. At pH 6.8 microbeads release higher content of drug by a non-Fickian diffusion mechanism. Their drug release rate depends upon the weight content of ethyl acrylate in the formulation as well as their size, increasing by increasing the former and decreasing the later.

Keywords: Microfluidics, ketoprofen, microbeads, ethyl acrylate, drug delivery

3.1.1 Introduction

Microencapsulation refers to the procedure by which solids, liquids and gases are enclosed in microparticles through the formation of thin coatings of wall material around an active substance (Dalmoro et al., 2012). This technology is widely used in several drug delivery systems since its first application in 1930. Administration of drugs in microparticle form benefits from protection of drug, controlled release, reduced administration frequency, patient comfort and compliance (Tran et al., 2011). Traditionally used method for microencapsulation lacks desired drug loading, monodispersity in size and batch to batch uniformity (Holgado et al., 2008; Xu et al., 2009). Therefore new techniques are required which yields microparticles with desired loading efficiency, homogenous shape and narrow size distribution (Holgado et al., 2008). Since the size of microparticles is a key parameter that influences drug distribution (Tran et al., 2011), degradation rate, stability of drug and release kinetics (Xu et al., 2009).

Microfluidics is concerned with small (10^{-9} to 10^{-18} liter) volumes of fluids constrained in microchannels of sub millimeter scale. Microfluidics allows synthesis of microparticles in single phase flow or multiphase flow and offers several advantages over batch process as significant reduction of reagents, mixing time, laminar flow and high heat and mass transfer (Park, 2010; Wang et al., 2011). Multiphase flow microfluidic devices allows the continuous generation of monodisperse droplets dispersed in a carrier phase which can be solidified in line downstream by chemical or physical means. For instance, hardening of liquid droplets may be produced by polycondensation, radical polymerization, ionic crosslinking, thermosetting, solvent evaporation or extraction (Park, 2010). Thus microfluidics produces polymer microparticles with coefficient of variation (CV) less than 5% (Serra and Chang, 2008) as compare to traditional method having CV between 10 to 50% (Takeuchi S, 2005). Furthermore, microfluidic devices provide microparticles with precise control over shape (sphere, rod etc.), morphology (core-shell, Janus, microcapsules etc.) and composition (hybrid, doped, etc.) (Serra and Chang, 2008). In recent times, UV light has become a powerful tool for initiating polymerization in droplet microfluidic due to certain significant advantages. The polymerization can be easily varied by controlling the light intensity and the exposure time (Ma et al., 2010). Moreover, UV technique could provide significant economic and environmental advantages by the elimination of solvents, low energy usage

requirements (Crivello, 1999) and is a faster and efficient industrial process than heat-curable processes (Xia et al., 2008).

Ketoprofen is a non-steroidal anti-inflammatory drug (NSAID) belonging to class II Biopharmaceutical Classification Systems (BCS) and was selected as a model for poorly water-soluble drug. It relieves the pain, tenderness, inflammation and stiffness caused by arthritis. It short half life necessitates frequent dosing thus exposing gastrointestinal tract (GIT) to high levels causing ulceration or bleeding (Arida and Al-Tabakha, 2007; Yu et al., 2010).

PDMS (polydimethylsiloxane) or PMMA (poly(methyl methacrylate)) based microchannels were used for fluorescein encapsulated poly(lactide-co-glycolic acid) (PLGA) microparticles (Hung et al., 2010), bupivacaine containing PLGA microparticles (Xu et al., 2009), BSA entrapped biopolymer microparticles (Fang and Cathala, 2011), tamoxifen encapsulated polycaprolactone microcapsules (Yang et al., 2009), 5-flurouracil containing genipin-gelatin microcapsules (Huang et al., 2009). These systems require rigorous cleaning, time consuming and are costly. In present study, we used an off-the-shelf capillary based co-axial microfluidic device which was assembled within fifteen minutes to emulsify dispersed phase in the absence of surfactant. Acrylate-based polymerizable ketoprofen-loaded droplets were cured downstream by an appropriate UV intensity, exposure time and wavelength far away from the maximum wavelength absorption of the drug. Thus monodispersed microbeads loaded with different amounts of drug will be produced. Drug encapsulation efficiency as well as release rate will be investigated with respect to the size of the microparticles and the weight content of the two co-monomers.

3.1.2 Experimental

I. *List of materials is given in Chapter 2 section 2.1*
II. *Description of the co-axial capillary-based device and overall particle synthesis process is provided in Chapter 2, section 2.2.1*
III. *Methods for particle characterization, encapsulation efficiency and release properties are detailed in Chapter 2, section 2.3, 2.3.1.2 and 2.3.1.7 respectively.*

3.1.3 Results and discussion

We successfully emulsified monomer phase without using surfactant and then obtained polymeric microbeads using the setup shown in Fig. 2.1 in chapter 2. Conditions adopted for synthesis were able to give us fully polymerized monodisperse microbeads with high encapsulation efficiency for acrylate monomers and unpolymerized microparticles with low encapsulation efficiency for methacrylate monomers. So, only fully polymerized formulations were used for further studies. We observed that ketoprofen solubility was 0.8 mg/mL at pH 5.8 which increased to 14 mg/mL at pH 8 (see Fig. S1 in the *Supplementary information section*). A probable reason may come from the fact that Ketoprofen is acidic in nature so it has low solubility in low pH but had good solubility in basic pH (I. E. Shohin, 2011).

3.1.3.1 Microdroplets and particle size analysis

All the formulations prepared under different continuous and dispersed phase flow rate ratios (Q_c/Q_d) were monodispersed, as per National Institute of Standards and Technology (*NIST*) definition (Table 3.1), having a CV less than 5%.

Table 3.1. Particle size information of various formulations

	Formulation	Q_c/Q_d	Mean particle diameter	Coefficient of variation (CV)*
1	Ke0	30 120	381 µm 288 µm	3.85% 1.23%
2	Ke2	30 120	352 µm 224 µm	4.48% 2.89%
3	Ke4	30 120	353 µm 217 µm	1.80% 4.01%
4	Ke6	30 120	346 µm 200 µm	1.29% 1.38%
5	Ke8	30	332 µm	2.70%
6	Ke85	30	332 µm	4.11%

*CV being equal to the ratio of the standard deviation to the mean particle diameter

Microparticles sizes are reported in Fig. 3.1 as a function of the value of Q_c/Q_d (= 30, 60 and 120), with different content of ethyl acrylate (EA). Illustrative pictures of the inline formation of the monomer microdroplets are reported Fig. 3.1a (see also video S1, S2 and S3 in the *Supplementary information* on web version of article), for Q_c/Q_d = 30, 60 and 120, and for %EA = 0, as well as micrographs of the polymerized microparticles Fig. 3.1c. Fig. 3.1b reports the sizes of the microdroplets before polymerization, and Fig. 3.1d reports the sizes of the microparticles after the complete polymerization. The size appears to be impacted by the Q_c/Q_d ratios and also decreased by the polymerization process. However, the EA amount does not induce significant variation of the sizes, even if a slight trend was drawn in Fig. 3.1 d reducing the size with an increase in %EA.

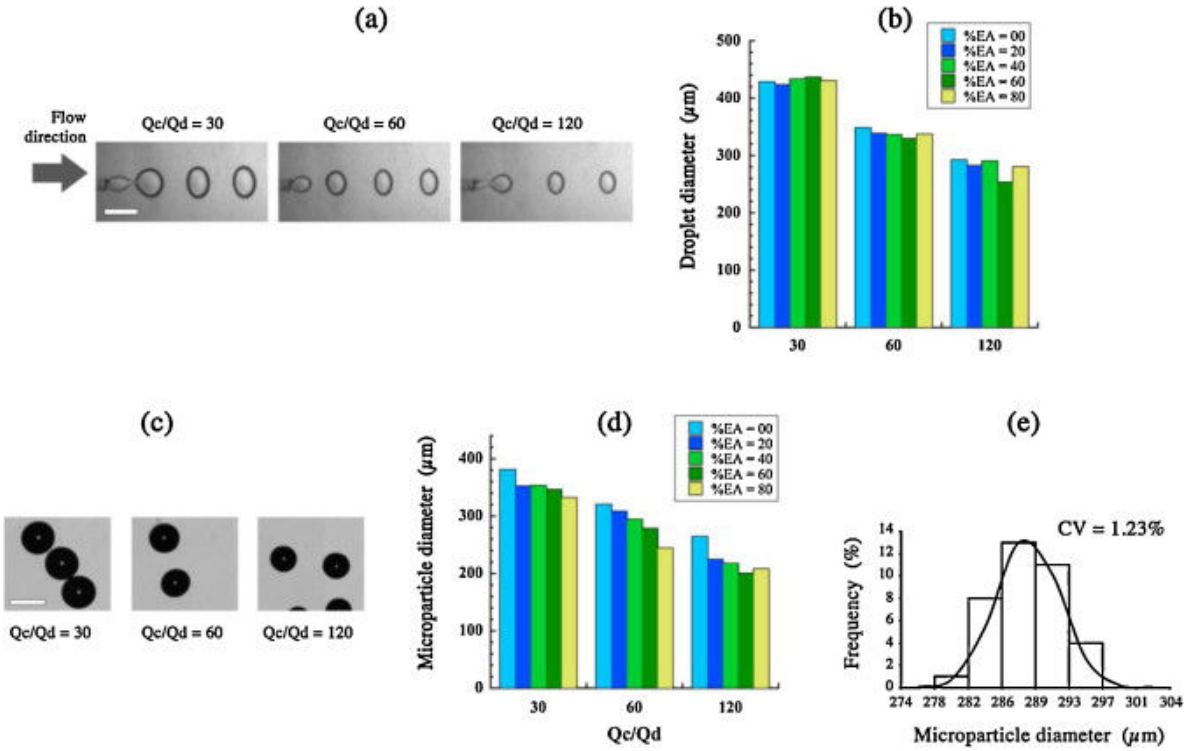

Fig. 3.1. Optical micrographs of droplet formation (a) and microbeads (c), scale bar is 500 µm. Influence of the continuous to dispersed phase flow rate ratio and ethyl acrylate weight content on the microdroplet (b) and microparticle (d) diameter. Typical microparticle size histogram for sample ke0 for Q_c/Q_d=120 (e).

It is known from literature that for given continuous and dispersed phase flow rates, the particles diameter decreases when the flow rate of the continuous phase increases or when the flow rate of the dispersed phase decreases (Bouquey et al., 2008). In addition, these results means that the flow-mediated droplet formation was not influenced by the

composition of the drops, and ethyl acrylate does not have significant interfacial activity to modify their size. After polymerization size contraction was observed which was likely due to reduced stiffness of polymer chain with reduction of TPGDA, and was in accordance with result of Tg of microbeads (Fig. 3.5).

Inter-droplet distance also increased with an increase in Q_c/Q_d ratio as shown in Fig. 3.1a (see also video S1, S2 and S3 in the *Supplementary information* section) but in all the cases system operated in dripping mode (Berkland et al., 2004).

Morphology and surface aspect of the polymeric microparticles were observed by scanning electron microscopy. The results are reported below in Fig. 3.2, showing different magnifications of the microparticles, for Q_c/Q_d = 30, 60 and 120, and for two representative ethyl acrylate contents, 60% and 80%. In order to facilitate the visual comparison of the samples, the scales are strictly the same between the different cases. The pictures reveal that microbeads are spherical in nature and have smooth surface. The influence of the flow rate ratio on the size was coherent with the optical measurements reported above in Fig. 3.1 d. In addition, SEM experiments disclose that, when the ethyl acrylate content was increased, the particles become rough and porous at highest content of EA (sizing around 1 to 4 µm) and reason is not known yet.

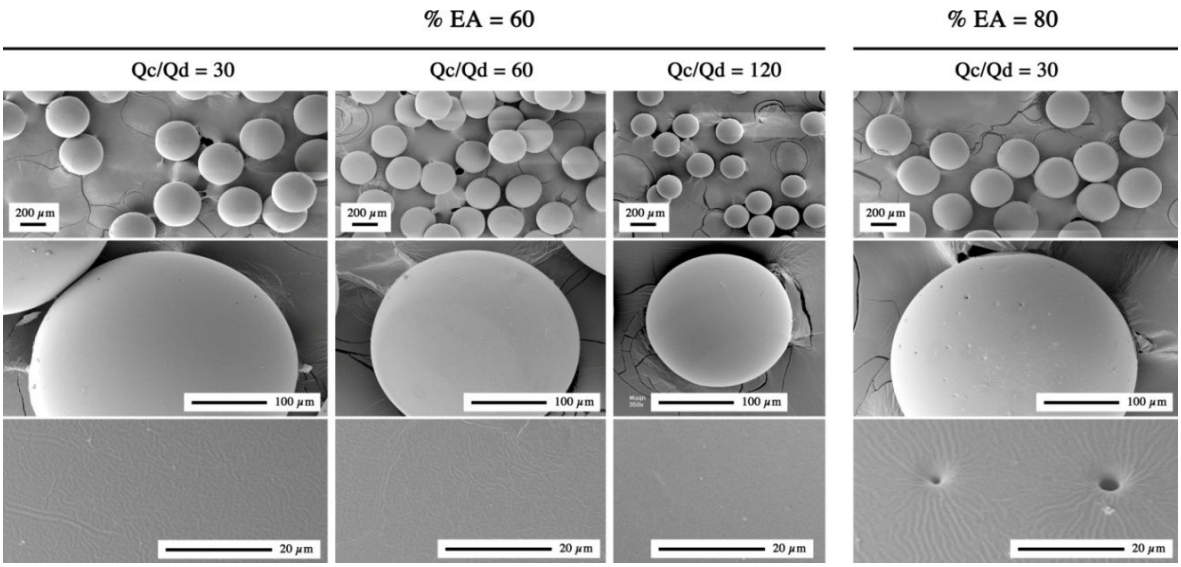

Fig. 3.2. Scanning electron microscopy of microbeads for different Q_c/Q_d ratio, for two different representative ethyl acrylate contents. Scales are the same over the different pictures.

3.1.3.2 Factors influencing encapsulation efficiency

Variation in the encapsulation efficiency as a function of the flow rate ratio and the EA content is presented in Fig. 3.3.

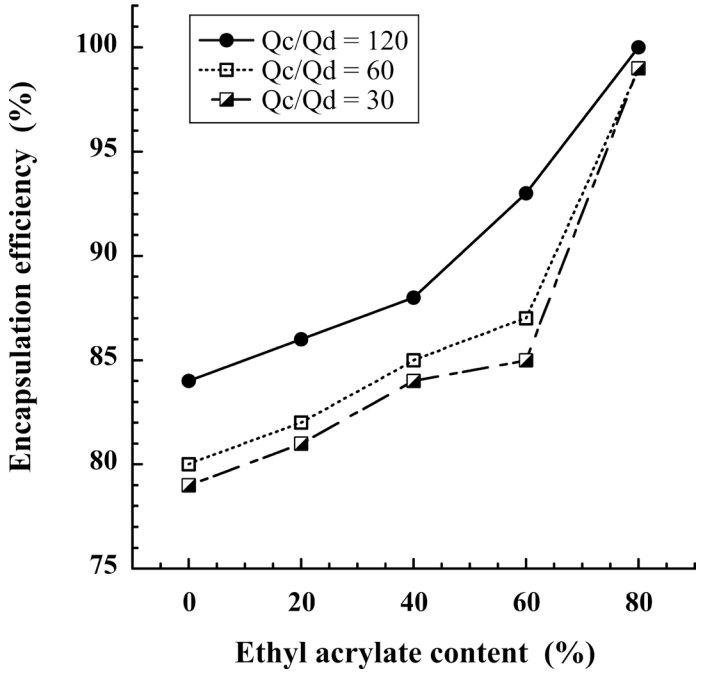

Fig. 3.3. Encapsulation efficiency of ketoprofen in microbeads, in function of the Q_c/Q_d ratio and ethyl acrylate content.

Values of the encapsulation efficiency appear significantly high around 80% to 100%, in function of the formulation parameters. *(a)* Increasing the EA content or *(b)* decreasing the microparticle size (directly linked to Q_c/Q_d), result in an increase in the encapsulation efficiency. Regarding the point *(a)*, a probable reason was due to abundant number of carbonyl groups in polymer chain. Caroboxyl group of ketoprofen will interact with carbonyl group and will not diffuse to surrounding media having pH around 6 to 7. Restani *et al.* found high encapsulation efficiencies in poly(1,3-glyceroldimethacrylate) (PGDMA) microparticles due to interaction between carboxylic group of ibuprofen and carbonyl and hydroxyl group of PGDMA network (Restani et al., 2010). As concerns the point *(b)* a probable reason for this is smaller droplet polymerizes faster than larger thus reducing the diffusion of ketoprofen. Berkland *et al.* found high encapsulation of piroxicam and rhodamine B in smaller size PLGA microspheres which is due to competition between diffusion and polymer precipitation (Berkland et al., 2003; Berkland et al., 2004).

3.1.3.3 FTIR analysis

Polymerization of monomer droplets were monitored by measuring absorbance of acrylate double bond stretching and bending vibrations at 1636 and 808 cm^{-1} respectively (Lee et al., 2003; Li et al., 2009). Under the provided conditions formulations containing methacrylate monomers (benzyl methacrylate and methyl methacrylate) failed to polymerize completely as one can see methacrylate double bond peaks in Fig. 4b; which may be due to slow reactivity of these monomers. But we do not see these peaks in formulations containing ethyl acrylate suggesting successful polymerization. FTIR of pure ketoprofen shows dimeric carboxylic acid carbonyl group stretching peak at 1692 cm^{-1} while the peak at 1652 cm^{-1} was referred to the ketonic carbonyl stretching vibration (Fig. 4a). The former was due to the fact that ketoprofen molecules are bound together in dimmers in a crystalline form (Fig. S2 in the *Supplementary information* section) which was in accordance with previous reports (Eerikäinen H, 2004; Sancin et al., 1999).

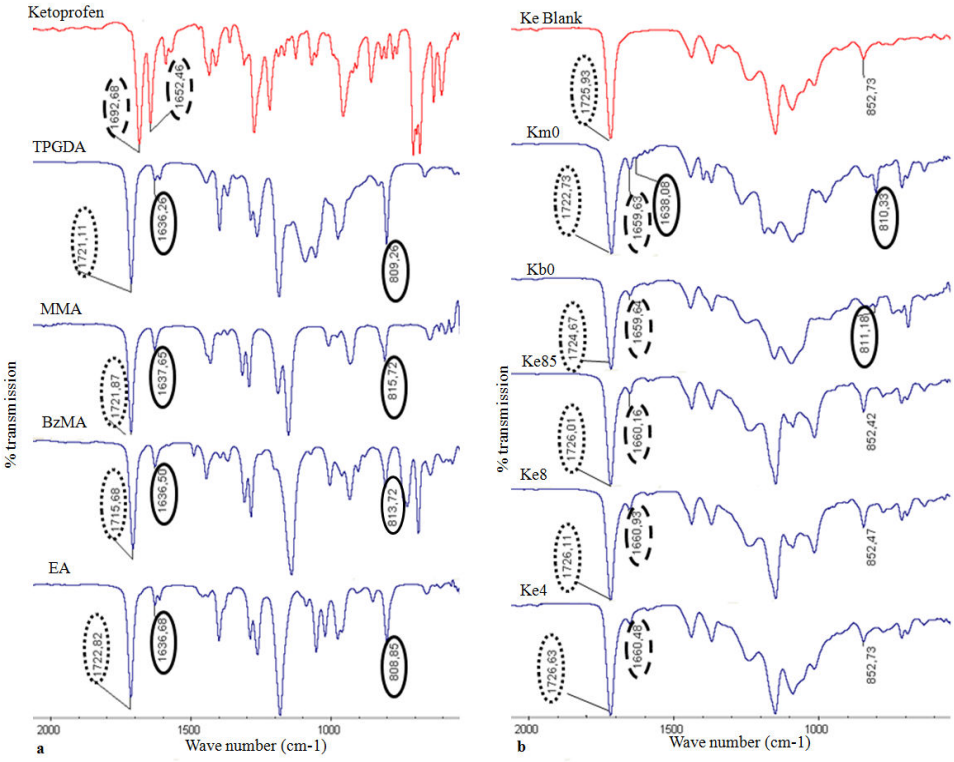

Fig. 4. (a) FTIR of ketoprofen and different monomers (b) FTIR of Blank microbeads containing TPGDA and ethyl acrylate in 50:50 ratios (ke Blank), Km0, Kb0, Ke85, Ke8 and ke4; (___) stretching and bending vibrations of acrylate, (.....) stretching vibrations of ester, (- - -) stretching vibrations of dimeric carboxylic and ketonic carbonyl group of ketoprofen.

In FTIR spectra of microbeads we observed ketoprofen ketonic peak at 1659 cm^{-1} but could not see carbonyl peak corresponding to 1692 cm^{-1} (Fig. 4b). It may be due to interaction between ketoprofen carboxylic group and carbonyl group of polymer resulting in disruption of crystalline dimer (Fig. S2 in the *Supplementary information* section) (Yu et al., 2010). Afterwards carboxylic acid stretching vibration was shifted to higher wavelengths and overlapped by strong ester vibrations of the polymer at 1725 cm^{-1}. We found some references of this kind in the literature (Blasi P, 2007; Eerikäinen H, 2004).

3.1.3.4 DSC measurements

Pure Ketoprofen gives endothermic peaks at 96˚C in DSC curves and is in agreement with literature (Del Gaudio P, 2009). In the drug loaded microbeads, endothermic peaks of ketoprofen disappeared suggesting the dispersion of drug at molecular level (Fig. 3.5). Yu *et al.* prepared solid dispersions of ketoprofen in nanofibers by electrospinning process with polyvinylpyrrolidone as the filament forming polymer and their DSC results reveals ketoprofen was distributed in the polymer nanofibers in an amorphous state (Yu et al., 2010). DSC also shows T_g of copolymers, which increases with an increase in the content of TPGDA. T_g of poly(TPGDA) microbeads was not clear from DSC graphs while T_g of copolymer lies between -15 to 20 ˚C. Thus incorporation of ethyl acrylate in copolymers helps to modify stiffness. Microbeads with low T_g were somehow sticky but the presence of TPGDA helps to maintain proper shape.

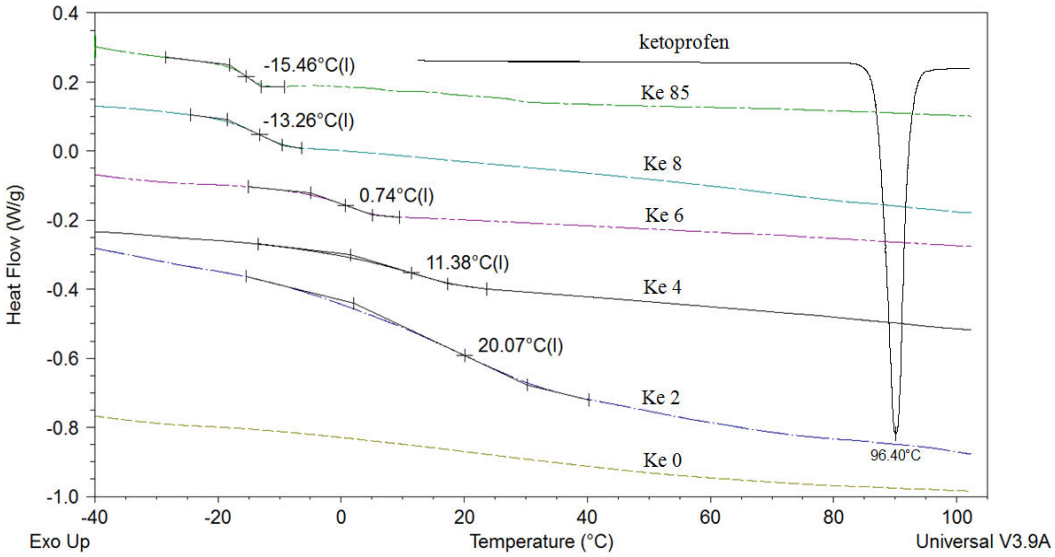

Fig. 3.5. DSC curves of pure ketoprofen and poly(TPGDA) and poly(TPGDA-co-EA) microbeads.

3.1.3.5 XRD analysis

XRD is one of the most sensitive techniques to acquire information about the molecular arrangement within the crystal (Khan IU et al., 2010). We obtained the diffraction patterns for pure ketoprofen, blank and different formulations. X-ray pattern demonstrates that the pure drug exhibited crystalline characteristics and these peaks show dramatic decline of intensity in all the formulations (Fig. 3.6) revealing the amorphous nature of ketoprofen in microbeads. This amorphous form will help to improve the drug's solubility in the dissolution media which finally may leads to better bioavailability.

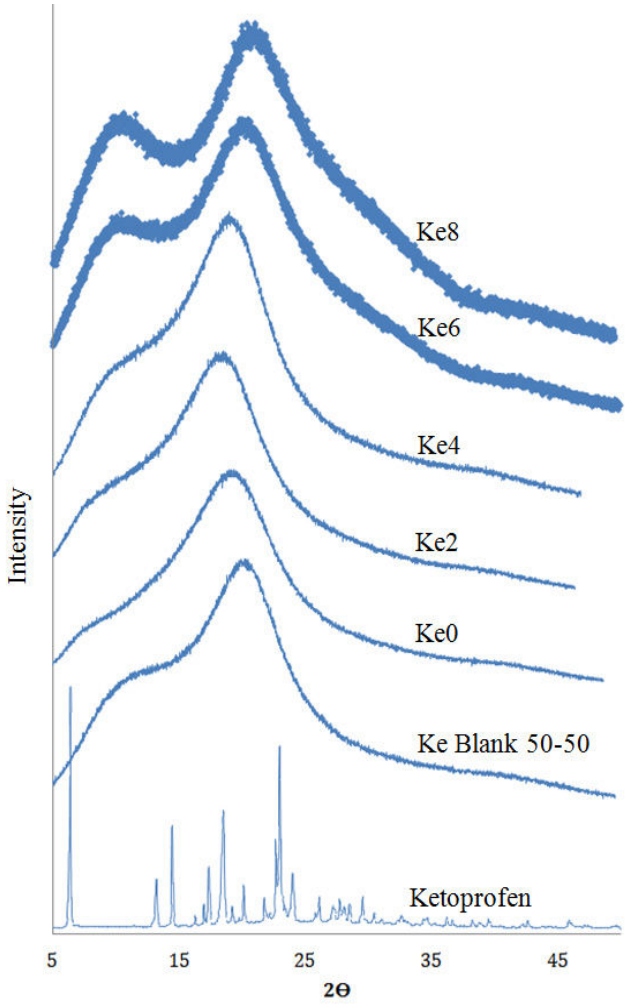

Fig.3.6. X-ray diffraction pattern of ketoprofen, blank and ketoprofen encapsulated microbeads.

3.1.3.6 *In vitro* ketoprofen release studies

Ketoprofen release from formulations containing different percentages of ethyl acrylate and TPGDA was investigated at pH 1.2 and 6.8 over a period of two and twenty four

hours respectively as shown in Fig. 3.7. At low pH (Fig. 3.7a) ketoprofen release within the residence time of stomach was less than 4% for all the formulations. Thus, our formulation will be able to protect the patient from peptic ulceration and anorexia associated with conventional dosage forms of this drug, administered thrice or four times orally (Silion et al., 2010). While at pH 6.8 (Fig. 3.7b) we observed gradual enhancement in cumulative percentage release, reaching 100% when ethyl acrylate concentration was varied from 20 to 85% in different formulations. As the drug release from microparticles depends on (1) imbibition of the release medium, (2) dissolution of the drug, and (3) drug release into the aqueous medium through a diffusion process (Stulzer et al., 2009). So, when the concentration of TPGDA was increased it forms a more compact and rigid polymer matrix which retards the chain relaxation and penetration of dissolution medium. Thus, at the highest concentration of TPGDA, ketoprofen cannot dissolve and remains in microbeads. But as we kept on increasing concentration of ethyl acrylate we get comparatively loose matrix, where surrounding fluid can diffuse easily to transport dissolved drug. Gander *et al.* found that drug release from dense macromolecular networks was rather slow due to extent of branching and entanglement of the polymeric chains which slows the diffusion process (Gander et al., 1989).

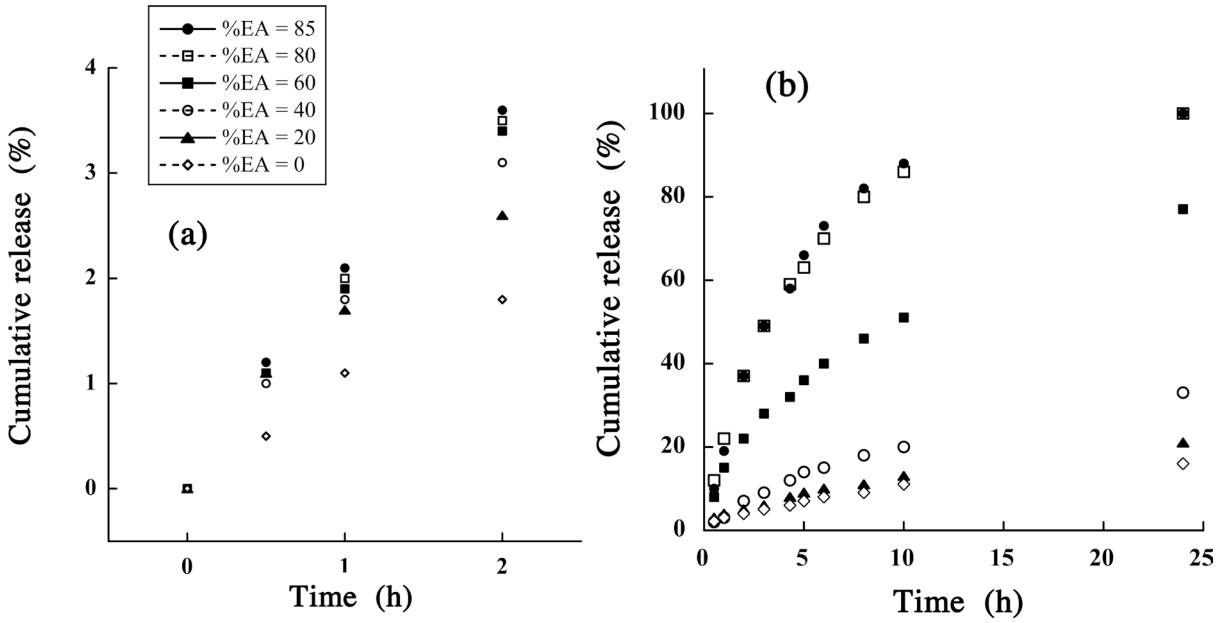

Fig. 3.7. Cumulative release profiles of ketoprofen encapsulated in microbeads for various ethyl acrylate contents at pH 1.2 (a) and pH 6.8 (b).

We were also able to improve the drug release rate from different formulation by reducing the size of microbeads as shown in Fig. 3.8. Yang *et al.* fabricated ampicillin loaded microparticles of different sizes in a microfluidic flow-focusing device and smaller microparticles showed faster release than bigger one (Yang et al., 2007). By reducing the size of the microbeads the specific surface area is increased (Mosharraf and Nyström, 1995) thus large surface area of smaller particles leads to faster release, on the other hand microbeads with larger diameters increased diffusion path length and decreased concentration gradient leading to slow release (Tran et al., 2011).

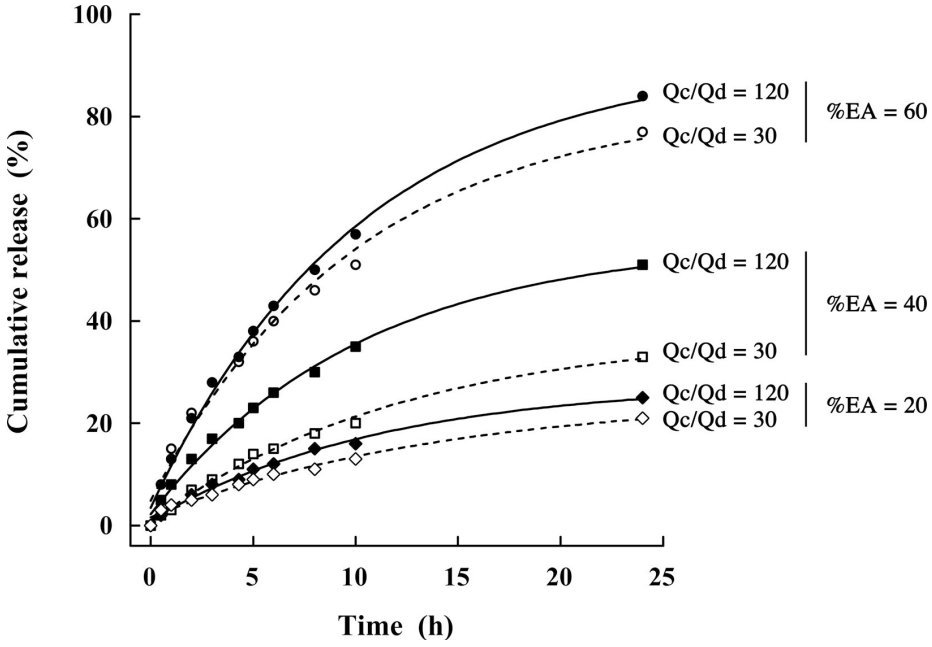

Fig. 3.8. Formulations prepared under various Q_c/Q_d (30, 120) showing different release profile as a function of particle size.

3.1.3.7 Drug release modeling

The drug release data from microbeads were evaluated by applying korsmeyers Peppas models. By plotting $\ln(M_t/M_\infty)$ versus $\ln(t)$, diffusional exponents were calculated from the slope by using linear regression analysis. The relative rate of diffusion and chain relaxation process is responsible for three different classes of diffusion, characterized by distinct values of the diffusional exponent (Silion et al., 2010). Table 3.2 shows that all of the formulations present good linearity ($R^2 \geq 0.98$) and values of the diffusion exponent (n) were between 0.5 and 1 suggesting that the ketoprofen release follows a non-Fickian diffusion mechanism.

Table 3.2 Ketoprofen modeling using Korsmeyer-Peppas model

S.No	Code	pH	Correlation coefficient (R^2)	Release rate constant (k)	Diffusion exponent (n)
1	ke85	1.2	0.9999	2.0882	0.79
		6.8	0.9894	2.9328	0.84
2	Ke8	1.2	0.9999	1.9797	0.82
		6.8	0.9940	3.0496	0.75
3	Ke6	1.2	0.9999	1.9182	0.82
		6.8	0.9869	2.6115	0.61
4	Ke4	1.2	0.9999	1.7787	0.80
		6.8	0.9864	1.2555	0.81
5	Ke2	1.2	0.9999	1.6948	0.62
		6.8	0.9810	1.3671	0.50
6	Ke0	1.2	0,9967	1.0203	0.84
		6.8	0,9921	1.0768	0.53

3.1.4 Conclusions

In this study we used an off-the-shelf co-axial microfluidic device for synthesizing poly(TPGDA-co-EA) microbeads with different EA weight contents encapsulating a lipophilic model drug (ketoprofen). This system allowed the rapid production of monodispersed microbeads in the size range of 200 to 380 µm with high encapsulation efficiency by environment friendly UV induced free radical polymerization. FTIR confirms the presence of ketoprofen molecules in all the formulations after UV polymerization. All formulations led to monodispersed microbeads having amorphous ketoprofen and smooth surface, but the surface becomes rougher with an increase in ethyl acrylate content. Ketoprofen encapsulation efficiency and release rate varied from 80% to 100% and from 16% to 100% respectively depending upon the EA weight content and particle size, both increasing by increasing the former and decreasing the latter. Moreover, some of the formulations allowed 100% sustained release of the drug at a constant rate over 24 h; thus will be useful to avoid side effect of multiple dosing and improving patient compliance. Finally, ketoprofen release from all formulations was successfully modeled by the Korsmeyer-Peppas equation for an anomalous diffusion mechanism. These results suggest that this setup hold great promise for efficient synthesis of polymeric microbeads for pharmaceutical applications.

In this section, it was shown that plain particle morphology was obtained, thanks to a simple but quite efficient capillary-base microdevice. Microbeads were able to deliver a single active molecule in a sustained release manner. However, one can question about the sustained release of two active molecules in GIT having different physicochemical properties, e.g. different solubility in monomer phase or incompatiblity. One answer lies in the Janus morphology. Thus the following section is dedicated to the synthesis of two drugs loaded Janus microparticles, thanks to a slight modifciation of the original capillary-based device presented in previous section.

3.1.5 Supplementary information

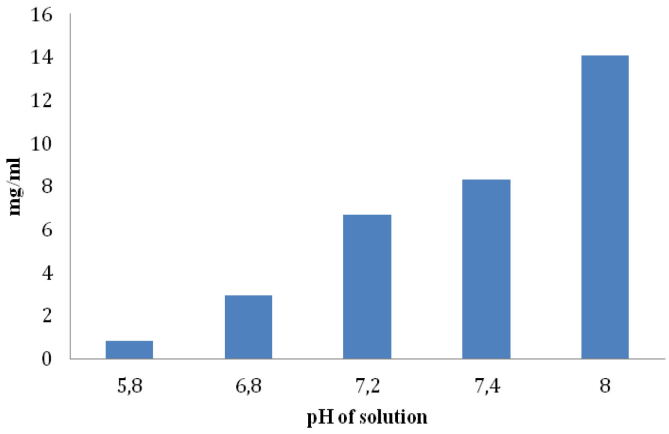

Fig. S1. pH solubility profile of ketoprofen.

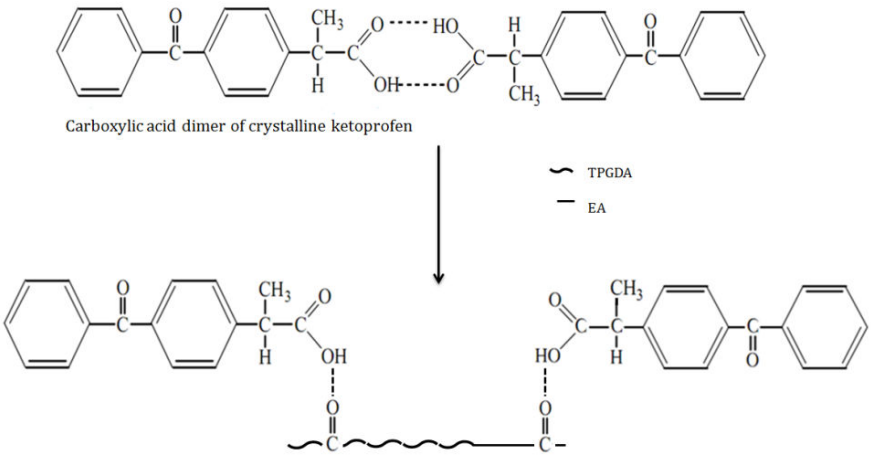

Fig. S2. Breakage of ketoprofen-ketoprofen intermolecular hydrogen bonding present in crystaline lattice.

Video S1: Droplet formation of Ke0 formulation at Qc/Qd 30 See web version of research article
Video S2: Droplet formation of Ke0 formulation at Qc/Qd 60 See web version of research article
Video S3: Droplet formation of Ke0 formulation at Qc/Qd 120 See web version of research article

References

Arida, A.I., Al-Tabakha, M.M., 2007. Encapsulation of ketoprofen for controlled drug release. European Journal of Pharmaceutics and Biopharmaceutics 66, 48-54.

Berkland, C., Kim, K., Pack, D.W., 2003. PLG Microsphere Size Controls Drug Release Rate Through Several Competing Factors. Pharmaceutical Research 20, 1055-1062.

Berkland, C., Kipper, M.J., Narasimhan, B., Kim, K., Pack, D.W., 2004. Microsphere size, precipitation kinetics and drug distribution control drug release from biodegradable polyanhydride microspheres. Journal of Controlled Release 94, 129-141.

Blasi P, S.A., Giovagnoli S, Perioli L, Ricci M, Rossi C., 2007. Ketoprofen poly(lactide-co-glycolide) physical interaction. AAPS PharmSciTech. 8, E1-E8.

Bouquey, M., Serra, C., Berton, N., Prat, L., Hadziioannou, G., 2008. Microfluidic synthesis and assembly of reactive polymer beads to form new structured polymer materials. Chemical Engineering Journal 135, Supplement 1, S93-S98.

Crivello, J.V., 1999. UV and electron beam-induced cationic polymerization. Nuclear Instruments and Methods in Physics Research Section B: Beam Interactions with Materials and Atoms 151, 8-21.

Dalmoro, A., Barba, A.A., Lamberti, G., d'Amore, M., 2012. Intensifying the microencapsulation process: Ultrasonic atomization as an innovative approach. European Journal of Pharmaceutics and Biopharmaceutics 80, 471-477.

Del Gaudio P, R.P., Rosaria Lauro M, Colombo P, Aquino RP., 2009. Encapsulation of ketoprofen and ketoprofen lysinate by prilling for controlled drug release. AAPS PharmSciTech. 10, 1178-1185.

Eerikäinen H, P.L., Raula J, Hirvonen J, Kauppinen EI., 2004. Nanoparticles containing ketoprofen and acrylic polymers prepared by an aerosol flow reactor method. AAPS PharmSciTech. 5, 129–137.

Fang, A., Cathala, B., 2011. Smart swelling biopolymer microparticles by a microfluidic approach: Synthesis, in situ encapsulation and controlled release. Colloids and Surfaces B: Biointerfaces 82, 81-86.

Gander, B., Gurny, R., Doelker, E., Peppas, N.A., 1989. Effect of Polymeric Network Structure on Drug Release from Cross-Linked Poly(Vinyl Alcohol) Micromatrices. Pharmaceutical Research 6, 578-584.

Holgado, M.A., Arias, J.L., Cózar, M.J., Alvarez-Fuentes, J., Gañán-Calvo, A.M., Fernández-Arévalo, M., 2008. Synthesis of lidocaine-loaded PLGA microparticles by flow focusing: Effects on drug loading and release properties. International Journal of Pharmaceutics 358, 27-35.

Huang, K.-S., Lu, K., Yeh, C.-S., Chung, S.-R., Lin, C.-H., Yang, C.-H., Dong, Y.-S., 2009. Microfluidic controlling monodisperse microdroplet for 5-fluorouracil loaded genipin-gelatin microcapsules. Journal of Controlled Release 137, 15-19.

Hung, L.-H., Teh, S.-Y., Jester, J., Lee, A.P., 2010. PLGA micro/nanosphere synthesis by droplet microfluidic solvent evaporation and extraction approaches. Lab on a Chip 10, 1820-1825.

I. E. Shohin, J.I.K., G. V. Ramenskaya, and G. F. Vasilenko, 2011. Evaluation of In Vitro Equivalence for Drugs Containing BCS Class II Compound Ketoprofen. Dissolution Technologies 18, 26-29.

Khan IU, Ranjha NM, HQ, M., 2010. Development of ethylcellulose-polyethylene glycol and ethylcellulose-polyvinyl pyrrolidone blend oral microspheres of ibuprofen. J. DRUG DEL. SCI. TECH. 20, 439-444.

Lee, T.Y., Roper, T.M., Jonsson, E.S., Kudyakov, I., Viswanathan, K., Nason, C., Guymon, C.A., Hoyle, C.E., 2003. The kinetics of vinyl acrylate photopolymerization. Polymer 44, 2859-2865.

Li, G., Guo, J., Wang, X., Wei, J., 2009. Microencapsulation of a functional dye and its UV crosslinking controlled releasing behavior. Journal of Polymer Science Part A: Polymer Chemistry 47, 3630-3639.

Ma, S., Song, G., Li, W., Fan, P., Tang, G., 2010. UV irradiation-initiated MMA polymerization to prepare microcapsules containing phase change paraffin. Solar Energy Materials and Solar Cells 94, 1643-1647.

Mosharraf, M., Nyström, C., 1995. The effect of particle size and shape on the surface specific dissolution rate of microsized practically insoluble drugs. International Journal of Pharmaceutics 122, 35-47.

Park, J., . Saffari, A,. Kumar, S,. Günther, A,. Kumacheva, E,. 2010. Microfluidic Synthesis of Polymer and Inorganic Particulate Materials. Annual Review of Materials Research 40, 415-443.

Restani, R.B., Correia, V.G., Bonifácio, V.D.B., Aguiar-Ricardo, A., 2010. Development of functional mesoporous microparticles for controlled drug delivery. The Journal of Supercritical Fluids 55, 333-339.

Sancin, P., Caputo, O., Cavallari, C., Passerini, N., Rodriguez, L., Cini, M., Fini, A., 1999. Effects of ultrasound-assisted compaction on Ketoprofen/Eudragit® S100 Mixtures. European Journal of Pharmaceutical Sciences 7, 207-213.

Serra, C.A., Chang, Z., 2008. Microfluidic-Assisted Synthesis of Polymer Particles. Chemical Engineering & Technology 31, 1099-1115.

Silion, M., Hritcu, D., Jaba, I., Tamba, B., Ionescu, D., Mungiu, O., Popa, I., 2010. In vitro and in vivo behavior of ketoprofen intercalated into layered double hydroxides. Journal of Materials Science: Materials in Medicine 21, 3009-3018.

Stulzer, H.K., Tagliari, M.P., Parize, A.L., Silva, M.A.S., Laranjeira, M.C.M., 2009. Evaluation of cross-linked chitosan microparticles containing acyclovir obtained by spray-drying. Materials Science and Engineering: C 29, 387-392.

Takeuchi S, G.P., Weibel DB, Whitesides GM, 2005. An Axisymmetric Flow-Focusing Microfluidic Device. Advanced Materials 17, 1067-1072.

Tran, V.-T., Benoît, J.-P., Venier-Julienne, M.-C., 2011. Why and how to prepare biodegradable, monodispersed, polymeric microparticles in the field of pharmacy? International Journal of Pharmaceutics 407, 1-11.

Wang, J.-T., Wang, J., Han, J.-J., 2011. Fabrication of Advanced Particles and Particle-Based Materials Assisted by Droplet-Based Microfluidics. Small 7, 1728-1754.

Xia, J., Xu, Y., Lin, J., Hu, B., 2008. UV-induced polymerization of urushiol without photoinitiator. Progress in Organic Coatings 61, 7-10.

Xu, Q., Hashimoto, M., Dang, T.T., Hoare, T., Kohane, D.S., Whitesides, G.M., Langer, R., Anderson, D.G., 2009. Preparation of Monodisperse Biodegradable Polymer Microparticles Using a Microfluidic Flow-Focusing Device for Controlled Drug Delivery. Small 5, 1575-1581.

Yang, C.-H., Huang, K.-S., Chang, J.-Y., 2007. Manufacturing monodisperse chitosan microparticles containing ampicillin using a microchannel chip. Biomedical Microdevices 9, 253-259.

Yang, C.H., Huang, K.S., Lin, Y.S., Lu, K., Tzeng, C.C., Wang, E.C., Lin, C.H., Hsu, W.Y., Chang, J.Y., 2009. Microfluidic assisted synthesis of multi-functional polycaprolactone microcapsules: incorporation of CdTe quantum dots, Fe3O4 superparamagnetic nanoparticles and tamoxifen anticancer drugs. Lab on a Chip 9, 961-965.

Yu, D.-G., Branford-White, C., Shen, X.-X., Zhang, X.-F., Zhu, L.-M., 2010. Solid Dispersions of Ketoprofen in Drug-Loaded Electrospun Nanofibers. Journal of Dispersion Science and Technology 31, 902-908.

3.2 Microfluidic conceived drug loaded Janus particles in side-by-side capillaries device

Graphical Abstract

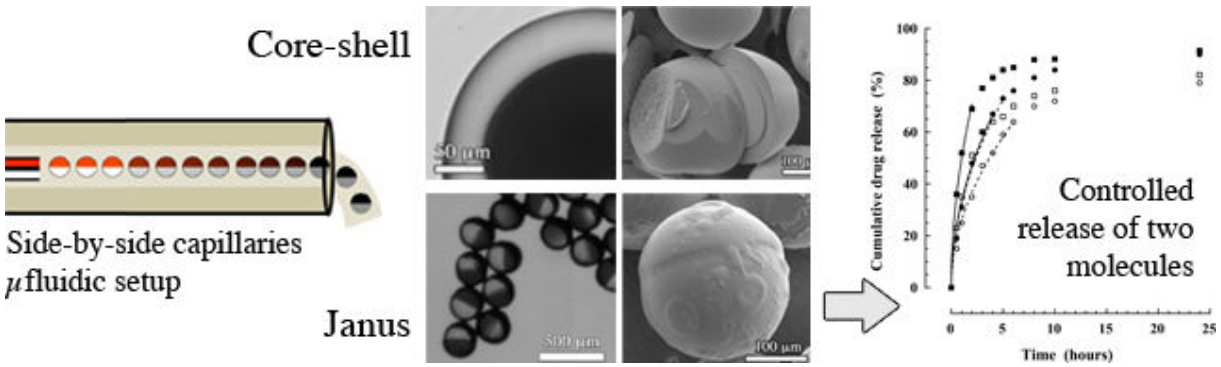

Abstract

A side-by-side capillaries microfluidic device was developed to fabricate drug loaded poly(acrylamide)/poly(methyl acrylate) Janus particles in the range of 59 to 240 µm by UV-assisted free radical polymerization. This system was characterized in terms of continuous and dispersed phases flow rates ratio (Q_c/Q_d), monomer composition of the two compartments, surfactant nature and concentration, outlet tube diameter and UV intensity. These factors were adequately controlled to get different particle shapes ranging from core-shell to bi-compartmental particles. For the latter, a low surfactant concentration (0.75 wt.%) was necessary when the two dispersed phases were pumped at equal flow rate, while at high surfactant concentration, dispersed phases flow rates have to be changed. FTIR analysis suggested complete polymerization of monomers and cytotoxicity test showed these particles were biocompatible having LD50 of 9 mg/mL. Both ketoprofen and sodium fluorescein were released in sustained release manner at pH 6.8 by following a diffusion type release mechanism. Drug release was faster for bigger particles and found to result from the irregular distribution of the two phases and indentation on bigger particles as revealed by SEM analysis. In comparison, sodium fluorescein release was slower which was attributed to low encapsulation but could be modified by decreasing crosslinker concentration.

Keywords: Microfluidics, Janus particles, drug delivery, poly(acrylamide), poly(methyl acrylate), cytotoxicity

3.2.1 Introduction

Active pharmaceutical ingredients (APIs) can be administered orally, intravenously, intramuscularly or subcutaneously but still oral route of administration remains most physiological and convenient way to deliver drugs (Delie and Blanco-Príeto, 2005). One can develop drug delivery systems that carry its payload in a sustained release manner or to a specific region within the gastrointestinal tract for a local or systemic action. Different dosage forms are used for oral administration but microparticles have certain advantages over single unit systems like less chance of dose dumping and local irritation, increased bioavailability, low dependence on gastric emptying time etc. Microencapsulation is a widely and well established method used to develop microparticles where active materials are entrapped in microparticles through formation of a thin coating for protection of drug from heat, light, surrounding environment etc., cosmetics, imaging, controlled release, reduced administration frequency, patient comfort and compliance (Chen et al., 2005; Khan et al., 2013b; Nokhodchi A, 2002; Pereira et al., 2014; Tran et al., 2011).

There are different kinds of microparticles among which Janus particles are currently attracting a lot of interest. These particles have two different areas with dissimilar chemistry, polarity, functionalization or other properties with roughly equal surface area (Yang et al., 2012). By now this definition is getting more general and includes multi-segment structures with regions of different compositions co-existing in asymmetric geometries.

These biphasic particles were first reported way back in 1970s by Xerox society with white and black plastic hemispheres and used in twisting-ball display (Marquis et al., 2012). In 1985, Cho and Lee (Cho and Lee, 1985) gave the name Janus after polymerization of asymmetric poly(styrene)/poly(methyl methacrylate) emulsion. Nowadays Janus particles are produced by templating, colloidal assembly, lithography techniques, glacing-angle deposition, nanosphere lithography, and microfluidic flow methods. Microfluidic devices and methods have some advantages over conventional encapsulation methods, for instance allowing the production of particle with narrow size distribution, high encapsulation efficiency not to mention the possibility to obtain different morphologies and shapes (Marquis et al., 2012). So far, considerable efforts are made to make drug loaded microgels, microcapsules, microbeads, core-shell particles and vesicular systems by microfluidics. These

attempts are discussed in detail in many review articles (Capretto et al., 2013; Khan et al., 2013b, c; Serra et al., 2013; Zhao, 2013). To date, Janus particles are gaining importance in optics, magnetics, plasmonics and chemistry owing to their fascinating properties. In formulation science, considerable interest is raised by the possibility to deliver two drugs or diagnostic agents simultaneously. In general, it is not suitable to encapsulate two molecules in single phase if they have dissimilar solubility and furthermore drugs with dissimilar physicochemical properties can cause difficulties in drug release (Xie et al., 2012). So encapsulating them in Janus particles would provide suitable alternative solution to above mentioned problems.

In the current study, we used capillary-based microfluidic device having two side-by-side capillaries. This setup gives rise to biphasic-droplets composed of hydrophilic and hydrophobic monomers and model drugs with different solubility range respectively. Further downstream, these droplets are polymerized by UV irradiation far away from maximum absorption wavelength of the two API to get drug loaded Janus particles while maintaining integrity of both molecules. To our best of knowledge this is first attempt to encapsulate APIs in Janus microparticles that will open new strategies to deliver combination of drugs.

3.2.2 Experimental

I. *List of materials is given in Chapter 2 section 2.1*
II. *Description of the side-by-side capillaries-based device and overall Janus particle synthesis process is provided in Chapter 2, section 2.2.2*
III. *Methods for particle characterization are detailed in Chapter 2, section 2.3.2 while encapsulation efficiency and release properties are determined following the procedure described in Chapter 2, section 2.3.1.2 and 2.3.1.7 respectively*

3.2.3 Results and discussion

Off-the-shelves capillaries-based microfluidic droplet generator was assembled within ten to fifteen minutes and used to produce size-controlled Janus particles. Two model drugs, with quite different physicochemical properties, namely ketoprofen (hydrophobic) and sodium fluorescein (hydrophilic) were incorporated in acrylamide/methyl acrylate Janus droplets and then photopolymerized (at 365 nm) to fix the droplet geometry far away from maximum absorption wave length of two active molecules. This insures integrity of drug in final product as already reported in our previously published work (Khan et al., 2013b).

3.2.3.1 Confirmation of Janus structure and particle size

Immediately after polymerization, particles were washed repeatedly with ethyl acetate to remove silicon oil then dried overnight at room temperature. Approximately fifty randomly selected dried polymerized Janus particles were imaged by optical microscopy and analyzed with Hiris version 3 (R & D Vision) software to determine average diameter and CV. In most of the cases CV was less than 5% (Fig. 3.13, 3.14, and 3.15). Size of particle was influenced by the flow rate of the two phases, outlet tubing internal diameter which will be discussed in detail in subsequent sections. In optical images one can clearly differentiate between two parts, thanks to presence of alcohol soluble nigrosin black in methyl acrylate phase. Raman signals from two segments of Janus particles were different, indicating different chemistry on two sides. Further confirmation was provided by SEM micrographs where one can clearly see two different sides in all the formulation tested (Fig.3.9).

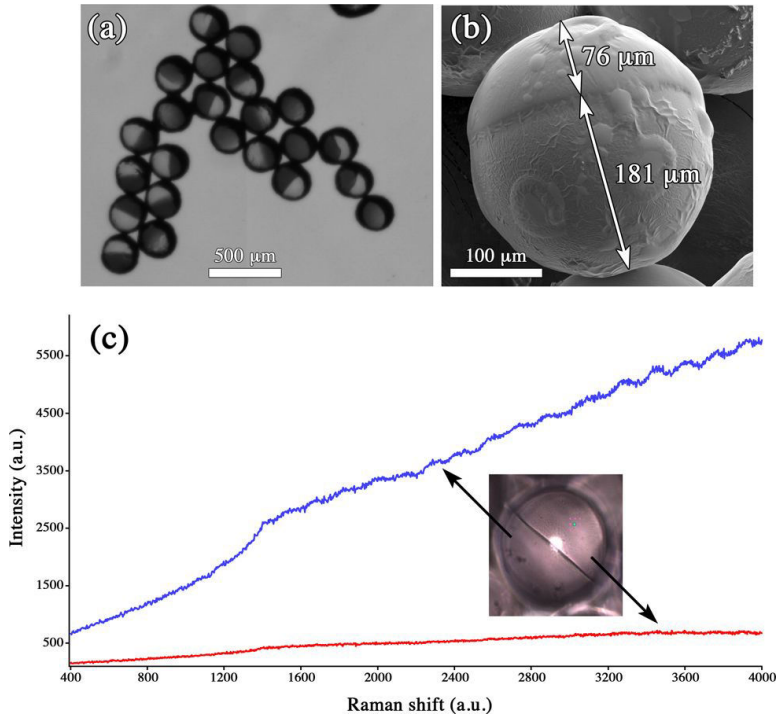

Fig. 3.9. Confirmation of Janus structure by: optical micrograph of formulation J1 after drying (a), SEM picture of J1 (250 µm) showing two compartments (181 and 76 µm for hydrophobic and hydrophilic portion respectively) containing two API of different hydrophilicities (b) and Raman spectra showing different peaks from separate compartments, ketoprofen (red) sodium fluorescein (blue) (c). Flow rate of the hydrophobic and hydrophilic phases were 5-2

µL/min respectively, whereas silicon oil was pumped at 240 µL/min. UV intensity was set to 40% and internal diameter of the collecting tube was 1.6 mm.

3.2.3.2 Effect of different factor on Janus structure

3.2.3.2.1 Effect of flow rate on Janus structure

The flow rate of two dispersed phases plays an important role in overall shape of Janus particles. Formulation J7 was used to study this effect. The flow rate ratio between hydrophobic and hydrophilic phase was set to 2-2, 3-2, 4-2, 5-2 µL/min while continuous phase was pumped at 240 µL/min. At same flow rates, core-shell structure was observed while when hydrophobic phase flow rate was increased one got acorn-like Janus particles and at even higher flow rates bi-compartmental Janus particles are observed. It was because at equal flow rate ratio concentration of surfactant (3 wt.%) was enough to emulsify the methyl acrylate phase. On increasing the flow rate of hydrophobic phase this concentration of surfactant was not enough to emulsify the whole methyl acrylate phase completely but rather partially to maintain interface between two phases. This gives to particles ranging from core-shell to bi-compartmental Janus just by changing flow rate (Fig. 3.10).

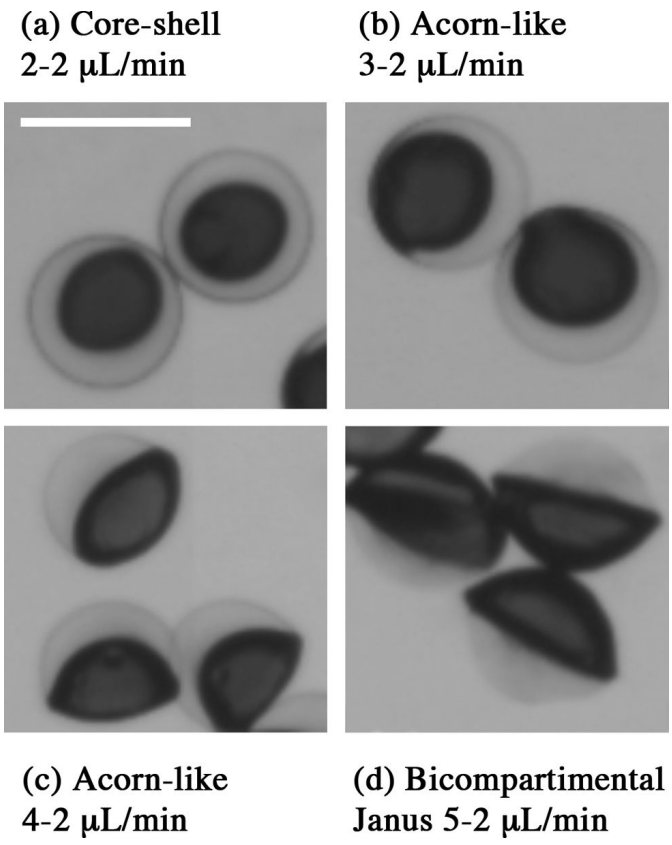

Fig. 3.10. Effect of flow rate of two dispersed phases by using formulation J7. The flow rates of hydrophobic and hydrophilic phases were 2-2 (a) 3-2 (b) 4-2 (c) 5-2 (d) µL/min, whereas silicon oil was pumped at 240 µL/min. Optical micrographs were taken immediately after photopolymerizing with 40% UV intensity and collecting tube having 1.6 mm ID. Scale bar represents 300 µm.

3.2.3.2.2 Effect of surfactant on Janus structure

Initial trials with acrylamide and ethyl acrylate suggested that surfactant is necessary to get bi-phasic particles (See supplementary information S3). Literature reveals that to form Janus particles from two immiscible liquids, both streams should run in parallel without disturbance and interface between these two liquids must be stable (Chen et al., 2009). Thus, interface can be stabilized by help of surfactants. Usually combination of surfactant is more effective. To study this effect, we used formulation J7, keeping the flow of two dispersed phases constant and only changing the surfactant concentration. One observed that putting high concentration of surfactant (3 wt.%) in hydrophilic phase resulted in a core-shell structure, while at low concentration (0.75 wt.%) Janus particles are obtained. Intermediate concentrations produced eccentric core-shell particles (Fig. 3.11).

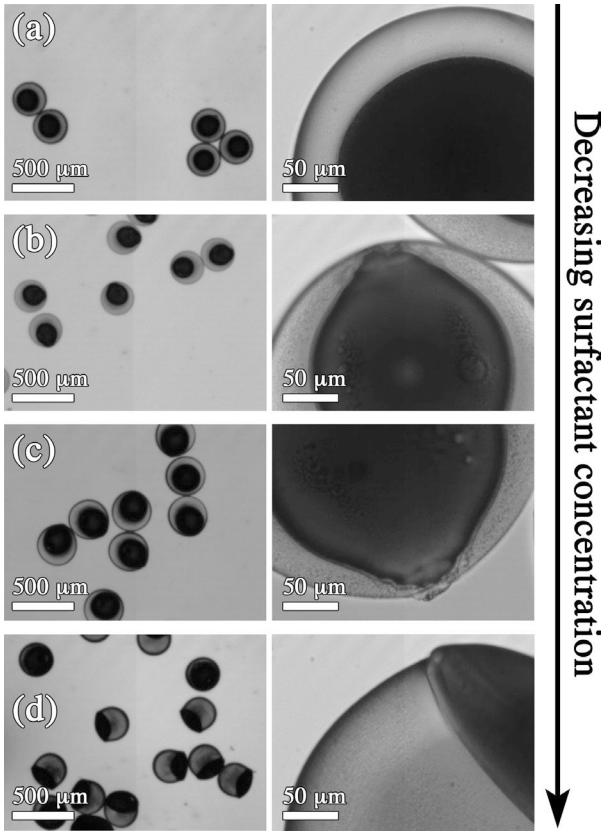

Fig. 3.11. Effect of surfactants concentration (wt.%). Constant evolution of Janus particle was seen as the concentration of surfactants decreased from formulation J7 to J11. Flow rates of hydrophobic and hydrophilic phases were kept constant at 2 µL/min, whereas silicon oil was pumped at 240 µL/min. Optical micrographs are taken immediately after polymerization at 40% UV intensity and outlet tubing having 1.6 mm ID.

Here, critical micellar concentration (CMC) of surfactants play important role. Amphiphilic structures are well known to forms core-shell like structures above CMC (Khan et al., 2013a). In our case when concentrations of surfactants were well above CMC (SDS 6 to 8mM or 0.1728 to 0.2304% w/v, Tween 80 0.012 mM or 0.0016% w/v) (Flores et al., 2001; Samanta and Ghosh, 2011; Shi et al., 2011) core-shell particles are obtained. When they are below the CMC surfactants align along the interface to stabilize it.

3.2.3.2.3 Effect of monomeric composition on Janus structure

Monomeric composition plays an important role in final particle characteristics. Addition of a bifunctional monomer was found to have a prominent effect on shape. Thus, in case of bicompartmental particles, addition of 7.5 wt.% of tripropyleneglycol diacrylate (TPGDA) resulted in a rugby shape Janus particles. Its presence in core-shell particles also gave a clear cut differentiation between core and shell which was not the case when methyl acrylate was used as core phase alone. It may be due to low glass transition (Tg) temperature of poly(methyl acryalte) which is around 9˚C. Addition of TPGDA to hydrophobic phase increases the Tg of polymer and can held core in a distinct shape (Fig. 3.12 d). In our previous study we observed increase in Tg of ethyl acrylate on addition of TPGDA to drug loaded poly(TPGDA-co-EA) microbeads (Khan et al., 2013b). Furthermore, on decreasing concentration of acrylamide to 20 and 10 wt.% resulted in two new morphologies which were named as helmet- and UFO-like Janus particles (Fig. 3.12 e and f).

3.2.3.3 Factors controlling the size of Janus microparticles

In microfluidic devices, particle size can be controlled by increasing viscosity and flow rate of continuous phase or decreasing the very same parameters for dispersed phase. It can also be decreased by decreasing the characteristic dimension of microchannels or capillaries. In current study, different strategies were investigated to modify particles size, namely (a)

outlet internal diameter, (b) combined effect of flow-focusing and flow rate and (c) UV intensity.

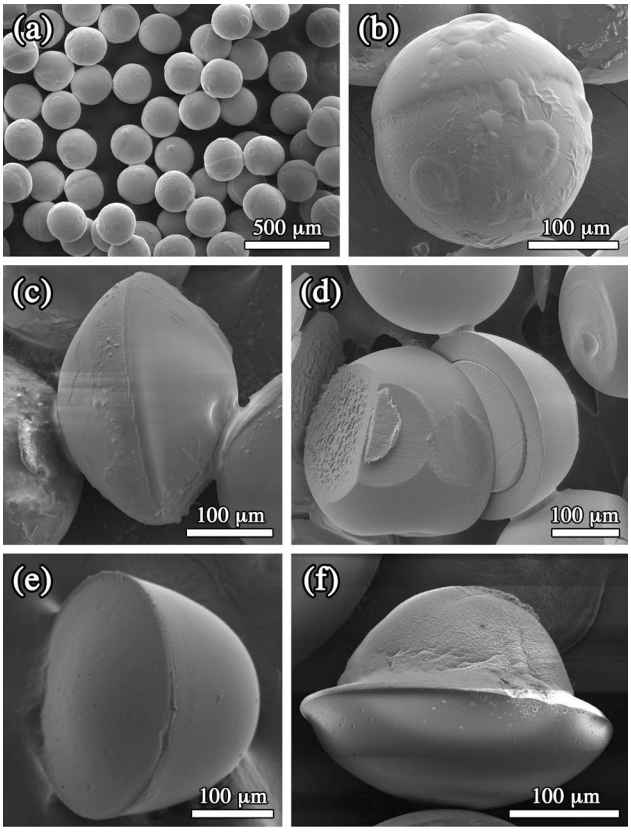

Fig. 3.12. SEM photographs showing effect of monomer contents and flow rates of hydrophobic and hydrophilic phases respectively on morphology: bicompartmental Janus particles, J1 5-2 µL/min (a, b); rugby-like Janus particle, J4 5-2 µL/min (c); core-shell particle, J4 2-2 µL/min (d); helmet-like Janus particle, J5 2-2 µL/min (e); UFO-like Janus particle, J6 2-2 µL/min (f). Silicon oil was pumped at 240 µL/min, UV intensity was 40% and collecting tube had an internal diameter of 1.6 mm.

To study first strategy (a), formulation J11 was operated under same conditions except changing outlet tube internal diameter (1.6, 1 and 0.5 mm). Changing this diameter changes the velocity of the continuous phase which in turn alters the shear rate acting on biphasic droplets during their formation at capillaries tips. The smaller the dimension of the collecting tube, the higher is the shear rate, the smaller are the droplets and subsequent particles after UV photopolymerization as shown in Fig. 3.13. All the particles were monodispersed except for collecting tube with 0.5 mm internal diameter where CV was 27%. This was because at higher shear rates frequency of droplet generation was high with

smaller inter droplet distance. Here, in the absence of surfactant in continuous phase, viscosity of silicon oil was not enough to prevent collision of droplets.

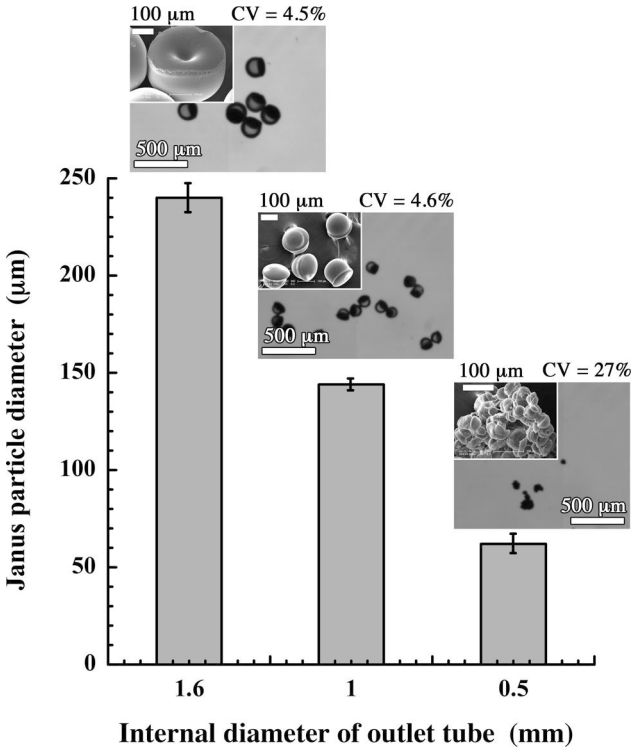

Fig. 3.13. SEM and optical micrographs showing the effect of outlet internal diameter on Janus particle size using formulation J11. Flow rates of hydrophobic and hydrophilic phases were kept constant at 2 µL/min, whereas silicon oil was pumped at 240 µL/min. UV intensity was 40%. Optical images are taken after drying. Error bar indicates standard deviation (n=3).

For strategy (b), we modified our original device to accommodate a flow-focusing section and combined this modification with different continuous to dispersed phase ratios (Q_c/Q_d). By reducing the cross section of the outlet tubing (down to 350 µm), the flow-focusing section increases locally the velocity of the continuous phase which in turn increases the shear force acting on the to-be formed droplets. Conversely to the co-flow configuration, where the droplet formation was observed at capillaries tips, the addition of the flow–focusing section made the droplet formation locus past the restriction (see Video V1 and V2 in supplementary section). This phenomena is well documented in the literature (Nie et al., 2008; Teh et al., 2008) and results from the high velocity of the continuous phase which elongates the droplet meniscus till restriction where sudden drop in continuous phase velocity induces droplet break-off (Fig. 3.14b and video V2 in supplementary section). Thus,

the higher symmetric shear imposed by the continuous phase on dispersed phases enabled smaller, controlled and stable generation of droplets (Teh et al., 2008). This results in smaller particles as compare to co-flow configuration under almost similar conditions (109 µm, CV 4.7% compared to 144 µm, CV 4.6%). Furthermore, when Q_c/Q_d was changed from 60 to 120 and 240 even smaller droplets with high droplet frequency was observed. At high frequency it was difficult to prevent the collision of droplets as silicon oil phase was devoid of surfactant, thus, resulting in Janus particles with higher CV (Fig. 3.14a and video V2b and c in supplementary section).

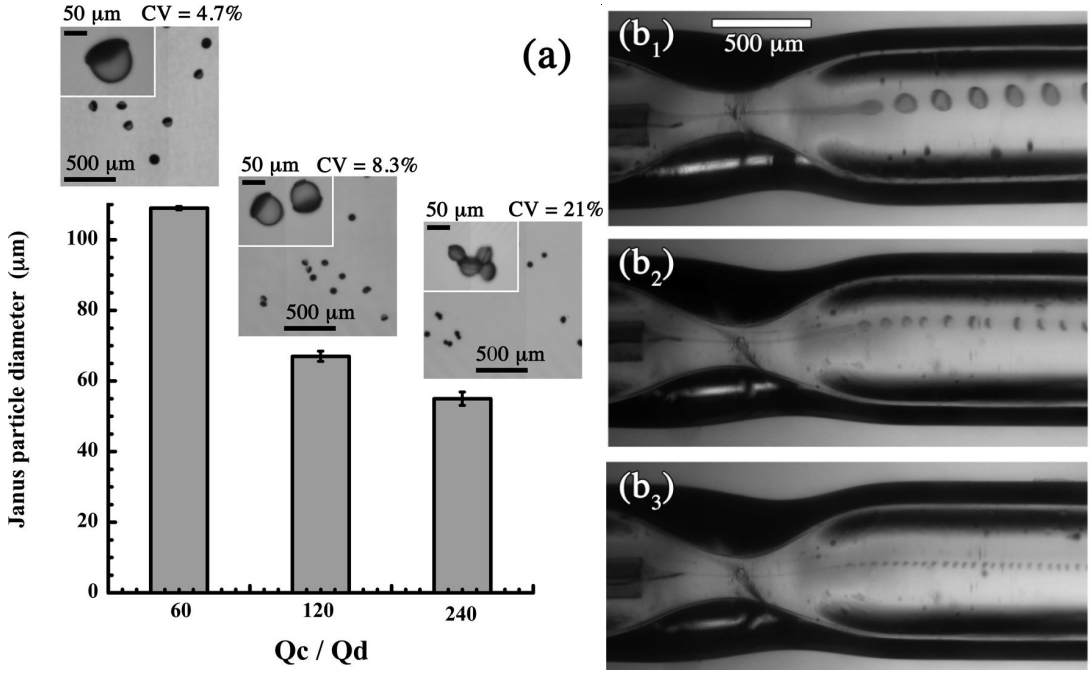

Fig. 3.14. Optical images of dried particles obtained with the flow-focusing section under different Q_c/Q_d ratios for formulation J11 (a); snapshots of droplet formation past the flow-focusing restriction under different Q_c/Q_d ratios: 60 (b_1) 120 (b_2) and 240 (b_3). Total flow rates of hydrophobic and hydrophilic phases were 4, 2 or 1 µL/min, whereas silicon oil was pumped at 240 µL/min. UV intensity was 40% and collecting tube ID 1 mm. Error bar indicates standard deviation (n=3).

In strategy (c), we polymerized formulation J11 under different UV intensities from 20 to 80%. In this set of experiments, the smallest Janus particles were obtained for 20% UV intensity. Hardening of the droplets was promoted by photopolymerization under UV irradiation. It is believed that at low UV intensity, a small amount of the photoinitiator was decomposed resulting in partially polymerized droplets which shrinked after dying. At higher

UV intensities, more monomer were polymerized which in turn gave larger particles (Fig. 3.15) but at 40 and 80% UV, no significant variation in size was observed i.e., 144 and 151 µm, respectively.

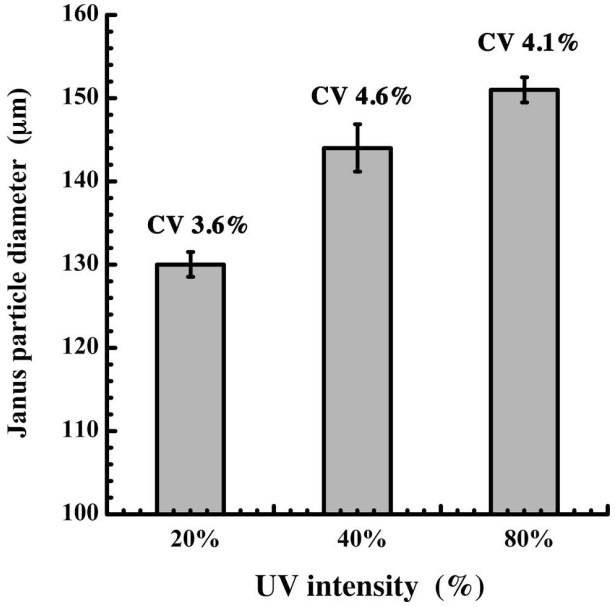

Fig. 3.15. Effect of UV intensity on particle size. All studies were carried out using formulation J11, flow rates of hydrophobic and hydrophilic phases were kept constant at 2 µL/min while silicon oil was pumped at 240 µL/min. The collecting tube internal diameter was 1 mm; UV intensity was varied from 20 to 80%. Error bar indicates standard deviation (n=3).

3.2.3.4 Analysis of polymerization

For pharmaceutical applications, it is utmost necessary to avoid any unreacted monomer in the final particle. FTIR is an appropriate technique to monitor the residual monomer. Monomers used contain a C=C double bond which gives characteristic peaks at 1636 and 808 cm^{-1} for acrylates (Lee et al., 2003; Li et al., 2009) while 1605 cm^{-1} for acrylamide (Özeroglu and Sezgin, 2007). Methyl acrylate shows a strong ester vibration at 1726 cm^{-1} (Khan et al., 2013b). –NH stretching of primary amide of acrylamide shows doublets between 3100 – 3500 cm^{-1}, while –C=O stretch of amide was observed between 1640 – 1690 cm^{-1} (Dweik et al., 2007; Özeroglu and Sezgin, 2007). In polymerized poly(acrylamide) and poly(methyl acrylate) particles (Fig. S4 c and d), C=C double bond peaks disappeared suggesting complete polymerization. Janus particles prepared from formulation J11 under 40 and 80% UV intensities (Fig. S4 e and f respectively) showed similar spectra. In

these spectra one can observe characteristic peaks of –NH stretching (3100 – 3500 cm^{-1}) and bending (1620 cm^{-1}) (Dweik et al., 2007), –C=O stretch (1649 cm^{-1}) for poly(acrylamide) (Alves et al., 2011) and ester vibration for poly(methyl acrylate) (1724 cm^{-1}). But one cannot distinguish characteristic peaks of unsaturated monomer (Fig. S4 e and f). Similar observations were already reported in literature by Özeroglu *et al.* and Khan *et al.* (Khan et al., 2013b; Özeroglu and Sezgin, 2007). These observations suggest that an optimal 40% UV intensity is enough to obtain Janus microparticles without residual monomers.

3.2.3.5 Encapsulation efficiency

Only fully characterized and optimal formulations were subjected to encapsulation efficiency. Particles having same composition but different size showed variation in encapsulation efficiency. Smaller particles have higher efficiency as compared to bigger particles (144 µm particles have 32 and 30% encapsulation efficiency for ketoprofen and sodium fluorescein respectively while 244 µm size particles have 30 and 29% encapsulation efficiency for same model drugs). A probable reason was that smaller droplets polymerize faster and prevents the loss of drug in continuous phase and washing media. These observations were in agreement with our previous experiments where small size ketoprofen loaded poly(ethyl acrylate-co-tripropylene glycol diacrylate) microbeads have higher encapsulation as compared to bigger ones (Khan et al., 2013b). It was further found that encapsulation of hydrophobic ketoprofen was comparatively higher than hydrophilic sodium fluorescein. In general, encapsulation efficiency of particles are affected by several factors like interaction between drug and polymer, solubility in continuous phase, polymer concentration and method of removal of solvent (Yeo and Park, 2004). In our case, Janus particles are allowed to dry at room temperature on filter paper (approximately 20° C) during which sodium fluorescein was lost along with water. Second probable reason was low affinity between hydrophilic drugs and polymer (Peltonen et al., 2004). Thirdly, encapsulation efficiency is affected by initial charged amount which was only 1 wt.% for sodium fluorescein. In comparison, ketoprofen have high encapsulation efficiency due absence of solvent in methyl acrylate phase, high initial charged amount (10 wt.%) and interaction between carboxyl group of ketoprofen and carbonyl group of poly(methyl acrylate). Couples of studies mentioning increased encapsulation by such interactions are already reported in literature (Khan et al., 2013b; Restani et al., 2010). Small amount of

ketoprofen was lost during washing procedure where ethyl acetate was used. We also observed an increase in encapsulation efficiency of sodium fluorescein while decreasing crosslinker concentration (from 27 to 48%) which could be related to a looser poly(acrylamide) gel part of Janus particles promoting more space for accommodation of hydrophilic molecule. Desai *et al.* found an increase in encapsulation efficiency of chitosan microspheres when crosslinker concentration was changed from 2 to 1% (Desai and Park, 2005).

3.2.3.6 *In vitro* cytotoxicity testing

Cytocompatibilty studies were carried out in BNL-CL2 cells. Cell cultures were observed before and after incubation of different concentration of Janus particles. These particles showed minimal cytotoxicity until 4 mg/mL (Fig. 3.16). LD50 of these particles was found to be around 9 mg/mL. MTT assay results were further confirmed by addition of propidium iodide and Calcein AM (acetomethoxy derivate of calcein) which have ability to stain dead and live cells respectively. In population of cell, dead cells appear as red due red-fluorescent nuclear and chromosome counterstain propidium iodide as it is only permeable to dead cells. Live cells will appear green because nonfluorescent Calcein AM was converted to a green-fluorescent calcein after acetoxymethoxy group was removed by intracellular esterases (Fig. 3.16).

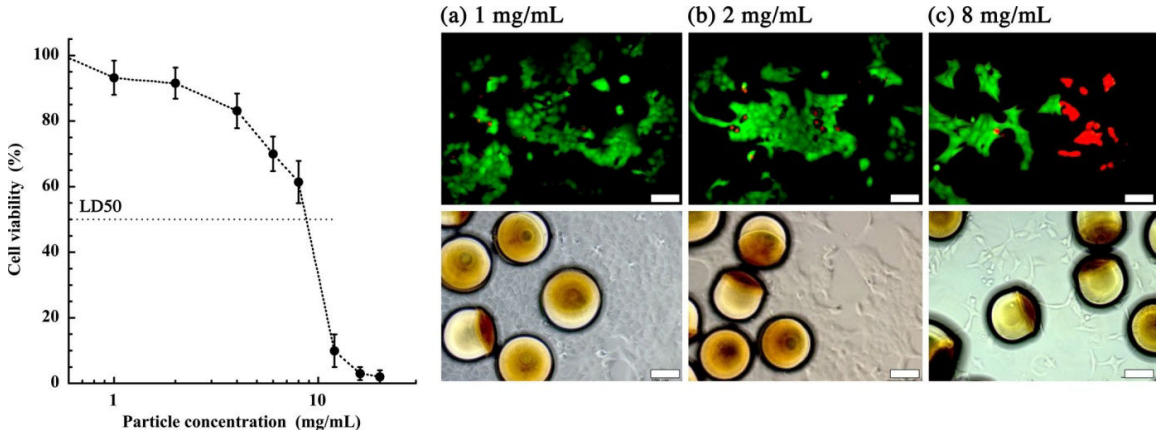

Fig. 3.16. Graph shows cell viability after exposure of BNL-CL2 hepatic cell line to different concentration of formulation J11. Lower figures a, b and c shows optical images of hepatic cell lines after incubation of Janus particles for 24 h. Upper figures shows overlayed fluorescent images taken after cell line treated with propidium iodide and Calcein AM which

were previously exposed to Janus particles. Scale bar represents 100 µm. Error bar indicates standard deviation (n=3). Error bar indicates standard deviation (n=3).

3.2.3.6 Drug release

Drug release studies were carried out at pH 1.2 and 6.8 in USP phosphate buffer solution. Two formulations having similar composition but polymerized in different size collecting tube were selected. It was observed that formulation having large particle size showed faster drug release as compared to small particles. Small particles released both drugs in more sustained release manner (Fig. 3.17). This was in contradiction to normal routine scientific observations. On further investigations, we observed that it was probably due to difference in shape. SEM micrographs showed large size Janus particles were dented on one side and there was no uniform distribution of the two phases (Fig. 3.17a). In case of small particles, we observed more uniform structure without defects (Fig. 3.17b). Hu *et al.* prepared microgels in a microfluidic device having different shapes. They observed uniform particles released drug in sustained manner while pear and mushroom-like particles released much faster. Authors attributed this observation to the difference in surface area and uniformity of particles (Hu et al., 2012). Furthermore, we observed ketoprofen release was higher compared to hydrophilic sodium fluorescein. We believe it is due to couple of reasons. First, in all the optimized formulations, the concentration of crosslinker and acrylamide in hydrophilic phase was quite high i.e. 6 wt.% and 30 wt.% respectively. These conditions may have promoted a highly dense crosslinked structure thus restricting the release of sodium fluorescein. Hussain *et al*. prepared ibuprofen loaded poly(acrylamide) gels using MBA as crosslinker. Drug release was carried out in gels containing 7, 8 and 9 wt.% acrylamide with 0.17, 0.20 and 0.22 wt.% of crosslinker respectively. They observed faster drug release in gels containing low concentration of acrylamide and crosslinker (Hussain MD et al., 1999). Second, initial loading amount of sodium fluorescein was 1 wt.% as compared to 10 wt.% of ketoprofen (Table 2.2 in Chapter 2). This could lead to slow drug release. Acetazolamide and timolol maleate were loaded in bi-component fibers comprising of semi-crystalline co-polymers, poly(ε-caprolactone) and poly(oxyethyleneb-oxypropylene-b-oxyethylene) using electrospining technique. Authors showed that fibers containing high loading showed a faster release than low loaded fibers. The later could not achieve 100% release, indicating drug was still entrapped (Natu et al., 2010). At pH 1.2 limited release of

encapsulated molecules (25 and 30% for sodium fluorescein and ketoprofen over two hours) was observed.

After comparing the drug release from various Janus particle sizes, it was concluded that particles developed in a 1 mm internal diameter collecting tubing gave better uniform size particles without any defects. So in next step, comparison was made by developing same J11 formulation in such collecting tube except that different UV intensities were investigated, i.e. 40 and 80%.

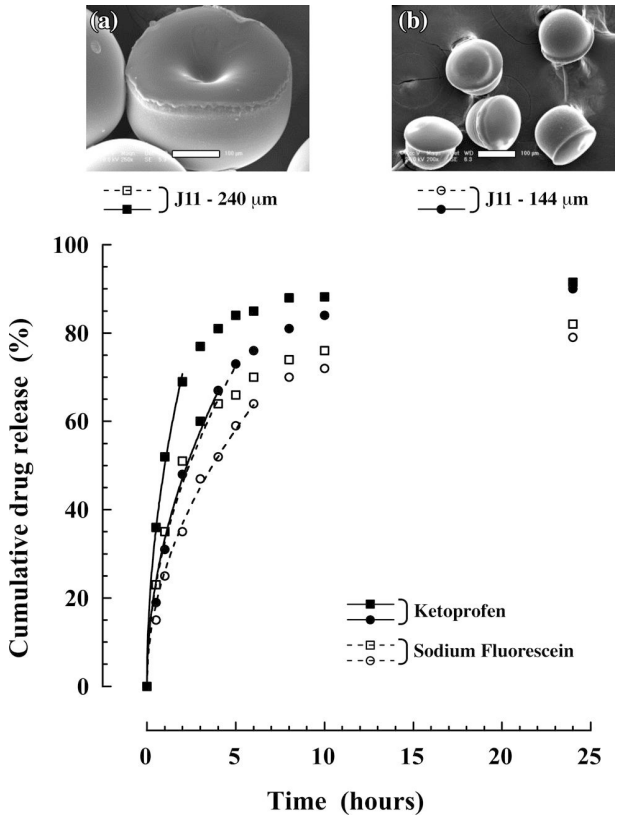

Fig. 3.17. Effect of morphology and particle size on drug release from formulation J11. The 240 µm Janus particle hardened in a 1.6 mm internal diameter collecting tube shows dents in SEM micrograph (a) while the 144 µm one developed in a 1 mm internal diameter collecting tube shows uniform structure without any defects (b). Release curve shows modified Fick's second law of diffusion on first 60% release. Flow rates of hydrophobic and hydrophilic phases were 2 µL/min and silicon oil was pumped at 240 µL/min. UV intensity was 40%. Scale bar in SEM images represents 100 µm.

Fig. 3.18a shows drug release of two formulations only differing in term of UV exposure intensity. There was no significant difference in release rate. Li *et al.* prepared

microcapsules containing dye (trade name D-8) and photopolymerizable core (TPGDA) by interfacial polymerization. They showed conversion of double bond in TPGDA could be controlled by exposure time to UV radiation, which in turn control the release rate of encapsulated dye. They showed decrease in dye release by increasing the UV curing time (Li et al., 2009). This suggest that both 40% and 80% UV intensity allowed full conversion of monomers as already emphasized by FTIR measurements (Fig. S4). Finally, concentration of crosslinker was reduced from 6 to 1.5 wt.% in formulation J12 and resulted in an increase in sodium fluorescein release (Fig. 3.18b). By decreasing crosslinker concentration, one decrease the crosslinking density and increase the mesh size which gave more freedom to movement of solvent and drug molecules. Several studies reported in literature pinpointed that crosslinker concentration can affect the release behavior of entrapped drug (Hezaveh and Muhamad, 2013; Jones et al., 2005). This demonstrates that, for these Janus particles, one can control the individual release rate of the two encapsulated drugs by controlling their respective compartment crosslinking density.

In order to further investigate the diffusion of drugs from the two polymer matrices, their diffusion coefficients were calculated using Fick's second law of diffusion. Herein polymers can be considered as homogeneous matrices in which the drug was either solubilized or trapped. As a consequence, the distance of diffusion of the solute is not constant but increases with time, following thereby a non-steady state diffusion regime generally described by the second Fick's law displayed in equation 1.

$$\mathrm{dC}/\mathrm{dt} = D\frac{d^2C}{dx^2} \qquad (1)$$

where *C* is the solute concentration, *D* the diffusion coefficient and *x* the diffusion distance (Higuchi, 1967). Equation 2, which is derived from equation 2, describes the case of homogeneous matrix systems like polymers and fits well the first part of the drug release profile ($0 \leq M_t/M_\infty \leq 0.6$).

$$\mathrm{M_t}/\mathrm{M}\infty = \frac{2S}{V}\left(\frac{Dt}{\pi}\right)^{1/2} \qquad (2)$$

where M_t is the mass of solute released at time *t*, M_∞ the total mass of solute, *S* the surface of the matrix and finally *V* the volume of the sample (including release medium).

Accordingly, this model was used to fit fluorescein salt and ketoprofen *in vitro* release data (see solid and dashed lines in Fig. 3.17 and 18). For all fits, correlation coefficients did not fall below 0.991. One can concludes that the release mechanism of these two model compounds from the polymer matrices was effectively the Fick's diffusion.

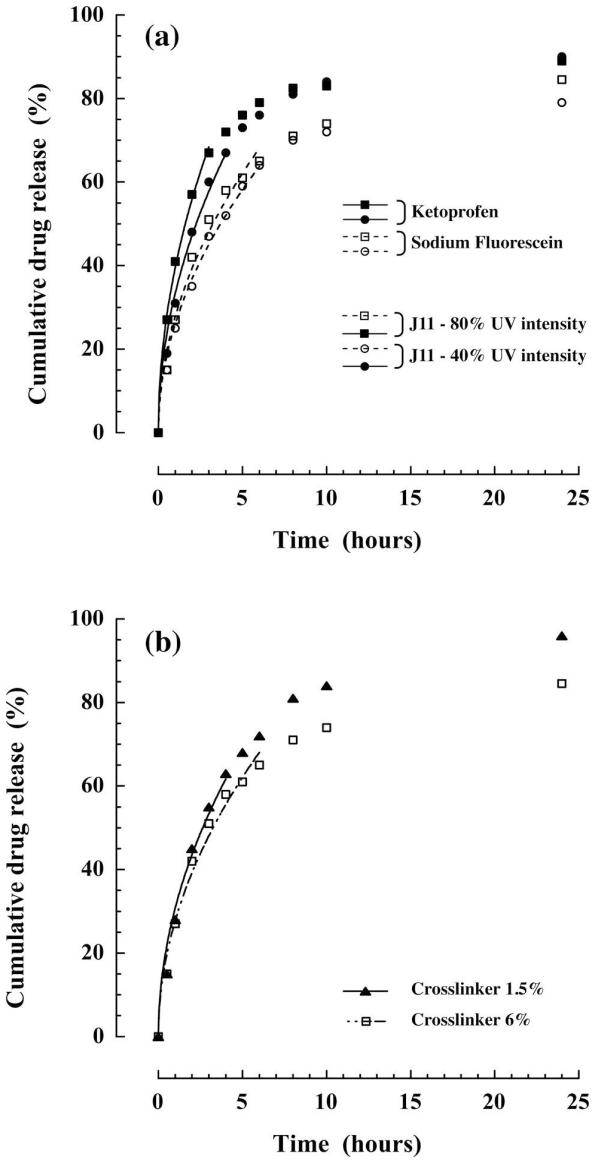

Fig. 3.18. Effect of UV intensity on drug release from formulation J11. Janus particle were hardened using UV intensity of 40 or 80%. Obtained particles were monodispersed in size and had a mean diameter of 144 and 151 µm for 40 and 80% UV intensity respectively (a). Comparison of sodium fluorescein release from formulation J11 and J12 having 6 and 1.5 wt.% crosslinker respectively polymerized using 80% UV (b). Release curve shows modified Ficks second law of diffusion on first 60% release. Flow rates of hydrophobic and hydrophilic

phases were 2 µL/min and silicon oil was pumped at 240 µL/min. Internal diameter of collecting tubing was 1 mm.

3.2.4 Conclusions

Side-by-side capillaries microfluidic device allowed rapid synthesis and incorporation of two molecules with different physicochemical properties in Janus particles for co-delivery. Biphasic droplet geometry was rapidly fixed by UV initiated free radical polymerization, far away from maximum absorption wavelength of ketoprofen and sodium fluorescein thus insuring their integrity. FTIR and MTT assay confirmed complete polymerization and biocompatibility respectively. Q_c/Q_d ratio as well concentration of surfactant allowed obtaining different particle morphologies ranging from core-shell to Janus particles. Size can be controlled by changing collecting tube internal diameter, flow rates ratio and a flow-focusing section. It was found that regular shaped particles released two entrapped molecules in more controlled release manner than the particles with irregular symmetry and indentation. We believe these biocompatible particles having ability to incorporate two different active ingredients in different sections will open a new horizon for the co-delivery of incompatible molecules or ones having different hydrophilic/hydrophobic nature. In future, these two sections particles could be designed to deliver molecules in different sections of the gastro intestinal tract.

3.2.5 Supplementary information

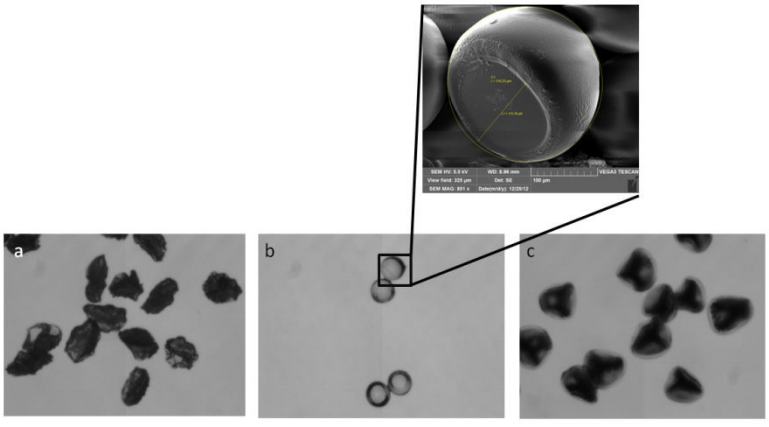

Fig. S3. Initial trials with 30 wt.% acrylamide in water phase and 80 wt.% ethyl acrylate in oil pahse. Formulation without surfactant fails to generate Janus particles (a). Presence of surfactant (3 wt.%) in acrylamide phase produces Janus particles as can be seen in optical

image after drying and related SEM micrograph. Flow rates of ethyl acrylate and acrylamide phases were 5-2 µL/min while silicon oil was pumped at 240 µL/min (b), Initial trials with 30 wt.% acrylamide in hydrophilic phase and 80 wt.% methyl acrylate in oil phase without surfactant. Flow rates of hydrophobic and hydrophilic phases were 2-2 µL/min while silicon oil was pumped at 240 µL/min (c). UV intensity was 40% and collecting tube internal diameter was 1.6 mm

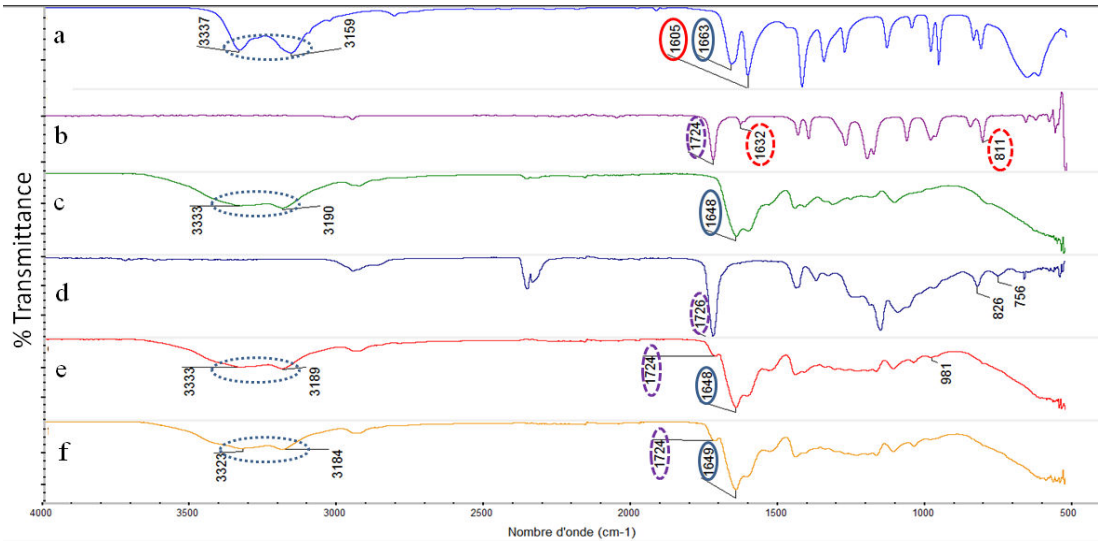

Fig. S4. FTIR spectra of acrylamide (a), methyl acrylate (b), poly(acrylamide) microparticles (c), poly(methyl acrylate) microparticles (d), formulation J11 formulated at 40% (e) and 80% (f) UV intensity respectively.
Amide N-H stretch (▪▪▪), amide C=O stretch (▬), –CH=CH2 Group frequency (▬), stretching vibration of ester (▬) and stretching and bending vibrations of acrylate double bond (▬).

Video V1: Janus droplet generation in side-by-side capillaries at Qc/Qd 60. See web version of research article
Video V2a, b and c: Janus droplet generation in flow focus set under different Qc/Qd 60, 120, 240. See web version of research article

References

Alves, T., Tavares, E., Aouada, F., Negrão, C., Oliveira, M., Duarte Júnior, A., Ferreira da Costa, C., Silva Júnior, J., Ribeiro Costa, R., 2011. Thermal analysis characterization of PAAm-co-MC hydrogels. J Therm Anal Calorim 106, 717-724.

Capretto, L., Carugo, D., Mazzitelli, S., Nastruzzi, C., Zhang, X., 2013. Microfluidic and lab-on-a-chip preparation routes for organic nanoparticles and vesicular systems for nanomedicine applications. Advanced Drug Delivery Reviews 65, 1496-1532.

Chen, C.-H., Shah, R.K., Abate, A.R., Weitz, D.A., 2009. Janus Particles Templated from Double Emulsion Droplets Generated Using Microfluidics. Langmuir 25, 4320-4323.

Chen, H.H., Le Visage, C., Qiu, B., Du, X., Ouwerkerk, R., Leong, K.W., Yang, X., 2005. MR imaging of biodegradable polymeric microparticles: A potential method of monitoring local drug delivery. Magnetic Resonance in Medicine 53, 614-620.

Cho, I., Lee, K.-W., 1985. Morphology of latex particles formed by poly(methyl methacrylate)-seeded emulsion polymerization of styrene. Journal of Applied Polymer Science 30, 1903-1926.

Delie, F., Blanco-Príeto, M., 2005. Polymeric Particulates to Improve Oral Bioavailability of Peptide Drugs. Molecules 10, 65-80.

Desai, K.G.H., Park, H.J., 2005. Preparation of cross-linked chitosan microspheres by spray drying: Effect of cross-linking agent on the properties of spray dried microspheres. Journal of Microencapsulation 22, 377-395.

Dweik, H., Sultan, W., Sowwan, M., Makharza, S., 2007. Analysis Characterization and Some Properties of Polyacrylamide Copper Complexes. International Journal of Polymeric Materials and Polymeric Biomaterials 57, 228-244.

Flores, M.V., Voutsas, E.C., Spiliotis, N., Eccleston, G.M., Bell, G., Tassios, D.P., Halling, P.J., 2001. Critical Micelle Concentrations of Nonionic Surfactants in Organic Solvents: Approximate Prediction with UNIFAC. Journal of Colloid and Interface Science 240, 277-283.

Hezaveh, H., Muhamad, I.I., 2013. Controlled drug release via minimization of burst release in pH-response kappa-carrageenan/polyvinyl alcohol hydrogels. Chemical Engineering Research and Design 91, 508-519.

Higuchi, W.I., 1967. Diffusional models useful in biopharmaceutics. Drug release rate processes. Journal of Pharmaceutical Sciences 56, 315-324.

Hu, Y., Wang, Q., Wang, J., Zhu, J., Wang, H., Yang, Y., 2012. Shape controllable microgel particles prepared by microfluidic combining external ionic crosslinking. Biomicrofluidics 6, 26502-265029.

Hussain MD, Rogers JA, Mehvar R, GK., V., 1999. Preparation and release of ibuprofen from polyacrylamide gels. Drug Development and Industrial Pharmacy 25, 265-271.

Jones, D.S., Andrews, G.P., Gorman, S.P., 2005. Characterization of crosslinking effects on the physicochemical and drug diffusional properties of cationic hydrogels designed as bioactive urological biomaterials. Journal of Pharmacy and Pharmacology 57, 1251-1259.

Khan, I.U., Ayub, G., Ranjha, N.M., 2013a. Assessment of Palmitoyl and Sulphate Conjugated Glycol Chitosanfor Development of Polymeric Micelles. BioImpacts 3, 97-100.

Khan, I.U., Serra, C.A., Anton, N., Vandamme, T., 2013b. Continuous-flow encapsulation of ketoprofen in copolymer microbeads via co-axial microfluidic device: Influence of operating and material parameters on drug carrier properties. International Journal of Pharmaceutics 441, 809-817.

Khan, I.U., Serra, C.A., Anton, N., Vandamme, T., 2013c. Microfluidics: A focus on improved cancer targeted drug delivery systems. Journal of Controlled Release 172, 1065-1074.

Lee, T.Y., Roper, T.M., Jonsson, E.S., Kudyakov, I., Viswanathan, K., Nason, C., Guymon, C.A., Hoyle, C.E., 2003. The kinetics of vinyl acrylate photopolymerization. Polymer 44, 2859-2865.

Li, G., Guo, J., Wang, X., Wei, J., 2009. Microencapsulation of a functional dye and its UV crosslinking controlled releasing behavior. Journal of Polymer Science Part A: Polymer Chemistry 47, 3630-3639.

Marquis, M., Renard, D., Cathala, B., 2012. Microfluidic Generation and Selective Degradation of Biopolymer-Based Janus Microbeads. Biomacromolecules 13, 1197-1203.

Natu, M.V., de Sousa, H.C., Gil, M.H., 2010. Effects of drug solubility, state and loading on controlled release in bicomponent electrospun fibers. International Journal of Pharmaceutics 397, 50-58.

Nie, Z., Seo, M., Xu, S., Lewis, P., Mok, M., Kumacheva, E., Whitesides, G., Garstecki, P., Stone, H., 2008. Emulsification in a microfluidic flow-focusing device: effect of the viscosities of the liquids. Microfluid Nanofluid 5, 585-594.

Nokhodchi A, F.D., 2002. Microencapsulation of Paracetamol by Various Emulsion Techniques Using Cellulose Acetate Phthalate. Pharm Technol 26, 54–60.

Özeroglu, C., Sezgin, S., 2007. Polymerization of acrylamide initiated with Ce(IV)- and KMnO4-mercaptosuccinic acid redox systems in acid-aqueous medium. eXPRESS Polymer Letters 1, 132–141.

Peltonen, L., Aitta, J., Hyvönen, S., Karjalainen, M., Hirvonen, J., 2004. Improved entrapment efficiency of hydrophilic drug substance during nanoprecipitation of poly(l)lactide nanoparticles. AAPS PharmSciTech 5, 115-120.

Pereira, G.G., Santos-Oliveira, R., Albernaz, M.S., Canema, D., Weismüller, G., Barros, E.B., Magalhães, L., Lima-Ribeiro, M.H.M., Pohlmann, A.R., Guterres, S.S., 2014. Microparticles of Aloe vera/vitamin E/chitosan: Microscopic, a nuclear imaging and an in vivo test analysis for burn treatment. European Journal of Pharmaceutics and Biopharmaceutics 86, 292-300.

Restani, R.B., Correia, V.G., Bonifácio, V.D.B., Aguiar-Ricardo, A., 2010. Development of functional mesoporous microparticles for controlled drug delivery. The Journal of Supercritical Fluids 55, 333-339.

Samanta, S., Ghosh, P., 2011. Coalescence of bubbles and stability of foams in aqueous solutions of Tween surfactants. Chemical Engineering Research and Design 89, 2344-2355.

Serra, C.A., Khan, I.U., Cortese, B., de Croon, M.H.J.M., Hessel, V., Ono, T., Anton, N., Vandamme, T., 2013. Microfluidic Production of Micro- and Nanoparticles, Encyclopedia of Polymer Science and Technology. John Wiley & Sons, Inc.

Shi, Y., Luo, H.Q., Li, N.B., 2011. Determination of the critical premicelle concentration, first critical micelle concentration and second critical micelle concentration of surfactants by resonance Rayleigh scattering method without any probe. Spectrochimica Acta Part A: Molecular and Biomolecular Spectroscopy 78, 1403-1407.

Teh, S.-Y., Lin, R., Hung, L.-H., Lee, A.P., 2008. Droplet microfluidics. Lab on a Chip 8, 198-220.

Tran, V.-T., Benoît, J.-P., Venier-Julienne, M.-C., 2011. Why and how to prepare biodegradable, monodispersed, polymeric microparticles in the field of pharmacy? International Journal of Pharmaceutics 407, 1-11.

Xie, H., She, Z.-G., Wang, S., Sharma, G., Smith, J.W., 2012. One-Step Fabrication of Polymeric Janus Nanoparticles for Drug Delivery. Langmuir 28, 4459-4463.

Yang, S., Guo, F., Kiraly, B., Mao, X., Lu, M., Leong, K.W., Huang, T.J., 2012. Microfluidic synthesis of multifunctional Janus particles for biomedical applications. Lab on a Chip 12, 2097-2102.

Yeo, Y., Park, K., 2004. Control of encapsulation efficiency and initial burst in polymeric microparticle systems. Arch Pharm Res 27, 1-12.

Zhao, C.-X., 2013. Multiphase flow microfluidics for the production of single or multiple emulsions for drug delivery. Advanced Drug Delivery Reviews 65, 1420-1446.

Chapter 4
Core-shell and Trojan particles

The first section of this chapter deals with the preparation of core-shell particles. They were produced by applying a slight modification of the previous single capillary-based setup. Here a two co-axial capillaries-based microfluidic setup was used to develop pH sensitive ketoprofen loaded poly(methyl acrylate) core – ranitidine HCl loaded poly(acrylamide-co-carboxyethyl acrylate) shell particles. As shown in the following, all particles were monodisperse and their overall size and core diameter can be controlled by modifying the three phase flow rates. These pH sensitive particles were able to deliver two different APIs to colonic region of GIT. The second section of this chapter describes a novel semi-continuous two step process based on nanoemulsions templating to elaborate Trojan particles for oral delivery of nanoparticles. Nanoemulsions were obtained in an elongation-flow micromixer and then polymerized in a single capillary-based setup to get Trojan particles of poly(acrylamide) embedded with ketoprofen loaded poly(ethyl acrylate) or poly(methyl acrylate) nanoparticles. These particles released ketoprofen and nanoparticles in simulated gastric medium.

This chapter is mainly composed of the following submitted research articles.

*1: **Khan, I.U**., **Stolch, L.**, Serra, C.A., Anton, N., Akasov, R., Vandamme, T.F. Microfluidic conceived pH sensitive core-shell particles for dual drug delivery. International Journal of Pharmaceutics **2015,** 478 (1), 78-87*

2: ***Khan, I.U***., *Serra, C.A.*, *Anton, N.*, Schmutz, M., Kraus, I., Messaddeq, N., Vandamme, T.F. Microfluidic conceived Trojan microcarriers for oral delivery of nanoparticles. *Submitted to International Journal of Pharmaceutics.*

Contents

4.1 Microfluidic conceived pH sensitive core-shell particles for dual drug delivery

Graphical Abstract

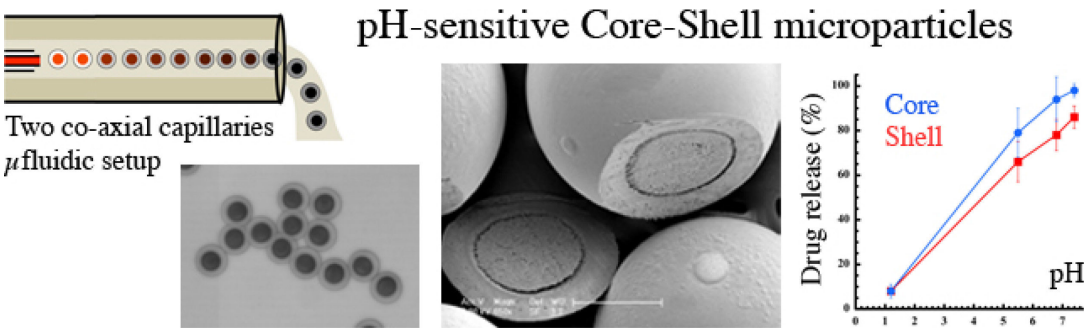

Abstract

In current study, we report on the synthesis of core-shell microparticles for dual drug delivery by means of a two co-axial microfluidic device and online UV assisted free radical polymerization. Before developing pH-sensitive particles, ketoprofen loaded poly(methyl acrylate) core – ranitidine HCl loaded poly(acrylamide) shell particles were produced. Influence of inner and outer phases flow rates on particle size, shape, core diameter, shell thickness and drug release properties was studied. All the particles were monodispersed with coefficient of variation below 5%. Furthermore their diameter ranged from 100 to 151 µm by increasing continuous (Q_c) to middle (Q_m) phase flow rate ratio (Q_c/Q_m). Core diameter varied from 58 to 115 µm by decreasing middle (Q_m) to inner (Q_i) phase flow rate ratio (Q_m/Q_i) at constant continuous phase flow rate as confirmed by SEM images. It was observed that an optimum concentration of acrylamide (30 wt.%) and an appropriate combination of surfactants were necessary to get core-shell particles otherwise Janus structure was obtained. FTIR confirmed the complete polymerization of core and shell phases. MTT assay showed variation in viability of cells under non-contact and contact conditions with less cytotoxicity for the former. Under non-contact conditions LD_{50} was 3.1 mg/mL. Release studies in USP phosphate buffer solution showed simultaneously release of ketoprofen and ranitidine HCl for non pH-sensitive particles. However, release rates of ranitidine HCl and ketoprofen were higher at low and high pH respectively. To develop pH-sensitive particles for colon targeting, the previous shell phase was admixed with few weight percentage of pH sensitive carboxyethyl acrylate monomer. Core and shell contained the same hydrophobic and hydrophilic model drugs as in previous case. The pH-sensitive shell

prevented the release of the two entrapped molecules at low pH while increasing significantly their release rate at higher pH with a maximum discharge at colonic pH of 7.4.

Keywords: Microfluidics, cytotoxicity, dual drug delivery, poly(acrylamide-co-carboxy ethyl acrylate), pH-sensitive.

4.1.1 Introduction

For many centuries man tried to treat diseases with different chemical entities but last century has seen a tremendous increase in the development of new active ingredients. These agents are delivered by suitable carriers called drug delivery systems. Emergence of new and more potent molecules necessitates the development of new controlled release drug delivery systems to counteract the problem raised with conventional systems. Controlled drug delivery systems in contrast offer several advantages like improved efficacy, reduced side effects and improved patient compliance. Currently polymeric micro- and nanoparticles and liposomes are widely used as controlled drug delivery systems (Wu et al., 2013). Still these drug delivery vehicles as simple as microparticles have numerous inherent issues, like burst effect, difficulty in achieving zero-order release and inability to incorporate and deliver two drugs in sequential or concurrent manner (Wang et al., 2010). Moreover these systems also suffer from large particle size distribution and uncontrolled drug release kinetics. Recently it was found that shape and size of particles can play an important role in initial burst effect and release kinetics (Wu et al., 2013).

Core-shell particles can provide an effective control on the drug release kinetics and initial burst effect. Indeed the drug is usually localized in the core compartment while the shell increases the diffusion path of water towards the core and that of drug to the surroundings which ultimately limit the initial burst release (Kong et al., 2013; Tran et al., 2011). On the other hand, the release kinetics is faster in case of small particles (Khan et al., 2013) and thus an effective control over the drug release rate requires monodisperse particles. However, conventional core-shell particles are usually polydisperse in size (Lee et al., 2002; Tran et al., 2011) because of their synthesis methods which involve time consuming multistep procedures and also lacks control over initial droplet size, a key parameter to control size of particles (Serra and Chang, 2008). Therefore new methods are required for precise control of core and shell dimensions.

Microfluidics refers to the manipulation of fluid segments in devices for which at least one of the characteristic dimensions lies in the micron range. Microfluidic techniques allow the synthesis of microparticles from single phase flow or multiphase flow and offer several advantages over their counterpart macroscale techniques such as uniform particle size with coefficient of variation (CV) less than 5%, minimum amount of reagents, short mixing time, laminar flow and high heat and mass transfers (Khan et al., 2013).

Core-shell particles have great promise in biomedical and pharmaceutical applications but their fabrication by conventional methods has limited their use. Conventional methods have several drawbacks like the necessity to rely on high energy to obtain double emulsions, the production of polydisperse particles, the poor encapsulation efficiency, the lack of reproducibility and control over other characteristics such as core diameter and shell thickness (Kong et al., 2013). Moreover, in certain cases, the core is developed at first and then a shell layer is applied by dipping in a suitable solution (Babu et al., 2006). On the other hand microfluidics has provided a facile approach to develop double emulsions that could serve as template for core-shell particles besides providing an efficient control over size and thickness of core and shell parts. So far many authors have tried to encapsulate a single molecule in the core and controlled its release kinetics by approaches like magnetism, network density tuning and thermal triggering (Gong et al., 2009; Kong et al., 2013; Rondeau E, 2012; Yu et al., 2012). All these approaches used preformed polymers dissolved in a suitable solvent to form multiple emulsions which are later transformed into core-shell particles.

In current paper we started with two different monomers admixed with active pharmaceutical ingredients of different hydrophilicities. Double droplets were obtained in a two co-axial capillaries-based microfluidic device. These droplets were then polymerized by UV initiated free radical polymerization to produce core-shell particles containing a hydrophobic model drug in the core and a hydrophilic model drug in the shell. Obtained microparticles were characterized in terms of FTIR, SEM, encapsulation efficiency, cytotoxicity testing and dual drug release as a function of their composition, size as well as pH of release medium.

4.1.2 Experimental

I. *List of materials is given in Chapter 2 section 2.1*

II. *Description of the capillary-based device and overall particle synthesis process is provided in Chapter 2, section 2.2.3*

III. *Methods for particle characterization are detailed in Chapter 2, section 2.3.3 while encapsulation efficiency and release properties are determined following the procedure described in Chapter 2, section 2.3.1.2 and 2.3.1.7 respectively*

4.1.3 Results and discussion

Core-shell microparticles were successfully prepared in a two co-axial capillaries-based setup using free radical polymerization, while insuring integrity of two active molecules separately encapsulated in core and shell parts of the particles. There integrity was maintained by using UV source (365 nm) far away from the maximum absorbance (260 and 315 for Ketoprofen and ranitidine HCl respectively) of the two APIs. It was further observed that to get a good morphology certain parameters must be adequately controlled. First, inner capillary tip should be 150-450 µm upstream to the middle capillary tip. Secondly, it was also necessary to align all three capillaries. Both of these factors are necessary to get perfect core-shell droplets. Otherwise droplets without core were obtained. Finally appropriate concentration of hydrophilic monomer and surfactant in middle phase was necessary to encapsulate core part.

4.1.3.1 Particle size analysis

For each formulation, approximately fifty fully polymerized particles were processed with imaging software do determine the average particle size.

Table 4.1. Average core-shell particle size and respective coefficient of variation of particle size distribution for the different formulations investigated

S. no	Formulation	Q_c/Q_m	Q_m/Q_i	Mean particle size (µm)	CV*
1	C1	120	1	144	4.2
2		180	1	113	4.1
3		240	1	100	4.9
4		120	1.3	139	4.1
5		120	2	148	2.3
6	C3	120	1	151	4.3

*CV is the ratio of the standard deviation to the mean particle diameter. In all formulations Q_m was kept constant at 2 µL/min.

In all the formulations tested, particles were spherical and their CV was less than 5%, indicating monodisperse particles (Table 4.1). SEM analysis also revealed that particles were spherical, monodisperse and had smooth surface (Fig. 4.1). To confirm the core-shell structure, particles were cut and observed at high resolution under SEM (Fig. 4.1). Core diameter was found bigger than shell's thickness at low middle to inner phase flow rate (Q_m/Q_i) ratio and decreased in size when Q_m/Q_i ratio is increased as seen in Figure 4.1.

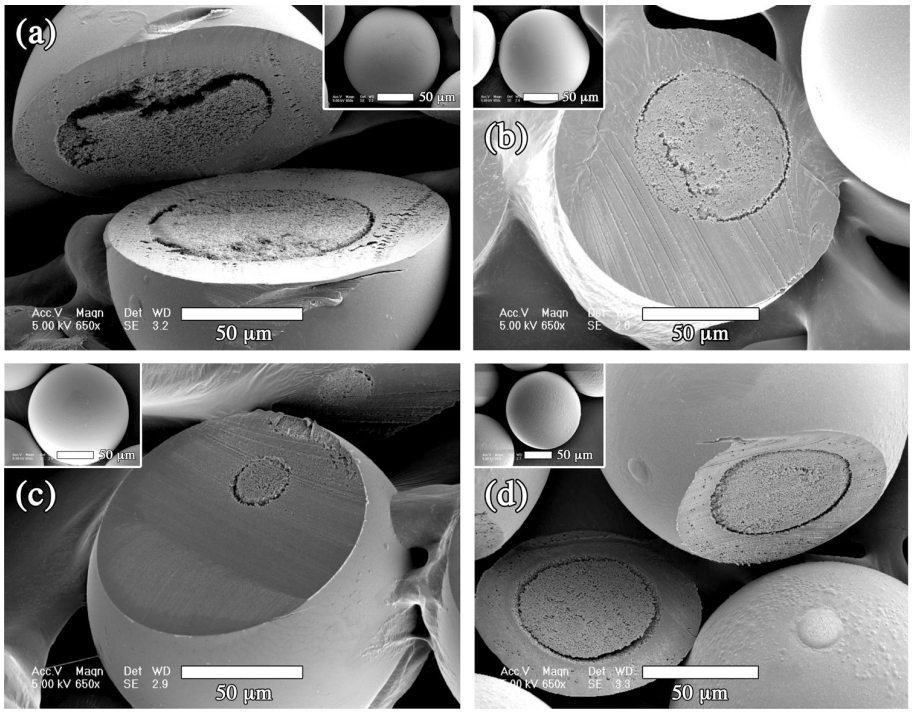

Fig. 4.1. SEM pictures of core-shell microparticles at same magnification showing transverse section for different formulations: C1 for a) Q_m/Qi = 1, b) 1.3, c) 2 and C3 for d) Q_m/Q_i = 1. Inset pictures show intact particles.

4.1.3.2 Effect of Q_c/Q_m

Q_c/Q_m flow rate ratio plays an important role in controlling the size of the particles. By increasing this ratio one can obtain smaller particles. Flow rates of hydrophobic inner (Q_i) and hydrophilic middle (Q_m) phases were kept constant at 2 µL/min while the continuous phase flow rate was either 240, or 360 or 480 µL/min; giving a Q_c over Q_m ratio of 120, 180 and 240 respectively. For Q_c/Q_m = 120, big particles were observed with an average diameter of 144 µm and a CV of 4.2%, whose size was reduced down to 113 µm with a CV of 4.1% for Q_c/Q_m = 180. This is due to the higher shear rate exerted by the continuous phase on dispersed phases when the continuous phase flow rate is increased (Bouquey et al., 2008;

Kong et al., 2013; Wang et al., 2014). No significant reduction of particle size was observed at Q_c/Q_m = 240 but CV was comparatively higher (Fig 4.2). It is probably because at this value of Q_c/Q_m, the plateau zone has been reached. Indeed, it was reported in the literature that CV is low in decreasing zone but relatively higher in plateau zone (Chang et al., 2009; Serra et al., 2007). Secondly in the absence of surfactant in the continuous phase, the viscosity of silicon oil (500 cts) was not high enough to prevent the collision of some of double droplets. We experienced such phenomena in our previous studies on Janus particles (Khan et al., 2014).

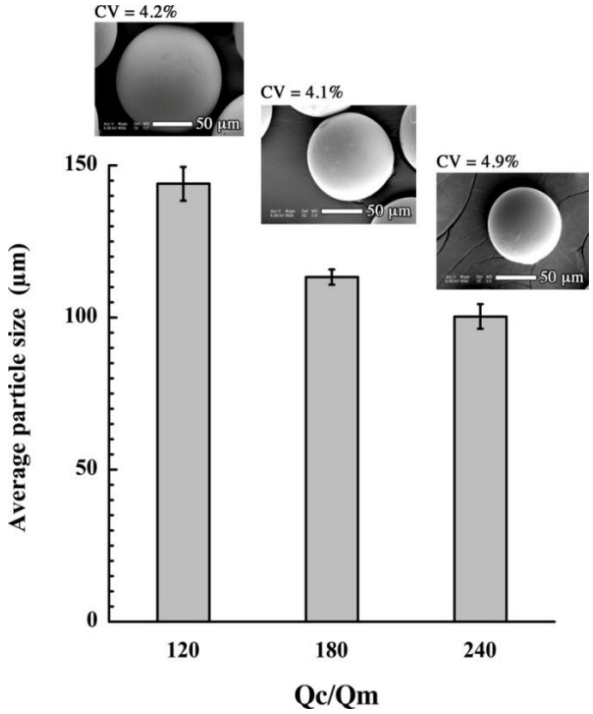

Fig. 4.2. Effect of Q_c/Q_m on average diameter of dried core-shell particles using formulation C1. SEM pictures confirm the decrease in size with an increase in Q_c/Q_m. Error bars indicate the standard deviation (n=3).

4.1.3.3 Variation of core diameter

We demonstrated that Q_c/Q_m can be adequately manipulated to control the overall size of the particles in formulation C1. Then we made use of another parameter, the middle phase to inner phase flow rates ratio (Q_m/Q_i), to easily control the shell's thickness and core's diameter of the particles. At low Q_m/Q_i, i.e. 1, core's diameter was 115 µm. It reduced down to 96 and 58 µm when Q_m/Q_i was increased up to 1.3 and 2 respectively while continuous phase was pumped at a constant flow rate of 240 µL/min (Fig. 4.3).

Q_m/Q_i was varied by lowering the inner phase flow rate. In such conditions and since the break-up times of shell and core thread are same, the core volume is reduced when Q_i is decreased. Thus core's diameter is smaller and shell's thickness larger when Q_m/Q_i is increased. Furthermore it was observed that at Q_m/Q_i = 2, eccentric core-shell particles are obtained. This observation was confirmed by cut sections of particles under SEM (Fig. 4.1c). Furthermore, particles developed under Q_m/Q_i = 1.3 and 2 presents small craters on their surface and required further investigations (See supplementary information S1). Finally, it was observed from SEM micrographs (Fig. 4.1a, b and c) as well as from inset pictures of Figure 4.3 that the overall size remained constant whatever the values of Q_i. This is consistent with previous studies where the overall particle's diameter was varied by changing Q_c/Q_m and was found independent of Q_i (Chang et al., 2009). As a consequence, the decrease in core's diameter resulted in an increase in shell's thickness.

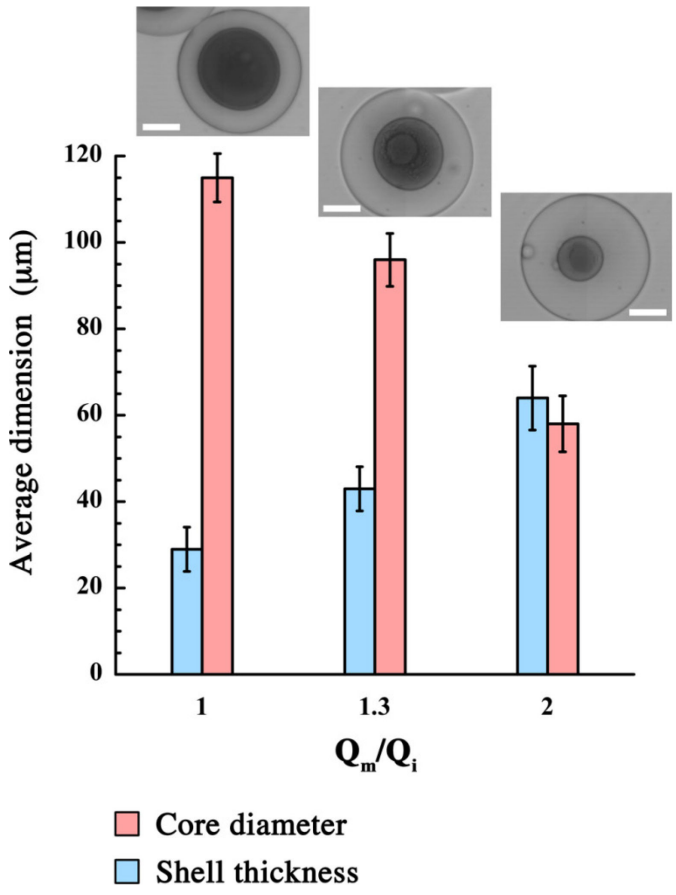

Fig. 4.3. Effect of Q_m/Q_i on core's diameter and shell's thickness for formulation C1 at different Q_m/Q_i. Inset pictures show the optical images of core-shell particles taken immediately after polymerization. Error bars indicate the standard deviation (n=3) and scale bars represent 55 µm.

4.1.3.4 Influence of composition on particle's morphology

By varying the weight content of acrylamide in the shell phase, it was observed that the particle's morphology adopted either a core-shell or Janus structure (Fig. 4.4).

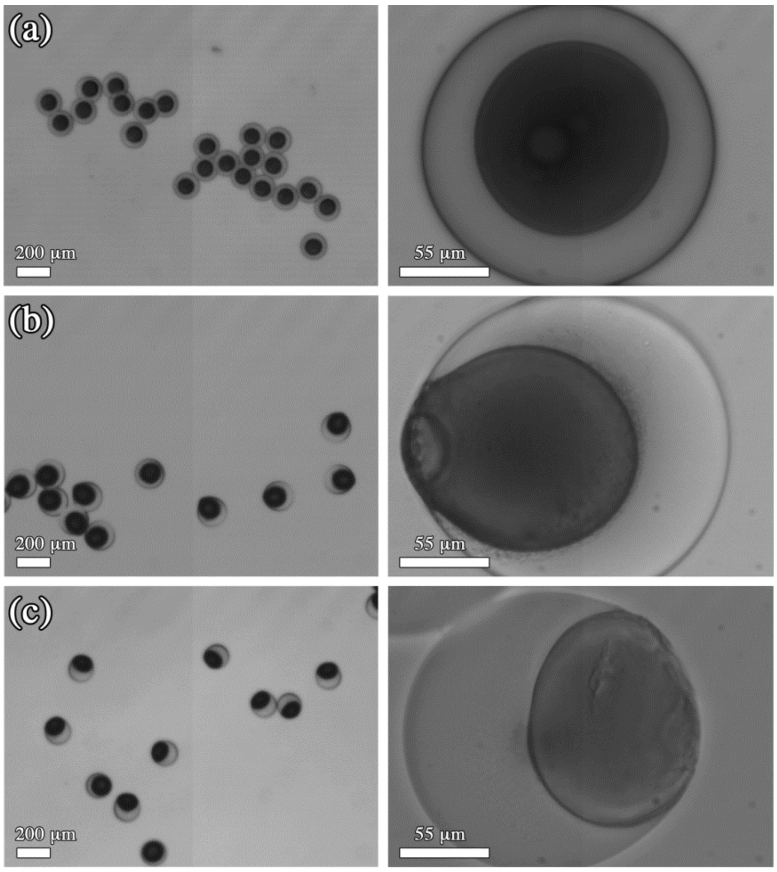

Fig. 4.4. Effect of acrylamide concentration on particle morphology: a) 30, b) 25 and c) 20 wt%. Pictures were taken immediately after polymerization.

Perfect core-shell structure was obtained with the highest concentration tested i.e. 30 wt.%. One probable reason is the increase in viscosity of shell phase when the concentration of acrylamide is increased (See supplementary information S2) which made the engulfment of core phase more stable. A second possibility may be related to relatively higher affinity between core phase with the silicon oil as compared to the shell phase. Afterwards the shell composition in acrylamide was kept constant at 30 wt.% and 20 or 40 wt.% of TPGDA were added to the core phase in order to modulate the release kinetics of ketoprofen. However, with such formulations, Janus particles were obtained for Q_m/Q_i =1, but as this ratio was increased to 2 core-shell particles were observed (See supplementary information S3).

4.1.3.5 Monitoring of polymerization

FTIR is a very efficient technique to monitor conversion of a monomer. Indeed under the influence of IR radiation each molecule gives its characteristic spectral bending or stretching vibration. These characteristic FTIR peaks are due to the presence of specific functional groups and are used as identification markers. For example in our study acrylate monomer contains a C=C double bond which gives two characteristic peaks at 1636 and 808 cm^{-1} (Lee et al., 2003; Li et al., 2009) and acrylamide shows a specific peak at 1605 cm^{-1} (Özeroglu and Sezgin, 2007). Methyl acrylate monomer exhibits strong ester vibration at 1726 cm^{-1}. –NH stretching of primary amide of acrylamide gives doublets between 3100 – 3500 cm^{-1}, while –C=O stretch of amide was observed between 1640 – 1690 cm^{-1} (Khan et al., 2014; Özeroglu and Sezgin, 2007). In polymerized core-shell particles peaks for unsaturated bonds were not observed suggesting complete polymerization (Fig. 4.5). But one can observe –NH stretching (3100 – 3500 cm^{-1}) (Dweik et al., 2007), –C=O stretch (1649 cm^{-1}) for poly(acrylamide) (Alves et al., 2011) and ester vibration for poly(methyl acrylate) (1724 cm^{-1}) (Khan et al., 2014; Khan et al., 2013). In formulated particles it was difficult to observe the characteristic peaks of ketoprofen and ranitidine HCl as their peaks are overlapped by strong vibrations of poly(methyl acrylate) core and poly(acrylamide) shell.

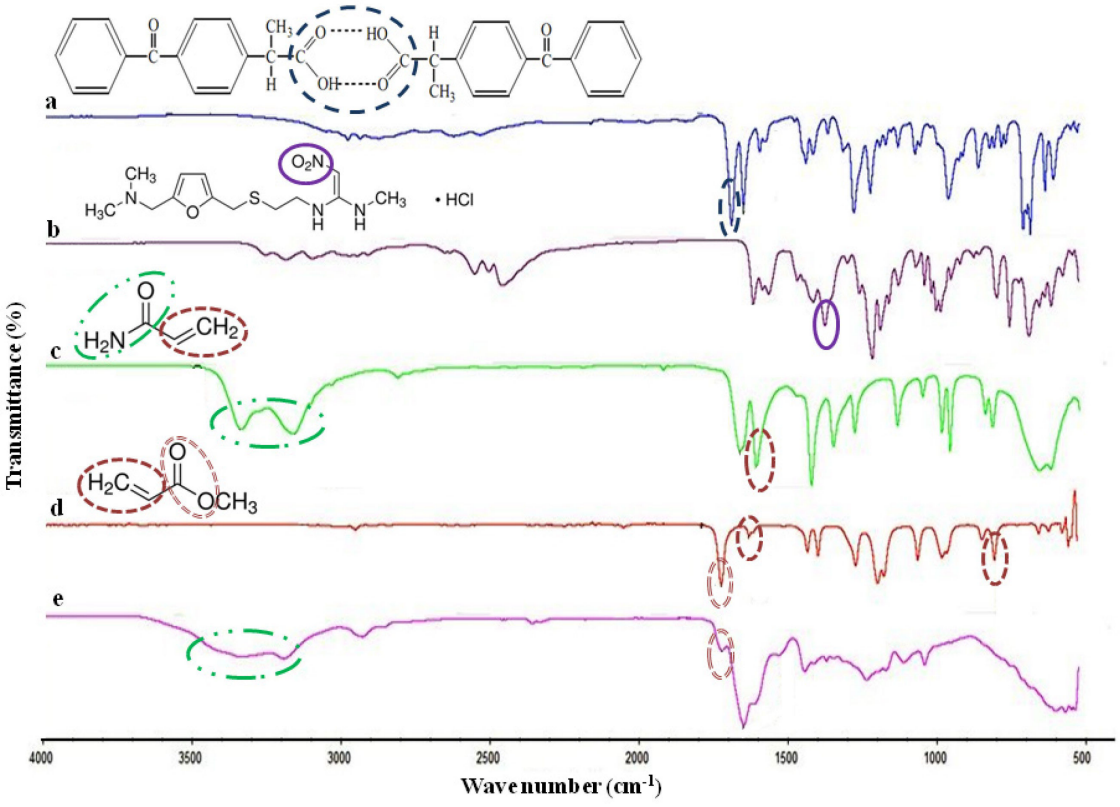

Fig. 4.5. FTIR spectra of a) ketoprofen, b) ranitidine HCl, c) acrylamide, d) methyl acrylate and e) formulation C1 at Q_m/Q_i = 1; (– -) stretching vibrations of dimeric carboxylic acid carbonyl group at 1691 cm^{-1} for ketoprofen, (—) -NO_2 group vibration at 1379 cm^{-1} for ranitidine HCl, (.. — ..) doublets for –NH group of primary amide in acrylamide and poly(acrylamide),(= =) ester vibration in acrylate, (– –) C=C for acrylates and acrylamide.

4.1.3.6 Encapsulation efficiency

Encapsulation efficiency of all the formulations tested was more than 80% for hydrophobic ketoprofen encapsulated in core. This is because shell provides protection to core and prevent loss of drug during encapsulation and washing procedure (Table 4.2). In comparison, ranitidine HCl, placed in shell, has low encapsulation efficiency. In general encapsulation of hydrophilic molecules is quite difficult. This may be due to poor affinity of ranitidine HCl with poly(acrylamide) shell, low initial charged amount i.e. 1wt.% and slow drying at room temperature where water diffuses slowly dragging ranitidine HCl out of the shell. This also explains the lower encapsulation efficiency of ranitidine HCl with higher shell's thickness (C1 at Q_m/Q_i = 1.3). We further observed an increase in encapsulation of ranitidine HCl with addition of carboxy ethyl acrylate in shell phase (formulation C3). We believe it is due to poly(acrylamide-co-carboxy ethyl acrylate) which prevented leakage of hydrophilic molecules by interacting with them. In literature interaction of ranitidine HCl by hydrogen bonding is reported with Eudragit E100 which is a mixture of acrylate monomers (Sarisuta et al., 2006) and number of other published reports also indicated a boost in encapsulation efficiency of drug by such interactions (Khan et al., 2014; Khan et al., 2013; Restani et al., 2010).

Table 4.2. Encapsulation efficiency (%) of the different formulations investigated

S. no	Formulation	Q_m/Q_i	Ketoprofen	Ranitidine HCl
1	C1	1	99	74
2		1.3	83	51
3	C3	1	100	87

4.1.3.7 Cytotoxicity testing

BNL-CL2 cells were incubated with specified concentrations of core-shell particles having same composition but different sizes of shell and core. They were observed before

and after incubation. MTT assay revealed that formulation C1 operated at low Q_m/Q_i was less toxic (LD_{50} was about 2.5 mg/mL) than the one formulated at high Q_m/Q_i (LD_{50} was about 2 mg/mL) (Fig. 4.6)**.** Note that formulation C1 operated at high Q_m/Q_i had a comparatively larger shell. We can propose that larger shell may contain small amount of non-reacted acrylamide monomer or other leachable species and it can lead to higher cytotoxicity, although we did not saw peaks of unreacted monomers in FTIR studies. Another proposition for the observed cytotoxicities is the direct physical contact with cell monolayer. To confirm our proposition we made non-contact MTT experiments in which particles were placed on the Transwell® polycarbonate membranes so that they did not have a physical contact with cell monolayer. At the same time soluble compounds could easily penetrate the membrane and influence cell viability. For non-contact conditions it was the same cytotoxicity ratio between formulation C1 operated at low (LD_{50} = 3.1 mg/mL and high (LD_{50} = 2.7 mg/mL) Q_m/Q_i. So we conclude that the main reason of cell toxicity is soluble compounds from the shell of particles (presumably acrylamide monomer, surfactants etc.). Surfactants also affect the viability of cells and it depends on concentration of surfactant and type of cell lines. In comparison surfactants containing organic counterions are less cytotoxic than those with inorganic counterions (Nogueira et al., 2011). In our particles presence of high concentrations of surfactants can contribute to the particle cytotoxicity, especially anionic SDS.

The difference between cell viability in contact and non-contact conditions may be explained with the physical properties of microparticles which are relatively big and heavy comparing to the cells, so in contact conditions they can move in medium causing cells trauma and death. The contribution of this factor is same for C1 formulated particles prepared at high and low Q_m/Q_i ratio (LD_{50} differed on about 0.6-0.7 mg/mL between the two types of tests) and its contribution was definitely less than one caused by soluble compounds.

We used live-dead test based on Calcein AM and Propidium iodide staining for visualization of cell viability. It confirmed the results of MTT-test and moreover allowed observing changes in the cell shape and in the intensity of staining caused by decreasing cell viability. The cells after treatment with microparticles had less bright green color compare to the control and shape which was close to round (Fig. 4.6).

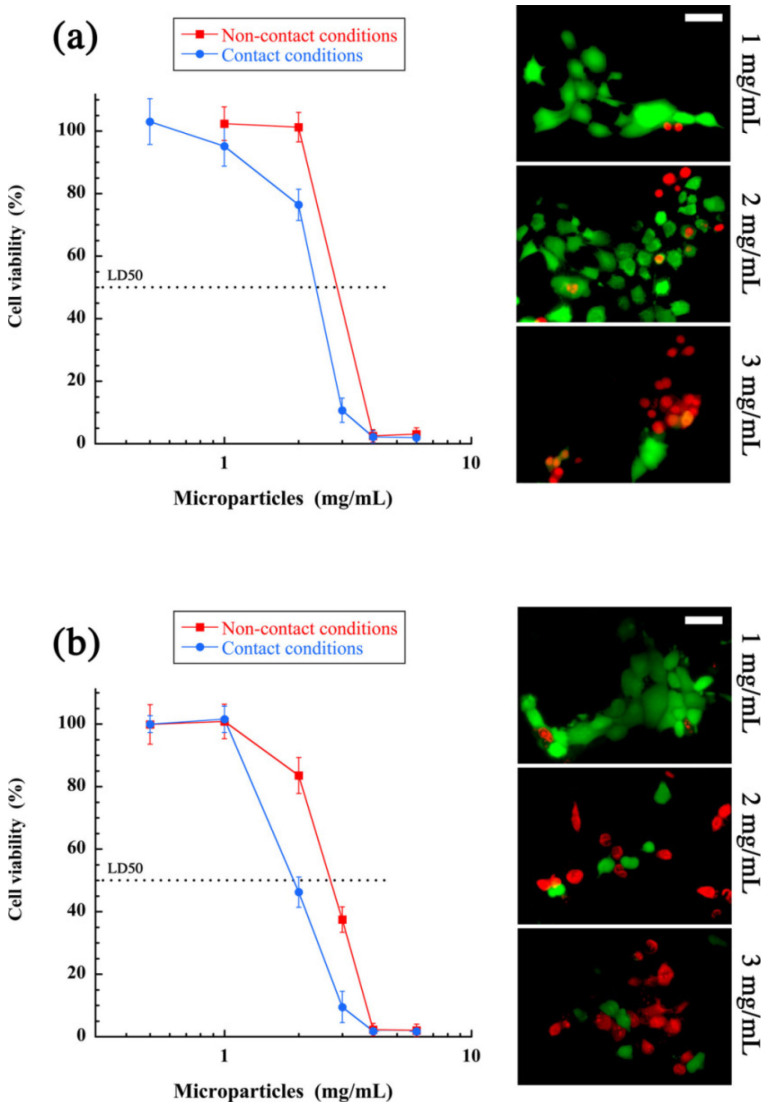

Fig. 4.6. Cell viability of BNL-CL2 hepatic cell line after exposure to different concentrations of C1 **at** a) Q_m/Q_i = 1 and b) Q_m/Q_i = 1.3 respectively. Figures shows overlaid fluorescent images of cell line after treatment with propidium iodide and Calcein AM. After exposure to core-shell particles dead cells appear red due to propidium iodide which is only permeable to dead cells while live cells appear green due to intracellular conversion of Calcein AM to green-fluorescent calcein after acetoxymethoxy group is removed by intracellular esterases. Scale bars represent 50 µm. Error bars indicate the standard deviation (n=3).

4.1.3.8 Drug release

Drug release of core-shell particles from formulation C1 obtained with Q_m/Q_i = 1 was carried out in USP buffer solution of pH 1.2 and 6.8. This formulation released higher quantity of ranitidine HCl (See supplementary Figure S 4) and ketoprofen at low and high pH respectively (Fig. 4.7).

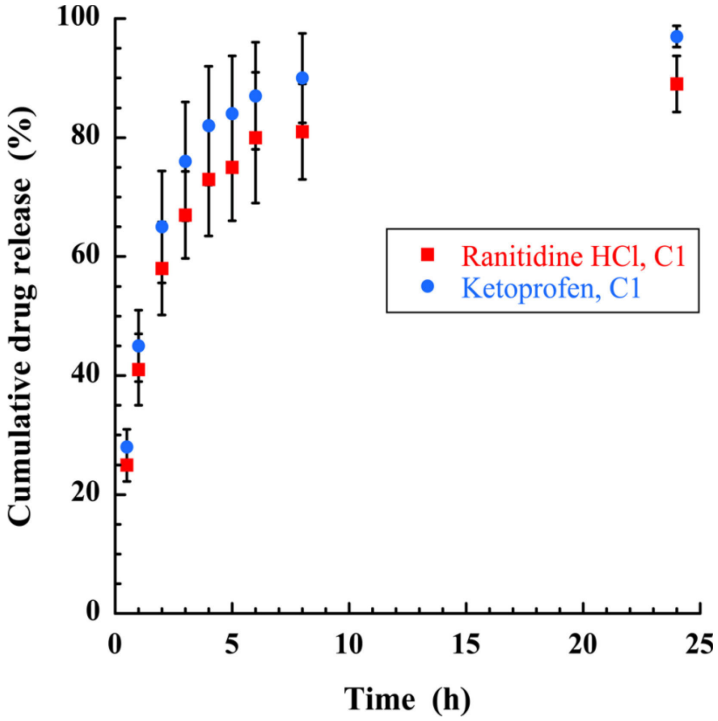

Fig. 4.7. Drug release of ranitidine HCl and ketoprofen from formulation C1 **at** Q_m/Q_i = 1 in USP phosphate buffer solution of pH 6.8.

Ketoprofen release from conventional dosage forms can cause serious systemic and gastric problems (Jachowicz et al., 2000). Although particulate dosage forms can reduce these side effects, the presence of a shell layer containing an antacid will further reduce the undesired effects and improve patients comfort. Here, higher release of ranitidine HCl at pH of stomach can suppress the gastric irritation effects like ulceration and bleeding commonly associated with nonsteroidal anti-inflammatory drugs (*NSAIDs*) like ketoprofen (Nagarsenker et al., 1997). At high pH, ketoprofen release was higher which was probably due to couple of reasons. a) Presence of high concentration of ketoprofen in core and low concentration of ranitidine HCl in shell. Babu *et al*. observed a slow release of 5-Fluorouracil from poly(acrylamide-*co*-methylmethacrylate) core-shell particles having lower amount of drug than ones having higher quantity b) High concentration of cross**s**linker and acrylamide, i.e. 6 and 30 wt. % respectively, made a dense crosslinked structure from where big molecules like ranitidine HCl (MW 350 g/mole) have difficulty to diffuse as compared to small ketoprofen (MW 254 g/mole). In our previous study with Janus particles, we observed a slow release of sodium fluorescein (MW 376 g/mole) at high concentration of crosslinker and monomer. Release rate of fluorescein sodium improved when crosslinker concentration dropped from 6 to 1.5 wt.% (Khan et al., 2014).

A further set of experiments aimed at enhancing the release rate of ranitidine HCl. This was done effortlessly by decreasing the flow rate of core phase in formulation C1, i.e. operating at high Q_m/Q_i. This resulted in a smaller core and subsequent thicker shell. Thus it prolonged the time and distance for dissolution media to reach the core, dissolve ketoprofen and diffuse drug in surrounding media while simultaneously increasing the concentration gradient for ranitidine. Kong *et al.* observed a decrease in burst release of hydrophobic drug from *poly(lactic-co-glycolic acid)* particles when they coated PLGA particles with an alginate layer in microfluidic device (Kong et al., 2013). In our experiments we observed a slight decrease in release rate of ketoprofen but on the other hand a fairly noticeable increase in the release rate of ranitidine HCl as shown in Figure 4.8.

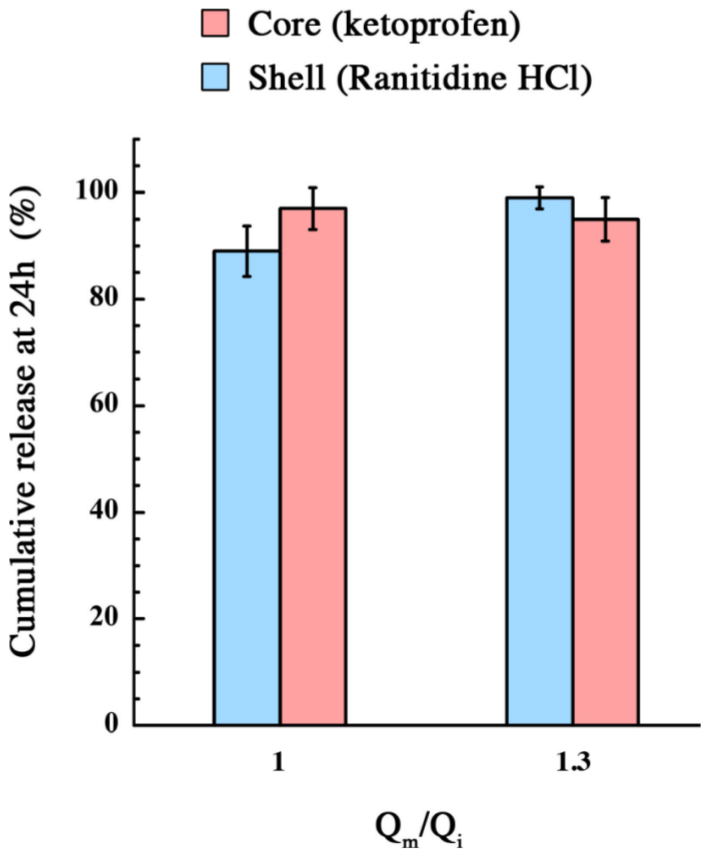

Fig. 4.8. Comparison of ketoprofen and ranitidine HCl release from core-shell particles obtained with formulation C1 for Q_m/Q_i = 1 and 1.3 having a shell thickness of 29 µm and 43 µm respectively. Shell thickness was measured immediately after polymerization.

Once formation and release properties of core-shell particles were elucidated, we moved to develop novel pH-sensitive particles where shell was composed of poly(acrylamide-co-carboxyethyl acrylate)(poly(AA-co-CEA)). pH-sensitive particles are highly

desirable to deliver active ingredients to colonic region of human intestine for topical treatment of local disorders such as colonic cancer, ulcerative colitis, amebiasis etc. Colonic drug delivery system delivers drug at target site thus increasing efficacy and reducing side effects (Ferrari et al., 2013; Wei et al., 2009).

So far, different strategies were investigated to target colonic region as time, pressure, pH, and enzyme based systems (Nunthanid et al., 2008; Wei et al., 2009). pH-sensitive systems for colon targeting are based on the assumption that pH increases from small intestine to large intestine. In stomach pH is about 1 to 2.5, 6.6 in the proximal small bowel, peaks at 7.5 in the terminal ileum and then falls down to 6.4 in the ascending colon and afterwards it rises again to values close to 7 (Ibekwe et al., 2006; Krogars et al., 2000). Nowadays, combination therapy to targeted organs is well established for effective treatment of cancer. The synergistic effect of drugs can be more beneficial if incorporated in multi drug delivery system (MDDS). These MDDS can overcome many of the conventional system limitations. Core-shell particles hold the ability to store drugs in core and shell.

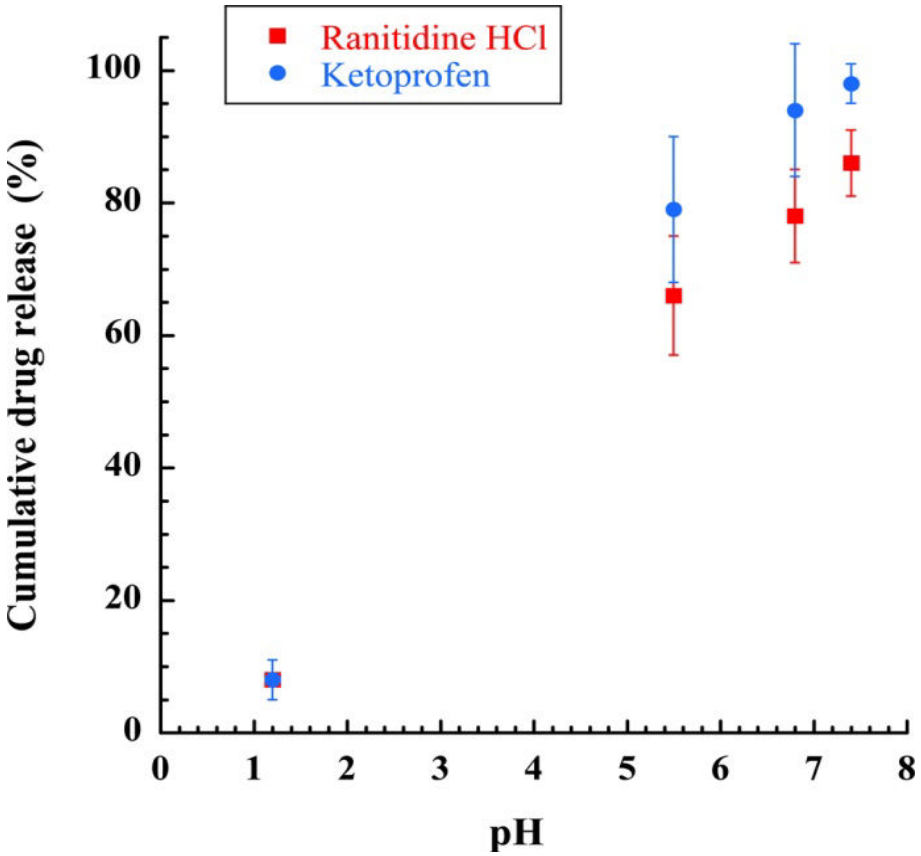

Fig. 4.9. Drug release from pH-sensitive core-shell particles with respect to the USP buffer solution pH. Error bars indicates the standard deviation (n=3).

In our study, pH-sensitive particles were obtained with formulation C3 (Table 2.3 chapter 2) where 10 wt.% of carboxyethyl acrylate were admixed to the shell phase of formulation C1. Thus it prevented the release of drugs at low pH but allowed to increase the release rate with pH (Figure 4.9). From the shape of curve, it seems that a maximum release was reached for a pH of 7.4. At low pH -COOH groups of poly(AA-co-CEA) shell remained in unionized form. But as the pH increases carboxyl groups dissociate to form carboxylate ions especially at neutral and basic pH. Charge repulsion arising from COO^- groups opened the polymeric network thus enhancing the drug diffusion with a subsequent faster release. In literature different pH-sensitive systems containing -COOH groups have shown such behavior (Kendall et al., 2009; Liu et al., 2013; Sohail et al., 2014). So, these pH responsive core-shell particles will be able to deliver two active molecules to diseases area in colon without fearing their solubility and incompatibility issues. As colon region of human intestine is less hostile in terms of enzymes as compared to stomach and small intestine. Accordingly, it is an ideal site to improve bioavailability of poorly absorbable drugs, proteins, peptides and vacciness (Chourasia and Jain, 2003; Yang et al., 2002).

4.1.4 Conclusion

A two co-axial capillaries-based microfluidic device was developed to provide an easy and facile approach for the production of droplets within droplets. These double droplets can be easily manipulated and hardened into core-shell microparticles with environment friendly UV assisted free radical polymerization while maintaining integrity of loaded APIs. Overall size of particles was controlled by adjusting continuous to middle phase flow rate ratio Q_c/Q_m whereas core's diameter and subsequent shell's thickness depended upon middle to inner phase flow rate ratio (Q_m/Q_i). A careful combination of monomers, surfactants and drug in either shell or core phases was necessary to get perfect core-shell structure. For non pH-sensitive particles under non-contact conditions LD_{50} was 3.1 mg/mL for formulation C1 at low Q_m/Q_i. Non pH-sensitive particles released higher concentration of shell located ranitidine at pH 1.2 as compare to core located ketoprofen and thus can prevent gastric injuries associated with NSAID's. A smart way was adopted to manipulate the release rate of two APIs by changing the dimensions of core and shell. Q_m/Q_i was increased to reduce the core's diameter and increase shell thickness while keeping the overall microparticle size constant. Colon targeted drug delivery systems can be used for local and

systemic treatment of different diseases. A facile approach is to use pH sensitive systems which prevent release at low pH, while releasing at colonic pH. Our novel pH-sensitive core-shell particles were able to release two model active compounds to colonic pH at the same time. It is believed that in the future this targeted dual delivery system will play an important role for better treatment of colonic diseases especially cancer by avoiding side effects and drug resistance. At the same time it gives additional benefits by delivering two APIs having incompatibility and different hydrophilicity in a single particle. Furthermore, these pH-sensitive core-shell particles will be a potential drug delivery system for protein in nature drugs.

In this section, core-shell particles were produced in a single step using a two co-axial capillaries-based microfluidic device. This morphology allowed protection of two incompatible APIs loaded in core and shell part respectively. Furthermore, these particles released simultaneously the two APIs at colonic pH and thus demonstrated their potential for targeted dual drug delivery. Core-shell particles provide protection to single core but what if one wants to encapsulate large number of nanoparticles. Such morphology, so-called Trojan, is quite difficult to obtain with conventional methods mainly because it implies numerous steps. The following section is devoted to the development of a novel semi-continuous two-step process for the production of nano-in-micro carriers that makes nanoparticles handling convenient and provides protection until they reach desired site in GIT.

4.1.5 Supplementary information

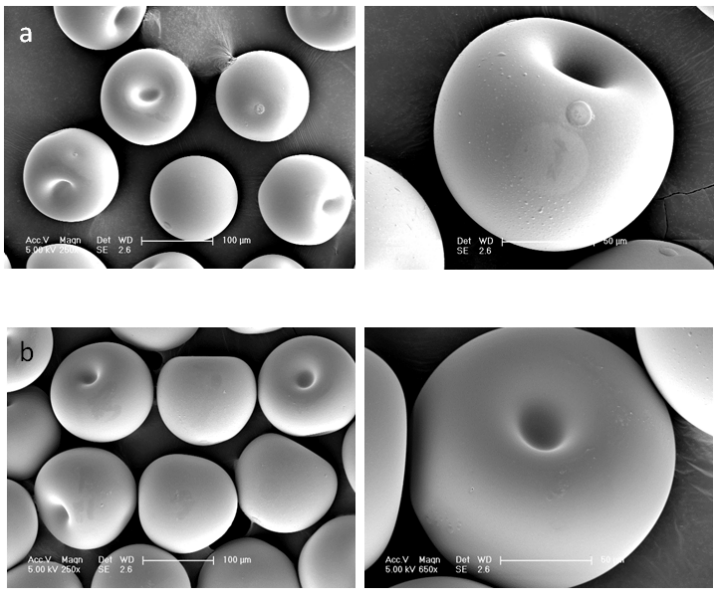

Fig. S1. SEM photographs of formulation C1 when Q_m/Q_i equals to a) 1.3 and b) 2. Enlarged images show indentation on one side.

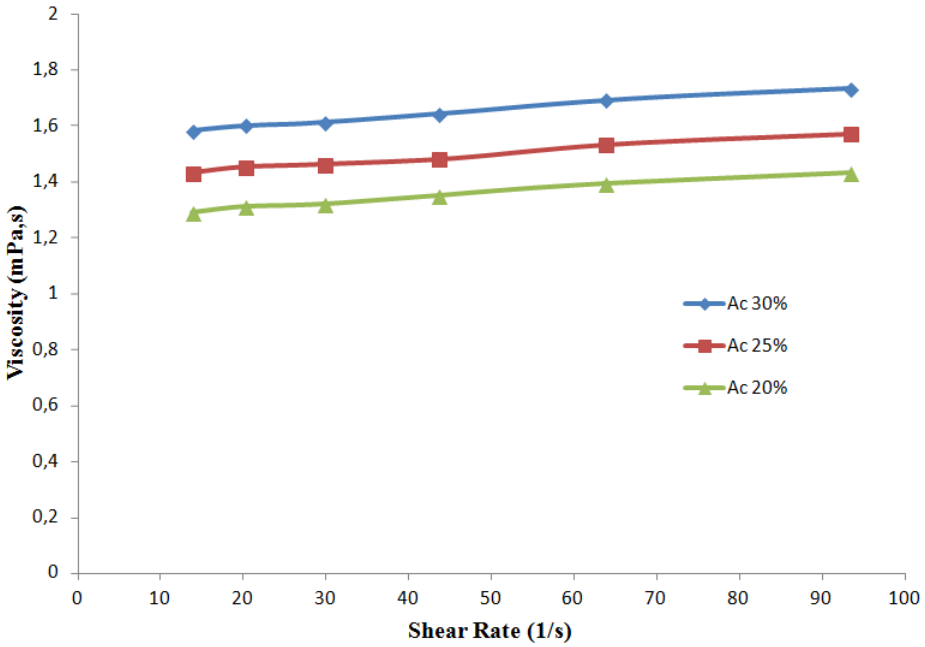

Fig. S2. Viscosity of shell phase solution as a function of acrylamide (Ac) weight content. All the viscosities were measured at 20°C using Anton Paar MCR 102 Rheometer.

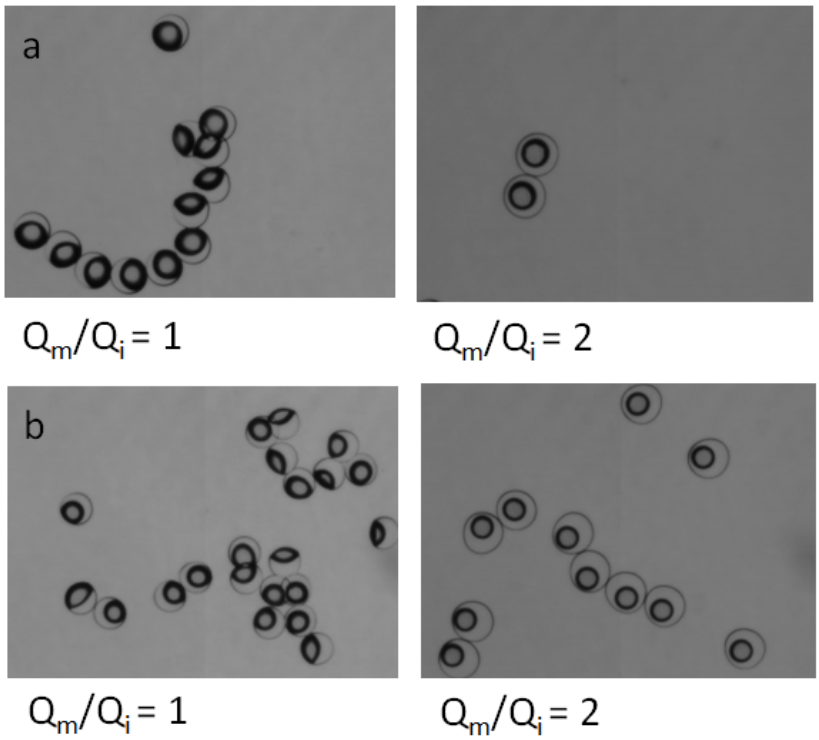

Fig. S3. Optical micrographs of particle structure for different middle to inner phase flow rate ratios in formulation C1 with a) 40 and b) 20wt.% of TPGDA in the core phase. Q_m was kept at 4 µL/min when Q_m/Q_i=2. Pictures were taken immediately after polymerization.

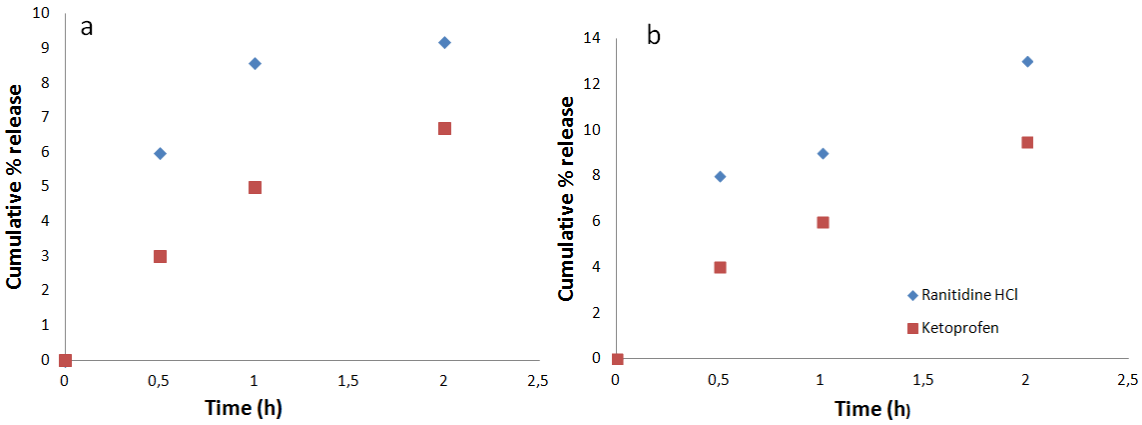

Fig. S4. Release of ketoprofen and ranitidine HCl from formulation C1 for Q_m/Q_i equals to a) 1 or b) 1.3 in USP buffer solution of pH 1.2.

References

Alves, T., Tavares, E., Aouada, F., Negrão, C., Oliveira, M., Duarte Júnior, A., Ferreira da Costa, C., Silva Júnior, J., Ribeiro Costa, R., 2011. Thermal analysis characterization of PAAm-co-MC hydrogels. J Therm Anal Calorim 106, 717-724.

Babu, V.R., Sairam, M., Hosamani, K.M., Aminabhavi, T.M., 2006. Development of 5-fluorouracil loaded poly(acrylamide-co-methylmethacrylate) novel core-shell microspheres: In vitro release studies. International Journal of Pharmaceutics 325, 55-62.

Bouquey, M., Serra, C., Berton, N., Prat, L., Hadziioannou, G., 2008. Microfluidic synthesis and assembly of reactive polymer beads to form new structured polymer materials. Chemical Engineering Journal 135, Supplement 1, S93-S98.

Chang, Z., Serra, C.A., Bouquey, M., Prat, L., Hadziioannou, G., 2009. Co-axial capillaries microfluidic device for synthesizing size- and morphology-controlled polymer core-polymer shell particles. Lab on a Chip 9, 3007-3011.

Chourasia, M.K., Jain, S.K., 2003. Pharmaceutical approaches to colon targeted drug delivery systems. J Pharm Pharm Sci. 6, 33-66.

Dweik, H., Sultan, W., Sowwan, M., Makharza, S., 2007. Analysis Characterization and Some Properties of Polyacrylamide Copper Complexes. International Journal of Polymeric Materials and Polymeric Biomaterials 57, 228-244.

Ferrari, P.C., Souza, F.M., Giorgetti, L., Oliveira, G.F., Ferraz, H.G., Chaud, M.V., Evangelista, R.C., 2013. Development and in vitro evaluation of coated pellets containing chitosan to potential colonic drug delivery. Carbohydrate Polymers 91, 244-252.

Gong, X., Peng, S., Wen, W., Sheng, P., Li, W., 2009. Design and Fabrication of Magnetically Functionalized Core/Shell Microspheres for Smart Drug Delivery. Advanced Functional Materials 19, 292-297.

Ibekwe, V.C., Fadda, H.M., Parsons, G.E., Basit, A.W., 2006. A comparative in vitro assessment of the drug release performance of pH-responsive polymers for ileo-colonic delivery. International Journal of Pharmaceutics 308, 52-60.

Jachowicz, R., Nürnberg, E., Pieszczek, B., Kluczykowska, B., Maciejewska, A., 2000. Solid dispersion of ketoprofen in pellets. International Journal of Pharmaceutics 206, 13-21.

Kendall, R.A., Alhnan, M.A., Nilkumhang, S., Murdan, S., Basit, A.W., 2009. Fabrication and in vivo evaluation of highly pH-responsive acrylic microparticles for targeted gastrointestinal delivery. European Journal of Pharmaceutical Sciences 37, 284-290.

Khan, I.U., Serra, C.A., Anton, N., Li, X., Roman, A., Messaddeq, N., Kraus, I., Vandamme, T.F., 2014. Microfluidic conceived drug loaded Janus particles in side-by-side capillaries device. International Journal of Pharmaceutics 473, 239-249.

Khan, I.U., Serra, C.A., Anton, N., Vandamme, T., 2013. Continuous-flow encapsulation of ketoprofen in copolymer microbeads via co-axial microfluidic device: Influence of operating and material parameters on drug carrier properties. International Journal of Pharmaceutics 441, 809-817.

Kong, T., Wu, J., Yeung, K.W.K., To, M.K.T., Shum, H.C., Wang, L., 2013. Microfluidic fabrication of polymeric core-shell microspheres for controlled release applications. Biomicrofluidics 7, -.

Krogars, K., Heinämäki, J., Vesalahti, J., Marvola, M., Antikainen, O., Yliruusi, J., 2000. Extrusion–spheronization of pH-sensitive polymeric matrix pellets for possible colonic drug delivery. International Journal of Pharmaceutics 199, 187-194.

Lee, T.H., Wang, J., Wang, C.-H., 2002. Double-walled microspheres for the sustained release of a highly water soluble drug: characterization and irradiation studies. Journal of Controlled Release 83, 437-452.

Lee, T.Y., Roper, T.M., Jonsson, E.S., Kudyakov, I., Viswanathan, K., Nason, C., Guymon, C.A., Hoyle, C.E., 2003. The kinetics of vinyl acrylate photopolymerization. Polymer 44, 2859-2865.

Li, G., Guo, J., Wang, X., Wei, J., 2009. Microencapsulation of a functional dye and its UV crosslinking controlled releasing behavior. Journal of Polymer Science Part A: Polymer Chemistry 47, 3630-3639.

Liu, W., Selomulya, C., Chen, X.D., 2013. Design of polymeric microparticles for pH-responsive and time-sustained drug release. Biochemical Engineering Journal 81, 177-186.

Nagarsenker, M.S., Tantry, J.S., Shenai, H., 1997. Influence of Hydroxypropyl-β-cyclodextrin on the Dissolution of Ketoprofen and Irritation to Gastric Mucosa After Oral Administration in Rats. Pharmacy and Pharmacology Communications 3, 443-445.

Nogueira, D.R., Mitjans, M., Infante, M.R., Vinardell, M.P., 2011. Comparative sensitivity of tumor and non-tumor cell lines as a reliable approach for in vitro cytotoxicity screening of lysine-based surfactants with potential pharmaceutical applications. International Journal of Pharmaceutics 420, 51-58.

Nunthanid, J., Huanbutta, K., Luangtana-anan, M., Sriamornsak, P., Limmatvapirat, S., Puttipipatkhachorn, S., 2008. Development of time-, pH-, and enzyme-controlled colonic drug delivery using spray-dried chitosan acetate and hydroxypropyl methylcellulose. European Journal of Pharmaceutics and Biopharmaceutics 68, 253-259.

Özeroglu, C., Sezgin, S., 2007. Polymerization of acrylamide initiated with Ce(IV)- and KMnO4-mercaptosuccinic acid redox systems in acid-aqueous medium. eXPRESS Polymer Letters 1, 132–141.

Restani, R.B., Correia, V.G., Bonifácio, V.D.B., Aguiar-Ricardo, A., 2010. Development of functional mesoporous microparticles for controlled drug delivery. The Journal of Supercritical Fluids 55, 333-339.

Rondeau E, C.-W.J., 2012. Formation of multilayered biopolymer microcapsules and microparticles in a multiphase microfluidic flow. Biomicrofluidics 6, 24125-2412516.

Sarisuta, N., Lawanprasert, P., Puttipipatkhachorn, S., Srikummoon, K., 2006. The Influence of Drug-Excipient and Drug-Polymer Interactions on Butt Adhesive Strength of Ranitidine Hydrochloride Film-Coated Tablets. Drug Development and Industrial Pharmacy 32, 463-471.

Serra, C., Berton, N., Bouquey, M., Prat, L., Hadziioannou, G., 2007. A Predictive Approach of the Influence of the Operating Parameters on the Size of Polymer Particles Synthesized in a Simplified Microfluidic System. Langmuir 23, 7745-7750.

Serra, C.A., Chang, Z., 2008. Microfluidic-Assisted Synthesis of Polymer Particles. Chemical Engineering & Technology 31, 1099-1115.

Sohail, K., Khan, I.U., Shahzad, Y., Hussain, T., Ranjha, N.M., 2014. pH-sensitive polyvinylpyrrolidone-acrylic acid hydrogels: Impact of material parameters on swelling and drug release. Brazilian Journal of Pharmaceutical Sciences 50, 173-184.

Tran, V.-T., Benoît, J.-P., Venier-Julienne, M.-C., 2011. Why and how to prepare biodegradable, monodispersed, polymeric microparticles in the field of pharmacy? International Journal of Pharmaceutics 407, 1-11.

Wang, W.-T., Chen, R., Xu, J.-H., Wang, Y.-D., Luo, G.-S., 2014. One-step microfluidic approach for controllable production of gas-in-water-in-oil (G/W/O) double emulsions and hollow hydrogel microspheres. RSC Advances 4, 16444-16448.

Wang, W., Zhou, S., Sun, L., Huang, C., 2010. Controlled delivery of paracetamol and protein at different stages from core–shell biodegradable microspheres. Carbohydrate Polymers 79, 437-444.

Wei, H., Li-Fang, F., Bai, X., Chun-Lei, L., Qing, D., Yong-Zhen, C., De-Ying, C., 2009. An investigation into the characteristics of chitosan/Kollicoat SR30D free films for colonic drug delivery. European Journal of Pharmaceutics and Biopharmaceutics 72, 266-274.

Wu, J., Kong, T., Yeung, K.W.K., Shum, H.C., Cheung, K.M.C., Wang, L., To, M.K.T., 2013. Fabrication and characterization of monodisperse PLGA–alginate core–shell microspheres with monodisperse size and homogeneous shells for controlled drug release. Acta Biomaterialia 9, 7410-7419.

Yang, L., Chu, J.S., Fix, J.A., 2002. Colon-specific drug delivery: new approaches and in vitro/in vivo evaluation. International Journal of Pharmaceutics 235, 1-15.

Yu, Y.-L., Zhang, M.-J., Xie, R., Ju, X.-J., Wang, J.-Y., Pi, S.-W., Chu, L.-Y., 2012. Thermo-responsive monodisperse core–shell microspheres with PNIPAM core and biocompatible porous ethyl cellulose shell embedded with PNIPAM gates. Journal of Colloid and Interface Science 376, 97-106.

4.2 Microfluidic conceived Trojan microcarriers for oral delivery of nanoparticles

Graphical Abstract

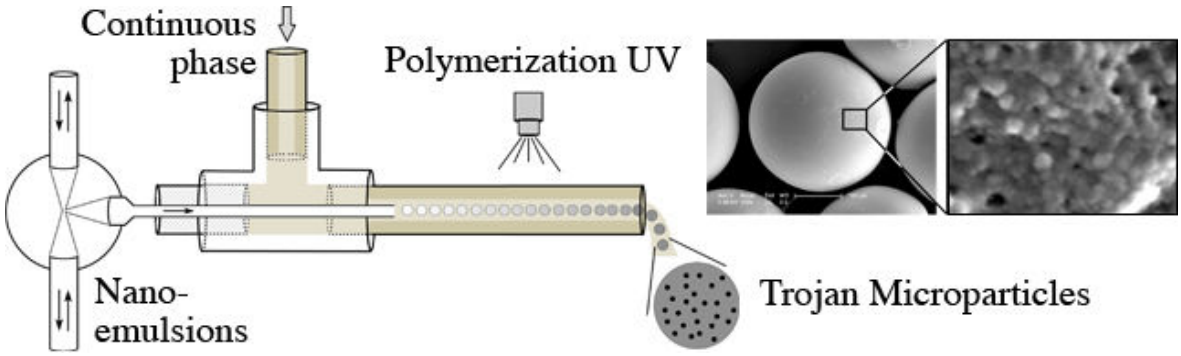

Abstract

In this study, we report on a novel method for the synthesis of poly(acrylamide) Trojan microparticles embedded with ketoprofen loaded poly(ethyl acrylate) or poly(methyl acrylate) nanoparticles. Thus, these microparticles have the potential to deliver nanoparticles in the gastro intestinal tract. A polymerizable nanoemulsion was used as a template to develop these microparticles. These nanoemulsions were obtained in an elongational-flow micromixer (µRMX) which was linked to a capillary-based microfluidic device for its emulsification into micron range droplets. Downstream, the droplets were hardened into Trojan particles in the size range of 213 to 308 µm by UV initiated polymerization. The nanoemulsion size varied from 98 to 132 nm upon changes in surfactant concentration and number of cycles in µRMX. SEM micrographs confirmed the Trojan morphologies and show that polymerization process reduces their sizes to 20-32 nm for poly(ethyl acrylate) nanoparticles, and to 10-15 nm for poly(methyl acrylate) ones. We show that Trojan microparticles released embedded nanoparticles on contact with suitable media as confirmed by transmission electron microscopy. In USP phosphate buffer solution of pH 6.8, Trojan microparticles embedded with poly(ethyl acrylate) nanoparticles released 35% of encapsulated ketoprofen over 24 hours. Low release of drug was attributed to overall low concentration of nanoparticles and attachment of some of nanoparticles to the poly(acrylamide) matrix.

Keywords: Trojan, nanoemulsions, elongational flow, poly(ethyl acrylate), poly(methyl acrylate), oral nanoparticle delivery

4.2.1 Introduction

The oral route is the most widely accepted route for delivering active pharmaceutical ingredients. But poor drug solubility, stability and absorption could lead to low bioavailability in blood stream (Ensign et al., 2012). Moreover, in conventional dosage some drugs can also cause irritation of gastrointestinal tract (GIT). One way to remove these hurdles is by encapsulating the drug into micro- or nanoparticles. It have been reported by many authors that these particles have the ability to accumulate in inflamed areas and also reduce the toxic effect of irritant drugs (Ranjha et al., 2009).

In nanotechnology, scientists manipulate drugs and polymers at nanoscales that give unique chemical, physical and biological properties, quite different from micro- and macro systems (Anton et al., 2012). So far, nanotechnology has provided us with significant improvement in drug solubility, drug delivery, cancer diagnosis and treatment (Bisht et al., 2008). Nanoparticles can be administered via parental, ocular, dermal, oral and inhalation routes. However, their administration involves numerous hurdles, for instance when administered by oral route multiple factors affect the fate of these nanoparticles like pH, ionic concentration, enzymes, mucus, motility etc. In GIT rapid secretion and shedding of mucus membrane along with motility primarily affect their accumulation and penetration through absorption site (Ensign et al., 2012). Secondly handling of nanoparticles can be more difficult than microparticles because sometimes former form aggregates while in suspension and can undergo hydrolysis or sedimentation (Gómez-Gaete et al., 2008).

Under such circumstances, a hybrid system combining the advantages of nanoparticles and microparticles would be a promising option. In such system nanoparticles are dispersed in microparticles that make their handling convenient while providing protection till their delivery near the site of absorption thus improving their effectiveness. These nano-in-micro system are called Trojan particles (Anton et al., 2012).

Nanoemulsions sometimes also referred as miniemulsions, ultrafine emulsions, submicron emulsions are transparent or translucent systems in the size range of 50–200 nm and requires oil, water, surfactant and energy to break large oil drops (in case of O/W) into smaller ones (Antonietti and Landfester, 2002; Solans et al., 2005; Tadros et al., 2004). This result in an increase in the Laplace pressure (p) defined as the difference between inside and

outside drop's pressures and is inversely proportional to the drop's radius (*R*) as shown in equation (1), where γ represents the interfacial tension. So for smaller droplets, high forces are required that are usually achieved by a more vigorous agitation (Anton et al., 2008; Tadros et al., 2004). Routine nano-emulsification processes include conventional devices such as ultrasonicator, high pressure homogenizer or microfluidizer® (Charles, 2011).

$$p = \frac{2\gamma}{R} \qquad 1$$

Conventional fabrication methods of Trojan particles usually follow a tedious and multistep procedure, *i.e.* nanoparticles are first synthesized usually in a batch reactor (by nanoprecipitation, miniemulsion polymerization, solvent extraction etc.) and then dispersed into microparticles by a spray drying process. However, these particles suffer from a large particle size distribution (Anton et al., 2012). In this paper, we report on a new semi-continuous process for the synthesis of Trojan microparticles based on nanoemulsion templates obtained by means of an elongational-flow micromixer. These microparticles have the potential to deliver a drug loaded nanoparticles in GIT. To the best of our knowledge this is a first step toward the continuous synthesis of Trojan particles using microfluidic tools.

4.2.2 Experimental

I. *List of materials is given in Chapter 2 section 2.1*
II. *Description of the microfluidic setup for Trojan particle synthesis is provided in Chapter 2, section 2.2.4*
III. *Methods for particle characterization are detailed in Chapter 2, section 2.3.4 while encapsulation efficiency and release properties are determined following the procedure described in Chapter 2, section 2.3.1.2 and 2.3.1.7 respectively*

4.2.3 Results and discussion

A new facile and semi-continuous microfluidic setup was reported to synthesize Trojan microparticles. This setup uses two different microfluidic devices namely a) an elongational-flow micromixer (μRMX) for the production of nanoemlusions and b) a co-axial capillary-based microfluidic device to generate microdroplets of the former polymerizable nanoemulsion. The latter device also allowed polymerizing downstream by UV source that converts nanodroplets into solid nanoparticles embedded in a microparticle (Fig. 2.4, Chapter 2). This was made possible due to the presence of hydrophobic (acrylate) and

hydrophilic (acrylamide) monomers and photoinitiators in oil and water phases respectively as well as surfactant in water phase (Table.2.4, Chapter 2). Later when exposed to UV irradiation, ethyl or methyl acrylate nanodroplets are converted to poly(ethyl acrylate) or poly(methyl acrylate) nanoparticles while microparticles matrix is formed upon polymerization of acrylamide.

4.2.3.1 Formation and size of nanoemulsions

This is a well established fact that formation of nanoemulsion depends on number of factors like interfacial tension, phases viscosity, phase transition region as well as surfactant structure and concentration (Anton et al., 2008; Bouchemal et al., 2004; Fernandez et al., 2004; Tadros et al., 2004). To form nanoemulsions, one need high shear forces or elongational flow (as in present paper) to break the to-be-dispersed phase into nanodroplets in the presence of surfactant which helps to decrease the interfacial tension. This reduction in interfacial tension is directly related to the concentration of surfactant as explained by Gibbs adsorption equation (Tadros et al., 2004).

Another factor which affects droplet size in nanoemulsions is the Ostwald ripening phenomenon where bigger droplets grow at expense of smaller ones due to difference in Laplace pressure between droplets of different sizes (Forgiarini et al., 2001; Tadros et al., 2004). According to Lifshitz–Slezov and Wagner (LSW) theory, Ostwald ripening rate in O/W emulsions is directly proportional to the solubility of the oil in aqueous phase. The addition of a second oil (Ostwald ripening inhibitor) having less solubility in aqueous solution can block this phenomenon (Solans et al., 2005). In this work, hexadecane was used for such purpose.

Immediately after preparation diluted samples of nanoemulsions were taken for DLS measurements. Results indicated monodisperse nanodroplets in the range of 98 to 132 nm with PDI as low as 0.160. The effect of surfactant concentration and composition on the nanoemulsion size distribution, corresponding to the two formulations T0 and T2 (reported in Table 2.4, Chapter 2), is presented in Figure 4.10 and appear negligible.

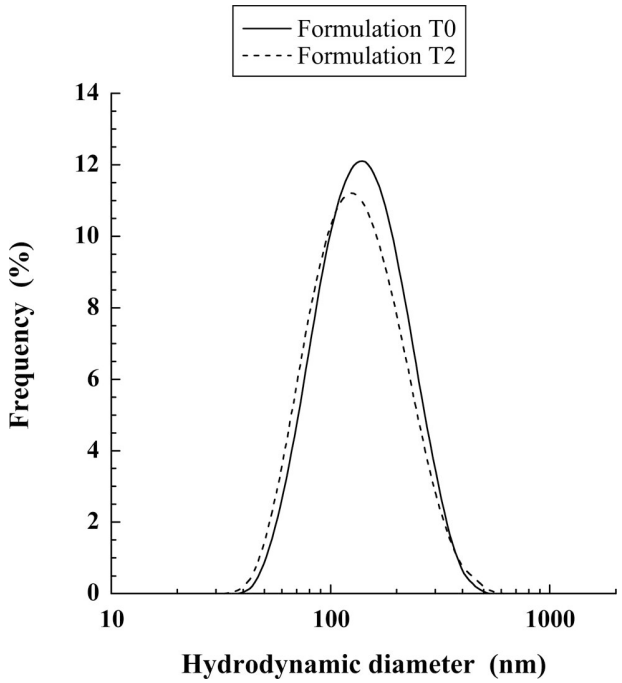

Fig. 4.10. Size of ethyl acrylate (T0) and methyl acrylate (T2) nanoemulsion as measured by DLS. Graph is reported after 30 cycles in µRMX and volume ratio between oil and water was 20:80.

4.2.3.2 Effect of cycles on nanodroplets

Prior to proper synthesis Trojan microparticles, it was necessary to evaluate the influence of µRMX operating parameters. Thus we kept constant all parameters (flow rate, composition of the dispersed and continuous phases) except the number of cycles for formulation T0. We observed a gradual reduction of the droplet size when the number of cycles was increased as shown in Figure 4.11. In the µRMX, droplets of oil phase are formed when the mixture was forced to pass through the restriction of 250 µm. As the number of cycles increases, droplets are broken into smaller droplets while at the same time they are stabilized by the presence of surfactants in the continuous phase. As mentioned above, surfactant plays an important role in the formation of nanoemulsions by decreasing the surface tension which in turn reduces the stress required to break the droplets. The surfactant also stabilizes newly formed droplets and prevent coalescence (Charles Lovelyn and Attama, 2011; Tadros et al., 2004). In our trials, a plateau value is obtained after 90 cycles. Such observation was also reported by Souilem *et al*. (Souilem et al., 2012) who claimed that equilibrium is reached between the forces resulting from the Laplace pressure (Eq. 1) and the hydrodynamic stress.

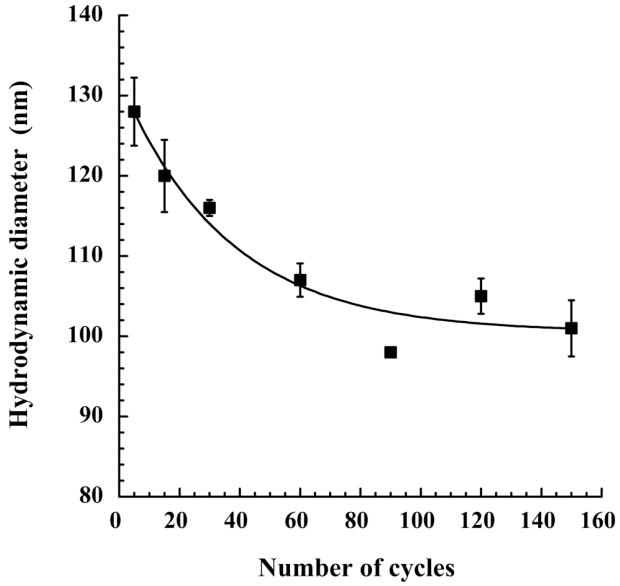

Fig. 4.11. Effect of the number of cycles on ethyl acrylate nanodroplets size obtained in the µRMX. Flow rate was set to 5 mL/min and volume ratio between oil and water to 20:80. Line is only to guide the eye. Error bars indicates the standard deviation (n=3).

4.2.3.3 Size and internal morphology of Trojan particles

All formulations studied led to monodisperse microparticles with a coefficient of variation less than 5% as shown in Table 4.3. Their size was dependent upon continuous to dispersed phase flow rate ratio (Q_c/Q_d) as reported in the literature (Jeong et al., 2012; Khan et al., 2014; Khan et al., 2013; Watanabe et al., 2011), decreasing when Q_c/Q_d is increased.

Table 4.3. Particle size of different formulations with coefficient of variation

	Formulation	Q_c/Q_d	Size (µm)	CV*
1	T0	30	308	2.32
		60	253	2.16
		120	213	0.83
2	T2	30	279	1.27

*CV is the ratio of the standard deviation to the mean particle diameter. In all formulation Q_c was kept constant at 240 µL/min.

Under SEM their surface appeared smooth and uniform. Their cross section revealed under high voltage and magnification (*i.e.* 20KV and 80000 or 1000000x) embedded ketoprofen loaded poly(ethyl acrylate) and poly(methyl acrylate) nanoparticles as shown in Figure 4. Poly(ethyl acrylate) nanoparticles were in the range of 20 to 32 nm (Figure 4.12a). But poly(methyl acrylate) nanoparticles were in the range of 10 to 15 nm (Figure 4.12b). The

slight difference in size for these two formulations is probably due to the difference in the concentration and combination of surfactants (Table 2.4, Chapter 2). Literature also supports the fact that the size of nanoemulsions is reduced with increasing concentration and type of surfactant (Antonietti and Landfester, 2002; Bouchemal et al., 2004; Tadros et al., 2004). Furthermore, it was observed a roughly 5 fold reduction in size when comparing the DLS results on nanoemulsion and SEM or TEM results on polymerized nanodroplets (*i.e.* nanoparticles). This could be due to different reasons. a) during polymerization of monomers there is always a reduction of size of the droplet/particle (Khan et al., 2013) due to the difference in density between polymer an nomoner; b) reduction may also originate from uncomplete polymerization leading to the shrinkage of the polymer nanoparticles when unreacted monomer is extracted during the washing procedure and/or SEM or TEM sample preparation; c) finally DLS measures a hydrodynamic diameter, *i.e.* the size of the dispersed phase nanodroplets plus the layer of ions around their surface.

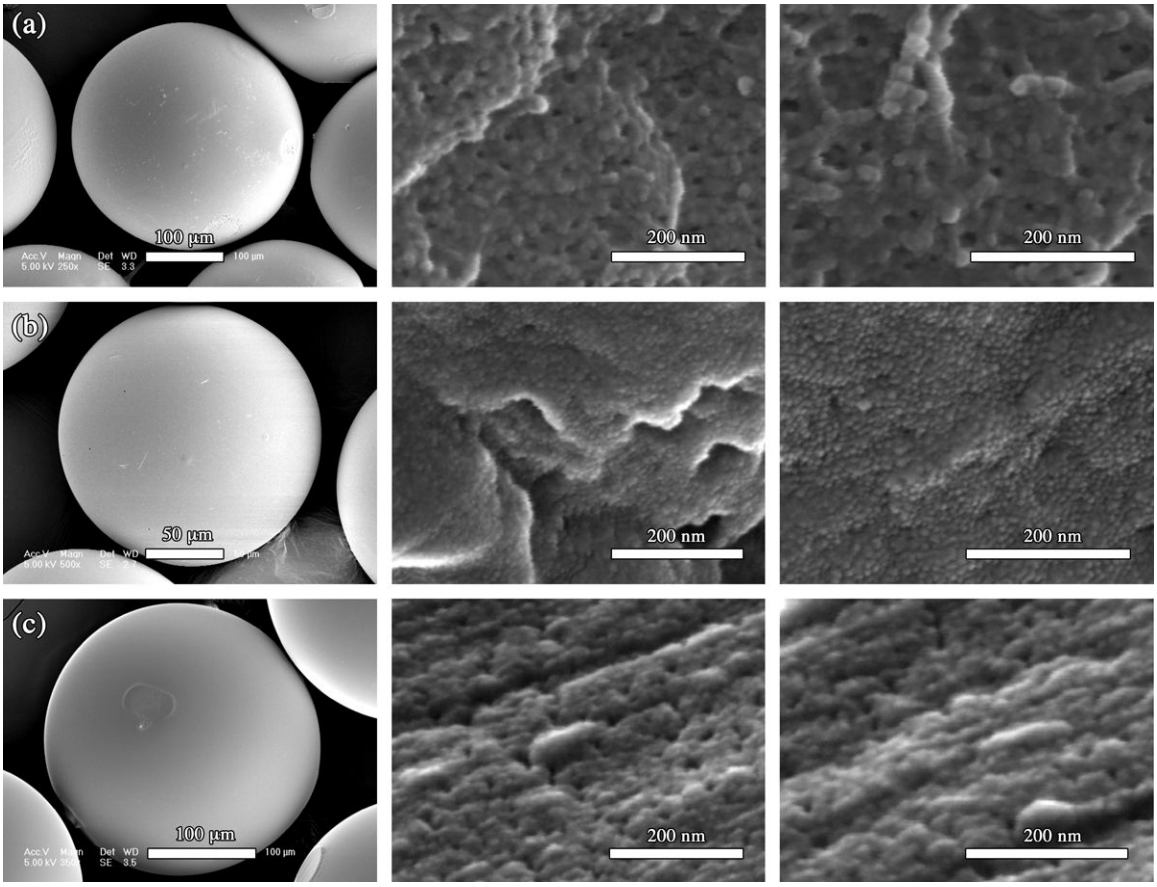

Fig. 4.12. SEM micrographs of microparticles and their cross section at different magnifications exhibiting embedded nanoparticles (except for (c)) obtained from the formulations T0 (a), T2 (b) and T2 blank (c) (i.e. without oil phase).

3.4 Release of nanoparticles

Trojan microparticles matrix was composed of a crosslinked network of poly(acrylamide) chains due to the use of a crosslinker (MBA) in the formulation. Since poly(acrylamide) is an hydrophilic polymer, the matrix acted as a hydrogel when immersed in water and swells by diffusion of the water through the network. Due to the presence of the nanoparticles inside the microparticle, when the matrix is swollen, after immersion in the release media and upon gently shaking, it released the entrapped nanoparticles which were detected in the release media by using TEM as shown in Figure 4.13.

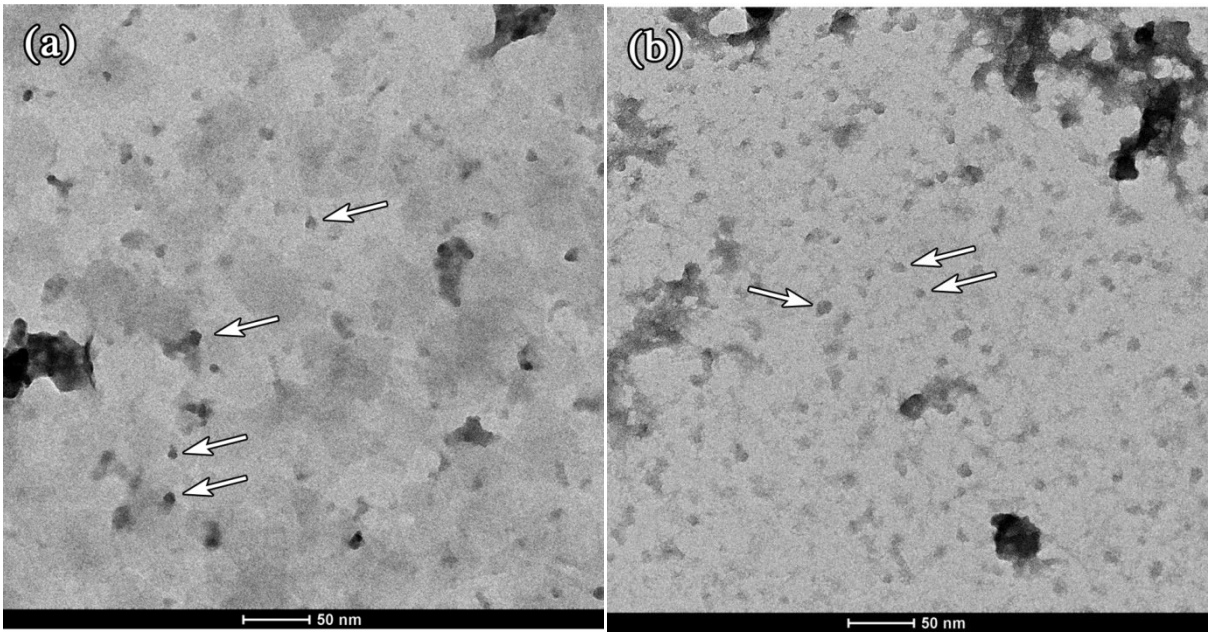

Fig. 4.13. TEM of ketoprofen loaded (a) poly(ethyl acrylate) and (b) poly(methyl acrylate) nanoparticles observed in release media after incubation of two hours and gentle shaking at 100 rpm in USP phosphate buffer solution of pH 6.8 at 37 °C.

3.5 Encapsulation efficiency and drug release

Encapsulation efficiency of formulation T0 was determined by encapsulating Trojan microparticles in PBS of pH 6.8 for 48 hours and was found to be around 81%. Then the release of ketoprofen from microparticles was measured at pH 6.8 in a phosphate buffer solution using dialysis tube. It was found that only 35% of encapsulated ketoprofen was released over 24 hours (Fig. 4.14). Limited release of drug is attributed to several reasons: a) overall concentration of nanoparticles in matrix was limited, as initial volume feed ratio

between ethyl acrylate and aqueous acrylamide solution was 20:80. Thus, only 20% of feed material was converted into nanoparticles; b) initial charged concentration of ketoprofen in formulation T0 was 2 wt.% (maximum solubility of ketoprofen in ethyl acrylate is 10 wt.%). In general drug release from polymeric matrices is governed by solute diffusion, polymeric matrix swelling and polymeric degradation (Fu and Kao, 2010). Solute diffusion in turn depends on initial concentration (Peppas and Narasimhan, 2014) which was less than 2 wt.% in case of Trojan microparticles designated as formulation T0.; c) polymeric matrix of Trojan microparticles swells when in contact with PBS solution. We believe this mechanism supports the release of entrapped poly(ethyl acrylate) nanoparticles.

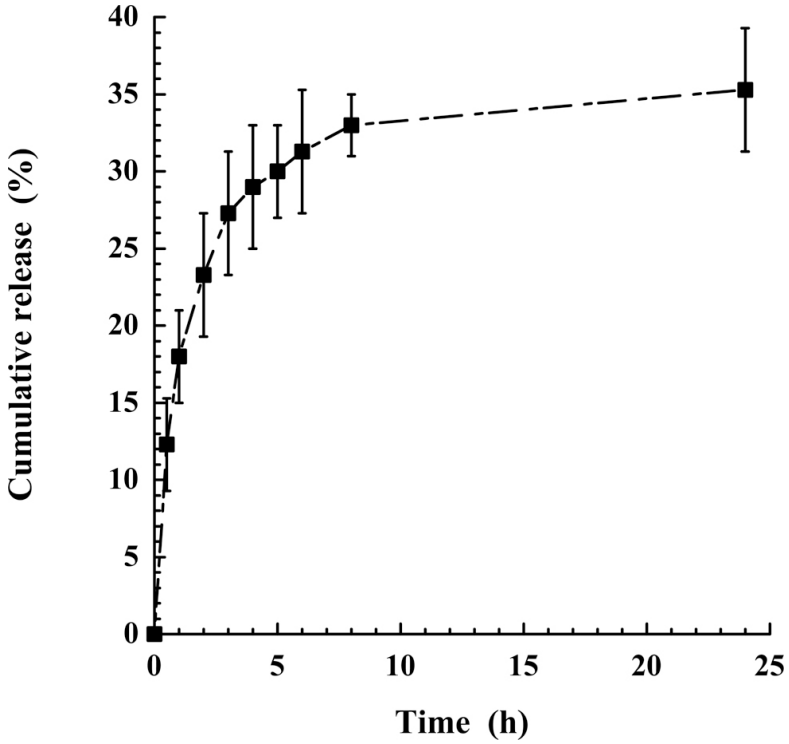

Fig. 4.14. Ketoprofen release from Trojan microparticles obtained from formulation T0 when Q_c/Q_d=30, in PBS of pH 6.8 after 24 hours. Error bars indicates the standard deviation (n=3).

On further investigation, it was revealed that some of drug loaded poly(ethyl acrylate) nanoparticles remain entrapped in poly(acrylamide) matrix. We believe this is related to high concentration of cross-linker that made a dense matrix and prevent the total release of nanoparticles. Secondly some of these nanoparticles might have bonded to the poly(acrylamide) matrix during free radical polymerization. This assumption was confirmed by observing the poly(acrylamide) matrix under TEM (Fig. 4.15) after 16 days of incubation in release media.

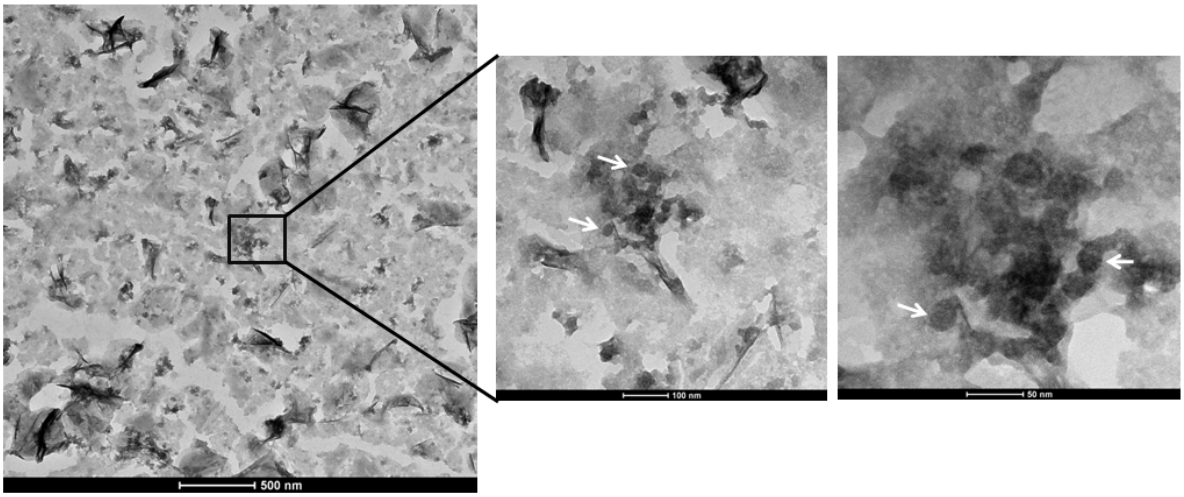

Fig. 4.15. TEM images of a Trojan microparticle's matrix obtained from formulation T0, after incubation in dissolution media for 16 days, under different magnifications showing the presence of embedded poly(ethyl acrylate) nanoparticles.

4.2.4 Conclusions

A new semi-continuous process based on nanoemulsion templating was developed for the synthesis of ketoprofen loaded Trojan microparticles. Polymerizable nanoemulsions were produced in an elongational-flow micromixer (μRMX) which was later linked to a co-axial capillary-based microfluidic setup for the production of uniform microdroplets. These droplets were then polymerized downstream by means of an UV source having wavelength far away from maximum absorbance wavelength of ketoprofen thus insuring its integrity. The size of the monodisperse nanodroplets was conveniently manipulated from 98 to 132 nm by controlling the surfactant concentration, type of monomer and the number of cycles in the μRMX. Poly(ethyl acrylate) nanoparticles in the range of 20 to 32 nm were found to be embedded in the microparticle's poly(acrylamide) matrix and to release loaded nanoparticles and ketoprofen in a suitable release media. This new semi-continuous process is a step forward toward an easy and facile approach to synthesize Trojan microparticles which otherwise requires usually multiple steps and time. The continuous process is also of an advantage to avoid any premature drug release or nano-emulsion droplet destabilization. In future, it is believed that these Trojan microparticles could be designed to targeted different locations in GIT.

References

Anton, N., Benoit, J.-P., Saulnier, P., 2008. Design and production of nanoparticles formulated from nano-emulsion templates—A review. Journal of Controlled Release 128, 185-199.

Anton, N., Jakhmola, A., Vandamme, T.F., 2012. Trojan Microparticles for Drug Delivery. Pharmaceutics 4, 1-25.

Antonietti, M., Landfester, K., 2002. Polyreactions in miniemulsions. Progress in Polymer Science 27, 689-757.

Bisht, S., Feldmann, G., Koorstra, J.-B.M., Mullendore, M., Alvarez, H., Karikari, C., Rudek, M.A., Lee, C.K., Maitra, A., Maitra, A., 2008. In vivo characterization of a polymeric nanoparticle platform with potential oral drug delivery capabilities. Molecular Cancer Therapeutics 7, 3878-3888.

Bouchemal, K., Briançon, S., Perrier, E., Fessi, H., 2004. Nano-emulsion formulation using spontaneous emulsification: solvent, oil and surfactant optimisation. International Journal of Pharmaceutics 280, 241-251.

Charles, L., ; Anthony, A. Attama, 2011. Current State of Nanoemulsions in Drug Delivery. Journal of Biomaterials and Nanobiotechnology, 2, 626-639.

Charles Lovelyn, Attama, A.A., 2011. Current State of Nanoemulsions in Drug Delivery. Journal of Biomaterials and Nanobiotechnology 2, 626-639.

Ensign, L.M., Cone, R., Hanes, J., 2012. Oral drug delivery with polymeric nanoparticles: The gastrointestinal mucus barriers. Advanced Drug Delivery Reviews 64, 557-570.

Fernandez, P., André, V., Rieger, J., Kühnle, A., 2004. Nano-emulsion formation by emulsion phase inversion. Colloids and Surfaces A: Physicochemical and Engineering Aspects 251, 53-58.

Forgiarini, A., Esquena, J., González, C., Solans, C., 2001. Formation and stability of nano-emulsions in mixed nonionic surfactant systems, in: Koutsoukos, P. (Ed.), Trends in Colloid and Interface Science XV. Springer Berlin Heidelberg, pp. 184-189.

Fu, Y., Kao, W.J., 2010. Drug release kinetics and transport mechanisms of non-degradable and degradable polymeric delivery systems. Expert Opinion on Drug Delivery 7, 429-444.

Gómez-Gaete, C., Fattal, E., Silva, L., Besnard, M., Tsapis, N., 2008. Dexamethasone acetate encapsulation into Trojan particles. Journal of Controlled Release 128, 41-49.

Jeong, W.-C., Lim, J.-M., Choi, J.-H., Kim, J.-H., Lee, Y.-J., Kim, S.-H., Lee, G., Kim, J.-D., Yi, G.-R., Yang, S.-M., 2012. Controlled generation of submicron emulsion droplets via highly stable tip-streaming mode in microfluidic devices. Lab on a Chip 12, 1446-1453.

Khan, I.U., Serra, C.A., Anton, N., Li, X., Akasov, R., Messaddeq, N., Kraus, I., Vandamme, T.F., 2014. Microfluidic conceived drug loaded Janus particles in side-by-side capillaries device. International Journal of Pharmaceutics 473, 239-249.

Khan, I.U., Serra, C.A., Anton, N., Vandamme, T., 2013. Continuous-flow encapsulation of ketoprofen in copolymer microbeads via co-axial microfluidic device: Influence of operating and material parameters on drug carrier properties. International Journal of Pharmaceutics 441, 809-817.

Peppas, N.A., Narasimhan, B., 2014. Mathematical models in drug delivery: How modeling has shaped the way we design new drug delivery systems. Journal of Controlled Release 190, 75-81.

Ranjha, N., Khan, I., Naseem, S., 2009. Encapsulation and characterization of flurbiprofen loaded poly(ϵ-caprolactone)–poly(vinylpyrrolidone) blend microphores by solvent evaporation method. J Sol-Gel Sci Technol 50, 281-289.

Solans, C., Izquierdo, P., Nolla, J., Azemar, N., Garcia-Celma, M.J., 2005. Nano-emulsions. Current Opinion in Colloid & Interface Science 10, 102-110.

Souilem, I., Muller, R., Holl, Y., Bouquey, M., Serra, C.A., Vandamme, T., Anton, N., 2012. A Novel Low-Pressure Device for Production of Nanoemulsions. Chemical Engineering & Technology 35, 1692-1698.

Tadros, T., Izquierdo, P., Esquena, J., Solans, C., 2004. Formation and stability of nano-emulsions. Advances in Colloid and Interface Science 108–109, 303-318.

Watanabe, T., Ono, T., Kimura, Y., 2011. Continuous fabrication of monodisperse polylactide microspheres by droplet-to-particle technology using microfluidic emulsification and emulsion-solvent diffusion. Soft Matter 7, 9894-9897.

Chapter 5
General discussion

Drug delivery can be considered as the field involving approaches, formulations, technologies and systems to transport an active pharmaceutical ingredient to desired site in the body in order to mitigate or cure a disease. These drug delivery systems should ensure safe, reliable and effective use of APIs by taking control of rate, time and place of release in body. Different macro drug delivery system like tablets, capsules, gastro retentive systems etc. are used for oral delivery of active ingredients but sometimes are restricted by dose dumping, side effects, dependence on gastric motility etc. Microparticle form of drug delivery systems, and especially those based on polymer materials, can overcome these limitations. However, it's a known fact that both the material and method of engineering drug delivery systems affect their properties. Standard encapsulation methods like solvent evaporation, solvent diffusion, crosslinking etc. using mechanical devices produces polydisperse particles with low encapsulation efficiency, initial burst release and batch to batch variation due to poor control over droplet generation in mechanical mixing processes. One can easily overcome above mentioned limitations if polymeric microparticles are engineered from monomer droplets where droplet formation is carefully controlled.

Recently microfluidic techniques have emerged as effective techniques to control the droplet formation. At macroscale, mass transport in fluids is determined by inertial and viscous forces. These inertial forces provide nonlinearity and are responsible for numerous instabilities such as turbulence. However in miniaturized system, inertial forces become negligible leading to laminar flow and much stable and controlled hydrodynamics which in turn allow an improved control over droplet formation. Thus, microfluidic device can efficiently achieve the production of monodisperse particles with high encapsulation efficiency and coefficient of variation less than 5%. Since microfluidic systems utilize small quantity of materials (ca 1 mg) and energy for the fabrication of carriers and thus are highly suitable for those a) involved in research and development of new delivery systems b) dealing with expensive or small available quantities of materials c) dealing with carcinogenic materials. Thus, these devices save time, material and thus money, not to mention that they reduce environmental impact and exposure to hazardous materials. Different microfluidic systems are developed to date but microchannel- and capillary-based systems are the most common ones. Capillary type systems are assembled in short span of time using commercially available chromatographic components and are as efficient as their

counterpart microchannel-based systems. Moreover, in capillary type systems, a slight change in design can result in particles with different morphologies, i.e. different properties.

In my thesis, I used capillary-based systems to develop four different drug loaded morphologies namely microbeads, Janus, Core-shell and Trojan particles to address different issues encountered during oral delivery of active ingredients. So far, microfluidic microparticles are developed by using different mechanisms like solvent evaporation, solvent diffusion, solvent extraction, ionic crosslinking etc. in combination with commercially available polymers. In my thesis, I chose to start from monomer and relied on UV-assisted free radical polymerization to get the microparticles. However, several issues had to be considered, e.g. UV light is usually considered harmful to active pharmaceutical ingredients, stability of active ingredient during free radical polymerization, solubility of drugs in monomer, conversion of monomers etc. During initial trials I found that by using a selective UV wavelength and suitable intensity far away from maximum absorbance wavelength of drug, one can maintain the integrity of active molecule while simultaneously completing polymerization. Use of UV light is economical and environment friendly and avoids a) the use of toxic solvents; b) the energy consumption to evaporate solvents. Secondly, when monomers were used as starting material it gives more flexibility to develop complex morphologies than polymers.

Each of the morphologies developed can tackle individual issues encountered in oral drug delivery. For instance, microbeads can release the drug with short half life in sustained release over extended period of time. Janus particles can store incompatible molecules in separate compartments and release them in sustained release manner. Core-shell particles have ability to deliver two incompatible molecules to targeted areas in GIT. Trojan particles can act as delivery vehicle for nanoparticles.

Ketoprofen loaded monodisperse microbeads of poly(tripropylene glycol diacrylate-co-ethyl acrylate) were fabricated using an off the shelf co-flow capillary-based microfluidic device and UV-assisted free radical polymerization under optimized conditions to maintain integrity of ketoprofen and confirmed by FTIR. All prepared microbeads were in the range of 200 to 380 µm with high encapsulation efficiency (80 to 100%). Release profile of these microbeads varied as function of size and composition of beads. Those having high content

of tripropylene glycol diacrylate released the drug very slowly due to the high crosslink density. On the other hand one having high content of ethyl acrylate released all the entrapped contents within 24 hours at pH 6.8 and limited release at pH 1.2. So these microbeads have potential to entrap and release drugs with short half life and gastric irritating effect in sustained release manner. Both of these features will improve the patient compliance and therapeutic effect of active molecules especially for NSAIDs like ketoprofen.

Microbeads have ability to deliver one molecule in sustained release manner. Certain clinical conditions demand administration of more than one API. Formulation of dosage form is a difficult task if the two APIs have different solubilities, physicochemical properties and are incompatible (e.g. when one molecule interferes with release profile of the second molecule). Under such circumstances, a bicompartmental particle will be quite useful. I chose Janus particles to tackle the above mentioned issues. Janus particles are prepared in a side-by-side capillaries-based microfluidic setup upon a slight modification of previous device use for the production of microbeads. Here each capillary carries a different monomer solution admixed with a specific active molecule namely ketoprofen and sodium fluorescein as hydrophilic and hydrophobic drug models. This setup produced Janus droplets which were polymerized by UV initiated free radical polymerization to form poly(acrylamide)/poly(methyl acrylate) Janus particles in the size range of 59 – 240 µm. As this was a new system, it was extensively characterized in terms of continuous and disperse phases flow rates, monomer composition of the two compartments, surfactant nature and concentration, outlet tubing diameter and UV intensity. It was observed that all of these factors could be adequately controlled to get different particle shapes ranging from core-shell to bi-compartmental particles. For the latter, a low surfactant concentration (0.75 wt.%) was necessary when the two disperse phases were pumped at equal flow rate, while at high surfactant concentration, disperse phases flow rates have to be changed. Small size particles were obtained by decreasing outlet tube internal diameter, increasing continuous to overall dispersed phase flow rates ratio (Q_c/Q_d) and using a flow-focusing section. Cytotoxicity tests showed these Janus particles were biocompatible, having LD_{50} of 9 mg/mL. Both ketoprofen and sodium fluorescein were released in sustained release manner at pH 6.8 and limited release at pH 1.2. Drug release was faster from bigger particles and found to result from the irregular distribution of the two phases and indentation on bigger particles as

revealed by SEM analysis. In comparison to hydrophobic model drug, hydrophilic sodium fluorescein release was slower which could be attributed to low initial loading and encapsulation efficiency. Furthermore, sodium fluorescein release could be modulated by changing crosslinker concentration. By decreasing crosslinker concentration, one decreased the crosslinking density and increased the mesh size which gave more freedom to movement of solvent and drug molecules. This demonstrates that, for Janus particles, one can control the individual release rate of the two encapsulated drugs by controlling their respective compartment crosslinking density. Thus Janus particles helps to deliver incompatible two APIs in sustained release manner but if one wants to deliver these incompatible molecules to a target site like colon in GIT, this morphology is not that much suitable. Answer lies in using morphology like core-shell particles which have a layer of polymer around core that encapsulates and protects the APIs in their shell and core respectively until they reach targeted site.

Core-shell particles are routinely prepared by non-microfluidic methods but they usually produce polydisperse particles and involve multiple steps procedures. In contrast, microfluidic methods produce monodisperse particles in one step and for the most of time for protection of API in core part. I slightly modified aforementioned co-flow capillary-based microfluidic setup to accommodate a second capillary. Both capillaries were co-axially arranged to form a double droplet generator. These double droplets were UV polymerized downstream to get ketoprofen loaded poly(methyl acrylate) core – ranitidine HCl loaded poly(acrylamide) shell particles. I managed to produce particles in the size range 100 to 151 µm by changing the continuous (Q_c) to middle (Q_m) phase flow rate ratio (Q_c/Q_m), while core diameter was varied between 58 to 115 µm by decreasing the middle (Q_m) to inner (Q_i) phase flow rate ratio (Q_m/Q_i). Core-shell structure was confirmed by optical and SEM analysis. It was further found that optimum concentration of surfactant, acrylamide and position of inner capillary (150 to 450 µm ahead of middle capillary) was necessary to produce core-shell particles otherwise particles without core were obtained. MTT assay showed LD_{50} of 3.1 mg/mL for non-contact conditions. LD_{50} was low in case of contact conditions which was attributed to combined effect of physical contact with cell line and release of leachable contents. Non pH sensitive particles released entrapped molecules in sustained release manner over 24 hours. Ketoprofen release was faster than ranitidine HCl

which was attributed to low initial loading of ranitidine HCl and higher molecular weight than ketoprofen. Ranitidine HCl release was augmented by increasing shell thickness and decreasing core diameter. In order to develop pH-sensitive particles for dual drug delivery to colonic region of human intestine, the shell phase was admixed with few weight percentages of pH sensitive carboxyethyl acrylate monomer. Core and shell contained the same model hydrophobic and hydrophilic drug as in previous case. Poly(acrylamide-co-carboxyethyl acrylate) shell retarded drug release at low pH but progressively increased its release with a maximum discharge at colonic pH of 7.4. So core-shell particles can deliver two molecules to targeted site.

Nanoparticles are desired for oral delivery in order to tackle the issue of solubility of drug and also to provide protection to protein in nature molecules. Furthermore, if delivered via oral route, patient can take them in the form of pills instead of receiving injections. Thus, nanoparticle form can improve patient compliance and avoid cost of injection manufacturing and administration. Unfortunately, oral delivery of nanoparticles is not successful yet due to different issues like aggregation of nanoparticles, rapid shedding of mucus membrane and motility of GIT which prevent their accumulation and penetration through absorption site. So a suitable carrier is required to alleviate these issues. One such system is composed of nanoparticles in microparticles so-called Trojan particles. In routine they are prepared in multiple steps i.e. a) preparation of nanoparticles b) dispersion of these nanoparticles in a microcarrier. These methods are time consuming and usually produce polydisperse particles. I have developed a two-step semi-continuous microfluidic process to easily produce Trojan microparticles from nanoemulsion templates. This system consists of two parts a) an elongational-flow micromixer and b) a co-flow capillary-based microfluidic device as used for the production of microbeads. The micromixer was used to produce size-controlled polymerizable nanoemulsions. Later on, the nanoemulsions were emulsified into miccrodroplets and immediately polymerized in the co-flow capillary-based setup to get monodisperse Trojan microparticles in the size range of 213 to 308 µm. To confirm the morphology, cross section of these particles were observed under SEM which revealed ketoprofen loaded poly(ethyl acrylate) nanoparticles embedded in a poly(acrylamide)matrix. After proving nanoparticles presence, there release was confirmed by observing release media under TEM. In USP phosphate buffer solution of pH 6.8, Trojan particles released 35%

of encapsulated drug in 24 hours. These initial trials confirmed that these microparticles can be prepared conveniently in a semi-continuous process saving time and cost of production. Further in future they can be designed to target specific area in gastro intestinal tract as well will be used for systemic delivery of nanoparticles.

So far, salient features of microfluidics have been discussed with focus on capillary-based devices to produce various drug loaded morphologies. But it would be unfair, not to highlight the shortcoming of this technique as observed during literature review and experimental work. As mentioned earlier microchannel type devices are commonly used but are limited by long, time consuming fabrication processes in clean room and are prone to clogging of channels. On other hand capillary-based systems are assembled in short span of time from commercially available chromatographic components and thus are easy to replace. Both systems produce particles at quite low rate (few mg/hr) and definitely needs to increase output to meet industrial scale production requirements. However, this issue has been resolved to some extent by the concept of numbering up which consists in the parallelization of several microdevices of same type.

Capillary based system used in my dissertation comes with some inherent drawbacks

1. It’s difficult to align capillaries especially when more than one capillary are assembled together as in side-by-side or two co-axial arrangements for Janus or core-shell droplets.
2. In case of complex capillary-based system, combination of hydrophilic and hydrophobic capillaries is necessary when hydrophilic and hydrophobic monomers are used.
3. Capillary-based microfluidic systems in current form are unable to deal with disperse phases with high viscosity.

To conclude, it necessary to give final remarks on the overall impact of microfluidic field on healthcare system. In the field of pharmaceutical applications, microfluidics is still at its infancy. So, it is difficult to figure out the exact area where this technique will flourish in the future. As a guess, one can foresee prospective domains for healthcare. One potential area on which scientist and pharmaceutical industries will probably focus in the future is targeted polymeric carriers with potential to deliver anticancer and protein drugs. One of

the most promising carrier morphology is the Janus-like structure which can store and deliver two anticancer drugs of different hydrophobicity simultaneously. Additionally, microfluidic 3D cancer models have better ability to identify cancer drug targets as compared to traditional animal models which lack the ability to simulate human structures and functions. Lastly, this technique is about to bring the point of care diagnostic to a new level since it would be much rapid, inexpensive and easy to use. This would enable health care personnel to rapidly diagnose and make onsite decision about treatment rather than waiting for results from traditional diagnostic test in clinical laboratories. So, integration of microfluidics and medical profession is about to set new era of safe, effective, rapid, easy and low-cost screening/diagnostic tools and dosage forms.

Chapter 6
Conclusion and perspectives

Conclusion

Microfluidics is a rather new field of science with a growing impact on pharmaceutics and drug delivery. Microfluidics has changed the way drug loaded particles are synthesized. Now simple and complex monodisperse microparticles with controlled-size, high encapsulation efficiency and batch to batch uniformity of drug release can be synthesized conveniently with off-the-shelves microfluidic tools. It is especially important to get complete clinical remedy of diseases condition with high patient's compliance. Encapsulation of multiple APIs in single complex morphologies like Janus and core-shell can serve both aforementioned goals. Microfluidic techniques use small quantity of reagents which is beneficial to research and development especially if one deals with toxic and expensive molecules. Microchannel- and capillary-based microfluidic devices are the most commonly used devices but most of times the former are used to develop simple morphologies. Little attention have been given to latter which are cheap, easily fabricated within short period of time and for which a slight change in the design gives new morphology as demonstrated in this doctoral research work. So far, different techniques like solvent evaporation, solvent diffusion, crosslinking, interfacial polymerization etc. were used for the fabrication of drug loaded microparticles. Little attention was given to UV initiated polymerization which can avoid the use of toxic solvents with minimum energy consumption.

During this work, it was demonstrated that monodisperse microbeads developed in a co-flow capillary-based device can be used as sustained release vehicle for short half life molecules. Release of active molecules from microbeads could be controlled by varying size and polymer composition. More complex morphology like Janus particles developed in a side-by-side capillaries-based device can deliver two immiscible and/or incompatible molecules in a sustained release manner. Release of APIs can be individually controlled from each compartment by varying size, crosslinking density and concentration of drug. Furthermore, a two co-axial capillaries-based device will produce core-shell particles for targeted dual drug delivery of active molecules to human colon or ensuring protection to the drug loaded in shell and core while traveling in the GIT. Trojan particles developed in a new semi-continuous microfluidic setup will probably open new horizons for oral delivery of nanoparticles.

Perspectives

In future there is need to focus on several issues related to the microfluidic production of drug loaded microparticles.

I. So far, per hour production of these microfluidic particles is quite low and there is definitely a need to develop methods that can increase the current throughput up to an industrial level. However, the concept of numbering up, i.e. mass parallelization of a single device, could be considered at first.

II. Under certain conditions, it was rather difficult to align capillaries. Further attention should be focused for rapid and reproducible alignment of capillaries.

III. Existing capillary-based devices lack online units for the separation and cleaning of microparticles from continuous phase.

IV. It would be interesting to complexify even more our Janus and core-shell droplet generators by accommodating a third capillary. This new setup could give core-multi shell or Janus core-shell particles for sequential or targeted release of three APIs.

V. Synthesis of Trojan particles needs further investigation in terms of µRMX restriction diameter, flow rate, oil to water phase ratio, drug and nanoparticle release

Appendices

Oral communications

- **T.F Vandamme**, I.U Khan, C.A. Serra, N. Anton. Microfluidic-conceived drug-loaded microcarriers. XXII International Conference on Bioencapsulation 21st Bratislava International Conference on Macromolecules, Bratislava, Slovakia, 17-19 September, 2014.
- **I.U Khan**, C.A. Serra, N. Anton and T. Vandamme. Droplet microfluidics: a tool to fabricate polymeric drug microcarriers with complex morphologies for new delivery strategies. *4th International Conference and Exhibition on Pharmaceutica*, San Antonio, TX USA, 24-26 March 2014.
- **I.U Khan**, C.A. Serra, N. Anton and T. Vandamme. Droplet microfluidics as a tool to develop copolymer drug micro-carriers with tunable drug release properties. *European Polymer Congress (EPF)* 2013 in Pisa (Italy), 16-21 June 2013.
- **I.U Khan**, C.A. Serra, T. Vandamme and N. Anton, Off-the-shelf microfluidic device for drug-loaded (co)polymer microbeads, In Proc. of *20th International Conference of Chemical and Process Engineering, Praha* (Czech Republic), 25-29 August 2012.
- **I.U Khan**, C.A. Serra, T. Vandamme and N. Anton, Off-the-shelf microfluidic device for drug-loaded (co)polymer microbeads *Seminar of LIPHT (ECPM)* on 28 July 2012 at Château de Lichtenberg France.

Poster communications

- **I.U Khan**, C.A. Serra, N. Anton and T. Vandamme **,** Droplet microfluidics: A tool to fabricate copolymer drug micro-carriers with tunable drug release properties, ***5th BBBB international Conference,*** held in Athens Greece on **26-28 September 2013.**
- Chang Z., C.A. Serra, M. Bouquey, I. Kraus, I.U. Khan, T. Vandamme, N. Anton, C. Ohm, R. Zentel, A. Knauer and M. Köhler, Engineering polymer microparticles by droplet microfluidics, In Proc. of *Microfluidics 2012*, Heidelberg (Germany), 3-5 December 2012.
- Chang Z., C.A. Serra, M. Bouquey, I. Kraus, I.U. Khan, T. Vandamme, N. Anton, C. Ohm, R. Zentel, A. Knauer, M. Köhler, Engineering polymer microparticles by droplet microfluidic, In Proc. of *11th International Workshop on Polymer Reaction Engineering*, Hamburg (Germany), 21-24 May 2013.
- **I.U Khan**, C. A. Serra, N. Anton and T. Vandamme, One step droplet microfluidic preparation and characterization of polymeric microbead drug carriers, *ERC Grantees Conference 2012, Frontier Research in Chemistry*, Strasbourg (France), 22-24 November 2012.

Original research articles

- **I.U Khan**, C.A. Serra, N. Anton and T. Vandamme, Continuous-flow encapsulation of ketoprofen in copolymer microbeads via co-axial microfluidic device: influence of operating and material parameters on drug carrier properties, Int. J. Pharm., 441 (1) (2013) 809-817.
- Serra C.A., **I.U Khan**, Z. Chang, M. Bouquey, R. Muller, I. Kraus, Marc Schmutz, T. Vandamme, N. Anton, C. Ohm, R. Zentel, A. Knauer and M. Köhler, Engineering polymer microparticles by droplet microfluidics, J. Flow Chem., (2013), 3(3): 66-75.
- **Khan, I.U.**; Serra, C. A.; Anton, N.; Li, X.; Akasov, R.; Messaddeq, N.; Kraus, I.; Vandamme, T. F. Microfluidic conceived drug loaded Janus particles in side-by-side capillaries device. International Journal of Pharmaceutics ***2014,*** 473 (1–2), 239-249.
- **Khan, I.U.**, **Stolch L**, Serra, C.A., Anton, N., Akasov R, Vandamme, T., 2013. Microfluidic conceived pH sensitive core-shell particles for dual drug delivery. International Journal of Pharmaceutics. ***2015,*** 478 (1), 78-87.
- **Ikram Ullah Khan**, Christophe A. Serra, Nicolas Anton, Marc Schmutz, Isabelle Kraus, Nadia Messaddeq, Thierry F. Vandamme, Microfluidic conceived Trojan microcarriers for oral delivery of nanoparticles, Submitted to International Journal of Pharmaceutics.

Review articles

- Serra C.A., B. Cortese, **I.U. Khan**, N. Anton, M.H.J.M. de Croon, V. Hessel, T. Ono and T. Vandamme, Coupling microreaction technologies, polymer chemistry and processing to produce polymeric micro and nanoparticles with controlled size, morphology and composition, Macromol. React. Eng., 7 (9) (2013) 414-439 (Invited article).
- **I.U Khan**, C.A. Serra, N. Anton and T. Vandamme. Microfluidics: a focus on improved cancer targeted drug delivery systems: Journal of controlled release (2013), 172(3):1065-74.
- **I.U Khan**, C.A. Serra, N. Anton and T. Vandamme. Production of nanoparticle drug delivery systems with microfluidic tools. Expert Opinion on Drug Delivery DOI:10.1517/17425247.2015.974547.

Book chapters

- Serra, C.A., **Khan, I.U.,** Cortese, B., de Croon, M. H. J. M., Hessel, V., Ono, T., Anton, N. and Vandamme, T. (2103) "Microfluidic Production of Micro- and Nanoparticles" in « Encyclopedia of Polymer Science and Technology », Wiley-VCH, Weinheim (Germany) (ISBN: 9780471440260).

- **Khan, I.U.,** Serra, C.A, Masood M.I, Shahzad Y, Vandamme T.F. Microfluidic-Conceived Drug-Loaded Micro-Carriers" (2014) Encyclopedia of Biomedical Polymers and Polymeric Biomaterials (Accepted).

Conference articles

- **I.U Khan** C.A. Serra, T. Vandamme and N. Anton, Off-the-shelf microfluidic device for drug-loaded (co)polymer microbeads, In Proc. of 20th International Conference of Chemical and Process Engineering, Praha (Czech Republic), 25-29 August 2012, 4 pages.
- Chang Z., C.A. Serra, M. Bouquey, I. Kraus, **I.U. Khan**, T. Vandamme, N. Anton, C. Ohm, R. Zentel, A. Knauer and M. Köhler, Engineering polymer microparticles by droplet microfluidics, In Proc. of Microfluidics 2012, Heidelberg (Germany), 3-5 December 2012, 10 pages.

Non peer reviewed article

- **I.U Khan**, C.A. Serra, N. Anton and T. Vandamme, Microfluidics: a new tool to get tunable release properties of drug loaded polymer microbeads, Newsletter of Bioencapsulation Research Group, June 2013.

Ikram Ullah KHAN

Microfluidic-assisted synthesis and release properties of multi-domain polymer microparticles drug carriers

Abstract

Characteristics and release properties of drug loaded microparticles depend upon material used and choice of production method. Conversely to most of the conventional ones, microfluidic methods give an edge by improving the control over droplet generation, size and size distribution. Capillary-based microfluidic devices were successfully used to obtain monodisperse drug(s) loaded microbeads, janus, core-shell and trojan particles using UV initiated free radical polymerization while keeping activity of active loaded molecules. These devices can be assembled in a short period of time and a slight change in design gives completely different microparticles morphologies. These particles were developed with the aim to address different issues experienced in oral drug delivery. For instance microbeads can be used to deliver NASIDs in a sustained release manner while janus particles can release two APIs with completely different properties (solubility, compatibility) also in a sustained release manner. Core-shell particles were designed to target colonic region of human intestine for dual drug delivery. Trojan particles were synthesized in a new semi-continuous microfluidic process, thus improving nanoparticles safety handling and release in simulated gastric fluid. Each system was fully characterized to insure batch to batch consistency and reproducibility. In general, the release of active ingredients was controlled by tuning the operating and material parameters like phases flow rates, nature and concentration of drug, (co)monomers, surfactant and crosslinker, pH of release media with the result of different particle morphologies, sizes and shapes or matrix crosslinking density.

Keywords: Microfluidics, capillary-based device, polymer, drug delivery, microbeads, janus particle, core-shell particle, trojan particle, cytotoxicity, pH sensitive, UV initiated polymerization

Résumé

Les caractéristiques et les propriétés de libération de microparticules chargées de médicament dépendent de la nature des matériaux employés, des propriétés physicochimiques des microparticules, du choix de la méthode de production, et enfin des propriétés des molécules encapsulées. A l'inverse de la plupart des méthodes conventionnelles, les méthodes microfluidiques présentent l'avantage de bien mieux contrôler la génération de gouttelettes, leur taille et leur distribution de tailles. Ainsi des dispositifs microfluidiques à base de capillaires ont été développés pour obtenir des microbilles de polymère mais également des microparticules de type janus, cœur-écorce ou troyenne, toutes monodisperses en taille et chargées de médicament(s). Ces particules ont été produites à partir de solutions de monomère qui furent polymérisées par irradiations UV de telle sorte à garder intacte l'activité des molécules chargées. Ces dispositifs peuvent être assemblés dans un court laps de temps et un simple changement dans leur conception permet d'obtenir des morphologies de particules très différentes. Ces particules ont été développées dans le but de résoudre les problèmes rencontrés dans l'administration orale de médicaments. Par exemple les microbilles peuvent être utilisées pour délivrer des anti-inflammatoires non stéroïdiens de manière continue tandis que les particules Janus peuvent libérer, simultanément et sur le même site, deux principes actifs possédant des propriétés complètement différentes (solubilité, compatibilité) également de manière prolongée. Quant aux particules cœur-écorce, elles ont été conçues pour cibler la région du côlon de l'intestin humain, et y libérer simultanément deux médicaments. Les particules troyennes furent synthétisées à l'aide d'un procédé microfluidique semi-continu qui a permis une manipulation plus sécurisée des nanoparticules vectrices ainsi que la libération continue d'un médicament dans un liquide gastrique simulé. Chaque système a été entièrement caractérisé pour assurer l'invariance entre lots et la reproductibilité. En général, la libération des ingrédients actifs a pu être facilement contrôlée/ajustée par le réglage des paramètres opératoires et de matériaux tels que les débits des différentes phases, la nature et la concentration du médicament, des (co)monomères, des agents tensioactif et de réticulation, le pH du milieu de libération. Ces différents paramètres influencent les propriétés des microparticules telles que leur morphologie, forme, taille et densité de réticulation du réseau polymère.

Mots-clés: Microfluidique, système capillaire, polymère, libération de médicament, microbille, particule janus, particule cœur-écorce, particule troyenne, cytotoxicité, pH répondant, polymérisation UV